

Dedicated to my supervisor and family

© Malaviya National Institute of Technology, Jaipur – 302017

All rights reserved



Department of Civil Engineering
Malaviya National Institute of Technology
Jaipur (Rajasthan) – 302017

CERTIFICATE

This is certified that the thesis entitled “**Electrochemical treatment of textile wastewater using 3D rotating anode**” is being submitted by **Aditya Choudhary** (ID – 2012RCE9021), to the Malaviya National Institute of Technology, Jaipur for the award of Degree of **Doctor of Philosophy** in Department of Civil Engineering is a bonafide record of original research work carried out by him. He has worked under my guidance and supervision, and has fulfilled the requirement for the submission of this thesis, which has revealed the requisite standard.

The results contained in this thesis have not been submitted in part or full, to any other University or Institute for the award of any degree or diploma.

Sanjay Mathur
Associate Professor
Department of Civil Engineering
MNIT Jaipur, India



Department of Civil Engineering
Malaviya National Institute of Technology
Jaipur (Rajasthan) – 302017

DECLARATION

I, **Aditya Choudhary**, declare that this thesis titled, “**Electrochemical treatment of textile wastewater using 3D rotating anode**” and the work presented in it, are my own. I confirm that:

- This work was done wholly or mainly while in candidature for a research degree at this university. Where any part of this thesis has previously been submitted for a degree or any other qualification at this university or any other institution, this has been clearly stated.
- Where I have consulted the published work of others, this is always clearly attributed.
- Where I have quoted from the work of others, the source is always given. With the exception of such quotations, this thesis is entirely my own work.
- I have acknowledged all main sources of help.
- Where the thesis is based on work done by myself, jointly with others, I have made clear exactly what was done by others and what I have contributed myself

Date:

Aditya Choudhary
2012RCE9021
Department of Civil Engineering
MNIT Jaipur, India

ACKNOWLEDGMENT

First and foremost, praises and thanks to God, the Almighty, for His showers of blessings throughout my research work to complete the research successfully.

The completion of my dissertation and subsequent Ph.D. has been a long journey and this thesis is the end of my journey in obtaining my Ph.D. At the end of my thesis, it is a pleasant task to express my thanks to all those who contributed in many ways to the success of this study and made it an unforgettable experience for me.

I express my sincere gratitude to my supervisor and advisor Dr. Sanjay Mathur, Department of Civil Engineering, MNIT, Jaipur. This work would not have been possible without his guidance, support and encouragement. Under his guidance I successfully overcame many difficulties and learned a lot. I appreciate all his contributions of time, ideas, and innovations to make my Ph.D. experience productive and stimulating. The joy and enthusiasm he has for this research was motivational for me, even during tough times in the Ph.D. pursuit. During the most difficult time of writing this thesis, he gave me the moral support and freedom I needed to move on. He always knew where to look for the answers to obstacles while leading me to the right source, theory and perspective. His patience, flexibility, genuine concern, and faith in me during the dissertation process enabled me to attend to life while also earning my Ph.D.

My thesis committee guided me through all these years. I am highly indebted and thankful to Prof. A.B. Gupta, Dr. U. Brighu and Dr. N. Kaul for being my major advisors. Their valuable advice, constructive criticism and extensive discussions around my work were a great help. During this work, I have used the expertise of Prof. Y.P. Mathur, Dr. Amar Patnaik and Dr. Amit Singh. I found them more than willing to share their treasure of knowledge with me. I wish to express my profound gratitude to them for their tender care and guidance. Their enthusiasm, encouragement and faith in me throughout have been extremely helpful. They were always available for my questions and generously gave their time and knowledge. I

am also thankful to the Head of Department (Civil), Prof. Gunwant Sharma for being a support. I extend my sincere thanks to Mr. Rajesh Saxena and Mr. S. Ansari for their motivation and support for completing the work. Their personal cheering is greatly appreciated.

I take this opportunity to sincerely acknowledge, Malaviya National Institute of Technology, Jaipur, for providing assistance which buttressed me to perform my work comfortably. I am grateful to Prof. U.R. Yaragatti, Director, MNIT, Jaipur, for his supportive gesture. I would also like to thank the team at the Materials Research Centre, MNIT, Jaipur for their help and support in testing various samples.

I am indebted to my colleagues for providing a stimulating and fun filled environment. I am ever indebted to Shilpi Singh, Kanika Saxena, Zainab Syed, Kavita Verma, Priya, Richa Sinha, Manish Yadav, Prakash Vijayvargia, Harish Pal, Neha Singh, Siddhant Srivastava, Rajneesh, Amit Patel, Saurabh Gupta, Prashant Gandhi, Narendra Sipani, Rakesh Gora, Praveen for their care and moral support. They have helped me survive all the stress and not letting me give up. I am also thankful to Achyut, Akansha, Priya, Tushali, Vipul, Akhil, Kuldeep, Ramchander, Priyesh, Sunder, Ashish, Santosh, Sandeep, Ravinder, Chotu Singh Ji, Chhatra Ram Ji who made the working environment worthwhile.

Finally, I would like to thank my family whom I owe a great deal. To my father, thank you for having faith in me and always stands beside me like a strong pillar and support. Hope, I made you proud. My brother, who motivated and helped me throughout my Ph.D work to handle all the difficulties with a smile. I finish with acknowledging, where the most basic source of my life energy resides: my MOTHER. Her support has been unconditional all these years. She has cherished with me every great moment and supported me whenever I needed it. Hence, great appreciation and enormous thanks are due to her, for without her understanding, I am sure this thesis would never have been completed.

I thank you all.

(Aditya Choudhary)

LIST OF PUBLICATIONS

In Journals:

1. A. Choudhary, S. Mathur, Performance evaluation of 3D rotating anode in electro coagulation reactor : Part I : Effect of impeller, *J. Water Process Eng.* 19 (2017) 322–330. doi:10.1016/j.jwpe.2017.08.020.
2. A. Choudhary, S. Mathur, Performance evaluation of 3D rotating anode in electro coagulation reactor: Part II: Effect of rotation, *J. Water Process Eng.* 19 (2017) 352–362. doi:10.1016/j.jwpe.2017.08.019.
3. A. Choudhary, S. Mathur (2017). Removal Kinetics and performance evaluation of 3D Rotating Cylindrical Anode Reactor for textile wastewater treatment, *Nature Environment and Pollution Technology (Accepted for Volume 16 Issue 4, 2017)*

In Conferences:

1. A. Choudhary, S. Mathur (2017). Performance Evaluation of Non Rotating And Rotating Anode Reactor In Electro Coagulation Process, *IOP Conf. Series: Materials Science and Engineering* 225, 012131 doi:10.1088/1757-899X/225/1/012131
2. A. Choudhary, S. Mathur (2016). Textile Wastewater Removal by Electrocoagulation in a 3D Rotating Cylindrical Anode Reactor: An Innovative Approach, *Trends and Recent Advances in Civil Engineering (TRACE – 2016)*
3. A. Choudhary, A. Dhar, S. Mathur (2013). Comparative Analysis of Treatment of Textile Wastewater by Electrocoagulation in Horizontal

Continuous and Horizontal Batch Reactor, *International Conference on
Water, Desalination, Treatment and Management (InDACON-2013)*

ABSTRACT

The electrochemical process is an immensely used treatment technology for industrial wastewater. Promising results have been obtained with EC, however, there exist various disadvantages of the process. These are in terms of electrode passivation, mixing, inconsistent coagulant dosing and other issues over long periods of operation that continue to limit the real application of EC. These are the factors of electrochemical reactor design/geometry which affects the mass transfer and in turn affects the process yield. So, the conventional electrochemical reactors are not sufficient in terms of mass transfer, mixing, flow dynamics and separate settling systems were required to handle the solid residues. These issues result in the fouling of electrode, lower efficiency of process, higher consumption of energy and anode material. The present scenario indicates sufficient scope to improve the process performance with better mixing and solid separation through better design of reactor and electrodes.

To avoid these unfavourable operating conditions which generally arise due to the geometry of the electrochemical reactor, a 3D perforated cylindrical rotating anode electrochemical reactor with hopper bottom was designed. This newly designed reactor was then evaluated through experiment and simulation of the fluid dynamics in the presented system. This helped in the evaluating the geometrical behaviour of the system. The expected improvements in performance are verified by treating the synthetic textile wastewater with the newly developed system.

The RTD and CFD were used to reveal the fluid dynamics of the electrochemical reactor. Both were applied to find the residence time and model the velocity, pressure and tracer profiles of the electrolyte/fluid inside the reactor. This helped to design the appropriate reactor configuration for enhancing the fluid dynamics and mass transfer inside the electrochemical reactor.

The flow dynamics of the reactor changed significantly when the perforated 3D anode was introduced into the reactor. For all studied flow rates, the pressure

profile showed 140 - 160% improvement in uniform pressure distribution inside the reactor due to the 3D anode. The velocity magnitude showed higher velocity zones created around the perforated 3D anode which indicates the turbulence caused by the introduction of the perforated 3D anode. The velocity vectors showed the generation of two vector zones imparting the fluid inside and out of the perforated 3D anode caused more turbulence as compared to the case where the perforated 3D anode was absent. The presence of perforated 3D anode caused a reduction in mixing time, in the range of 18 to 44%. The tracer mass fraction curve indicated symmetrical shape in a case where the impeller was present as compared to when the impeller was absent. The short circuiting index also decreased with increase in the flow rate when the impeller was present, and it was always less than the case where the impeller was absent. The flow regime tended to become plug flow when the impeller was present with an increase in flow rate. This showed that the introduction of impeller imparted more turbulence in the reactor which in turn provided better mixing and made the flow regime plug flow.

The 3D rotating anode clearly affected the performance of the reactor and increased the mean residence time of the fluid inside the proposed reactor configuration. The CFD and RTD helped to evaluate and simulate the performance and hydrodynamics of the reactor. The effective volume ratio increased with increasing rotation speed and found out to be best suited at flow rate of 60 lph with anode rotation speed set at 60 rpm. The short circuiting index was also found out to be minimum at these values. The 3D rotating anode acted as a turbulence enhancer for the configuration and in turn increased the mass transfer inside the reactor. The passivation of the anode, dead volume, short circuiting was not present in the proposed configuration.

The treatment capacity of the 3D rotating anode reactor was analysed by treating simulated textile wastewater using the reactor configuration. The plackett-burman design was employed and showed that the anode rotation was the significant operating parameter immensely affecting the process followed by current density, pH, and flow rate as per the pareto chart. The batch reactor showed an efficiency of 92.85% in terms of COD removal and 98.86% in terms of color removal. The batch re-circulation configuration was the best among three batch reactor configuration employed giving an efficiency of 94.40% at 60 lph. The Box-Behnken design was

then employed to optimize the process for COD removal and specific electrical energy consumption. It showed if anode rotation was kept in range of 50-60 rpm with current density ranging between 5.88 to 6.26 mA/cm², with flow rate of 65-75 lph and supporting electrolyte concentration of 3 – 3.50 g/l; the COD removal efficiency shoots upto 96.50% with SEEC of 0.026 J/mg COD. The textural analysis of EC generated sludge shows that all the residues were mesoporous in nature and TGA revealed that the EC solid residue can be used in making fuel briquettes.

The comparison of perforated 3D anode in stationary condition and commonly used plate electrode reactors revealed that stationary 3D anode system results in higher COD and color removal efficiency and lesser specific electrical energy consumption. The maximum COD and color removal with 3D perforated anode was found to be 85.12% and 97.97% respectively; against 78.91% and 93.89% respectively with plate electrode. The specific electrical energy consumption with 3D stationary anode was found to be about 20% lesser than the same with plate electrode for all current densities. A higher COD removal efficiency (96.40%), color removal efficiency (99.88%) and low specific energy consumption (0.028 J/mg) are observed vis-à-vis stationary 3D anode reactor.

TABLE OF CONTENTS

ACKNOWLEDGMENT.....	iv
LIST OF PUBLICATIONS	vi
ABSTRACT.....	viii
LIST OF FIGURES	xvi
LIST OF TABLES.....	xxi
NOMENCLATURE	xxiii
ABBREVIATIONS	xxiv
CHAPTER 1	1
INTRODUCTION	1
1. Background of the problem	1
1.1 Electrochemical Technology and Reactors	3
1.2 Selection of Electrochemical Reactors.....	5
1.3 Performance/Geometrical analysis of the Electrochemical Reactor	6
1.4 3D rotating anode electrochemical reactor.....	7
1.5 Objectives of the present work.....	8
1.6 Outline of the present work.....	9
1.7 Organization of the present thesis	10
CHAPTER 2	12
LITERATURE REVIEW	12
2. Background.....	13
2.1 Fundamentals	14
2.2 Sacrificial anode materials for electro coagulation	17
2.2.1 Iron and steel anodes.....	18
2.2.2 Aluminium anode.....	19
2.3 Pollutants removal mechanisms	20
2.3.1 Heavy metals removal.....	21
2.3.2 Organics removal	21
2.4 Factors affecting electro coagulation	22
2.4.1 Effect of electrode material.....	22
2.4.2 Effect of pH.....	22
2.4.3 Effect of current density and type.....	23

2.4.4	Effect of supporting electrolyte	23
2.4.5	Current density supply and time of treatment.....	24
2.4.6	Effect of temperature	24
2.4.7	Conductivity of the solution.....	24
2.4.8	Effect of agitation speed	25
2.4.9	Inter-electrode gap	25
2.4.10	Electrode arrangements.....	25
2.5	Electro coagulation reactors	26
2.6	Design of the EC cell	27
2.7	Mass transfer measurement.....	28
2.8	Residence Time Distribution (RTD).....	29
2.9	Computational Fluid Dynamics (CFD).....	31
2.10	Response Surface Methodology.....	33
2.11	Electro coagulation applications	34
2.11.1	Non-metallic inorganic species.....	34
2.11.2	Heavy Metals	36
2.11.3	Organic pollutants.....	38
2.11.4	Actual effluents.....	39
CHAPTER 3	41
MATERIAL AND METHODS	41
3.	Analysis of flow pattern in reactor with perforated anode.....	41
3.1	The 3D rotating anode reactor.....	41
3.2	Geometric Specification of the reactor.....	42
3.3	Performance of the 3D rotating anode reactor.....	44
3.3.1	Residence time distribution (RTD).....	45
3.3.2	Computational fluid dynamics (CFD)	47
3.4	Experimental Investigation on textile wastewater	49
3.4.1	Synthetic textile wastewater	49
3.4.2	Materials/Chemicals	49
3.4.3	Equipments	50
3.4.4	Experimental strategy during EC treatment of STW.....	51
3.5	Microscopic Analysis Scattering Analysis.....	56
3.5.1	Zeta potential analysis.....	56

3.6	Solid Residue Generation and Analysis	56
3.6.1	Thermo-gravimetric analysis (TGA)	57
3.6.2	Field emission scanning electron microscope (FE-SEM) and energy dispersive X-ray analysis (EDX)	57
3.6.3	Powder X-ray diffraction (PXRD).....	58
3.6.4	Surface area and pore size distribution analysis	59
CHAPTER 4	60
RTD & CFD ANALYSIS of 3D ROTATING ANODE REACTOR.....		60
4.	RTD and CFD Analysis.....	61
4.1	Residence Time Distribution (RTD) Model.....	61
4.1.1	Effect of Flow Rate on Exit Age Distribution	64
4.1.2	Effect of Rotation Speed on Exit Age Distribution	64
4.2	Comparison of RTD with Model	65
4.2.1	Unequal Volume ($V_1 \neq V_2 \neq V_3$)	65
4.2.2	Equal Volume ($V_1 = V_2 = V_3$)	66
4.2.3	Active Center Compartment Volume	66
4.3	CFD Analysis	67
4.3.1	Specification of Problem.....	68
4.3.2	Material and Flow Properties.....	68
4.4	CFD of 3D Stationary Anode.....	69
4.4.1	Pressure Distribution.....	70
4.4.2	Velocity Vector and Magnitude Contour.....	73
4.4.3	Turbulent Intensity.....	76
4.4.4	Normalized Mixing Time	76
4.4.5	Tracer Mass Fraction	77
4.4.6	Plug Flow Index	79
4.4.7	Short Circuiting Indexes	80
4.5	CFD of 3D rotating anode.....	82
4.5.1	Effective Volume Ratio	82
4.5.2	Effect of flow rate and rotation on Short Circuiting Index	83
4.5.3	Pressure Distribution.....	84
4.5.4	Velocity Magnitude Contour	86
4.5.5	Velocity Vector.....	89

4.5.6	Reynolds Number and Turbulent Kinetic Energy	91
4.5.7	Comparison between simulated and experimental mixing patterns ..	92
CHAPTER 5	94
TREATMENT OF STW USING 3D ROTATING ANODE	94
5. EC Treatment of synthetic textile wastewater (STW) with 3D rotating anode electrochemical reactor		95
5.1	The Electrochemical treatment.....	95
5.2	Criteria for Reactor performance	95
5.3	The 3D rotating anode reactor.....	96
5.4	Screening of the operating parameters using Plackett-Burman (PB) Design	97
5.4.1	Method of Steepest ascent/descent	100
5.5	Performance of the 3D rotating anode (Batch Studies).....	101
5.5.1	Batch Reactor.....	101
5.5.2	Effect of Anode Rotation Speed	103
5.5.3	Effect of Current Density.....	105
5.5.4	Effect of the initial pH (pH ₀)	106
5.5.5	Effect of NaCl/electrolyte concentration	108
5.5.6	Effect of type of supporting electrolyte	109
5.5.7	EC Treatment time (t)	110
5.5.8	Rate Constant	110
5.5.9	Batch Recirculation Reactor	112
5.5.9.1	Effect of the Electrolyte Flow Rate	112
5.5.10	Single Pass System	114
5.6	Response Surface Methodology (RSM).....	115
5.6.1	Interaction and optimization of parameters	115
5.6.2	Development of regression equation	116
5.6.3	Adequacy	120
5.6.4	Combined Effects of operating parameters on COD and SEEC.....	123
5.6.5	Optimization of Model and its verification.....	129
5.7	Comparison of Plate Electrode and 3D stationary anode reactor.....	130
5.7.1	Color Removal	130
5.7.2	COD Removal.....	131

5.7.3	Energy Consumption	132
5.8	Comparison of 3D stationary and rotating anode reactor	134
5.8.1	Color Removal	134
5.8.2	COD Removal.....	135
5.8.3	Anode Consumption	136
5.8.4	Energy Consumption	137
5.9	Zeta Potential.....	138
5.10	Adsorption study	139
5.10.1	Adsorption isotherms	139
5.10.2	Reaction kinetics	140
5.10.3	Adsorption mechanism	141
5.11	Solid Residue Generation and Analysis	141
5.11.1	XRD Analysis	141
5.11.2	SEM-EDAX and Pore size distribution of solid residue	143
5.11.3	Thermal Degradation Analysis	144
CHAPTER 6	146
CONCLUSIONS AND RECOMMENDATIONS	146
6.1	Hydrodynamics of the 3D rotating anode electrochemical reactor with RTD and CFD	146
6.2	Treatment of synthetic textile wastewater using 3D rotating anode	148
6.3	Recommendations	150
BIBLIOGRAPHY	152
BRIEF BIO-DATA	196

LIST OF FIGURES

Figure 1-1: Major factors affecting the EC process.....	3
Figure 1-2: Classification of electrochemical reactors according to electrode geometry and configuration	5
Figure 1-3: Outline of the research work.....	9
Figure 2-1: Conceptual representation of the electrical double layer (Vepsäläinen, 2012)	15
Figure 2-2: Typical reactions during the EC treatment (Chaturvedi, 2013)	16
Figure 2-3: Concentrations of soluble monomeric hydrolysis products of Fe(III) and Al(III) in equilibrium with the amorphous hydroxides at zero ionic strength and 25°C (Vepsäläinen, 2012).....	20
Figure 3-1: Front View of the Proposed Reactor.....	43
Figure 3-2: Side View of the Proposed Reactor.	43
Figure 3-3: Geometry of Proposed Reactor. 1) 3D Aluminum perforated cylindrical anode. 2) Aluminum rod cathode. 3) Conical Hopper Bottom for Sludge collection. 4) Mechanical stirrer. 5) DC Power Supply Unit. 6) Inlet for Wastewater. 7) Outlet for Treated Water.....	44
Figure 3-4: Experimental setup for RTD studies: 1) 3D Aluminum perforated cylindrical anode. 2) Aluminum rod cathode. 3) Conical Hopper Bottom for Sludge collection. 4) Mechanical stirrer. 5) DC Power Supply Unit.....	45
Figure 4-1: C (t) vs time of RTD	63
Figure 4-2: E (t) vs time of RTD	63
Figure 4-3: E (t) (s ⁻¹) vs time of RTD	64

Figure 4-4: Pressure Contour for different flow rates in absence of impeller (a) 5 lph, (b) 15 lph, (c) 30 lph, (d) 60 lph, (e) 90 lph, and (f) 120 lph; and in presence of impeller (g) 5 lph, (h) 15 lph, (i) 30 lph, (j) 60 lph, (k) 90 lph, and (l) 120 lph.	71
Figure 4-5: Velocity Vector and Magnitude Contour for different flow rates in absence of impeller (a) 5 lph, (b) 15 lph, (c) 30 lph, (d) 60 lph, (e) 90 lph, and (f) 120 lph; and in presence of impeller (g,m) 5 lph, (h,n) 15 lph, (i,o) 30 lph, (j,p) 60 lph, (k,q) 90 lph, and (l,r) 120 lph.....	75
Figure 4-6: Normalized Mixing Time in absence and presence of Impeller	77
Figure 4-7: Tracer Mass Fraction at different flow rates (a) in the absence of Impeller (b) in the presence of Impeller	78
Figure 4-8: Plug flow Index in absence and presence of impeller for different flow rates	79
Figure 4-9 : Short Circuiting Index in absence and presence of impeller for different flow rates.....	80
Figure 4-10: The distance of S_{ib} from ideal PFR	81
Figure 4-11: The distance of Q_{sc} from ideal PFR	82
Figure 4-12: Effective Volume Ratio at different flow rates (5-120 lph) with varying rotation speed (0-100 rpm)	83
Figure 4-13: Short Circuiting index at different flow rates (5-120 lph) with varying rotation speed (0-100 rpm).....	84
Figure 4-14: Total Pressure profile for the flow rates of 5 (a-c), 60 (d-f) and 120 (g-i) lph with anode rotation speed of 20 – 100 rpm respectively.....	85
Figure 4-15: Velocity Magnitude Contour for the flow rates of 5 (a-c), 60 (d-f) and 120 (g-i) lph with anode rotation speed of 20 – 100 rpm respectively.	88
Figure 4-16: Velocity Vector profile for the flow rates of 5 (a-c), 60 (d-f) and 120 (g-i) lph with anode rotation speed of 20 – 100 rpm respectively.	91

Figure 4-17: Comparison of simulated, experimental and ideal mixing line for anode rotation of (a) 0 rpm, (b) 20 rpm, (c) 40 rpm, (d) 60 rpm, (e) 80 rpm, and (f) 100 rpm respectively.....	93
Figure 5-1: Schematic display of the various operating parameters influencing the EC process performance.	96
Figure 5-2: Geometry of Proposed Reactor. 1) 3D Aluminium perforated cylindrical anode. 2) Aluminium rod cathode. 3) Conical Hopper Bottom for Sludge collection. 4) Mechanical stirrer. 5) DC Power Supply Unit. 6) Inlet for Wastewater. 7) Outlet for Treated Water.....	97
Figure 5-3: Pareto chart of standardized effects for the Plackett-Burman design for response (a) Color removal and (b) COD removal.....	100
Figure 5-4: Effect of Anode rotation speed on percentage COD removal. (CD =6 mA/cm ² , pH = 6, initial COD = 861 ppm).....	104
Figure 5-5: Effect of Anode rotation speed on percentage Color removal. (CD =6 mA/cm ² , pH = 6, initial COD = 861 ppm).....	104
Figure 5-6: Effect of Current density on percentage COD removal. (Anode Rotation Speed = 60 rpm, pH = 6, initial COD = 861 ppm)	106
Figure 5-7: Effect of pH on percentage COD removal. (Anode Rotation Speed = 60 rpm, current density = 6 mA/cm ² , initial COD = 861 ppm)	107
Figure 5-8: Effect of conductivity on percentage COD removal. (Current density = 6 mA/cm ² , Anode Rotation Speed = 60 rpm, pH = 8, initial COD = 861 ppm)....	109
Figure 5-9: Actual vs Predicted COD Removal Efficiencies	121
Figure 5-10: Actual vs Predicted Specific Electrical Energy Consumption.....	121
Figure 5-11: Normal probability curve for COD Removal	122
Figure 5-12: Normal probability curve for Specific Electrical Energy Consumption (SEEC).....	122

Figure 5-13: Combined Effects of supporting electrolyte concentration and anode rotation speed on percentage COD removal: (a) Contour plot and (b) Response Surface	124
Figure 5-14: Combined Effects of current density and anode rotation speed on percentage COD removal: (a) Contour plot and (b) Response Surface.....	125
Figure 5-15: Combined Effects of flow rate and anode rotation speed on percentage COD removal: (a) Contour plot and (b) Response Surface	126
Figure 5-16: Combined Effects of supporting electrolyte concentration and anode rotation speed on specific electrical energy consumption: (a) Contour plot and (b) Response Surface.....	127
Figure 5-17: Combined Effects of current density and anode rotation speed on specific electrical energy consumption: (a) Contour plot and (b) Response Surface	128
Figure 5-18: Combined Effects of flow rate and anode rotation on specific electrical energy consumption: (a) Contour plot and (b) Response Surface	129
Figure 5-19: Effect of current density on COD removal efficiency of plate electrode reactor and 3D stationary anode reactor	132
Figure 5-20: Effect of current density on SEEC of plate electrode reactor and 3D stationary anode reactor	133
Figure 5-21: Color Removal comparison between continuous 3D stationary and rotating Reactor.....	134
Figure 5-22: Effect of detention time on COD removal efficiency of Non Rotating and rotating 3D cylindrical anode reactor.....	136
Figure 5-23: Effect of anode rotation speed on electrode consumption	137
Figure 5-24: Specific Electrical Energy consumption	138

Figure 5-25: XRD Analysis of Sludge generated during electrolysis at pH ~ 6
(Major Species are Al(OH)_3 , Aluminium chloride Hydroxide Hydrate and
Aluminium Oxide Chloride Hydroxide)..... 143

LIST OF TABLES

Table 2-1: Removal of various compounds using electro coagulation.....	35
Table 2-2: Removal efficiency of heavy metals by using electro-coagulation.....	36
Table 3-1: Dimensions of the Reactor Configuration with electrode	44
Table 3-2: Mesh quality of the reactor.....	48
Table 3-3: Composition of synthetic textile wastewater (STW)	49
Table 3-4: Levels and units of the factors used in Plackett-Burman design.....	51
Table 3-5: Plackett-Burman matrix used for EC treatment of STW	52
Table 3-6: Range of variables used in STW degradation	54
Table 3-7: Box-Behnken (BB) matrix used for EC treatment of STW	55
Table 4-1 : Variation of reactor active volumes (V_1 , V_2)	66
Table 4-2: Parameters used for non-moving/stationary case.....	68
Table 4-3: Parameters used for moving impeller (anode) case.....	69
Table 4-4: Mean Turbulent Intensity in absence and presence of impeller for different flow rates.....	76
Table 4-5: Reynolds number and type of flow	91
Table 4-6: Comparison of turbulent kinetic energy for different flow rates with rotation speed.....	92
Table 5-1: Regression coefficient and their significances for responses (COD and Color) in the Plackett-Burman design.....	98
Table 5-2: Range of operating parameters used in STW degradation for batch and Box-Behnken (BB) design.....	101

Table 5-3: Effect of the anode rotation (n) on the performance of 3D rotating anode batch reactor.....	111
Table 5-4: Effect of the current density (j) on the performance of 3D rotating anode batch reactor.....	111
Table 5-5: Effect of the initial pH (pH_0) on the performance of 3D rotating anode batch reactor.....	112
Table 5-6: Effect of the electrolyte flow rate (q) on the performance of 3D rotating anode batch recirculation reactor.	113
Table 5-7: Effect of the flow rate (q) on the performance of 3D rotating anode single pass system.	114
Table 5-8: Effect of the current density (j) on the performance of 3D rotating anode single pass system.	114
Table 5-9: Range of variables used in textile wastewater degradation.....	116
Table 5-10: Design of Experiments using RSM.....	116
Table 5-11: ANOVA for (a) COD removal and (b) specific electrical energy consumption (SEEC)	118
Table 5-12: Comparison of optimized and experimental results for COD removal and specific electrical energy consumption (SEEC).....	129
Table 5-13: Color Removal efficiency comparison between conventional plate electrode reactor and 3D stationary anode reactor.....	131
Table 5-14: Isotherm parameters for EC removal of STW.....	140
Table 5-15: Textural characteristics of solid residues	144

NOMENCLATURE

Sh	Sherwood Number
Re	Reynolds Number
Sc	Schmidt Numbers
d	Effective Diameter
D	Diffusion Coefficient
μ	Fluid Viscosity
ρ	Fluid Density
N	Rotational Speed
b	Mass transfer correlation constant
a	Exponent of Reynolds number
\emptyset	Velocity along x, y, and z direction
U	Temperature or mass fraction
p	Pressure
ν	Kinematic viscosity
α	Concentration of species in solution
D_{turb}	Diffusion coefficient of species in turbulent liquid phase
Sc_{turb}	Turbulent Schmidt Number
τ	Hydraulic Residence Time
(τ_p)	Peak Time
(τ_m)	Mean Residence Time
λ_{max}	Wavelength corresponding to maximum absorbance of the dye
Co	Concentration of COD before treatment
C	Concentration of COD after treatment
Ao	Absorbance of dye before treatment
A	Absorbance of dye after treatment
ELC_t	Theoretical metal consumption
M_w	Molecular weight of the anode
Z	Chemical equivalence
F	Faraday's constant
ELC_e	Experimental amount of anodic dissolution
V	Voltage
I	Current
T	Time
p_0	Saturated Vapour Pressure
σ	Surface Tension,
θ	Wetting Angle
R	Gas Constant
r_k	Kelvin's Radius
v	Volume of gas adsorbed at the equilibrium pressure
v_m	Liquefaction
D/uL	Mixing in axial direction of the flow
V^*	Inlet volumetric flow rate
e	Effective Volume Ratio
(t_{mean})	Mean retention time

$I(\Theta)$	Internal Age Distribution
N	Impeller rotation
n	Anode Rotation Speed
j	Current Density
q	Flow Rate
t	EC time
pH_0	Initial pH
m	Supporting Electrolyte Concentration
V_e	Effluent Volume
A_e	Effective Anode Area
i	Current Density
a_s	Specific Anode Surface
C_0	Initial COD
z	Number of electrons involved in the electrochemical reaction
C	COD at the time t
F	Faraday Constant
k	Rate Constant
q	Input Flow Rate
t_c	Contact Time
t	Sampling time of the process
V_R	Volume of the reactor
V	Total volume used

ABBREVIATIONS

3D	Three Dimensional
AC	Alternating Current
ANOVA	Analysis of Variance
BB	Box-Behnken

BET	Brunauer-Emmett-Teller
BJH	Barrett-Joyner-Halenda
CFD	Computational Fluid Dynamics
Cm	Centimetres
COD	Chemical Oxygen Demand
CSTR	Continuous Stirred Tank Reactor
DC	Direct Current
DLVO	Derjaguin-Landau-Verwey-Overbeek
DOC	Dissolved Organic Carbon
DTA	Derivatives Thermal Analysis
DTG	Differential Thermo Gravimetric
EC	Electro Coagulation
EDX	Energy Dispersive X-Ray Analysis
FE-SEM	Field Emission Scanning Electron Microscope
FTIR	Fourier Transformation Infrared
g/l	Grams Per Litres
Kg/m ³	Kilograms Per Cubic Metre
l/h	Litres Per Hour
Lph	Litres Per Hour
m/s	Metres Per Second
mA/cm ²	Milliampere Per Square Centimetre
MAC	Multistage Agitated Contactor
MBR	Membrane Bioreactor
min	Minutes
MP-P	Monopolar Electrodes In Parallel Connections
MP-S	Monopolar Electrodes In Serial Connections
PB	Plackett -Burman
PFR	Plug Flow Reactor
PSD	Particle Size Distribution
PXRD	Powder X-Ray Diffraction
R	Resistance
RCE	Rotating Cylindrical Electrode
RNG	Renormalization Group Method
rpm	Rotation Per Minute
RSM	Response Surface Methodology
RTD	Residence Time Distribution
SEEC	Specific Electrical Energy Consumption
SEM	Scanning Electron Microscope
SS	Stainless Steel
STW	Synthetic Textile Wastewater
TA	Thermal Analyzer
TGA	Thermo-Gravimetric Analysis
XRD	X-Ray Diffraction

CHAPTER 1

INTRODUCTION

This chapter deals with the brief description of the background on which the present research work was based upon. The outcome of the background study was identification of the research gaps that are required to be targeted and which in turn propagate the present work. This chapter also deals with the outlines and framework of the present thesis along with the objectives of this research work.

The electrochemical process was studied to understand the problems incur at the time of application. It was found that the geometry of the electrochemical process plays a major role in the performance of the process as the mixing pattern and mass transfer were dependent on electrochemical reactor design. The conventional electrochemical reactors are not sufficient in terms of mass transfer, mixing, flow dynamics and separate settling systems were required to handle the solid residues. This results in the fouling of electrode, lower efficiency of process, higher consumption of energy and anode material. The present scenario indicates sufficient scope to improve the process performance with better mixing and solid separation through better design of reactor and electrodes.

To avoid these unfavourable conditions generally developed due to the geometry of the electrochemical reactor. A 3D cylindrical rotating anode electrochemical reactor with hopper bottom was designed. This newly designed reactor was then evaluated as per the objectives of this thesis through experiments and simulation of the fluid dynamics in the presented system. This helps in the evaluating the geometrical behaviour of the system. The expected improvements in performance are verified by treating the synthetic textile wastewater with the newly developed system.

1. Background of the problem

In current scenario, water consumption and wastewater generation is becoming a cosmic issue in this era of industrial revolution. The conventional technologies

presently available are costly and have become inefficient due to their own limitations to treat the wastewater to a desired level. The introduction of electrochemical technologies for the treatment of industrial wastewater is of great influence and readily replacing the conventional treatment technologies. It is considered to be an effective, comparatively inexpensive (in comparison to advance oxidation methods) technology and is characterized by its easy operation, reduction in sludge volume and equipment costs for the treatment of industrial wastewater (Butler *et al.*, 2011a; Chopra, Kumar Sharma and Kumar, 2011; Fu and Wang, 2011; J.N. Hakizimana *et al.*, 2017; Moreira *et al.*, 2017). In recent years, various treatment electrochemical technologies have been used such as advanced electro oxidation, photo oxidation, electro coagulation, electro floatation, etc. (S. Lin and Peng, 1994; Pérez *et al.*, 2002; Anglada, Urriaga and Ortiz, 2009; Zodi *et al.*, 2009a; Kushwaha, Srivastava and Mall, 2010; Sinha, Singh and Mathur, 2014). The major factors that affect the performance of the electrochemical reactor are depicted in Figure 1-1.

Further, being an effective technique there are also some disadvantages associated with the present electrochemical treatment systems. These issues are mainly associated with the design and operations of the electrochemical treatment system. So, with increasing popularity of the EC technology; there exist the difficulties/limitations of the technology viz.

- a.) Dissolution of sacrificial electrodes,
- b.) Dead Zone formation inside the electrochemical reactor,
- c.) Oxide layer formation leading to loss of efficiency,
- d.) Fouling of the electrode,
- e.) Short circuiting inside the electrochemical reactor hampering the efficiency,
- f.) Solid and Scum generation and its handling system,
- g.) High energy consumption.

Keeping all these limitations in mind and requirement of an innovative and robust system is the need of this era. The design of electrochemical reactor plays an important role in the process of treatment. It drives the dynamics of the fluid to be treated inside the electrochemical reactor. The effective geometry and design may solve most of the issues that come into play with regular electrochemical reactors. The proper design and geometry of the electrochemical reactor helps the fluid to be treated

in a uniform fashion leaving no dead zones, short circuiting, channeling and fouling of electrode (Kuramitz *et al.*, 2002; Martínez-Delgadillo *et al.*, 2010; Ibrahim *et al.*, 2013a; Rodríguez *et al.*, 2015). These issues can be addressed with efficient mixing inside the electrochemical reactor (Alvarez *et al.*, 2002; Arratia *et al.*, 2004; Essadki *et al.*, 2008, 2010).

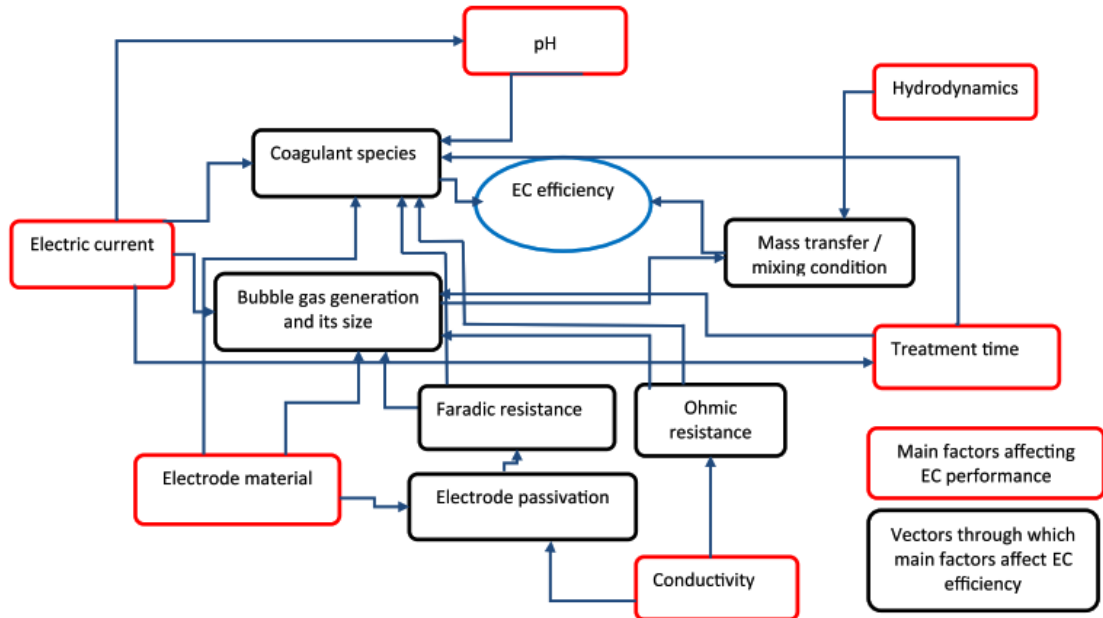


Figure 1-1: Major factors affecting the EC process

So, the better design/geometry of the electrochemical reactor can be the answer to this problem. Therefore, a new electrochemical reactor was needed to be designed, analysed and checked for its performance for treatment of industrial wastewater.

1.1 Electrochemical Technology and Reactors

Electrochemical science plays an important role in providing environmentally-friendly technology for chemical synthesis, separations, fuel cells, etc. The uniqueness of electrochemical technology is versatility, energy efficiency for automation, environmental compatibility and economy (Jüttner, Galla and Schmieder, 2000).

Electrochemical technology has contributed to zero discharge in the chemical process industries by providing advanced treatment methods such as electro-coagulation, electro-oxidation, electro-deposition etc.

Electrochemical technology continues to assist in environmental treatment, recycling, and monitoring, which includes (Walsh, 2001):

- i) Treatment by electrochemically generated species,
- ii) Removal of harmful contaminants, such as metal ions and organics coming from industrial wastewater and,
- iii) Using photovoltaic devices and fuel cells for the conversion of chemical to electrochemical energy.

The knowledge of electrochemical technology is essential for the design and operation of electrochemical reactors. In general, electrochemical reactors are classified based on electrode geometry and configuration. Various electrochemical reactors are used in the chemical process industry for various applications ranging from small scale reactors to large scale reactors.

The design or selection of appropriate electrochemical reactor is very imperative in electrochemical process as the reactor geometry plays an important role in the performance and process yield. In general, electrochemical reactors are classified based on either flow pattern or mode of electrical connection. The Figure 1-2 shows the outlines of electrochemical reactor classifications (R. Saravanathamizhan, Paranthaman, Balasubramanian and Basha, 2008a).

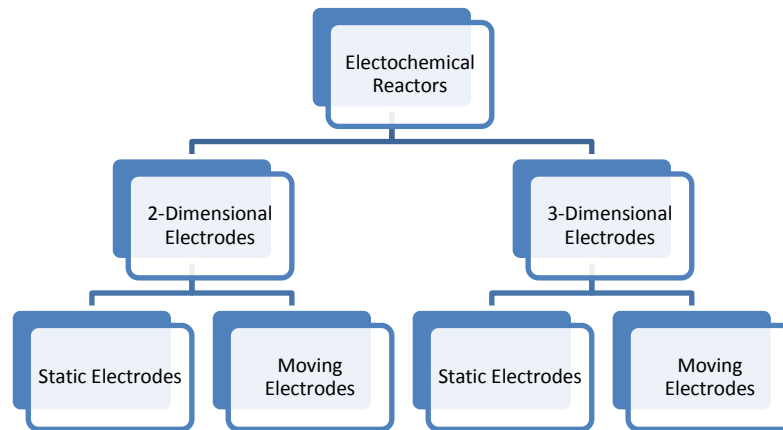


Figure 1-2: Classification of electrochemical reactors according to electrode geometry and configuration

1.2 Selection of Electrochemical Reactors

The selection of appropriate electrochemical reactor is important to achieve maximum efficiency and process yield. General guidelines for selection of electrochemical reactor are:

- (a) Highly active per unit volume of electrode area, that results in a compact reactor which is capable of achieving a considerable conversion, even at low concentrations of the reactants.
- (b) The controlled distribution of electrode potential over the electrode surface. The concentric cylinder and the parallel plate are common electrode geometries that promote a uniform potential distribution over the electrode.
- (c) A high value of current efficiency is desirable, in order to minimize the issues with the side reactions generated at the time of treatment and to provide good energy efficiency.
- (d) A high current density, in order to provide a rapid reaction rate per unit electrode area.
- (e) A high rate of mass transfer inside the electrochemical reactor by enhancing the relative movement in between the electrode surface and the electrolyte.

This can be achieved by promoting turbulence inside the reactor, using high linear fluid velocity and by rotating of the electrode also.

- (f) A lower electrical energy consumption to economize the treatment process which can be done by reducing the inter-electrode gaps, by using conductive electrodes and, by increasing the conductivity of the solution.
- (g) Other practical aspects such as ease in operation and control, low maintenance requirements, long-term stability of reactor components and the mode of product removal (Walsh and Pletcher, 2014).

1.3 Performance/Geometrical analysis of the Electrochemical Reactor

The performance of the electrochemical reactor can be analysed using the residence time distribution (RTD) and computational fluid dynamics (CFD). These experimental and computational tools have been widely used in the geometrical analysis of the electrochemical reactor to establish the flow behaviour inside the reactors. All the reactors are generally categorised into plug flow reactor (PFR) and Continuous stirred tank reactor (CSTR). The concept of ideal reactor doesn't apply in real reactors. The main reasons of the non-ideal behaviour of the real reactors are (Fogler, 2006b):

- i) Residence time distribution (RTD) of the system,
- ii) State of aggregation and,
- iii) Earliness or lateness of mixing.

In ideal reactors it is assumed that all the reactants have the same residence time equal to time space. It is possible when all the molecules move with same velocity. In real reactors some molecule may move faster compared to the other. The presence of channelling is reflected in RTD results. In ideal reactors all molecules are considered in micro level size and they all are free to move. In reality, group of molecules may combine together or aggregate to produce macro molecules and results in slower movement than that of micro molecules. Thus, the state of aggregation causes non ideal behaviour. In real reactors molecules might go for early or late stage of mixing unlike ideal reactors where molecules are uniformly mixed. The scenario makes it

imperative to understand actual flow pattern in reactor for better estimation of performance, which can be carried out with RTD experiment and CFD simulations. The tracer can be injected into the reactor by pulse and step input to study the RTD of the reactor. A tracer should be easy to analyse, stable and inactive compound generally NaCl. The computational fluid dynamics (CFD) models the flow behaviour of the reactor in terms of pressure distribution, velocity and vector contours, vorticity magnitude, radial and axial velocities, computational analysis of residence time and results can be verified using experimental RTD. The CFD also provides the analysis regarding the channelling, dead zone index and other behaviour of the reactors. This helps in understanding the developing a novel reactor that is free from these drawbacks generally encountered in the conventional reactors.

1.4 3D rotating anode electrochemical reactor

Though many type of electrochemical reactor are being used with their own limitation and advantages over conventional electrochemical reactors. A new type of electrochemical reactor was designed and studied in the present study to address most the issues faced in electrochemical reactors, presently, in use.

A novel 3D perforated rotating anode electrochemical reactor was designed which has a simple operation mechanism. The motion of rotation was being imparted to the anode rather than a separate agitation assembly. The perforated cylindrical anode drags the solution inside the reactor and due to centrifugal force solution moves away from the centre of the anode making a swirl motion due to perforation. Due to this action, solution to the surface of the anode was replenished by the bulk solution in every rotation. This results in mass transfer increment due to forced convection and it strongly depends on angular and radial velocity of the anode. A detailed description of the same is presented in Chapter 3.

1.5 Objectives of the present work

As it was evident for the diversity of the application areas, the study of hydrodynamic behaviour of the electrochemical reactor was very important in proper designing of the reactor. Often the behaviour of the reactor was found non-ideal and it has profound effect on the conversion of reactants to products. The non ideal behaviour can be depicted well using RTD and CFD. Thus, keeping in mind the gaps in the conventional electrochemical reactors the objectives of the present study were framed. The present study as described below; was to design a new cylindrical hopper bottom electrochemical reactor with a cylindrical 3D type electrode. The 3D electrode apart from its main function also acts as a turbulence enhancer/promoter inside the reactor. The present design of the electrochemical reactor was an endeavour to overcome the drawbacks (back mixing, channelling/short circuiting, formation of dead zones) practised with the conventional electrochemical reactors, presently in use. These drawbacks hamper the mass transfer inside the reactors and advances to efficiency losses at pilot scale plants (Djoudi, Aissani-Benissad and Ozil, 2012).

Therefore, to attain the above mentioned scope the following objectives were framed and completed:

- Design and Fabrication of New cylindrical hopper bottom electrochemical reactor with a cylindrical 3D type rotating anode acting as electrode and turbulence enhancer.
- Study the experimental exit age distribution in 3D RCE reactor. Validation of the experimental data of RTD with reported residence time distribution model.
- Development of the CFD model for 3D RCE reactor and to compare the model simulation with experimental observations.
- Study of the degradation of textile wastewater using 3D RCE and assessment of the effects of operating parameters. Development of Regression equation and Optimization of EC process using RSM and CCD approach for minimum energy input to achieve maximum COD and Color Removal.

- Analyses of the sludge composition using XRD, SEM-EDAX, textural characteristics, and TGA of samples.

1.6 Outline of the present work

The present research work has been broadly classified into two parts: RTD and CFD of the proposed reactor and its performance evaluation using synthetic textile wastewater (STW). A description of the present work is outlined in the Figure 1-3.

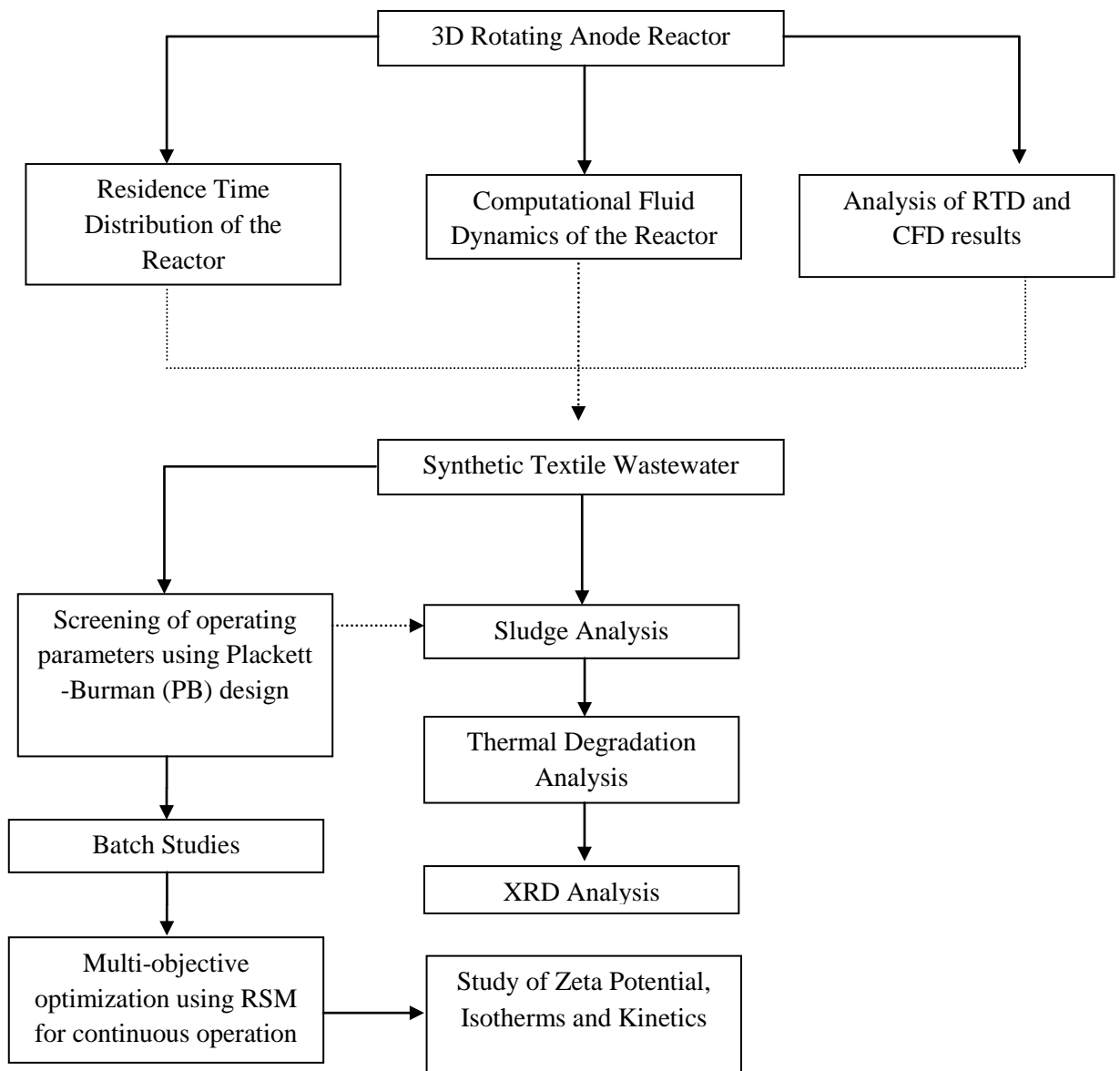


Figure 1-3: Outline of the research work

1.7 Organization of the present thesis

The entire thesis is summed up in six chapters. Presented below are the highlights of the chapters.

Chapter 1: This chapter presents the overview of the problem statement, gaps in the present research approach, and problems with conventional electrochemical reactors and outlines the tasks performed for present work.

Chapter 2: This chapter includes a critical review of literature, designed to provide the summary of the knowledge available in the literature involving research gaps and interests. This chapter has been divided into 4 sections. The first section gives the insight of electrochemical treatment process. The second section describes about the various reactor designs and operation mechanism used in electrochemical treatment of pollutants. The third section presents the residence time distribution and Computational fluid dynamics involved in the electrochemical reactors. The fourth section presents the statistical methods used for optimization of experimental data using response surface methodology and central composite design.

Chapter 3: This chapter presents the detailed description of methodology used in this research. It also introduces the experimental, computational and analytical techniques used for the completion of research.

Chapter 4: This chapter includes the RTD and CFD analysis of proposed reactor in presence and absence of 3D rotating anode. This chapter also includes the effect of anode rotation and its analysis using RTD and CFD and comparison of the same with stationary 3D electrode reactor of same configuration. The pressure distribution, velocity distribution and vector profile, short circuiting index etc. of the proposed reactor was studied using CFD to analyse the hydrodynamic behaviour of the proposed reactor.

Chapter 5: This chapter includes the screening of significant operating parameters using PB design, experimental investigation and optimization of operating parameters using response surface methodology and central composite design. The degradation of

simulated textile wastewater (STW) using 3D RCE and assessment of the effects of selected operating parameters were also studied. This chapter also includes the analysis of zeta potential, kinetics and adsorption isotherms to reveal the reaction mechanism taking place inside the reactor. This chapter also includes physic-chemical and textural characterization, and thermal degradation of the solid residues generated during EC process in order to understand the removal mechanism and final disposal alternative of the solid residues.

Chapter 6: This is the concluding chapter, which includes the main findings of the present research work and future recommendations based on the outcome of the present study.

CHAPTER 2

LITERATURE REVIEW

This chapter deals with the analysis of available literature which points out the validity of the EC approach for the elimination of different pollutants from wastewaters, at lab and pilot plant scale.

EC has achieved higher removal efficiencies by using principally Fe or Al anodes being considered as an economical technology. This electrochemical technology is able to reduce high pollutant contents considerably, although it does not achieve complete removal, in some cases. Furthermore, the alternative use of inexpensive and renewable energies (sunlight or wind power) in EC should also be investigated to make much more attractive eco-sustainable processes in practice.

Promising results have been obtained with EC, however, electrode passivation, mixing, inconsistent coagulant dosing and other issues over long periods of operation continue to limit the real application of EC. These are the factors of electrochemical reactor design/geometry which affects the mass transfer and in turn affects the process yield. The effect of these limiting factors can effectively be reduced by increasing the mass transfer inside the electrochemical reactor.

The RTD and CFD used in the literature revealed the fluid dynamics of the electrochemical reactor. Both were applied to find the residence time and model the velocity, vorticity, pressure and tracer profiles of the electrolyte/fluid inside the reactor. This helps to design the appropriate reactor configuration for enhancing the fluid dynamics and mass transfer inside the electrochemical reactor.

The geometry of the reactor plays an important role and the search of web of science revealed that there is plentiful research on electrochemical treatment while searching for rotating electrode within the scope, revealed that under the electrochemistry there were only 173 research articles published on the same. Narrowing the search further revealed that there are only 23 articles available in the literature which was not specifically related to rotating anode as it has given all the results containing the term rotating and anode. So, there is very less literature available regarding the use of

rotating cylindrical anode which can be a possible solution to the geometrical issue of the electrochemical reactor to enhance mass transfer.

The development of the emerging advanced EC processes is of great interest due to the removal efficiency enhancement. Several other complementary EC procedures that can remove with higher efficiencies the pollutants with lower energy requirements or combined/hybrid EC technologies as pre-/post-treatments can be used. Future developments will rely upon the close collaboration of analytical chemists, engineers and electrochemists to ensure effective application and exploitation of these electrochemical technologies.

2. Background

Water recycling is one of the greatest environmental challenges and necessity of 21st century due to limited fresh water sources and its ever-increasing demand (UNESCO, 2012). Nowadays due to the technological development and the industrial activity the pollutants contained in waters are completely different from those in ancient times. The physico-chemical processes for water treatment are the most used technologies because these have been known and applied since centuries to make water drinkable for human intake (Bratby, 2006). In this context, EC or electro coagulation is an electrochemical technology with a wide range of application that can effectively reduce several pollutants in the water from heavy metals to persistent organic pollutants. This chapter discusses EC fundamentals, its principles, parameters of influence, removal mechanisms and applications (Butler *et al.*, 2011b; Khandegar and Saroha, 2013; Kuokkanen *et al.*, 2013, 2015; Sahu, Mazumdar and Chaudhari, 2014; Jean Nepo Hakizimana *et al.*, 2017) and summarizes the fundamentals of EC technologies including, the advanced EC with *in situ* generation of oxidant species to improve the pollutants removal efficacy as well as the coupling of *on-line* electro analytical technologies to follow the pollutants abatement.

2.1 Fundamentals

The traditional process of coagulation is a physico-chemical treatment which involves phase separation for the purification of wastewaters before discharge to the environment (J.N. Hakizimana *et al.*, 2017). The process of Electro Coagulation is directly related to conventional coagulation process, which has been used as a method (as early as 2000 BC) for water clarification and potabilization (Bratby, 2006) and nowadays, it is still extensively used (Sahu and Chaudhari, 2013).

The conventional process of coagulation-flocculation is based on the formation and aggregation of a colloidal system by the use of the coagulating agents. Inorganic and organic pollutants are separated from the aqueous phase by their precipitation with the coagula and subsequently removed from the treated water by clarification (Pernitsky and Edzwald, 2006; Jiang, 2015). The aggregates formation is explained by the famous Derjaguin-Landau-Verwey-Overbeek (DLVO) theory where it is assumed that the formation of an aggregate depends on the interaction forces which is the sum of Van der Waals and double layer forces (Matilainen, Vepsäläinen and Sillanpää, 2010). The simplest consideration is the symmetric system (homo-aggregation) where the double layer force is repulsive and the Van der Waals forces attractive; then, the attractive force has to overcome the repulsive force in order to destabilize the colloids and form the aggregate or the micro flocs (Garcia-Segura *et al.*, 2017). Consequently, zeta potential is used to measure the effective charge of the particle as it moves through the solution, providing a direct indication to particle stability as depicted in Figure 2-1.

However, DLVO theory cannot totally explain the coagulation phenomena because in this complex system other interactive forces than electrostatic repulsion (e.g.: hydration, hydrophobic interactions and so on) are involved in the colloids stabilization (Santo *et al.*, 2012).

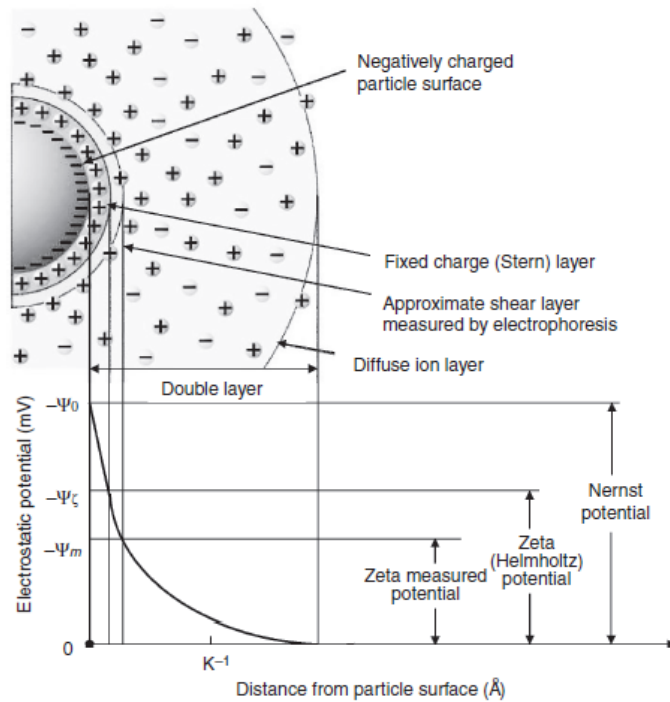


Figure 2-1: Conceptual representation of the electrical double layer (Vepsäläinen, 2012)

In coagulation-flocculation process, the addition of coagulating agents (such as Fe^{3+} or Al^{3+} salts) favours the neutralization of charged pollutants and their aggregation (Lee, Robinson and Chong, 2014), and after that, their physical separation from water by precipitation or flotation (Balla *et al.*, 2010; Verma, Dash and Bhunia, 2012). Considering the EC approach, similar effects like conventional coagulation can be produced (Chen, 2004; Brillas and Martínez-Huitle, 2015). This technique incorporates current to dissolve Fe, Al or other metals as sacrificial anodes immersed in the polluted water instead of using coagulants. The electro-dissolution induces an increase of the metal ions in solution as well as their complexed species with hydroxide ion depending on the pH conditions and the sacrificial anode used (Cañizares *et al.*, 2007; W.-L. Chou, Wang and Huang, 2010; Kamaraj and Vasudevan, 2015). These species act as coagulants or destabilization agents and separate pollutants from the wastewaters (Gregory and Duan, 2001).

In general, specific steps take place during an EC treatment given in Figure 2-2 (Can, Bayramoglu and Kobya, 2003; MOLLAH *et al.*, 2004; Al Aji, Yavuz and Koparal, 2012):

- (i) Metal ions from anodes are produced causing electro-dissolution, and H₂ gas is evolved at the cathode,
- (ii) Destabilization of the organic and inorganic pollutants, suspensions and breaking emulsions,
- (iii) Formation of aggregates of the destabilized pollutants and its coagulation in the wastewater as flocs,
- (iv) Removal of coagulated pollutants by sedimentation or by electro-flotation by evolved H₂ (electro-flotation can be used to disperse the coagulated particles via the bubbles of H₂ gas produced at the cathode from water reduction reaction, transporting the solids to the top of the solution),
- (v) Electrochemical and chemical reactions promoting the cathodic reduction of organic impurities and metal ions onto the cathode surface.

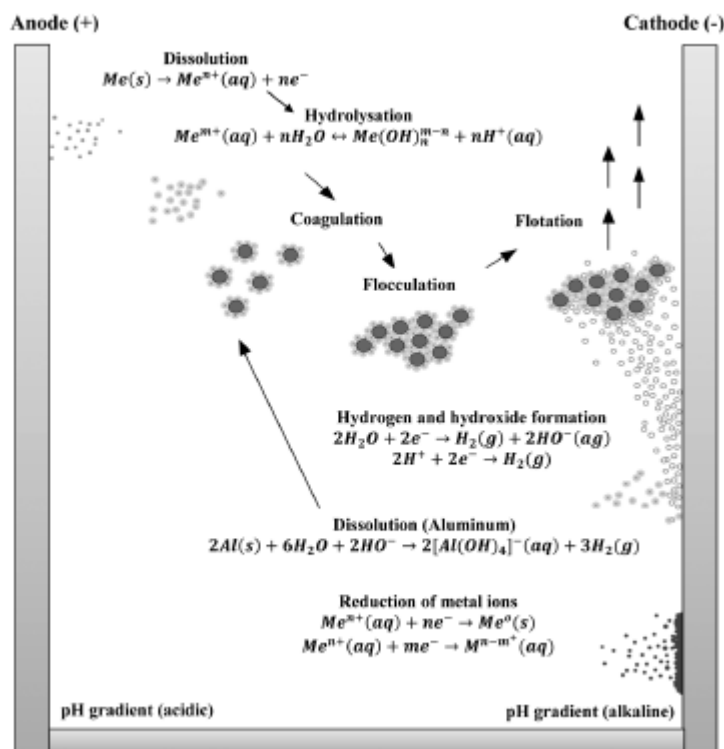


Figure 2-2: Typical reactions during the EC treatment (Chaturvedi, 2013)

The main advantages that have been reported by several authors (S. H. Lin and Peng, 1994; Meunier *et al.*, 2006; Brillas and Martínez-Huitle, 2015) are listed below:

- (i) Effective separation of organic matter separation than in conventional coagulation,
- (ii) Less dependent on pH,
- (iii) Coagulants are directly electro-generated, thus there is no extra competitive anions like chloride or sulphate ions,
- (iv) The highly-pure electro-generated coagulant improves the pollutants removal, then, a smaller amount of chemicals is required,
- (v) A direct consequence of (iv) is the lower amount of sludge produced,
- (vi) The operating costs are much lower than conventional technologies.

However, this method presents some major disadvantages as mentioned below (Garcia-Segura *et al.*, 2017):

- (i) The possible passivation of anode or/and sludge deposition on the electrodes can inhibit the electrolytic process in continuous operation mode,
- (ii) Even though lower amount of sludge is produced in comparison with coagulation, the treated effluents still present high concentrations of iron and aluminium ions in the effluent that avoid their direct release to the environment. Thus, a post-treatment to reduce the metallic ions concentration after the electrochemical process is required in order to attend the environmental legislations,
- (iii) There is requirement of periodical replacement of sacrificial anodes
- (iv) Deposition of hydroxides of calcium, magnesium, etc., onto the cathode, avoiding the release of H₂ and the pass of current, when using actual wastewaters. This can be solved using alternate current with same anode and cathode materials.

2.2 Sacrificial anode materials for electro coagulation

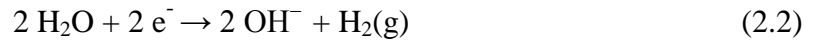
The dissolution of the anodes releases coagulants in the water that are responsible for the pollutants removal. Below discussed are the main materials used as sacrificial anodes in EC.

2.2.1 Iron and steel anodes

When iron, steel (St) or stainless steel (SS) anode is used in EC, Fe^{2+} is dissolved in the treated wastewater by Fe oxidation at the anode, as follows (Daneshvar, Ashassi-Sorkhabi and Tizpar, 2003; Zodi *et al.*, 2009b):



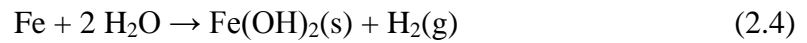
Meanwhile, hydroxide ion and H_2 gas are generated at the cathode from the water reduction reaction:



Significant OH^{-} production from reaction (2.2) causes an increase in pH during electrolysis leading to the formation of different iron hydroxo-complexes in solution. The formation of insoluble $\text{Fe}(\text{OH})_2$, which favours the coagula precipitation, can be written as:



and the overall reaction for the electrolytic process from the sequence of reactions (2.1 to 2.3) is:



Even though Fe(II) species can generate coagulates, the Fe(III) species are those that present higher charge density favouring even more the coagulation-flocculation process.



where protons can be neutralized with the OH^{-} produced in reaction or directly reduced to H_2 gas at the cathode by means of reaction (2.7):



All these species with different protecting charge and electrostatic attraction favour the coagulum formation/precipitation, in more or less extent, depending on the pollutant characteristics. However, among all the iron(III) species, $\text{Fe}(\text{OH})_3$ is considered to be the preferred coagulant agent and the main responsible specie for pollutant removal (Garcia-Segura *et al.*, 2017).

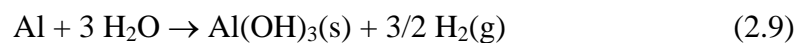
2.2.2 Aluminium anode

In the case of EC with Al, the anodic reaction (2.8) leads soluble Al^{3+} (Daneshvar *et al.*, 2007; Modirshahla, Behnajady and Kooshaiian, 2007) while the cathodic reaction produces hydroxide ion and H_2 gas by reaction.



Aluminium ions in the aqueous medium present a complex equilibrium with different monomeric species such as $\text{Al}(\text{OH})^{2+}$, $\text{Al}(\text{OH})_2^+$, $\text{Al}(\text{OH})_3$ and $\text{Al}(\text{OH})_4^-$ depending on the pH conditions (Figure 2.3) (Cotillas *et al.*, 2013).

Various polymeric species are formed by polymerization of monomeric species as $\text{Al}_2(\text{OH})_2^{4+}$, $\text{Al}_6(\text{OH})_{15}^{3+}$, $\text{Al}_7(\text{OH})_{17}^{4+}$, $\text{Al}_8(\text{OH})_{20}^{4+}$, $\text{Al}_{13}\text{O}_4(\text{OH})_{24}^{7+}$ and $\text{Al}_{13}(\text{OH})_{34}^{5+}$ (Duan and Gregory, 2003; Kobyas, Demirbas, *et al.*, 2006; Daneshvar *et al.*, 2007). However, the main responsible specie for the formation of the flocs is $\text{Al}(\text{OH})_3$, which is formed by complex precipitation mechanisms from the soluble monomeric and polymeric cations. Being the overall reaction (2.9) in the bulk:



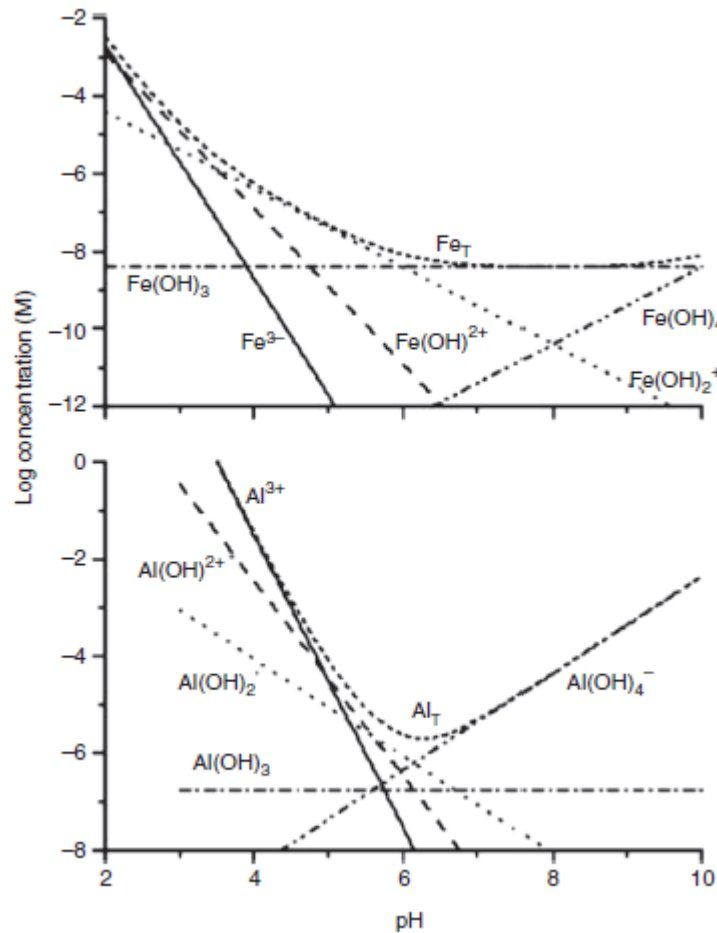


Figure 2-3: Concentrations of soluble monomeric hydrolysis products of Fe(III) and Al(III) in equilibrium with the amorphous hydroxides at zero ionic strength and 25°C (Vepsäläinen, 2012)

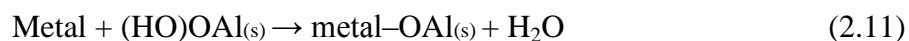
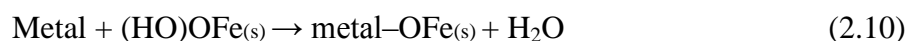
2.3 Pollutants removal mechanisms

The mechanisms involved in EC are not clearly understood yet (Mollah *et al.*, 2004), but during the last decade several researchers (Zaroual *et al.*, 2006; Moreno-Casillas *et al.*, 2007; Aoudj *et al.*, 2015) have tried to elaborate the mechanisms involved in coagulation. This subsection presents a brief overview to give an insight on the most important mechanisms considered during EC for removing pollutants from water. These are classified into two main groups:

2.3.1 Heavy metals removal

Heavy metals are mainly removed by EC by two mechanisms: (i) surface complexation and (ii) electrostatic attraction. Meanwhile, other mechanisms occur, such as (iii) adsorption and (iv) direct precipitation by the formation of the pollutant metal hydroxides.

The complexation mechanism considers that the heavy metal can act as a ligand to form a complex bond to the hydrous moiety of the coagulant floc (mainly $\text{Fe}(\text{OH})_3$ or $\text{Al}(\text{OH})_3$) yielding a surface complex. Subsequently, the formation of these complexes; superior aggregates are formed and the coagula precipitate, allowing the separation of the pollutants from the aqueous phase:



The second mechanism considers electrostatic attraction between the heavy metal pollutant and the coagulant floc. It is important to note that coagulation is not the only removal mechanism of heavy metals in EC but also electrochemical reduction of these species onto the cathode surface is also feasible, improving the removal efficiencies of these pollutants (Heidmann and Calmano, 2008a).

2.3.2 Organics removal

The different nature of organic pollutants, depending on their structures and functional groups, has an important influence on the mechanisms, involving their coagulation. The main mechanisms of organic pollutants are: complexation, charge neutralization, entrapment, adsorption and/or the combination of them (Jarvis, Jefferson and Parsons, 2004; Moreno-Casillas *et al.*, 2007).

The complexation mechanism occurs where the organic pollutant acts as a ligand and is coordinated to the metallic centre by their functional groups and precipitates within the coagulant floc. Also, the charge neutralization or destabilization is one of the most common mechanisms with organics (Garcia-Segura *et al.*, 2017).

The last mechanism is called adsorption, which presents similarities to entrapment approach but with a slight difference. While in entrapment the pollutant is physically dragged by the coagula; the pollutant presents physico-chemical interactions that favour its adsorption onto the coagulant species surface during adsorption approach.

The predominance of each mechanism is influenced by organic pollutant nature (charge, size, hydrophobicity, etc), the coagulant type and its dosage and pH (Matilainen, Vepsäläinen and Sillanpää, 2010).

2.4 Factors affecting electro coagulation

2.4.1 Effect of electrode material

The electrode material influences the performance, efficiency and cost of the process. In this frame, higher charge valence metal-ionic coagulants are preferred due to their greater electrical double-layer compression that enhances the pollutants coagulation. Typically, aluminum and iron electrodes are used because of the coagulating properties of multivalent ions (Pearse, 2003). Nevertheless, other feature is that aluminium and iron chloride salts are the most used coagulants and the most conventionally accepted in coagulation water-treatment (Verma, Dash and Bhunia, 2012). Besides, these materials are also preferred for their easily availability, their low cost and their high electro-dissolution rates.

2.4.2 Effect of pH

Different species are formed in equilibrium depending on the pH: the metal ionic species, the monomeric hydroxide complexes and the polymeric hydroxide complexes. Each one of them present different interactions with pollutants, giving different coagulation performances and consequently different removal mechanisms. The species in high alkaline conditions for aluminium and iron anodes are Al(OH)^{4-} and Fe(OH)^{4-} , respectively. These species present poor coagulation activity (Kim *et al.*, 2002). The coagulation is performed at slightly acidic conditions (Fe: 4-5 and Al: 5-6). pH conditions significantly vary the physiochemical properties of

coagulants, such as: (i) the solubility of metal hydroxides, (ii) the electrical conductivity of metal hydroxides and (iii) the size of colloidal particles of coagulant complexes (Vasudevan, Lakshmi and Sozhan, 2011; Ganesan *et al.*, 2013). Thus, neutral and alkaline media are preferred for coagulation.

2.4.3 Effect of current density and type

The applied current density (j) controls the electrochemical reactions that take place (Brillas and Martínez-Huitle, 2015; J.N. Hakizimana *et al.*, 2017) in solution (e.g.: electro-dissolution rate, gas evolution, electro-flotation, water reactions, etc. (Balla *et al.*, 2010) as well as their extension and kinetics. Consequently, the j defines (with the applied potential) the energy consumption associated to the operation of the electrochemical process.

Generally, direct current (DC) is more extensively used in EC (Vasudevan, Lakshmi and Sozhan, 2011). The passivation of the sacrificial anode increases the ohmic resistance (R), and consequently, the cell potential rises, increasing the operational costs, but the passivation decreases considerably the EC efficiency (Eyvaz *et al.*, 2009). Alternatively, the use of alternating current (AC) can be considered as the continuous changes of polarity avoid or reduce the formation of passivation layers and enlarge the operational life of the sacrificial anodes (Pi *et al.*, 2014).

2.4.4 Effect of supporting electrolyte

In electrochemical processes, the supporting electrolyte is required in solution that avoids migration effects and contributes to increase the solution conductivity, diminishing the ohmic drop and the energy consumption (J.N. Hakizimana *et al.*, 2017). Alternatively, the electrolyte has appreciable effects on the electro-dissolution kinetics of the sacrificial anodes and it can also influence the double layer shielding by the coagulants to form the flocs (Izquierdo *et al.*, 2010). Several studies on EC process with different supporting electrolytes (Yilmaz *et al.*, 2008; Aoudj *et al.*, 2010; W. L. Chou, Wang and Huang, 2010; Hu, Lo and Kuan, 2014; Thiam *et al.*, 2014) suggests the different influences are usually associated to the anion effects rather than cations (Trompette and Vergnes, 2009). Some authors have reported an appreciable affinity of

sulphate species to form complexes with aluminium (Huang, Chen and Yang, 2009) passivating the anodic surface.

2.4.5 Current density supply and time of treatment

Current density is regarded as an important factor because it influences the coagulant dosage rate, bubble formation rate, size, and development of flocs, as they affect the efficiency of the EC process. The anode dissolution rate is directly proportional to the current density. Coagulant concentration produced by electrolysis on anodes is typically directly proportional to the electric charge added per volume (coulombs per litre). The removal rate of pollutant is also a function of the electrolysis time. The pollutant removal efficiency increases with an increase in the electrolysis time (Naje *et al.*, 2017).

2.4.6 Effect of temperature

A high temperature when used with aluminium electrode causes a shrinkage of large pores of the $\text{Al}(\text{OH})_3$ gel, which causes the formation of dense flocs that are more likely to be deposited on the electrode surface. Increase in temperature and reduction of electrolysis time significantly improves the removal efficiency without difference in cost and energy consumption. In fact, due to the increase in temperature, the mass transfer increases, and the kinetics of particle collision improves. In addition, high temperature favors formation of large hydrogen bubbles, enhanced flotation speed, and reduction in the adhesion of suspended particles (Naje *et al.*, 2017).

2.4.7 Conductivity of the solution

In the electrolysis process, the contaminant elimination efficiency and working cost are direct functions of the solution conductivity. The conductivity of the solution helps the flow of the electric current through it. Salt additives, such as sodium chloride or sodium sulfate, are added to the solution before treatment for adjusting the pH (Naje *et al.*, 2017).

2.4.8 Effect of agitation speed

In the process of electro coagulation agitation helps to maintain uniform conditions and avoids the formation of the concentration gradient in the electrolysis cell. Further, the agitation in the electrolysis cell imparts velocity for the movement of the generated ions. With an increase in the agitation speed up to the optimum agitation speed, there is an increase in the pollutant removal efficiency. This happens because of early floc formation attributed to increase in the mobility of the generated ions. Further, the pollutant removal efficiency at a particular electrolysis time increases (Bayar, Yıldız, *et al.*, 2011; Naje *et al.*, 2017).

2.4.9 Inter-electrode gap

The space between the electrodes has a direct influence on the IR-drop that is minimized decreasing the distance between anode and cathode. However, lower removal efficiencies of the pollutants from water can be achieved when short distances between the electrodes are used because several phenomena can be affected (e.g.: coagulation, flocculation, precipitation, electro-flotation, etc.). These effects impact the flocs formation and their precipitation (Vázquez, Rodríguez and Lázaro, 2012), and avoids the formation of aggregates because of the high electrostatic effect that hinders the collision of particles (Modirshahla, Behnajady and Mohammadi-Aghdam, 2008). In contrast, an excessive distance between electrodes decreases significantly the formation of flocs (Ghosh, Medhi and Purkait, 2008; Ghosh, Solanki and Purkait, 2008).

2.4.10 Electrode arrangements

The connection mode of the electrodes in the EC cell affects not only the removal efficiency but also the energy consumption and the cost (Kobyas, Bayramoglu and Eyvaz, 2007; Kobyas *et al.*, 2011). The most typical arrangements (Kobyas, Hiz, *et al.*, 2006; Kobyas, Bayramoglu and Eyvaz, 2007; Modirshahla, Behnajady and Mohammadi-Aghdam, 2008; Sahu, Mazumdar and Chaudhari, 2014) are monopolar

electrodes in parallel connections (MP-P), monopolar electrodes in serial connections (MP-S) and bipolar electrodes in serial connections (BP-S).

In monopolar electrodes arrangement, each one of the electrode work as anode or cathode depending on its electrical polarity in the electrochemical cell. In the MP-P, each sacrificial anode is directly connected with other anode in the cell; using the same condition for cathodes. Meanwhile, in the MP-S configuration, each pair anode-cathode is internally connected but they are not connected with the outer electrodes.

In the case of the bipolar electrodes, each one of the electrodes, except the external ones, which are monopolar, present different polarity at each one of the electrode sides depending on the charge of the electrode in front of it. The connection of bipolar electrodes is always in serial mode.

It is noteworthy to mention that higher potential differences are required when a serial arrangement is used, but the same current is distributed between all electrodes. Conversely, in a parallel mode, the electric current is divided between the interconnected electrodes, as a function of their resistance, in the electrochemical reactor. The results of performance of these different electrode arrangements are not completely conclusive because the relative efficiencies strongly depend on operating parameters discussed previously as well as the water matrix and the nature of the pollutant (Kobyas, Hiz, *et al.*, 2006; Golder, Samanta and Ray, 2007a; Kobyas, Bayramoglu and Eyvaz, 2007; Ghosh, Solanki and Purkait, 2008; Sahu, Mazumdar and Chaudhari, 2014).

2.5 Electro coagulation reactors

The type of EC reactor not only influences the process performances but it also affects its operation and scale-up. The reactor most extensively used is the open batch cell with plate electrodes. The electrodes are submerged in the solution, and the effluent is conventionally stirred to be homogenized.

A variation of the cylindrical reactor was reported by Un and co-workers (Tezcan Un, Koparal and Bakir Ogutveren, 2013), where the anode is a cylindrical electrode but the cathode consists in a rotating impeller with two metallic blades to homogenize mechanically the solution and prevent the particles settling in the reactor during EC.

Other electrochemical reactor considerably used for EC is the typical filter press-cell, continuous reactors with rotating screw type electrodes. Other novel EC systems are the continuous reactors with rotating screw type electrodes. These have been used to treat cheese whey wastewater (Tezcan Un *et al.*, 2014) and groundwater (Hamdan and El-Naas, 2014). These cells are designed with a symmetrical section to favour uniform velocity distribution of the flowing liquid around a sacrificial anode rod with a helical cathode, and both electrodes are placed in the middle of the EC reactor (with or without rotation).

2.6 Design of the EC cell

To harness the maximum efficiency of an EC cell it becomes important to consider the following factors:

- The IR-drop between the electrodes must be minimized
- The accumulation of O₂ and H₂ gas bubble nucleates at the electrode surfaces need to be minimized
- Impairment to mass transfer through the spaces between the electrodes should be minimized

Further, the IR-drop depends on the following:

- The conductivity of the electrolyte solution;
- The distance between the two electrodes;
- The electrode geometry.

The overall voltage (U/V) is dependent on equilibrium potential difference, anode and cathode over potentials, mass transfer overvoltage, and ohmic potential drop in the solution. Alteration in analyte concentration occurs near the electrode surface because the electrode reaction causes concentration over potential, also called as mass transfer or diffusion over potential. This is attributable to the variation in the electro-active species concentration between the bulk solution and the electrode surface. This takes place if the electrochemical reaction is significantly fast to the inferior surface concentration of electro-active species below that of the bulk solution. The concentration over potential is negligibly less when reaction rate constant is much smaller than the mass transfer coefficient. The increase in masses of the metal ions

transported from the anode surface to the bulk of the solution reduces mass transport over potential. This mass transportation is achievable by increasing the turbulence of the electrolyte solution using some mechanical means (Khaled *et al.*, 2014; Lekhlif *et al.*, 2014).

2.7 Mass transfer measurement

One of the most significant constraints for design and operation of chemical reactors is the mass transfer coefficient. Coefficient of mass transfer mainly depends on fluid flow either under laminar or turbulent conditions. Mass transfer takes place from a range of high chemical potential to a range of low chemical potential, minimizing any difference within the system. To measure these coefficients experimentally, electrochemical method or limiting current method can be used. This technique has been widely used in evaluating solid-liquid mass transfer coefficients for a rough surface in complex flow regimes or chemical reaction systems. It is based on measurement of the maximum achievable current through an electrode for a particular electrochemical process. The limiting current technique can be used for various electrochemical reactors to analyze the effect of electrode configuration on mass transfer rates.

The accuracy of measuring the mass transfer coefficient is better than that obtained using other techniques such as dissolution method that depends on removal efficiency of pollutants to find the mass transfer coefficient. The most important advantages of limiting current methods include controllability of the driving forces and in situ current monitoring.

The technique of dimensional analysis can be used to study mass transfer phenomenon of EC process when using rotating electrodes. The application of this analysis to the description of mass transfer yields three non-dimensional groups, namely, the Reynolds (Re), Sherwood (Sh), and Schmidt numbers (Sc), respectively,

$$Sh = K_m d/D \quad (2.12)$$

$$Re = \rho N d^2 / \mu \quad (2.13)$$

$$Sc = \mu / \rho D \quad (2.14)$$

Where, d , D , N , ρ , and μ represent effective diameter (cm), diffusion coefficient (cm^2/s), rotational speed (rps), fluid density (g/cm^3), and fluid viscosity ($\text{g}/\text{cm}\cdot\text{s}$), respectively. However, no previous studies use rotating electrodes in the EC process. Accordingly, mass transfer data are correlated experimentally using the following dimensionless relationship, which is considered valid for a great variety of electrolytic reactor designs:

$$Sh = b Re^a Sc^{0.33} \quad (2.15)$$

Where, b is a mass transfer correlation constant and a is the exponent of Reynolds number. The values of these parameters can be obtained experimentally, or from differential equations. Such mass transfer correlations are useful for reactor design optimization, as well as for analysis of chemical kinetics. The development of these mass transfer correlations is crucial to understanding mass transfer processes (Khaled *et al.*, 2014; Lekhlif *et al.*, 2014; Naje *et al.*, 2015).

2.8 Residence Time Distribution (RTD)

The residence time distribution (RTD) of a reactor represents the characteristics of the mixing that occurs in a chemical reactor. It is projected for investigation of hydrodynamic flows in chemical apparatuses on the base of stimulus - response technique. The RTD gives insights on how long the various elements have been in the reactor, but it does not provide any information about the exchange of matter between the fluid elements. Its importance lies in the fact that it provides a quantitative measure of the degree of back-mixing within a system (Fogler, 1999b), thus provides accurate kinetic modelling of the system, and facilitates the reactor design to achieve a desired flow pattern more thorough comparison between systems with different configurations or different zones of the reactor could be achieved by RTD and it appears to be an important tool in successful process scale-up.

It provides the powerful tools and convenient interface for: initial processing of the experimental data, model creation of the flow in reactor by using the predefined flow

patterns as the building blocks, estimation of the flow model parameters, simulate the system for the response to the input signals of different types and creation of a user-defined flow patterns.

The residence time distribution analysis is a classical technique for predicting yields in isothermal, homogeneous reactors; and in some cases, the general concept of a reaction history distribution can be applied to heterogeneous or even non-isothermal reactors. The residence time distribution determines the yield of a first order reaction in a unique manner. The experimental determination of RTD is done by injecting an inert chemical, molecule, or atom, called a tracer, into the reactor at some time $t = 0$ and then the tracer concentration, C , is measured in the effluent stream as a function of time. The chosen tracer should be nonreactive, easily detectable, should have same physical properties to reactor liquid, and should be completely soluble in the mixture (Fogler, 1999a). The two used methods of injection are pulse input and step input. In a pulse input, a certain amount of tracer is injected into the reactor in very short time duration.

Capela et al. (2009) studied the hydrodynamic characteristics of a full-scale anaerobic contact reactor treating evaporator condensate from a sulphite pulp mill. The methodology applied was based on the RTD technique using lithium as a tracer (Capela *et al.*, 2009). Egedy et al. 2013 studied a compartment model structure based on the results of physical experiments performed in a stirred reactor. The most important aspect of this study is that a suitable structure identification algorithm was created, and tested (Egedy, Varga and Chován, 2013). Wang et al (2009), reported the flow profile and hydraulic conditions of Membrane Bioreactor (MBR) that predicts the performance of design was not evolved. The author used a concept of RTD to characterize the hydraulic conditions in MBR (Wang *et al.*, 2009). Jones et al (2008), studied the variations in CSTR feed geometry, impeller speed and inlet flow rate through RTD. The measured RTD was also used to characterize the degree of plug flow behaviour and short-circuiting (Jones, Özcan-Taşkin and Yianneskis, 2009). Qingfeng Yang et al (2007), used to diagnose the flow characteristics in spiral wound Reverse Osmosis (RO) modules by RTD techniques (Yang *et al.*, 2007). Lifeng Zhang et al (2007), studied the RTDs in a multistage agitated contactor (MAC)

for Newtonian fluids and presented a suitable Computational Fluid Dynamics (CFD) simulation (Zhang, Pan and Rempel, 2007).

2.9 Computational Fluid Dynamics (CFD)

Computational fluid dynamics (CFD) has become an inevitable tool for solving engineering problems. CFD simulates the details of how processes work and offers easier evaluation and optimization of the simulated system by providing a computational solution, even before building the prototypes. The CFD has become a convenient and useful method for engineering processes as it offers various features of simulation, such as low cost, short lead times, and satisfactory accuracy. The fluid flow (hydrodynamics) equipment design, CFD gives a better understanding and information for design. The analyses of flow comprise turbulence, chemical reactions, and/or heat and mass transfer, which limit and reduce design accuracy due to the three-dimensional nature of the problems. However, all three parameters are handled by CFD appropriately; it overcomes many of the limitations influencing traditional analysis.

Flow field variables like velocities, temperatures, or a mass concentration are considered in CFD. The three main elements of CFD codes are: (i) a pre-processor, (ii) a solver, and (iii) a post-processor (Thilakavathi *et al.*, 2012). Investigation of the flow pattern is required prior to simulation of mass transfer processes in chemical engineering. The fluid is defined as a continuum, and the major equations of fluid dynamics, the mass, momentum, and energy equations provide the cornerstone for CFD. These equations have significant commonalities so that a general variable can be used to describe the traditional form fluid flow equations, inclusive of scalar quantities such as temperature and concentration. This common governing equation is written in the following form:

$$\frac{\partial(\rho\phi)}{\partial t} + \nabla \cdot (\rho \mathbf{U} \phi) + \nabla \cdot D_{\phi}(\nabla\phi) + S_{\phi} \quad (2.16)$$

Where, the variable ϕ can be velocity along x, y, and z direction, U is temperature or mass fraction, ρ is the density of fluid, D_{ϕ} is the diffusion coefficient, and S_{ϕ} is the source term.

The governing equation if further simplified:

$$\nabla \cdot \mathbf{U} = 0 \quad (2.17)$$

$$\frac{\partial \mathbf{U}}{\partial t} + \nabla \cdot (\mathbf{U}\mathbf{U}) - \nabla \cdot \nu \nabla \mathbf{U} = -\frac{p}{\rho} \quad (2.18)$$

Where, \mathbf{U} is the velocity, ν is the kinematic viscosity, ρ is the density, and p is the pressure. For the case of mass transfer into the fluid bulk, the dimensionless concentration of species in solution, α , was modelled using a scalar transport equation with turbulent diffusivity contributions:

$$\frac{d\alpha}{dt} + \nabla \cdot (\mathbf{U} \alpha) - \nabla \cdot D_{turb} \nabla \alpha = 0 \quad (2.19)$$

where D_{turb} is the diffusion coefficient of species in turbulent liquid phase, consisting of the binary diffusivity, D_{AB} , and an enhancement factor dependent on the turbulent eddy viscosity, ν_{turb} , and a turbulent Schmidt number, Sc_{turb} :

$$D_{turb} = D_{AB} + \left(\frac{\nu_{turb}}{Sc_{turb}} \right) \quad (2.20)$$

The most common condition simulated in CFD is turbulent flow, which causes the formation of eddies in extensive choices of length and time scales. Electrodes are important for process and design as they affect the inner flow of the reactor, ultimately influencing the performance. Numerous researchers reported the influence of the hydrodynamic limitations on the performance of reactor such as turbulence intensity, velocity and vorticity distribution map for the fluid (Vegini *et al.*, 2008; Naje *et al.*, 2017).

CFD modelling has been used to describe fluid flow in three-dimensional electrochemical rotating cylinder reactor to show the influence of the counter electrode geometry. Four design configurations were explored by authors, wherein both size and number of counter electrodes were varied. It was observed that electrode arrangement and counter electrodes affect the streamlines of the flow. This generates high-velocity zones within the reactor, mainly at the surface of the electrode and at the bottom of the reactor (Enciso *et al.*, 2017).

It has been suggested that the standard K - ϵ model is suitable for predicting flows with low curvature, whereas as the curvature increases, the RNG K - ϵ model is more precise for capturing the turbulence fluctuation of swirl flows (Delgadillo and Rajamani 2005, Enciso et al. 2012).

2.10 Response Surface Methodology

Optimization in conventional multifactor experiments, optimization is generally carried out by varying a single factor while all other factors are fixed at a specific set of conditions. It consumes a lot of time and is also usually incapable of reaching the true optimum due to ignoring the interactions among variables. On the other hand, the RSM has been proposed to determine the influences of individual factors and their interactive influences. The RSM is important in designing, formulating, developing, and analyzing new scientific studying and products. It is also efficient in the improvement of existing studies and products. One important fact is whether the system contains a maximum or a minimum or a saddle point, this has resulted in increased use of RSM in the industry.

Bahadir Korbahti (2007) studied the electrochemical degradation of Levafix Blue CA, Levafix Red CA and Levafix Yellow CA reactive dyes in textile dye wastewater by using iron electrodes. RSM was used to optimize the effect of various operating parameters on COD removal, dye removal and turbidity removal (Körbahti, 2007).

Barbara Bianco et al (2011) studied the experimental factorial analysis on wastewaters samples taken from a real treatment plant in different periods, were used to construct a model response function to be applied in operative conditions. The modification of second-order model was done to include the initial COD as an independent variable in order to account for the wide range of initial COD in the treatment plant. The regression gave an excellent quantitative agreement between the predicted and measured values of COD for different experimental conditions. For the optimum condition, the removal of 80% COD was obtained (Bianco, De Michelis and Vegliò, 2011).

2.11 *Electro coagulation applications*

EC has been largely used on the wastewater treatment process to remove different pollutants that have been classified as follows: non-metallic inorganic species, heavy metals, organic pollutants and actual industrial effluents.

2.11.1 Non-metallic inorganic species

The human development and the extensive use of fertilizers and detergents have resulted in an increasing amount of non-metallic inorganic species in waters. Thus, there is a need to concentrate efforts to reduce the environmental impact of these pollutants. More than 80% of concentration removal has been achieved for ammonia, boron, cyanide, fluoride, nitrite, nitrate, phosphate, powdered activated carbon, silica particles, sulphide and sulphite when Al, Fe and SS electrodes were used. In the case of ammonia, the configuration of Al-SS electrodes favours the efficient elimination of this inorganic compound from wastewaters (Mahvi *et al.*, 2011), while that, Al-Al removed 80%. Meanwhile, the use of Fe-Fe electrodes did not achieve significant elimination of ammonia, obtaining up to 15% (Lin and Wu, 1996).

In several cases, the EC arrangement preferentially used was MP-P reactor. On the other hand, no significant differences were observed when supporting electrolyte was changed (Hanay *et al.*, 2003). In several cases, the EC arrangement preferentially used was MP-P reactor. Regarding the pH conditions, the efficacy of EC approach was improved when pH about 7.0 –8.0 was employed during boron removal (Bektaş *et al.*, 2004; Yilmaz *et al.*, 2005, 2008, Yilmaz, Boncukcuoğlu and Kocakerim, 2007a, 2007b; Vasudevan *et al.*, 2010; Subramanyan Vasudevan and Lakshmi, 2012; Vasudevan, Lakshmi and Sozhan, 2013; Isa *et al.*, 2014; Henry Ezechi *et al.*, 2015). Even when the nature of electrode was not noteworthy parameter for removing boron, the effective combination of Fe, Al or SS electrodes represents a substantial reduction on the electrolysis time, depending on the boron concentrations in the effluent. Other electrode combinations such as Mg-SS (Vasudevan *et al.*, 2010) and Zn-SS (Vasudevan, Lakshmi and Sozhan, 2013) were used, obtaining removal efficiencies

between 86.3% to 97.3%. The removal of various compounds using electro coagulation is given in Table 2-1.

Table 2-1: Removal of various compounds using electro coagulation

Compound	[C0] mg/L	Anode -cathode	Arrangement	Electrolyte	pH	j (mA/cm ²)	Removal %	Time (min)	Reference
Ammonia (NH ₄ ⁺)	50	Al-SS	MP-P	n.d.	7.0	16.7	99.0	60	(Mahvi <i>et al.</i> , 2011)
	20	Fe-Fe	MP-P	2000 mg/L NaCl	7.0	33	15.0	30	(Lin and Wu, 1996)
Boron (B)	24	Al-Al	MP-P	Real geothermal water	8.0	6.0	96.0	30	(Yilmaz <i>et al.</i> , 2008)
	2500	Al-Al	MP-P	0.1 g/L NaCl	8.0	20.0	90.0	50	(Bektaş <i>et al.</i> , 2004)
Cyanide (CN ⁻)	300	Fe-Fe Fe-Al Al-Al Al-Fe	MP	n.d.	11.5	15.0	87.0 93.0 35.0 32.0	20	(Moussavi, Majidi and Farzadkia, 2011)
Fluoride (F ⁻)	42	Al-Al Fe-Fe	MP-P	0.025 M Na ₂ SO ₄	3.0	5.0	87.0 56.7	90	(Aoudj <i>et al.</i> , 2015)
	20	Al-Al	MP-P	n.d.	7.0	10 AC 10 DC	93.0 91.5	60	(Vasudevan <i>et al.</i> , 2011)
Phosphate (PO ₄ ³⁻)	30	Al-Fe	MP-P	1.0 g/L NaCl real wastewater	5.0	10	96.0 93.0	15 60	(Kuokkanen <i>et al.</i> , 2015)
	83	Al-Al Fe-Fe	MP-P	500 mg/L Na ₂ SO ₄	9.0	3.0	100 100	30 120	(Lacasa <i>et al.</i> , 2011a)
Powdered Activated Carbon (C)	20	Al-Al	MP-P	n.d.	7.5	10.0	95.0	50	(Vu <i>et al.</i> , 2014)
Silica particles	70 NTU of turbidity	Fe-SS	MP-P	n.d.	9.5	1.4	95.0	60	(Den and Huang, 2005)
Sulphide (S ²⁻)	100 500	Fe-Fe	MP-P	30 mg/L Cl ⁻	7.0	32	99.0 65.0	15	(Murugananthan, Raju and Prabhakar, 2004)

Sulphite (SO ₃ ²⁻)	100 500	Fe-Fe	MP- P	30 mg/L Cl ⁻	7.0	62	85.0 46.2	15	(Muruganathan, Bhaskar Raju and Prabhakar, 2004)
Sulphate (SO ₄ ²⁻)	100 500	Fe-Fe	MP- P	30 mg/L Cl ⁻	7.0	62	71.3 30.0	15	(Muruganathan, Bhaskar Raju and Prabhakar, 2004)

2.11.2 Heavy Metals

Heavy metals are not biodegradable and are bio-accumulative affecting the whole food chain. As an important parameter, the combination of electrodes employed as well as the EC reactor influence significantly the removal efficiency achieved in some cases, such as arsenate, arsenite, cadmium, manganese and silver (R. Parga *et al.*, 2005; Rodriguez, Friedrich and Stopić, 2007; Jewel A.G. Gomes *et al.*, 2007; Heidmann and Calmano, 2008b; Pocięcha and Lestan, 2010; Shafaei *et al.*, 2010; Kumar and Goel, 2010; Lakshmanan, Clifford and Samanta, 2010; Vasudevan and Lakshmi, 2011; Vasudevan, Lakshmi and Sozhan, 2011; Wan *et al.*, 2011; Hanay and Hasar, 2011; Kobya *et al.*, 2011; Nuñez *et al.*, 2011; Al Aji, Yavuz and Kopal, 2012; Ganesan *et al.*, 2013; Hu, Lo and Kuan, 2014). The efficient elimination depends on the pH, current density and kind of the effluent due to the parallel reactions that are involved during the formation of complex or flocs with coagulant material. The removal efficiencies of various heavy metals are given in Table 2-2.

Table 2-2: Removal efficiency of heavy metals by using electro-coagulation

Compound	[C0] mg/L	Anode cathode	Arrangement	Electrolyte	pH	j(mA/cm ²)	Removal %	Time (min)	Reference
Antimony [Sb ³⁺]	28.6	Al-Al	BP-S	Mine water	2.0	22	96.5	60	(Zhu <i>et al.</i> , 2011)
Arsenite (III) [AsO ₃ ³⁻]	13.4	Fe-Fe Al-Al Fe-Al	MP-P	4 g/L NaCl	2.4	4.0 4.0 30 (AC)	99.6 97.8 99.6	60	(Jewel A G Gomes <i>et al.</i> , 2007)
Arsenate (V) [AsO ₄ ³⁻]	0.10	Fe-Fe MP-P	None	1 mg/L PO ₄ ³⁻ 5 mg/L SiO ₂	7.0	0.14	99.9	15 60 15	(Wan <i>et al.</i> , 2011)
	10	Fe-Fe Al-Al	MP-P	1000 mg/L NaCl	7.0	3.0	99.9 99.9	60	(Lacasa <i>et al.</i> , 2011b)

Cadmium [Cd ²⁺]	20	Zn-Zn	MP-P	n.d.	7.0	2.0 AC 2.0 DC	97.8 96.9	120	(Vasudevan and Lakshmi, 2011)
Caesium [Cs ⁺]	5 Mg-Zn	Al-Zn Zn-Zn Fe-Zn	MP-P	n.d.	6.8	0.8	96.8 92.4 90.6 90.0	80	(Kamaraj and Vasudevan, 2015)
Chromium (III) [Cr ⁺³]	1700	Fe-Fe	MP-P BP-S	1820 mg/L Cl [□]	3.4	10.8 4 32.5 2	81.5 99.9	50	(Golder, Samanta and Ray, 2007b)
Chromium (VI) [CrO ₄ ²⁻] [Cr ₂ O ₇ ²⁻]	50	Al-Al Fe-Fe	MP-P	0.025 M Na ₂ SO ₄	3.0	5.0	25.2 99.8	90	(Aoudj <i>et al.</i> , 2015)
Cobalt [Co ²⁺]	400 100 25	Al-Al	MP-P	NaCl	7.0	6.25	95.5 100 100	60 35 15	(Shafaei <i>et al.</i> , 2010)
Copper [Cu ²⁺]	250	Fe-Fe	MP-P	n.d.	5.5	25	98.0	40	(Al Aji, Yavuz and Kopalal, 2012)
Indium [In ³⁺]	20	Fe-Al Al-Fe Fe-Fe Al-Al	MP-P	100 mg/L NaCl	2.5	20 V	78.3 70.1 31.4 15.8	90	(Wang, Chou and Kuo, 2009)
Iron [Fe ²⁺]	25	Al-Al	MP-P	Tap water	7.5	0.4	99.2	35	(Ghosh, Solanki and Purkait, 2008)
	220	Al-Al	MP-P	n.d.	7.1	64	88.6	20	(Pociecha and Lestan, 2010)
Lead [Pb ²⁺]	300	Al-Al	MP-P	0.5 mol/L NaNO ₃	7.0	11.8 7.9 3.9	100 100 100	45 75 90	(Eiband <i>et al.</i> , 2014)
Manganese [Mn ²⁺]	2.0	Mg-Zn	MP-P	None 5 mg/L CO ₃ ²⁻ 5 mg/L PO ₄ ³⁻ 5 mg/L H ₂ AsO ₄ [□] 5 mg/L Silicate	7.0	0.5	97.2 72.8 64.7 54.6 82.4	100	(Ganesan <i>et al.</i> , 2013)
Mercury (II) [Hg ²⁺]	0.4	Fe-Fe Al-Al	MP-P	NaCl	7.0	25	99.9	15 25	(Nanseu-Njiki <i>et al.</i> , 2009)
Nickel [Ni ²⁺]	250 100 50	Al-Al	BP-S	1700 mg/L NaNO ₃	5.5	3.3	100 100 100	20 10 5	(Heidmann and Calmano, 2008b)
Silver [Ag ⁺]	50 20 10	Al-Al	BP-S	1700 mg/L NaNO ₃	5.5	3.3	66.0 60.0 90.0	50 30 30	(Heidmann and Calmano, 2008b)
Strontium	5	MgZn	MP-P	n.d.	6.8	0.8	97.0	80	(Kamaraj

[Sr ²⁺]		Fe-Zn Al-Zn Zn- Zn					95.2 91.4 89.6		and Vasudevan, 2015)
---------------------	--	-----------------------------	--	--	--	--	----------------------	--	----------------------------

2.11.3 Organic pollutants

During the last decade, organic pollutants have started to be considered of high concern and hazardous pollutants as it is stated in the UNESCO's World Water Report (World Water Assessment Programme, 2012). The several hazardous effects associated to organics pollution are toxicity, carcinogenic and mutagenic effects. Therefore, effluents must be pre-treated before their disposal as ineludibly environmental requirement (Sánchez-Bayo, 2006; Yu *et al.*, 2014). EC treatment could be considered an alternative to reduce the fate and the presence of these pollutants in water bodies.

Several comparative EC studies with Fe and Al anodes have been performed for synthetic dyes like Reactive Red 43 (Amani-Ghadim *et al.*, 2013) and Crystal Violet (Durango-Usuga *et al.*, 2010) dyes used in the textile industry. For these kinds of dyes, the use of Fe is advantageous compared to Al for colour removal. The superiority of Fe in most cases can be related to the reduction of dyes by Fe⁺² ions supplied to the medium, a fact that not takes place using Al since dyes are only removed by pure adsorption and coagulation (Patel, Ruparelia and Patel, 2011). However, the decay of the colour was significantly influenced by the anions in solution, for example, when 1.8 L of 50 mg/L of Reactive Red 43 in the presence of several common anions at neutral pH were treated employing Al-Al electrodes by applying 2.5 mA cm⁻² (Amani-Ghadim *et al.*, 2013).

In the case of pesticides, these organic pollutants were treated by peroxi-EC treatment (Boye, Brillas and Dieng, 2003; Boye, Dieng and Brillas, 2003; Brillas *et al.*, 2003). Fe-ADE arrangement of electrodes was mainly used in 0.05M of Na₂SO₄ with an addition of H₂O₂ to promote the electro-chemical reactions in the bulk of solution. Higher efficiencies (100%) of organic compound removal were achieved in all cases by applying lower current densities (10 mA cm⁻²) under acidic conditions (pH 3), in short times of EC treatment, approximately 40 min. However, DOC decays ranging from 35% to 66% at 40 min of treatment, for this reason, the EC was extended up to

120 or 360 min in many cases, obtaining more than 85% of DOC removal. MP-P reactor was frequently used, and the concentration of the pesticides varied from 186 to 270 mg/L.

2.11.4 Actual effluents

Different kind of wastewaters have been treated by EC approaches, obtaining several removal efficiencies in terms of an specific organic compound or in terms of colour, COD and DOC, such as almond industry (Valero *et al.*, 2011), baker's yeast wastewater (Kobyta and Delipinar, 2008; Gengec *et al.*, 2012), bilge water (Rincón and La Motta, 2014), biodiesel wastewater (Chavalparit and Ongwandee, 2009; Siles *et al.*, 2011), carwash wastewaters (Panizza and Cerisola, 2010), cheese whey wastewater (Tezcan Un *et al.*, 2014), chemical mechanical polishing (CMP) wastewater (Lai and Lin, 2003, 2004; Hu *et al.*, 2005; Drouiche *et al.*, 2007), cigarette industry wastewater (Bejankiwar, 2002), coal seam water (Millar *et al.*, 2014), cookies and pasta processing wastewater (Roa-Morales *et al.*, 2007), dairy effluents (Şengil and özacar, 2006; Tchamango *et al.*, 2010; Yavuz *et al.*, 2011), distillery effluent (Kannan, Karthikeyan and Tamilselvan, 2006; Kirzhner, Zimmels and Shraiber, 2008; Thakur, Srivastava and Mall, 2009; Krishna *et al.*, 2010; Davila, MacHuca and Marrianga, 2011; Khandegar and Saroha, 2012), domestic wastewater (Kurt *et al.*, 2008); dyebath effluent (Arslan-Alaton *et al.*, 2009), food-processing wastewater (Barrera-Díaz *et al.*, 2006), gelatin production effluent (Lakshmi Kruthika *et al.*, 2013), industrial wastewater (Meas *et al.*, 2010; Zodi *et al.*, 2010), landfill leachate (Bouhezila *et al.*, 2011; Li *et al.*, 2011; Top *et al.*, 2011; Orkun and Kuleyin, 2012; Ricordel and Djelal, 2014), laundry wastewater (Ge *et al.*, 2004; Wang, Chou and Kuo, 2009; Janpoor, Torabian and Khatibikamal, 2011), oily bilge water (Asselin, Drogui, Brar, *et al.*, 2008), olive oil mill wastewater (Inan *et al.*, 2004; Hanafi, Assobhei and Mountadar, 2010; Coskun *et al.*, 2012; Fajardo *et al.*, 2015), olive packaging industry (García-García *et al.*, 2011), paint manufacturing industry (Akyol, 2012), palm oil mill wastewater (Agustin, Sengpracha and Phutdhawong, 2008), paper industry black liquor (Zaied and Bellakhal, 2009), paper industry bleaching effluent (Sridhar *et al.*, 2011), paper mill effluents (Uğurlu *et al.*, 2008; Katal and Pahlavanzadeh, 2011; Zodi *et al.*, 2011), petrochemical wastewater (Dimoglo *et al.*,

2004), petroleum refinery sulfidic spent caustic wastes (Ben Hariz *et al.*, 2013), petroleum refinery wastewater (El-Naas *et al.*, 2009), plugboard wastewater (Zhao *et al.*, 2012), potato chips manufacturing (Koby, Hiz, *et al.*, 2006), pulp mill effluents (Vepsäläinen *et al.*, 2011), restaurant wastewater (Chen, Chen and Yue, 2000), slaughterhouse effluent (Bayramoglu *et al.*, 2006; Koby, Senturk and Bayramoglu, 2006; Asselin, Drogui, Benmoussa, *et al.*, 2008; Bayar, Yildiz, *et al.*, 2011), tannery effluent (Şengil, Kulaç and Özacar, 2009), textile effluent (S. H. Lin and Peng, 1994; Bayramoglu *et al.*, 2004; Can *et al.*, 2006; Bayramoglu, Eyvaz and Koby, 2007; Zodi *et al.*, 2009b), transport container wastewater (Kara, 2013), vegetable oil refinery wastewater (Tezcan Un, Koparal and Bakir Ogutveren, 2009), wet-spun acrylic fibres manufacturing wastewater (Gong *et al.*, 2014), yogurt industry wastewater (Tezcan Un and Ozel, 2013) and chemical-mechanical-planarization wastewater (Den and Huang, 2005).

Thus, EC can be effectively used for treating different type of waste waters. However necessary pre-and post-treatment may be applied along with EC.

CHAPTER 3

MATERIAL AND METHODS

This chapter deals with the description of materials and methods used for experimental and analytical investigations in the present thesis. A 3D rotating anode is used in an electrochemical reactor to improve the mixing regime with hopper bottom for sludge collections.

Tracer studies were conducted with 6.5 M NaCl solution and results were used to study residence time distribution. The results of RTD analysis were used to develop a model for CFD analysis. CFD analysis is carried out to investigate changes in mixing patterns due to the perforated cylindrical anode in stationary and rotating scenarios.

A series of experiments were carried out to verify advantages of improved mixing patterns due to the perforated 3D anode during electrochemical treatment (in both, stationary and rotating conditions). The experimental investigations were carried out on textile wastewater. For the sake of consistency, synthetic textile wastewater prepared in the laboratory was used.

The screening of significant operating parameters was done using Plackett-Burman (PB) design and the batch experiments were conducted in accordance. The series of experiments were designed using Box-Behnken (BB) design for continuous flow regime. The results were used for development of mathematical relation between operating parameters which was further used for optimization. The zeta potential analysis and pore size distribution analysis were conducted to understand the expected reaction mechanism in the reactor. Sludge characterization was used to evaluate its calorific value for possible use as fuel briquettes.

3. Analysis of flow pattern in reactor with perforated anode

3.1 The 3D rotating anode reactor

The conventional electrochemical reactors like plate electrode reactors etc. incur different design issues and many issues were encountered in these reactors. The issues

like short circuiting, development of dead zones, the formation of an oxide layer on anodesurface, etc. which hinders the performance of the reactor.

These issues lead to a further improvement of the technology to eliminate these problems. So, we have developed a unique reactor to solve these problems, leading to the development of a new advanced EC system.

An innovative electrochemical reactor for the EC treatment of waste water was designed. The reactor was made up of a perplex cylinder with hopper bottom in a cone shape to effectively collect and separate the sludge produced during electrochemical treatment. The inlet of water is through a pipe of 0.5 cm diameter above the hopper bottom and at the end of the cylinder as shown in the front view of the proposed reactor (Figure 3-1). A rotating three-dimensional cylindrical aluminum anode was developed to induce high turbulence even at low rotational speeds in the solution (Winnick, 1996). The anode was a cylinder with 40% perforations to induce turbulence and cathode was a long rod. This in turn reduces the soiling of the electrode, the formation of the oxide layer as the concentration polarization decreases, and hence reduces the passivation tendency of the anode which severely impairs the performance of the EC process. This also reduces the dissolution of the anode into the solution. In this light, it is expected that the use of a rotating 3D perforated cylindrical anode would improve the process of textile waste water treatment by electrochemical treatment by increasing the mass transfer of Al^{3+} from the surface of the anode to the solution to be treated (El-Ashtoukhy and Yasmine, 2014).

3.2 Geometric Specification of the reactor

A conical hopper bottom vessel used as a reactor with the 3D perforated rotating cylindrical impeller acting as an anode is shown schematically in Figure 3-1 - Figure 3-2. The total volume of the reactor was 4 litres with one inlet stream pipe and two outlet collection pipes to vary the volume of the reactor. Table 3-1 shows the dimension of 3D rotating anode reactor along with electrode dimensions. The connections in line with the reactor are shown in Figure 3-3. The DC power unit supplies negative current to the long rod making it cathode and positive to perforated cylinder making it anode. This was a hydrodynamic electrode system in which

electrode (anode) rotates during the electrolysis inducing a flux of analyte to the electrode. The 3D rotating cylindrical impeller was designed to facilitate better mixing during the electrolysis process. The additional advantage it would offer is prevention of oxide layer formation, which in turn would slow down the fouling of electrode. The surface of the electrode was kept perforated to further improve the mixing phenomenon for better yield of the process.

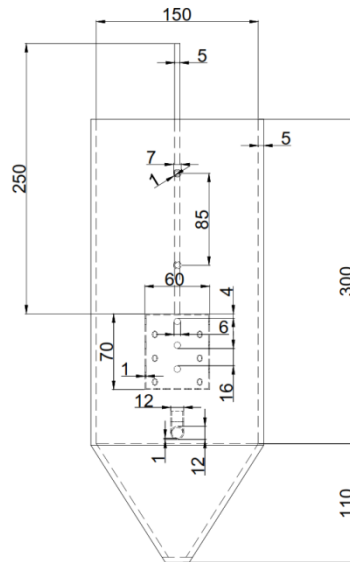


Figure 3-1: Front View of the Proposed Reactor.

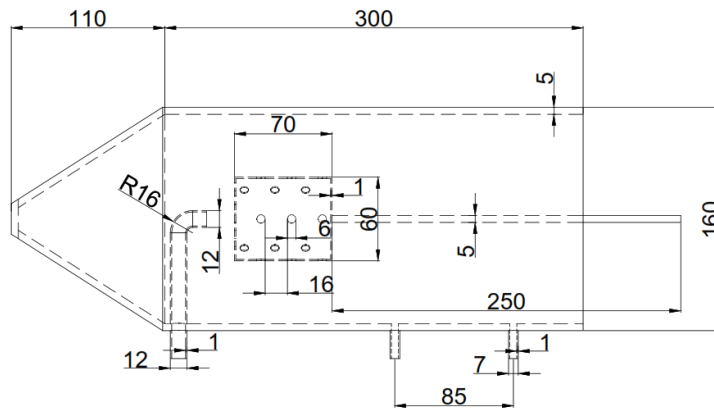


Figure 3-2: Side View of the Proposed Reactor.

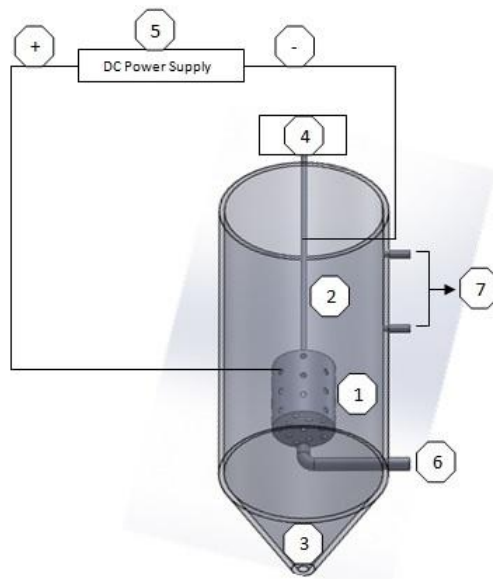


Figure 3-3: Geometry of Proposed Reactor. 1) 3D Aluminum perforated cylindrical anode. 2) Aluminum rod cathode. 3) Conical Hopper Bottom for Sludge collection. 4) Mechanical stirrer. 5) DC Power Supply Unit. 6) Inlet for Wastewater. 7) Outlet for Treated Water

Table 3-1: Dimensions of the Reactor Configuration with electrode

Reactor Volume	4.0 L
Diameter of the Cathode	1 cm
Inside diameter of the Anode	4 cm
Thickness of the Anode	0.5 cm
Area of the Anode	254.82 cm ²
Inlet and Outlet Diameter	0.5 cm

3.3 Performance of the 3D rotating anode reactor

Knowledge on Electrochemical Engineering is very essential for design and operation of electrochemical reactors. In general electrochemical reactors are classified based on electrode geometry and configuration. Different electrochemical reactors are used in chemical process industries for various applications; small scale electrode to large

scale commercial reactors. The behavior of a reactor treating wastewater has been studied using RTD (Residence time distribution) and simulated with CFD (Computational fluid dynamics).

3.3.1 Residence time distribution (RTD)

Experimental setup for RTD studies is given in Figure 3-4. Experiments were conducted for residence time distribution. For RTD studies, the 3D rotating anode was operated with water as electrolyte. A saturated solution (6.5 M Solution) of 10 ml NaCl was chosen as a tracer, the tracer concentration was measured through conductance meter at the outlet of the reactor. Time taken to inject the tracer was maintained less than 5 sec of mean residence time. Sampling was done using a grab sample method at definite time intervals of 30 seconds and 4 to 5 times the mean residence time to ensure consistency. The experiment ended when the electrical conductivity value decreased to the normal raw water conductivity levels.

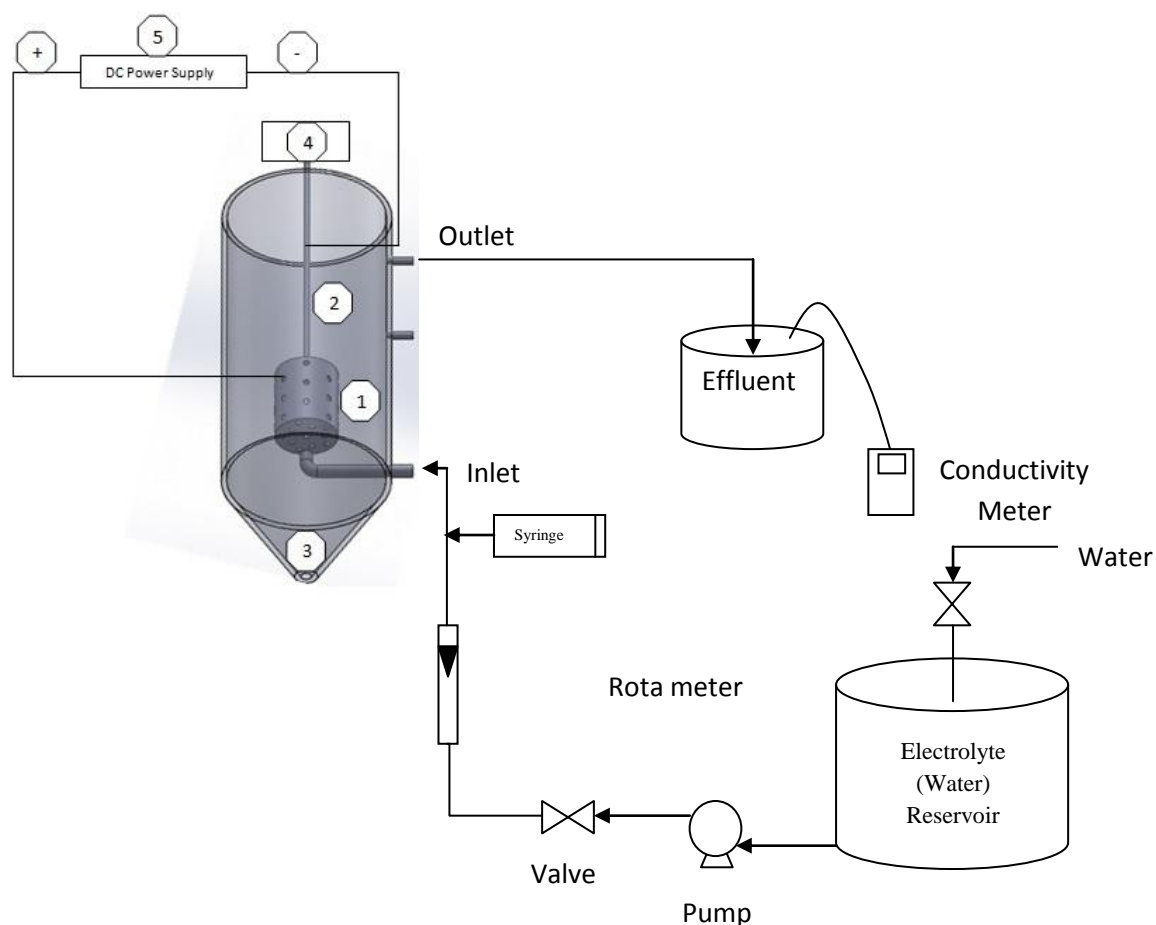


Figure 3-4: Experimental setup for RTD studies: 1) 3D Aluminum perforated

cylindrical anode. 2) Aluminum rod cathode. 3) Conical Hopper Bottom for Sludge collection. 4) Mechanical stirrer. 5) DC Power Supply Unit.

The RTDs are determined experimentally by classical tracer response technique. The $E(t)$ can be calculated from the following equation (Fogler, 2016):

$$E(t) = C(t) / \int_0^{\infty} C(t) dt \quad (3.1)$$

The relationship between hydraulic residence time (τ), peak time (τ_p) and mean residence time (τ_m) is assessed using RTD profiles. These can be calculated from following relations (Fogler, 2006a; Brannock *et al.*, 2009; Wang *et al.*, 2009):

$$PlugFlowIndex = \tau_p - \tau \quad (3.2)$$

$$DeadZoneIndex = \tau_m - \tau \quad (3.3)$$

$$ShortCircuitingIndex = 1 - (\tau_p - \tau_m) \quad (3.4)$$

The RTD was used to analyze the residence time of the tracer inside the reactor. This helps in calculating the dead zone index, plug flow index and short circuiting index using RTD.

RTD was used efficiently to characterize the non-ideal flow within the chemical reactors. For this, many type of models have been developed. The two most frequently used hydraulic models are the dispersion model and Tank-in-Series model. In this study, tank-in-series model has been used to describe the flow characteristics of the electrolyte in a 3D rotating anode. The total volume of the reactor was divided into three parts constituting total volume ($V = V_1 + V_2 + V_3$), where V_1 and V_3 are the volumes of annular space between the agitators and reactor wall and V_2 is the volume near the multistage agitated section around the 3D rotating anode. The model equations were compared with experimental $E(t)$ to explain the flow characteristics of the 3D rotating anode.

3.3.2 Computational fluid dynamics (CFD)

The enhancement of computational fluid dynamics (CFD) during the last few years drives the improvement and optimization of the chemical reactor design. It is used to evaluate complex reactors as it provides insight of the reactor dynamics. The degree of dispersion is mainly affected by flow behavior and mixing characteristics inside the reactor. The comparison and evaluation of experimental residence time distribution and simulated CFD model data provide better perception of geometrical complexities and flow behavior of the chemical reactor (Thilakavathi *et al.*, 2012; Jean Nepo Hakizimana *et al.*, 2017).

The modelling was performed using the code ANSYS 14.0, where Fluent™ is used to compute the governing equations of the fluid as well as the mass balance, momentum balance, and turbulence effect. The RTD experiments data was used to simulate the same tracer experiment in the CFD. This helps to compare and understand the variations in experimental and simulated results. The governing equations are the continuity and Navier-Stokes equations in three dimensions and thus require significant computational effort. The solution of these equations and the turbulence effect were performed with computational fluid dynamics (CFD).

A 3-Dimensional computational grid domain model for Rotating Cylindrical Anode has been generated in Ansys Meshing software with appropriate boundary conditions. The boundary conditions for the shaft and rotating cylinder has been considered as moving wall; the reactor and cathode wall were taken as a stationary wall with no slip.

Anode zone, shaped as a cylinder that acts as an impeller, is defined as Moving Reference Frame (MRF). The additional element was introduced because the impeller is not a revolving body in fluent. By using this method of defining a zone, we introduce a rotating reference frame, and the Navier-Stokes system has two additional terms: Coriolis acceleration and centripetal acceleration. K- Epsilon Turbulent model was used for all simulations with numerical discretization by Semi-implicit pressure-linked equation (SIMPLE) method.

The reactor domain was divided into two parts to generate a stable and independent mesh. The first section was the rotating anode and counter electrodes, and the second section was the tank where the electrolyte is present. The separation of the two sections allowed for the construction of a better mesh. An independent solution of the mesh was obtained, and the size of the mesh was changed until the solution did not vary for each reactor arrangement. Table 3-2 presents the number elements, nodes and skewness for each reactor. A good-quality mesh should have a skewness factor above 95%. In mesh *c*, the maximum skewness factor achieved was 98.25%. So, the mesh *c* was used.

Table 3-2: Mesh quality of the reactor

Reactor Type	Elements	Nodes	Skewness Factor
a	1,150,458	247,879	97.85%
b	9,63,578	129,687	94.14%
c	1,223,969	250,397	98.25%
d	9,57,867	131,478	95.26%

The result of RTD's helps in defining the boundary conditions for the CFD model. The system was defined as a static wall in the reactor and counter electrodes, and in the top of the reactor, the system was defined as a pressure outlet of 1 atm. The aluminum cylinder (anode) was defined as a moving reference frame wall spinning at different (0-100) rpm in contact with the electrolyte. An interface was defined at the boundary of the electrolyte and air. The definition of this interface was very important because this definition allows for a free flow of the fluid imposed by the rotating cylinder. The momentum was transferred between the interface, and the equations were solved for the air and electrolyte section.

3.4 Experimental Investigation on textile wastewater

3.4.1 Synthetic textile wastewater

The STW was synthetically prepared using azo-red dye as per the method reported in the literature using chemicals which are commonly found in the textile wastewater (Alinsafi *et al.*, 2005; Körbahti and Tanyolaç, 2008, 2009, Singh, Srivastava and Mall, 2013a, 2013c) as shown in Table 3-3. The desired concentration of dye solution was prepared by dilution of the stock solution with tap water.

Table 3-3: Composition of synthetic textile wastewater (STW)

S.No.	Chemical required	Amount	For 100 l
1.	Dye	0.3 g/l	30 g
2.	Sodium chloride	3 g/l	300 g
3.	Hydrolyzed starch	0.00556 g/l	0.56 g
4.	Ammonium sulfate	0.0174 g/l	1.174 g
5.	Disodium hydrogen phosphate	0.0174 g/l	1.174 g
6.	Liquid detergent	Few drops	Approx. 50 ml

3.4.2 Materials/Chemicals

All the chemicals used in this study were of analytical grade. The red azo dye was used for the preparation of synthetic textile wastewater (STW).

SM ultrapure reagent grade deionized water was used for the preparation of all analytical standards and for dilution of the samples. Tap water was used to prepare the synthetic textile wastewater (STW). The aluminum (Al) cylinder and rod used as electrode material were of 99.9% purity connected via mono polar connections.

3.4.3 Equipments

3.4.3.1 UV-visible spectrophotometer

Double beam UV visible spectrophotometer (Shimadzu UV 1800) designed on split-beam for multiple analyte analysis with an accuracy of 1 nm and resolution of 0.1 nm having multi wavelength scanning facility from 190-1100 nm was used for analysis of chemical oxygen demand (COD) by closed reflux method (American Public Health Association, American Water Works Association and Water Environment Federation, 1999). It was also used to analyze the color of the untreated and treated samples. The concentration of dye (λ_{\max}) was determined by measuring the absorbance of the unknown sample at wavelength and then comparing the value to the previous drawn calibration curve of absorbance versus known concentrations i.e. standard curve. The change in λ_{\max} determined by UV-visible spectral analysis during the treatment helped in determining the dye degradation mechanism.

3.4.3.2 DC Power Supply

The variable DC (direct current) power supply unit was used for the current distribution in the reactor configuration. The make and model of the power supply were Kusum-Meco (KM-PS-305D-II; 0-30 V/0-5 A Dual output).

3.4.3.3 Conductivity Meter

The conductivity of the solution after and before RTD experiments was analyzed using Lutron CD-4302 conductivity meter. The STW prepared was also checked for conductivity for smooth transfer of electrons with minimum resistance.

3.4.3.4 pH Meter

The pH of the solution was adjusted by adding 0.1 N NaOH or 0.1 N H₂SO₄, respectively. The pH of the solution was measured by Hanna pHep®5 - HI-98128 with a reading range of 0 – 14 pH with a least count of 0.01 pH.

3.4.3.5 Closed Reflux Digester

The samples for the measurement of chemical oxygen demand (COD) were digested using Hach DRB200 digital reactor for 2 hrs at the temperature of 150⁰C. The digestion was used to oxidize the trivalent chromium and quantify the remaining amount by measuring the absorbance at 600 nm using a spectrophotometer. The COD was measured by using closed reflux method (American Public Health Association, American Water Works Association and Water Environment Federation, 1999).

3.4.4 Experimental strategy during EC treatment of STW

3.4.4.1 Plackett-Burman (PB) design

Plackett-Burman (PB) design has been used for screening and evaluating the important variables that influence the response of a particular process (Montgomery, 2000, 2012; Tanyildizi, 2011; Singh, Srivastava and Mall, 2013a). A total (n) of six parameters (*anode rotation (n)*, *current density (j)*, *flow rate (q)*, *EC time (t)*, *initial pH (pH₀)*, *supporting electrolyte concentration (m)*) were investigated using PB design to identify the variables that significantly affect the COD and color removal efficiency. Each variable was responded at two levels, high and low, denoted by (+) and (-) signs respectively. Table 3-4 illustrates the factors under investigation as well as levels of each factor used in the experimental design. Table 3-5 shows the PB matrix used for EC treatment of STW.

Table 3-4: Levels and units of the factors used in Plackett-Burman design

Factors	Units	Level	
		Low (-)	High (+)
A. Anode Rotation	rpm	10	500
B. Current Density	mA/cm ²	1	20
C. Flow Rate	Lph	1	150
D. EC time	Min	10	120

E. Initial pH	-	2	10
F. Supporting electrolyte concentration	g/l	0	5

Table 3-5: Plackett-Burman matrix used for EC treatment of STW

Std. order	A	B	C	D	E	F
1	1	-1	1	-1	-1	-1
2	1	1	-1	1	-1	-1
3	-1	1	1	-1	1	-1
4	1	-1	1	1	-1	1
5	1	1	-1	1	1	-1
6	1	1	1	-1	1	1
7	-1	1	1	1	-1	1
8	-1	-1	1	1	1	-1
9	-1	-1	-1	1	1	1
10	1	-1	-1	-1	1	1
11	-1	1	-1	-1	-1	1
12	-1	-1	-1	-1	-1	-1

3.4.4.2 Path of steepest ascent/descent

The initial estimate of the optimum operating conditions for any system by PB design is far from the actual optimum. Therefore, variables that significantly influenced the desired responses were optimized by performing experiments as per steepest ascent/descent method (Montgomery, 2012). The PB design was used to screen out the variables (operating parameters with range) that significantly affect the COD and color removal efficiency. Then these operating parameters were used for the input in batch studies and Box-Behnken (BB) design to optimize the process performance.

3.4.4.3 Batch Studies

The batch studies were performed using the 3D rotating anode reactor to assess the effect of significant operating parameters screened out using PB design. The 3D rotating anode batch, batch recirculation and single pass system were compared. All EC experiments were conducted in the designed 3D rotating anode reactor in batch mode. The batch was run for 60 minutes, and after that the analysis of color, COD and

specific electrical energy consumption was done. The reaction time (t) was measured from the time when the power supply was switched on. The current density (j) was maintained constant during each experimental run. The cleaning of the electrode was not done to check the requirement of cleaning interval.

The performance of proposed configuration was evaluated in terms of color removal efficiency, COD removal efficiency, electrode consumption and energy consumption.

The color and COD removal efficiency (RE%) were calculated using the following equations:

$$\text{COD Removal Efficiency (\%)} = \frac{C_0 - C}{C_0} * 100 \quad (3.5)$$

Where; C_0 and C are the concentration of COD before and after treatment, respectively, in ppm or mg/L.

$$\text{Color Removal Efficiency (\%)} = \frac{A_0 - A}{A_0} * 100 \quad (3.6)$$

Where; A_0 and A are the absorbance of dye before and after treatment, respectively.

The theoretical amount of anodic dissolution (ELC_t) was calculated using Faraday's law (Ghosh, Solanki and Purkait, 2008; Singh, Srivastava and Mall, 2013b):

$$ELC_t = \frac{It_{EC}M_w}{Z_{FV}} \quad (3.7)$$

Where, ELC_t is the theoretical metal consumption (Kg/m^3), M_w is the molecular weight of the anode (g/mol) in the EC reactor, Z is the chemical equivalence, and F is the Faraday's constant (96485.3 C/mol). Actual or experimental amount of anodic dissolution (ELC_e) was calculated by weighing the anode before and after the experiment.

The specific electrical energy consumption per mg COD removed (E_{COD}) was

calculated as follows:

$$E_{cod} = V * I * \frac{t}{C_0 - C} * 60 \quad (3.8)$$

Where, V is voltage, I is current, t is time (usually taken as 60 min for specific energy consumption), C₀ and C are the initial and final COD concentrations.

3.4.4.4 Box-Behnken (BB) design of Response Surface Methodology (RSM) for the study of continuous flow regime

The response surface methodology (RSM) was used to determine the relationship between percentage of chemical oxygen demand removal and operating parameters such as current density, electrolyte flow rate, supporting electrolyte concentration and anode rotation speed along with specific electrical energy consumption and electrode consumption. Response surface methodology is a resourceful tool that is being used comprehensively in chemical process optimisation (Saravanathamizhan *et al.*, 2007; R Saravanathamizhan *et al.*, 2008; Montgomery, 2012; Palani and Balasubramanian, 2012).

Table 3-6 provides the operating parameters along with their ranges. The current density, electrolyte flow rate, supporting electrolyte concentration and anode rotation speed are referred to by uncoded variables as A, B, C and D respectively. A total of 27 experiments were conducted as per BB design (Table 3-7). All the experiments were performed in triplets and the average of removal efficiencies were used.

Table 3-6: Range of variables used in STW degradation

Factor	Variable	Unit	Range and Levels		
			-1	0	+1
A	Current Density	mA/cm ²	2	6	10
B	Flow Rate	LPH	5	60	120
C	Supporting Electrolyte Concentration	g/l	1	3	5
D	Anode Rotation Speed	RPM	0	60	100

The Box–Behnken experimental design of response surface methodology was being chosen to find the relationship between the response functions and variables using the statistical software tool Design Expert 7 trial version. The three-level second-order design requires a moderately lesser number of experimental data for specific prediction (Palani and Balasubramanian, 2012). A total number of 27 experiments with three centre points are carried out to investigate the percentage of COD removal with specific electrical energy consumption for the same. RSM is used to study the interaction between the variables and the analysis of variance (ANOVA). The value of R^2 determines the quality of the fit for this model.

Table 3-7: Box-Behnken (BB) matrix used for EC treatment of STW

Set No.	A: Current Density	B: Flow Rate	C: Supporting Electrolyte Concentration	D: Anode Rotation
	mA/cm²	lph	g/l	rpm
1	6	120	3	100
2	10	5	3	60
3	2	60	1	60
4	10	120	3	60
5	6	60	5	0
6	6	5	1	60
7	6	5	3	0
8	6	5	3	100
9	2	60	5	60
10	6	60	1	0
11	2	60	3	0
12	6	5	5	60
13	6	120	5	60
14	6	120	3	0

15	10	60	3	100
16	6	60	3	60
17	6	60	5	100
18	10	60	5	60
19	10	60	1	60
20	6	60	3	60
21	6	60	1	100
22	6	120	1	60
23	2	5	3	60
24	6	60	3	60
25	10	60	3	0
26	2	60	3	100
27	2	120	3	60

3.5 Microscopic Analysis Scattering Analysis

3.5.1 Zeta potential analysis

Dynamic light scattering (DLS) technique was employed for determining the zeta potential and particle size distribution (PSD) of colloids present in the solutions. Malvern Nano Zetasizer was used to measure the colloidal suspension stability during EC process using a non-invasive technique. Zeta potential measurements of the samples helped in understanding the role of the electrostatic interaction between aluminum species and the dye molecules.

3.6 Solid Residue Generation and Analysis

The mechanism of dye degradation and treatment efficiency were studied by various physicochemical analysis. The characterization of solid residues was performed using various techniques as described in the subsequent text.

In EC treatment with 3D rotating anode reactor, some amount of solid residues (scum and sludge) also get generated. Despite small amount these solid residues containing the electrode material as heavy metal needs to be disposed off in an environmentally friendly manner. The sludge generated during the EC experiments was collected after the experiment and dried in the oven for moisture removal.

3.6.1 Thermo-gravimetric analysis (TGA)

Thermo-gravimetric analysis of the generated solid residue has given the information regarding the potential use of sludge as a fuel in the boilers/incinerators for recovering energy. Thermal analysis of the solid residue was carried out by using a thermal analyzer (TA) instrument. Thermo gravimetric (TGA), differential thermo gravimetric (DTG) and the derivatives thermalanalysis (DTA) were carried out from the data and the plot obtained from the instrument (Perkin Elmer Pyris Diamond) having a flow rate of 200 ml/min in the temperature range from room temperature to 1000⁰C with heating rate of 10⁰C/min. Aluminum was used as the reference material. The continuous weight loss of a sample during TGA under oxidative (air or oxygen) and the inert gas atmosphere was a function of temperature (or time) and governed by the thermal event (volatilization) or chemical reaction (combustion).

3.6.2 Field emission scanning electron microscope (FE-SEM) and energy dispersive X-ray analysis (EDX)

Scanning electron microscope (SEM) is one of the most versatile and well known analytical techniques. Compared to the conventional optical microscope, an electron microscope offers advantages, including high magnification, large depth of focus, great resolution and ease of sample preparation and observation. Electrons generated from an electron gun enter a surface of a sample and generate many low energy secondary electrons. The intensity of these secondary electrons is governed by the surface topography of the sample. An image of the sample surface is therefore constructed by measuring secondary electron intensity as a function of the position of the scanning primary electron beam. EDX analysis is widely used for chemical

analysis. The characteristic X-rays emitted from the sample serve as fingerprints and give elemental information of the samples to know the external morphology of sludge and electrodes, SEM was used. SEM was performed using Nova Nano FE-SEM 450. It gives a resolution of 1:4 kV (TLD-SE) and 1 nm at 15 kV (TLD-SE). The samples were coated with Platinum to ensure conductivity. The SEM uses a focused beam of high-energy electrons to generate a variety of signals at the surface of solid specimens. The signals that derive from electron-sample interactions reveal information about the sample including external morphology (texture), chemical composition, crystalline structure and orientation of materials making up the sample. The FE-SEM is coupled to an EDX detector for measuring the elemental chemical composition. EDX analysis usually involves the generation of an Xray spectrum from the entire scan area of the SEM. The Y-axis shows the counts (number of X-rays received and processed by the detector) and the X-axis shows the energy level of those counts.

3.6.3 Powder X-ray diffraction (PXRD)

Powder X-ray diffraction (PXRD) analysis is based on constructive interference of monochromatic X-rays and a crystalline sample. The X-rays are generated by a cathode ray tube, filtered to produce monochromatic radiation, collimated to concentrate, and directed towards the sample. The interaction of the incident rays with the sample produces constructive interference (and a diffracted ray) when conditions satisfy Bragg's Law ($n\lambda = 2d \sin \theta$). This law relates the wavelength of electromagnetic radiation to the diffraction angle and the lattice spacing in a crystalline sample. These diffracted X-rays are then detected, processed and counted. By scanning the sample through a range of 2θ angles, all possible diffraction directions of the lattice should be attained due to the random orientation of the powdered material. Conversion of the diffraction peaks to d-spacings allows identification of the mineral because each mineral has a set of unique d-spacings. Typically, this is achieved by comparison of d-spacings with standard reference patterns. The composition of sludge produced after the EC process was analyzed by XRD technique. The XRD measurements were carried out by PAN analytical Xpert powder.

3.6.4 Surface area and pore size distribution analysis

Pore size distribution, porosity and pore surface area of solid samples, were determined using liquid nitrogen adsorption-desorption isotherms measured at a temperature of 77 K with Micromeritics apparatus. The surface and pore analysis of the solid sample was done to understand the solid structure and potential application of different phases of alumina present in the solid residue. Brunauer-Emmett-Teller (BET) (Barrett, Joyner and Halenda, 1951; Do, Herrera and Nicholson, 2011) surface area was calculated using the following equation:

$$\frac{p}{v(p_0-p)} = \frac{1}{v_m C} + \frac{(C-1)p}{v_m C p_0} \quad (3.9)$$

Where, p_0 is the saturated vapour pressure at (-200⁰C), v is the volume of gas adsorbed at the equilibrium pressure, and v_m is the liquefaction (Q_1) of nitrogen gas.

Pore size distribution analysis was done by using Barrett-Joyner-Halenda (BJH) method (Barrett, Joyner and Halenda, 1951; Singh, Srivastava and Mall, 2013a):

$$\ln\left(\frac{p}{p_0}\right) = -2\sigma v \cos\left(\frac{\theta}{r_k R}\right) \quad (3.10)$$

Where, σ is the surface tension, θ is the wetting angle, R is the gas constant and r_k is the Kelvin's radius. Before the analysis, the sample was degassed at 300⁰C for about 6 h. The surface area was obtained using BET model for adsorption data in a relative pressure range of 0.05 to 0.30. The total pore volume was calculated from the amount of N₂ vapor adsorbed at a relative pressure of 0.99.

CHAPTER 4

RTD & CFD ANALYSIS of 3D ROTATING ANODE REACTOR

This chapter deals with the residence time distribution studies and computational fluid dynamics of the 3D rotating anode reactor. The RTD and CFD were used to understand the hydrodynamics of the 3D rotating anode reactor. The fluid dynamics of the reactor in absence and presence of stationary 3D anode (also refereed as impeller in text) and with the rotation of 3D anode was studied.

The flow dynamics of the reactor changes significantly when the perforated 3D anode was introduced into the reactor. For all studied flow rates, the pressure profile shows 140 - 160% improvement in uniform pressure distribution inside the reactor due to the 3D anode. The velocity magnitude shows higher velocity zones created around the perforated 3D anode which indicates the turbulence caused by the introduction of the perforated 3D anode. The velocity vectors show the generation of two vector zones imparting the fluid inside and out of the perforated 3D anode causing more turbulence as compared to the case where the perforated 3D anode was absent. The presence of perforated 3D anode causes a reduction in mixing time, in the range of 18 to 44%. The tracer mass fraction curve indicates symmetrical shape in a case where the impeller was present as compared to when the impeller was absent. The short circuiting index also decreases with increase in flow rate when the impeller was present, and it was always less than the case where the impeller was absent. The flow regime tends to become plug flow when the impeller was present with an increase in flow rate. This shows that the introduction of impeller imparts more turbulence in the reactor which in turn provides better mixing and makes the flow regime plug flow.

The 3D rotating anode clearly affects the performance of the reactor and increases the mean residence time of the fluid inside the proposed reactor configuration. The CFD and RTD help to evaluate and simulate the performance and hydrodynamics of the reactor. The effective volume ratio increases with increasing rotation speed and found out to be best suited at flow rate of 60 lph with anode rotation speed set at 60 rpm. The short circuiting index was also found out to be minimum at these values. The 3D rotating anode acts as a turbulence enhancer for the configuration and in turn

increases the mass transfer inside the reactor. The passivation of the anode, dead volume, short circuiting was not present in the proposed configuration.

4. RTD and CFD Analysis

4.1 Residence Time Distribution (RTD) Model

RTD measurements were obtained with a wide range of operating conditions. The exit age distribution $E(t)$ can be calculated from tracer output using the standard equations. The experiments conducted to yield $C(t)$ curves in time t , which were normalized in $E(t)$ curves using:

$$E(t) = \frac{c(t)}{\int_0^{\infty} c(t)dt} \quad (4.1)$$

Where, τ_m represents the mean residence time, and the represents the variance of the $E(t)$ curves; they were computed using equations (4.2) and (4.3) respectively:

$$\tau_m = \int_0^{\infty} tE(t)dt \quad (4.2)$$

$$\sigma^2 = \int_0^{\infty} ((1 - \tau_m))^2 E(t)dt \quad (4.3)$$

In terms of dimensionless form, equations (4.1) - (4.3) can be represented as:

$$E(\theta) = \tau_m \cdot E(t) \quad (4.4)$$

$$\theta = \frac{t}{\tau_m} \quad (4.5)$$

$$\sigma_{\theta}^2 = \frac{\sigma^2}{\tau_m^2} \quad (4.6)$$

The hydraulic residence time is defined as the quotient of the streamed volume V and the volumetric flow rate Q;

$$\tau_m = V/Q \quad (4.7)$$

The dimensionless variance σ_{θ}^2 can be related to the dispersion number D/uL by the following equation

$$\sigma_{\theta}^2 = 2 \left(\frac{D}{UL} \right) - 2 \left(\frac{D}{UL} \right) \cdot \left(1 - e^{-\frac{UL}{D}} \right) \quad (4.8)$$

The dispersion number D/uL represents the mixing in axial direction of the flow. For an ideal plug flow system, the dispersion number tends to 0 and for a highly mixed system it tends to ∞ .

The electrolyte behaviour in a 3D RCE has been carried out in pulse tracer input using the tanks-in-series model cases. Experimental observation of the exit age distributions are given in Figure 4-1 to Figure 4-3 for three different flow rates and rotations speed. The exit age distribution E(t) was obtained from the exit concentration from the reactor. It was evident from the obtained RTD that as the flow rate increases with rotation speed, the curve attains symmetrical shape in lesser time indicating efficient mixing and less short circuiting. When the anode rotation is 0 i.e. stationary anode, the curve shows the mixing by eddies caused by the perforated anode. This confirms that the presence and rotation of the perforated anode improves the mixing, turbulent intensity, pressure, velocity profile and decreases the chances of short circuiting inside the reactor.

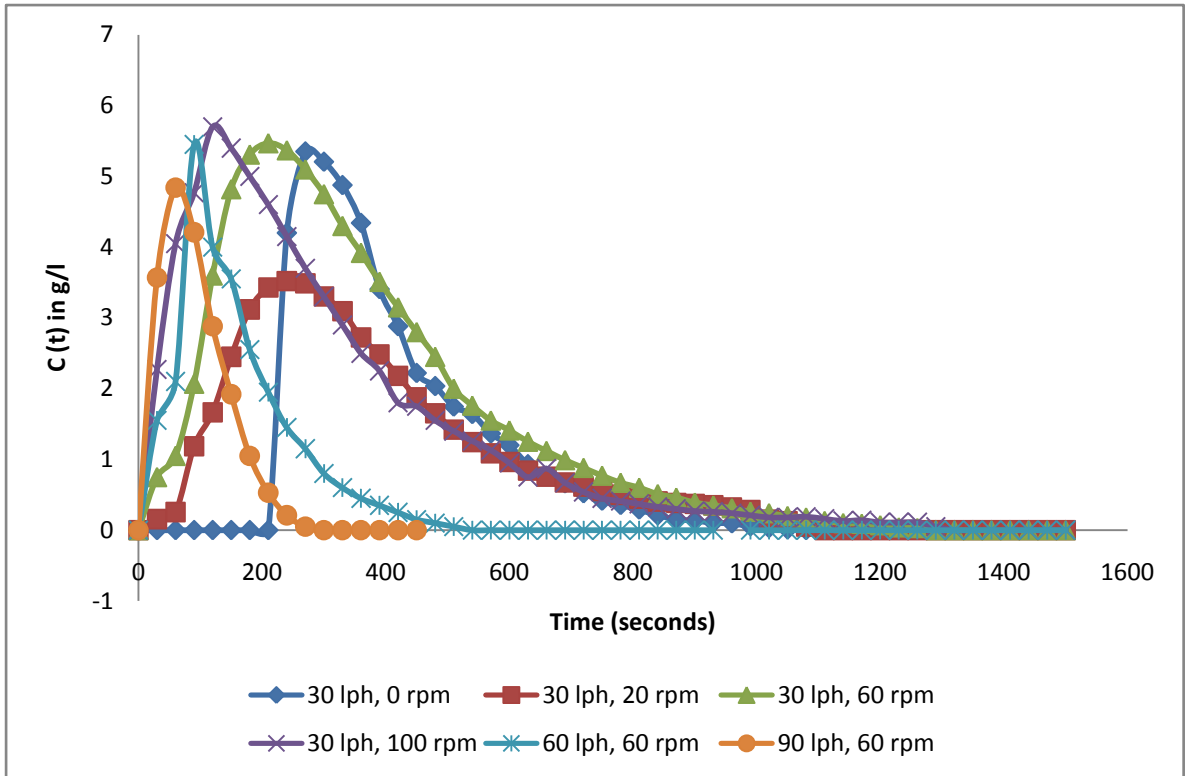


Figure 4-1: $C(t)$ vs time of RTD

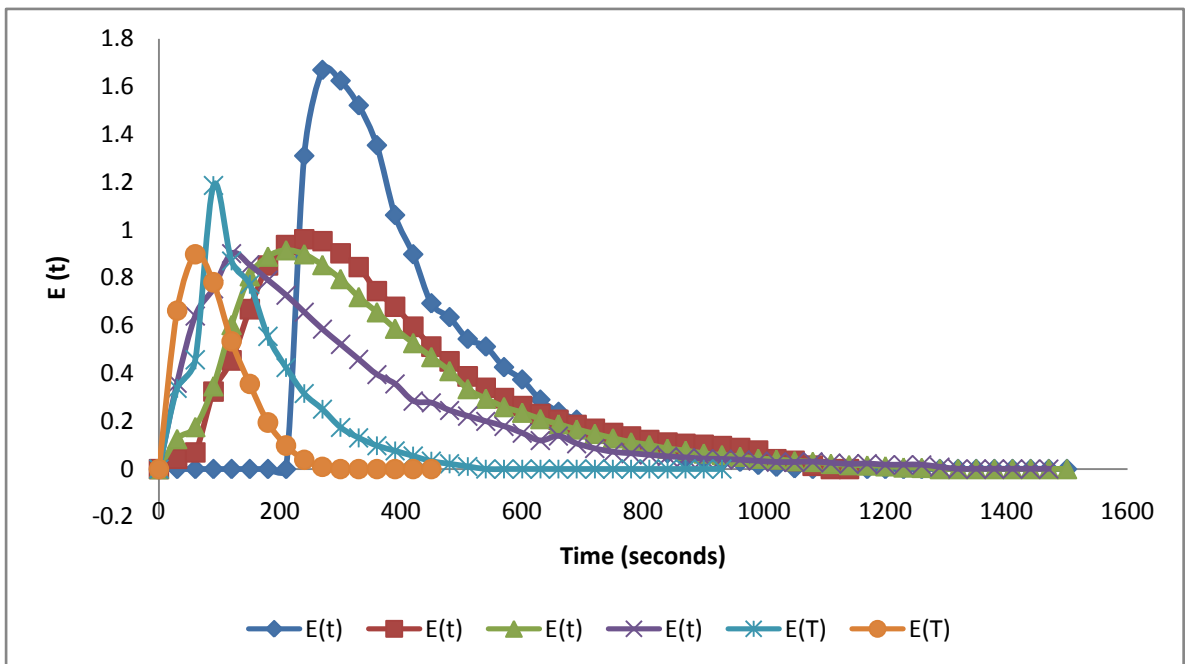


Figure 4-2: $E(t)$ vs time of RTD

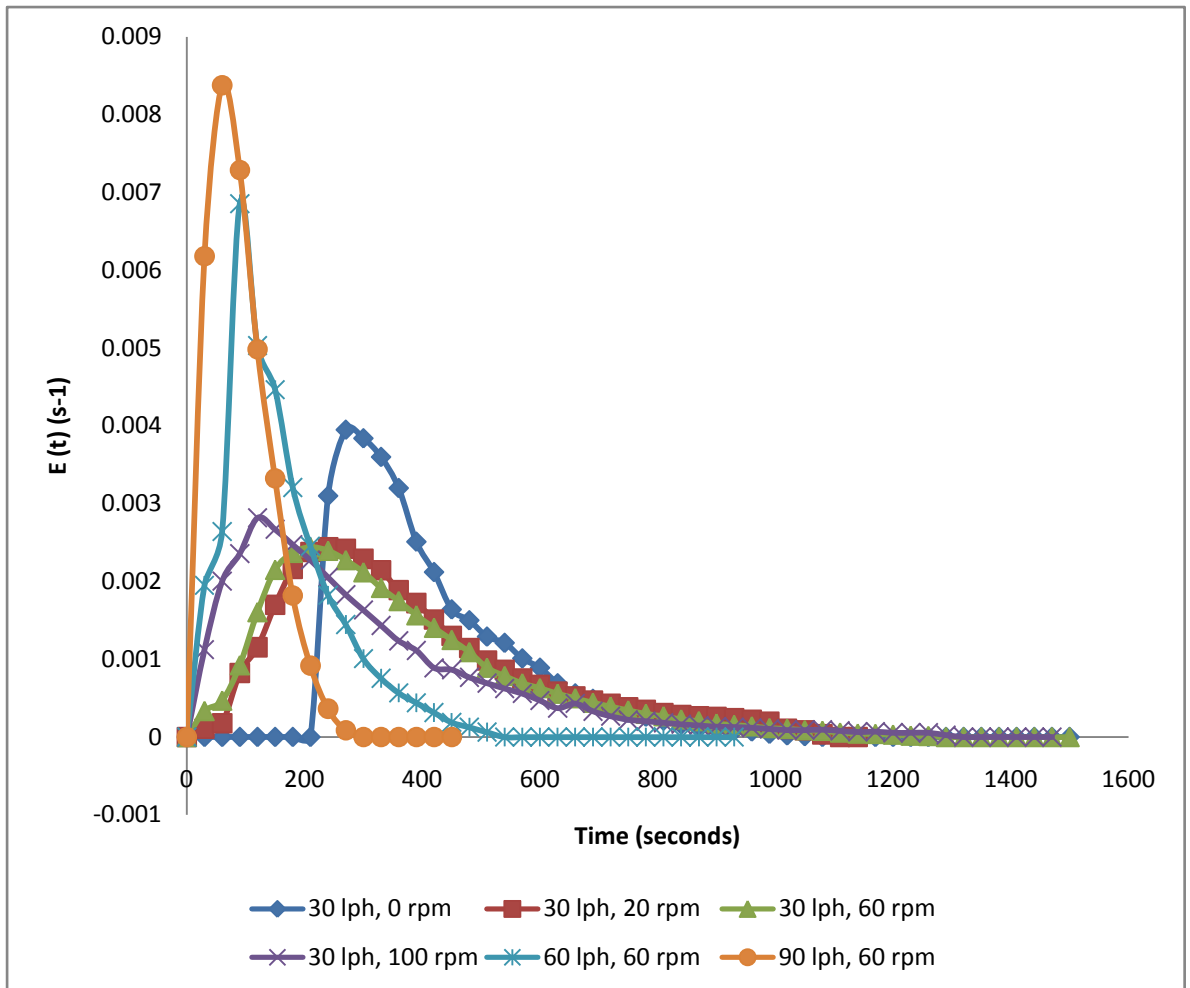


Figure 4-3: $E(t) (s^{-1})$ vs time of RTD

4.1.1 Effect of Flow Rate on Exit Age Distribution

Initially the perforated anode was kept stationary and the experiments were performed for various flow rates. The residence time of electrolyte decreases with flow rate. Dimensionless variance and dispersion increases to some extent with an increase in the flow rate. This observation may be due to the fact that the perforation of the anode inside the reactor promotes the spreading of the tracer at stationary condition. This trend is observed for all flow rates without applying rotation.

4.1.2 Effect of Rotation Speed on Exit Age Distribution

The phenomenon of back mixing significantly affects the performance of the reactor and can be described with the help of n or D/uL based on tank-in-series of equal volume model and by axial dispersion model. Back mixing is an important

parameter affecting the performance of any reactor and can be explained by parameters n or D/uL based on tank-in-series of equal volume and axial dispersion model. The dispersion numbers D/uL increases for the whole range of plug flow to mixed flow when the flow rate with anode rotation increases. This shows that the anode rotation increases the axial dispersion inside the reactor and decrease in short circuiting index. The phenomenon of back mixing was strong at lower flow rates and when the anode rotation increases, the value of n tends to move towards 1, resulting in a completely mixed system.

With an increase in rotation speed, the spread of residence time distribution increases as reflected in the values. Variance is increasing from 0.358 to 0.725, when the rotation speed increases from 0 to 100 rpm, confirms more back flow is created when go for the higher rotational speed (Palani, AbdulGani and Balasubramanian, 2017). Beyond 100 rpm of anode rotation speed facilitates an earlier occurrence of the RTD peaks and a broader distribution. If back mixing is to be contained then high rotation speed should not be employed. It can also be contained if inlet flow rate can be maintained. However, further increase in the anode rotation at constant inlet flow rate decreases the volumetric efficiency of the electrochemical reactor and this can be confirmed by the reduction of mean residence time (Ibrahim *et al.*, 2013b).

4.2 Comparison of RTD with Model

The RTD obtained was compared with the three models as unequal volume, equal volume and active center compartment model to effectively find out the suitable model for the present system (R. Saravanathamizhan, Paranthaman, Balasubramanian and Ahmed Basha, 2008; R. Saravanathamizhan, Paranthaman, Balasubramanian and Basha, 2008b).

4.2.1 Unequal Volume ($V_1 \neq V_2 \neq V_3$)

The model of unequal volume, was taken into consideration. It was ascertained that the simulated exit age distribution shows wide deviation from experimental observations. This shows that this model do not fit into the proposed system.

4.2.2 Equal Volume ($V_1=V_2=V_3$)

The simulated exit age distribution shows a much greater variation along the experimental observation. This deviation represents that the assumption of dividing the reactor into equal volume was not a realistic representation of the reactor.

4.2.3 Active Center Compartment Volume

The active center compartment model divides the reactor into 3 parts with the center part as active due to the presence of anode. Various ratios for the compartments were varied and the best fit was obtained. Model simulations were carried out by varying the center compartment volume as put forward by Saravanathamizhan model. From Table 4-1, we could observe the variation of reactor active volume with variation in anode rotation speed.

Table 4-1 : Variation of reactor active volumes (V_1, V_2)

SNo	N(rpm)	V ₁ (litre)	V ₂ (litre)
1	20	0.98	2.18
2	60	0.75	2.55
3	100	0.32	1.98

This shows that, as the anode rotation increases, the volume of center compartment increases and there was only marginal increase in volume of side compartment. And as the anode rotation speed increased from 20 rpm to 60 rpm, there was around 22.5% increment in the center compartment volume. The ratios that best fitted the reactor system were 1:2:1, 1:3:3:1 and 1:3:7:1 for 20, 60 and 1000 rpm respectively and in accordance with the Saravanathamizhan model.

4.3 *CFD Analysis*

Mixing is an important feature for continuous reactors. Good mixing improves the efficiency of heat and mass transfer. If the reactants are fed into the reactor premixed, the reaction can start from the entry of reactor itself. On the other hand, under non premixed conditions, reactants must first come in contact for reaction to occur. The mixing time depends on contact time. In general mixing can occur due to diffusion, pumping fluid in the reactor and also due to presence of mechanical agitator.

Diffusional mixing relies on concentration or temperature gradients within the fluid inside the reactor. This approach is common with micro reactors where the channel thicknesses are very small and heat can be transmitted to and from the heat transfer surface by conduction. In larger channels and for some types of reaction mixture (especially immiscible fluids), mixing by diffusion is not practically acceptable because of low rate of mixing.

In a continuous reactor, the product is continuously pumped through the reactor. This pump can also be used to promote mixing. If the fluid velocity is sufficiently high, turbulent flow conditions exist (which promotes mixing). The disadvantage with this approach is that it leads to long reactors with high pressure drops and high minimum flow rates. This is particularly true where the reaction is slow or the product has high viscosity. This problem can be reduced with the use of static mixers. Static mixers are baffles in the flow channel which are used to promote mixing. They are able to work with or without turbulent conditions. Static mixers can be effective but still require relatively long flow channels and generate relatively high pressure drops. The oscillatory baffled reactor is specialized form of static mixer where the direction of process flow is cycled. This permits static mixing with low net flow through the reactor. This has the benefit of allowing the reactor to be kept comparatively short.

In most cases, the continuous reactors use mechanical agitation for mixing (rather than the product transfer pump). Whilst this adds complexity to the reactor design, it offers significant advantages in terms of versatility and performance. With independent

agitation, efficient mixing can be maintained irrespective of product throughput. It also eliminates the need for long flow channels and high pressure drops.

4.3.1 Specification of Problem

The purpose of this work was to find out the tank Reynolds number, which accounts the inlet flow energy, sufficient for ideal mixing condition in case of stationary anode. It was also required to find out the minimum number of impeller (anode) rotation sufficient to reach ideal mixing in moving stirrer case. For ideal mixing of the liquid solely by the inlet energy, the following relations must be fulfilled (Burghardt and Lipowska, 1972).

$$R_e = \frac{4V^*\rho}{\pi D\mu} \geq 13.5 \quad (4.9)$$

Where R_e is the tank Reynolds number based on the tank diameter, and ρ and μ are the liquid density and viscosities respectively, V^* is the inlet volumetric flow rate.

4.3.2 Material and Flow Properties

The liquid used in present work was water. The properties of the solution are given in Table 4-2 and Table 4-3.

Table 4-2: Parameters used for non-moving/stationary case

Flow Rate (l/h)	Inlet Diameter (cm)	Density (Kg/m ³)	Viscosity (cP)	Velocity (m/s)	Reynolds Number	τ (min)	Flow
5	1	1000	1	0.017684	176.84	48.00	Laminar
15	1	1000	1	0.053052	530.52	16.00	Laminar
30	1	1000	1	0.1061	1061	8.00	Laminar
60	1	1000	1	0.21221	2122.1	4.00	Laminar

90	1	1000	1	0.31831	3183.1	2.67	Transient
120	1	1000	1	0.42441	4244.1	2.00	Turbulent

Where τ , is the time constant or holdup time of the reactor and is defined as

$$\tau = \frac{V}{V^*} \quad (4.10)$$

Table 4-3: Parameters used for moving impeller (anode) case

RPM	Impeller Diameter (cm)	Density (Kg/m³)	Viscosity (cP)	Reynolds Number	Flow
10	5.8	1000	1	33640	Turbulent
20	5.8	1000	1	67280	Turbulent
40	5.8	1000	1	134560	Turbulent
60	5.8	1000	1	201840	Turbulent
80	5.8	1000	1	269120	Turbulent
100	5.8	1000	1	336400	Turbulent
150	5.8	1000	1	504600	Turbulent
200	5.8	1000	1	672800	Turbulent
500	5.8	1000	1	1682000	Turbulent
1000	5.8	1000	1	3364000	Turbulent

4.4 CFD of 3D Stationary Anode

The effect of 3D stationary anode configuration was studied in this section. This mainly deals with the mixing pattern in absence and presence of the 3D stationary anode. The CFD model studies on pressure, velocity, magnitude, dead zone formation, short-circuiting etc. to validate the fluid dynamics of the proposed configuration.

4.4.1 Pressure Distribution

Pressure distribution profile of the reactor provides substantial information regarding the fluid dynamics behaviour in terms of pressure drop. The parts of the reactor where pressure drop was negative implies the low mixing zones created due to short circuiting/channelling or due to low inlet fluid velocity. Uniform pressure distribution resembles the proper mixing inside the reactor and reduces the chances of short circuiting/channelling.

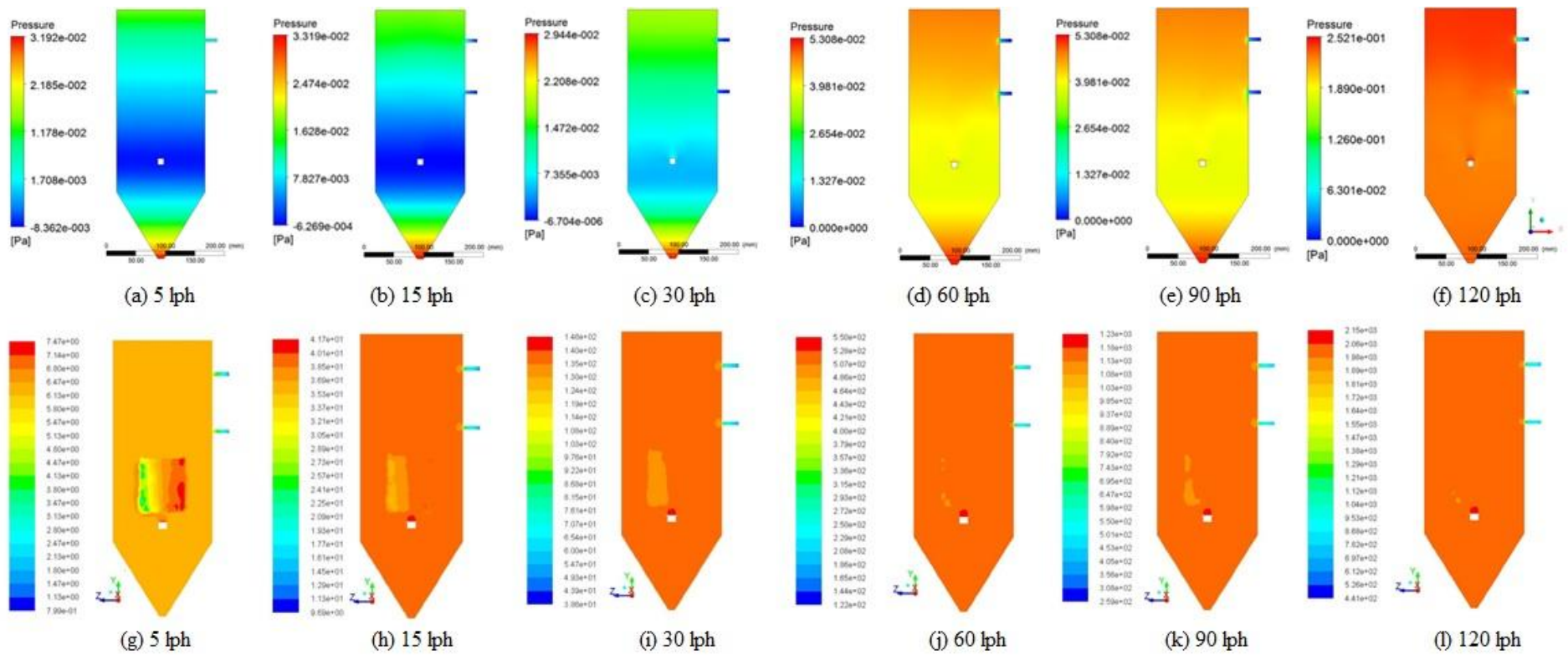


Figure 4-4: Pressure Contour for different flow rates in absence of impeller (a) 5 lph, (b) 15 lph, (c) 30 lph, (d) 60 lph, (e) 90 lph, and (f) 120 lph; and in presence of impeller (g) 5 lph, (h) 15 lph, (i) 30 lph, (j) 60 lph, (k) 90 lph, and (l) 120 lph.

The pressure contours for the flow rates of 5, 15, 30, 60, 90 and 120 lph in the absence and presence of impeller in the reactor are presented in Figure 4-4. For the flow rate of 5 lph, Figure 4-4 (a), the pressure was increasing towards the bottom of the reactor. There was a negative pressure zone created around the inlet which means that the pressure of this zone is less than the other parts of the reactor which imply that at low flow rate the fluid moves away from the inlet zone and creates a low-pressure contour. The bottom zone of the reactor indicates a slightly high pressure index than the other parts of the reactor. The pressure near the outlet shows mid pressure index implying releases of fluid through the outlet. For the same flow rate of 5 lph when the impeller is introduced inside the reactor, Figure 4-4 (g), the pressure profile changes significantly indicating better distribution of pressure all along the reactor. Different pressure contours were present around the impeller which indicates that the introduction of the impeller has significantly changed the dynamics of the reactor, as there is no low pressure zone present inside the reactor in this case. The reactor shows a uniform distribution of pressure zone from bottom to top of the reactor. The impeller in accordance with pressure index can be divided into right and left half as can be clearly seen in Figure 4-4 (g). The pressure index shows high pressure zones in the right part of the impeller and slightly low pressure zone on the left part of the impeller. This confirms the movement of fluid from right to left of the impeller.

As the flow rate is increased to 60 lph as shown in Figure 4-4 (d) the case where the impeller was absent, the pressure around the inlet was lower than the pressure along the other parts of the reactor. The pressure around the inlet was lower than the other parts due to the distribution of fluid along the reactor. So, with increased flow rate the pressure index also increases.

The pressure contours in the reactor for the same flow rate when the impeller was present are indicated in Figure 4-4 (j). It can be seen that the pressure increases throughout the reactor except for few zones on the left side of the impeller. The highest pressure zone was present around the inlet of the reactor.

The pressure contours for increased flow rate of 120 lph are shown in Figure 4-4 (f) in the absence of impeller. The difference in pressure between high and low pressure

zone was less than compared to previous two cases. A comparatively higher pressure zone was visible near outlets indicating movement of fluid towards this part.

The pressure contours in the reactor for the same flow rate when the impeller was present are indicated in Figure 4-4 (l). The pressure was uniform throughout the reactor. There was no low pressure zone, and a uniform distribution of pressure implies around 160% improvement in pressure profile as compared to the same flow rate in the absence of impeller.

It is clear that for all flow rates the presence of impeller has significantly changed the pressure distribution inside the reactor.

4.4.2 Velocity Vector and Magnitude Contour

The fluid velocity vector is one of the most important variables in fluid dynamics. The velocity magnitude and vector study gives us the insight of movement of fluid in the reactor. The magnitude provides the rate at which dispersion of fluid occurs in the reactor. The vector provides the direction of flow.

Several researchers have used ε - κ turbulence model for quantitative assessment of radial and tangential velocity. The present model is also developed on similar lines (Fimbres-Weihs and Wiley, 2010; Singh, Fletcher and Nijdam, 2011).

The velocity vector and magnitude contours for the flow rates of 5, 15, 30, 60, 90 and 120 lph in the absence and presence of impeller in the reactor are presented in Figure 4-5.

For the flow rate of 5 lph, Figure 4-5 (a), the velocity magnitude diminishes as we move away from the inlet. The distribution of fluid was facilitated by the inlet velocity at which it enters. The velocity vector shows a non-uniform behaviour escaping towards the bottom of the reactor.

The velocity magnitudes for the same flow rate when the impeller was present are indicated in Figure 4-5 (g). The velocity magnitude in the reactor was uniform, and

around the impeller, it was changing. It shows the movement of fluid through the impeller which confirms the distribution of fluid due to turbulence caused by the impeller. The velocity vector distribution of fluid inside the reactor was uniform, and the movement was upward as presented in Figure 4-5 (m). There was a swirl movement below the impeller from left to right side of the impeller which indicates the turbulence caused by the impeller in the reactor.

For the flow rate of 60 lph, Figure 4-5 (d), the velocity magnitude increases. The magnitude around the inlet and outlets were more than the other parts of the reactor. The velocity vector shows a uniform distribution making it like a waterfall towards the left and right side of the inlet.

The velocity magnitudes for the same flow rate when the impeller was present are indicated in Figure 4-5 (j). The velocity magnitude at the base of the impeller was more than the other parts. There was a uniform distribution of magnitude throughout the reactor. The velocity vector profile was presented in Figure 4-5 (p). It shows the formation of zones around the impeller which indicates the turbulence caused by the impeller. The bottom hopper zone was also divided into two vector zones imparting the fluid directly inside the impeller.

For the flow rate of 120 lph, Figure 4-5 (f), the velocity magnitude increases with increase in the flow rate. The highest magnitude can be seen around the outlets. The vector distribution follows a similar pattern as it was for 60 lph, but the intensity was low due to the reduction in mean residence time at higher flow rate.

The velocity magnitudes for the same flow rate when the impeller was present are indicated in Figure 4-5 (l). The magnitude distribution is similar to 60 lph when the impeller was present. This shows that when the flow rate was increased the magnitude changes only around the impeller and outlets. Figure 4-5 (r) indicates the velocity vector profile for 120 lph. It shows more turbulence than the 60 lph flow rate, but the distribution was in a similar fashion. The fluid moves inside out along the impeller with inlet flow rate which provides better distribution of fluid in the reactor.

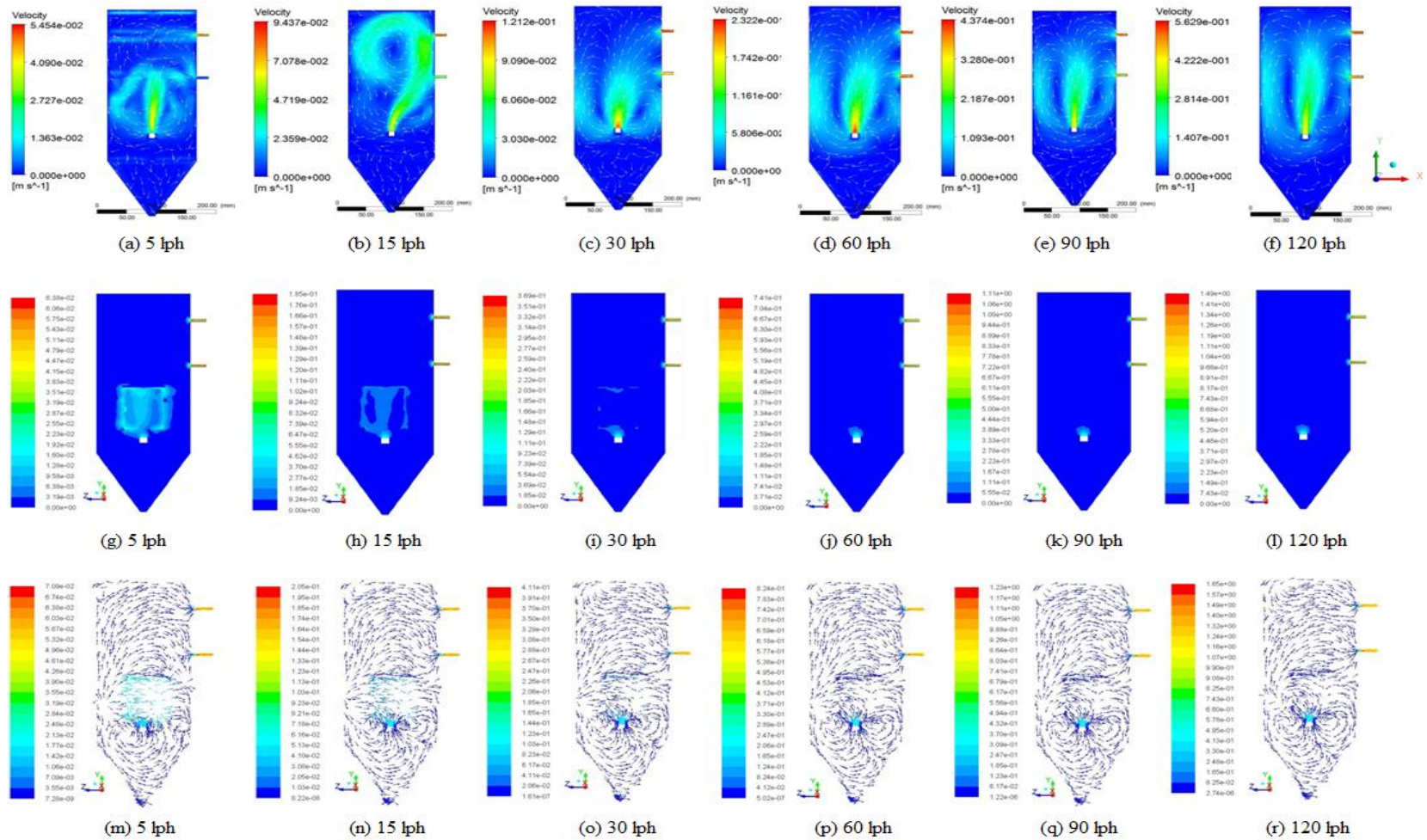


Figure 4-5: Velocity Vector and Magnitude Contour for different flow rates in absence of impeller (a) 5 lph, (b) 15 lph, (c) 30 lph, (d) 60 lph, (e) 90 lph, and (f) 120 lph; and in presence of impeller (g,m) 5 lph, (h,n) 15 lph, (i,o) 30 lph, (j,p) 60 lph, (k,q) 90 lph, and (l,r) 120 lph.

4.4.3 Turbulent Intensity

The turbulent intensity in presence and absence of impeller for different flow rates is shown in Table 4-4. The mean turbulent intensity was higher in the presence of impeller which indicates the significance of impeller. The turbulence was only caused by the inlet flow rate when the impeller was absent in the reactor. As the impeller was introduced, the turbulent intensity increases with increase in flow rate. This signifies that the impeller was imparting turbulence inside the reactor which is also presented and confirmed by the velocity vector profile.

Table 4-4: Mean Turbulent Intensity in absence and presence of impeller for different flow rates

Flow Rate (lph) ⇒	5	15	30	60	90	120
Turbulent Intensity (In absence of Impeller)	0.007	0.010	0.011	0.013	0.015	0.017
Turbulent Intensity (In presence of Impeller)	0.775	0.916	1.232	1.405	1.765	1.967

4.4.4 Normalized Mixing Time

The normalized mixing time was always found higher in the absence of impeller. When the flow rate increases, the normalized mixing time decreases in both cases. At the same flow rate of 5, 60 and 120 lph, the normalized mixing time was lower in about 18.75%, 35.71%, and 44.11% when compared to the case in which impeller is absent as shown in Figure 4-6. This signifies that the mixing time also improved when the impeller was introduced at same flow rates in the reactor. Hence enhancing the mass transfer inside the reactor and thus improving its efficiency.

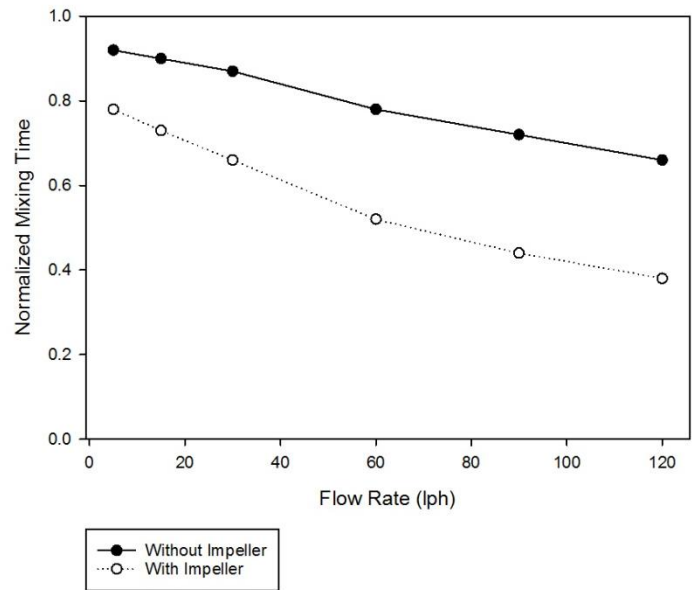
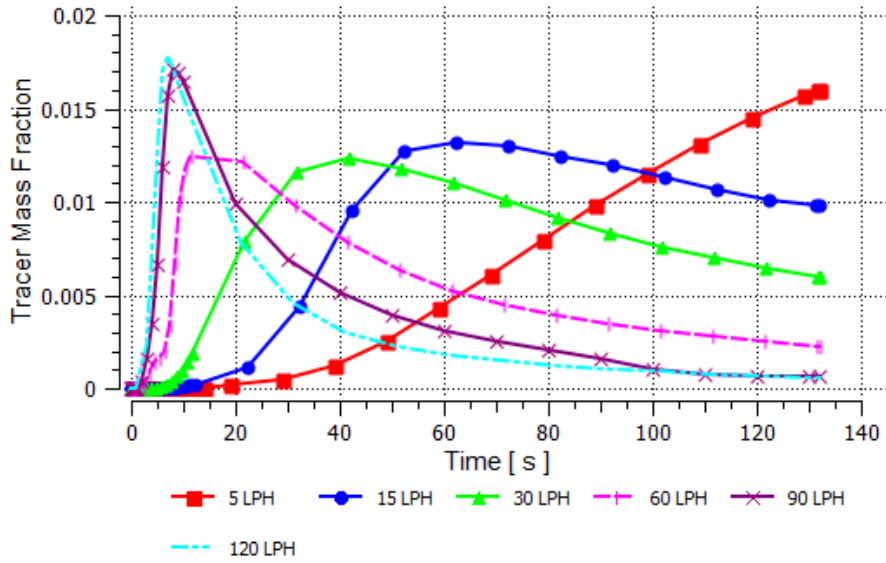


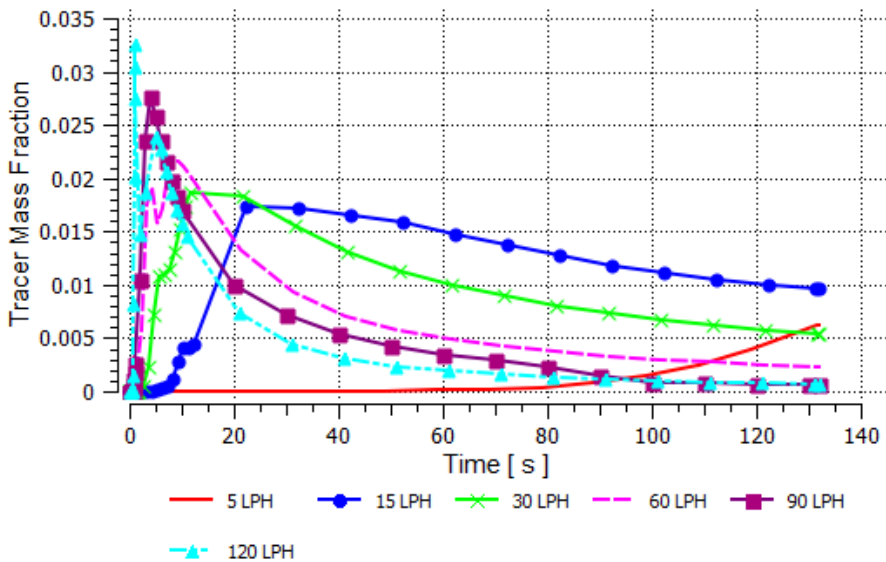
Figure 4-6: Normalized Mixing Time in absence and presence of Impeller

4.4.5 Tracer Mass Fraction

As shown in Figure 4-7 (a), the case where the impeller was absent. The tracer mass fraction shows a delayed peak point for low flow rates of 5, 15 and 30 lph. The peak points were visible with increasing flow rates. The early peak points implies the mixing due to inlet flow rate. The non-symmetrical curve in Figure 4-7 (a) indicates the presence of short circuiting along the length of the reactor.



(a)



(b)

Figure 4-7: Tracer Mass Fraction at different flow rates (a) in the absence of Impeller
(b) in the presence of Impeller

As shown in Figure 4-7 (b), the case where the impeller was present. The mean tracer mass fraction increases at similar flow rates as compared with the case where the impeller was absent. The symmetrical curve can be seen in Figure 4-7 (b) which indicates better mixing inside and along the length of the reactor. The higher flow

rates in the presence of impeller provide the better mixing efficiency which was also verified by the mean turbulent intensity. At the flow rates of 60 – 120 lph, the curve attains a symmetrical shape in lesser time which confirms the absence of short circuiting along the reactor. This confirms that the presence of impeller improves the mixing, turbulent intensity, pressure, velocity profile and decreases the chances of short circuiting inside the reactor.

4.4.6 Plug Flow Index

As depicted in Figure 4-8, the plug flow index increases with increase in flow rate for both the cases in absence and presence of impeller. The plug flow index for a given flow rate was always higher and short circuiting index was lower in the presence of impeller. This confirms that the impeller increases the turbulence and better mixing inside the reactor. It tends the flow regime towards the ideal plug flow which was better than then the case where the impeller is absent.

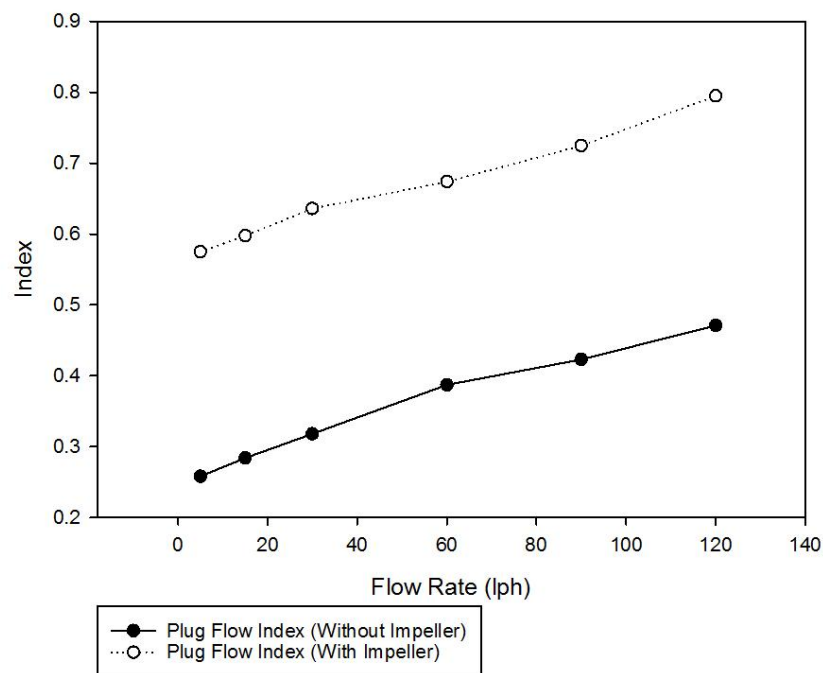


Figure 4-8: Plug flow Index in absence and presence of impeller for different flow rates

4.4.7 Short Circuiting Indexes

Short circuiting is a perplexing phenomenon as it largely affects the performance of the reactor and also hinders the successful design of a novel reactor (Persson, 2000). This in turn results in formation of dead zones and to reduce reactor functions (Dierberg *et al.*, 2002, 2005; Tchobanoglous *et al.*, 2003). This is that one key factor which results into poor hydraulic efficiency of the reactor (Singh *et al.*, 2009; Xanthos *et al.*, 2011; Tsai, Ramaraj and Chen, 2012).

As the plug flow index increases, the short-circuiting index decreases. For the flow rate of 5, 60 and 120 lph; the short-circuiting index falls by 25.69%, 32.51%, and 35.16% respectively as compared to the case when the impeller was absent as depicted in Figure 4-9. This clearly shows that presence of impeller effectively controls the short-circuiting phenomenon in the reactor. Moreover, impeller helps to establish the plug flow regime in the reactor.

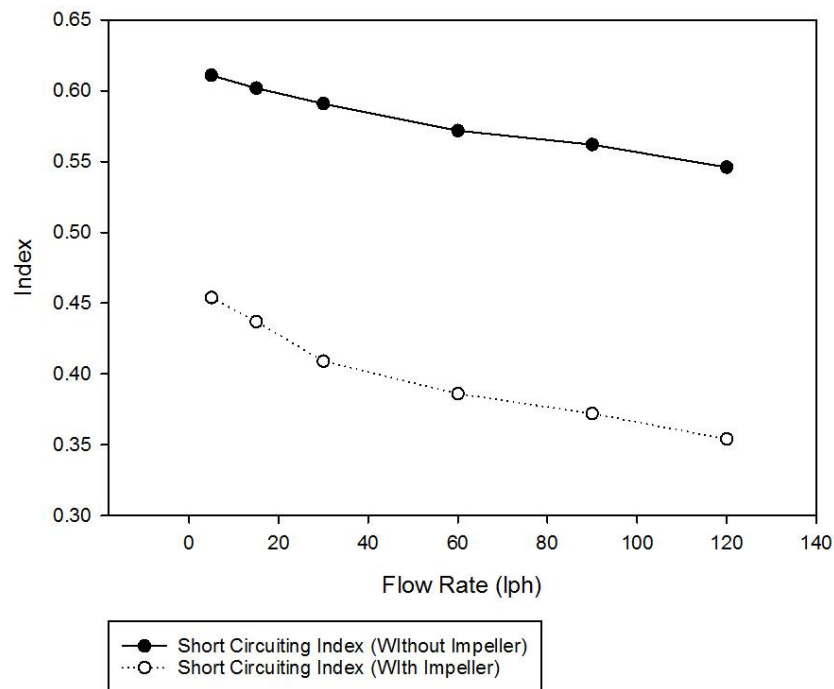


Figure 4-9 : Short Circuiting Index in absence and presence of impeller for different flow rates

4.4.7.1 *Ta and Brignal Index*

Ta and Brignal Index ($S_{tb}=t_{16}/t_{50}$) S_{tb} was being developed to analyse the level of short-circuiting from circulation inside the electrochemical reactor. The tracer flowing out at (t_{16} and t_{50}) devices this index (TA and BRIGNAL, 1998). 0.205 & 0.432 were maximum estimated value in the absence and presence of impeller at the flow rate of 120 lph respectively. Considering $S_{tb} = 1$ in ideal PFR, the distance from the ideal value is 0.795 in the absence of impeller and 0.568 in the presence of impeller. This indicates a lower degree of short-circuiting with impeller as shown in Figure 4-10 .

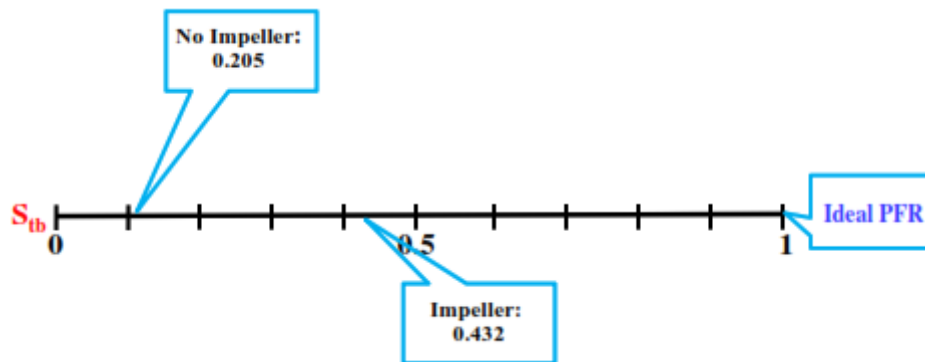


Figure 4-10: The distance of S_{tb} from ideal PFR

4.4.7.2 *Index of Short Circuiting Flow*

Index of Short-Circuiting Flow ($Q_{sc} = Q_{in}(1 - \tau/t_{mean})$) is highly related to τ/t_{mean} . If $t_{mean} < \tau$ or $t_{mean} > \tau$, then dead volume or short-circuiting flow will occur in the reactor (Tsai, Ramaraj and Chen, 2012). As t_{mean} was longer than τ in both absence and presence of impeller, the short circuiting is prevalent because of it and it is 43.8% in the absence of impeller and 19.8% in the presence of impeller as depicted in Figure 4-11. This shows and confirms that short circuiting in the presence of impeller was lower than the absence of impeller.

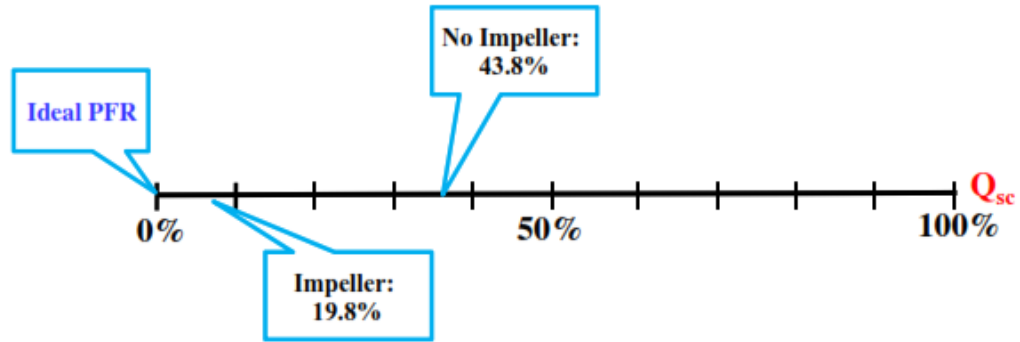


Figure 4-11: The distance of Q_{sc} from ideal PFR

4.5 CFD of 3D rotating anode

4.5.1 Effective Volume Ratio

Effective Volume Ratio ($e = t_{\text{mean}} / \tau$) was used to evaluate useful volume in proposed reactor. If reactor volume was effectively used, the mean retention time (t_{mean}) should be very close to τ . The value of e for an ideal CSTR would be equal to 1. The degree of short-circuiting is significantly affected by e . The data acquired from RTD experiments were used to calculate the values of e for each rotation speed with input flow rate as presented in Figure 4-12. It was evident that for lower flow rates of 5 and 15 lph, the values of e at different rotation speed were significantly away from ideal value of 1 indicating the long retention time. The up-flow design and vigorous circulation inside the proposed system might be the reasons to delay t_{mean} . From definition for short-circuiting, $e > 1$ represents longer t_{mean} than τ . It exhibits the existence of short-circuiting (Tsai, Ramaraj and Chen, 2012).

Similarly, the values of e for flow rate, 90 and 120 lph were also significantly away from ideal value of $e=1$, which indicates either short circuiting or development of dead zones/bypass volume. The value of e for flow rate 60 lph, are closest to 1, which indicates minimum short circuiting. It was also worth noting that at higher flow rate

with higher rotation speed the value of e were moving away from 1 which may be due to high turbulence and back mixing which may not favour the treatment requirement.

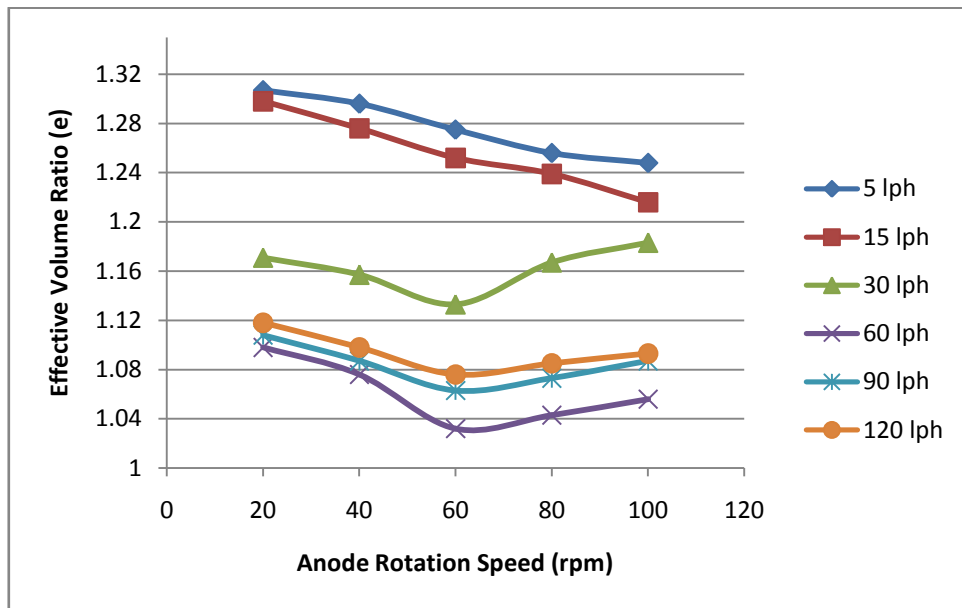


Figure 4-12: Effective Volume Ratio at different flow rates (5-120 lph) with varying rotation speed (0-100 rpm)

4.5.2 Effect of flow rate and rotation on Short Circuiting Index

The short-circuiting index for different flow rates are presented in Figure 4-13. For the flow rate of 5, 15 and 30 lph; the short-circuiting index decreases with an increase in rotation speed. For the flow rate of 60 lph; the short-circuiting index was minimum among all flow rates. It decreases with an increase in rotation speed till 60 rpm and thereafter, increases slightly with the increasing RPM. This was in line with the trends for effective volume, indicates that at flow rates of 60 lph, the reactor performs best, with minimum short-circuiting index, dead volume, and by-pass volume.

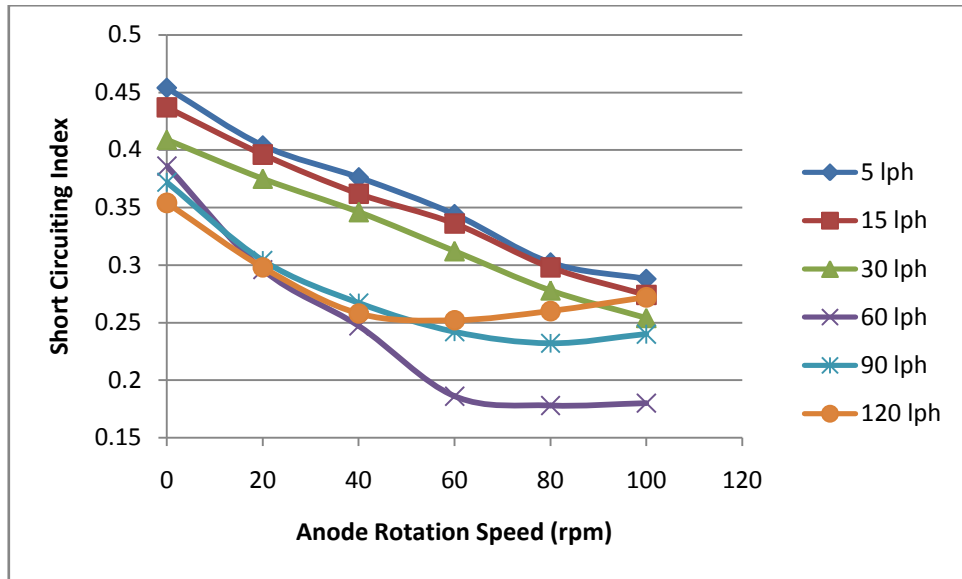
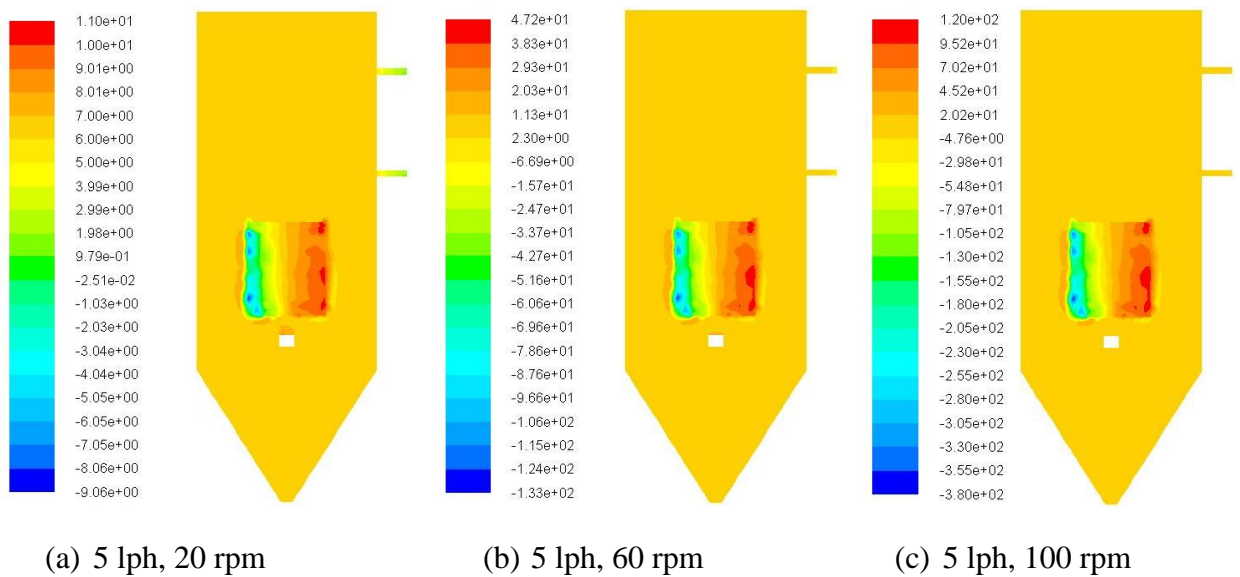
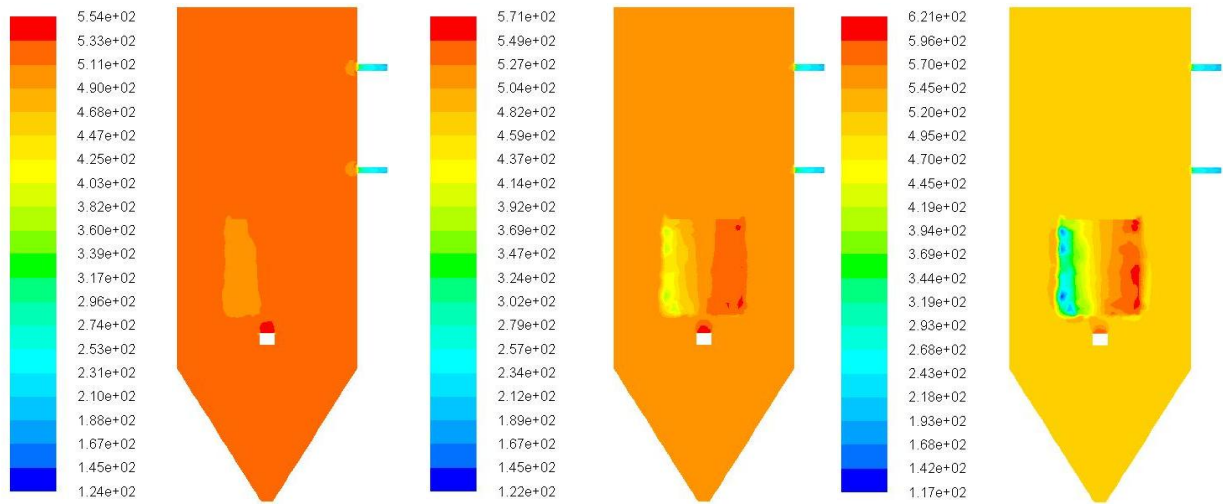


Figure 4-13: Short Circuiting index at different flow rates (5-120 lph) with varying rotation speed (0-100 rpm)

4.5.3 Pressure Distribution

Pressure distribution profile of the reactor provides substantial information regarding the fluid dynamics behaviour in terms of pressure drop. The part of the reactor where pressure drop was negative implies the low mixing zones exists due to short circuiting/channelling or due to low inlet fluid velocity. Uniform pressure distribution resembles the proper mixing inside the reactor and reduces the chances of short circuiting/ channelling/back mixing.

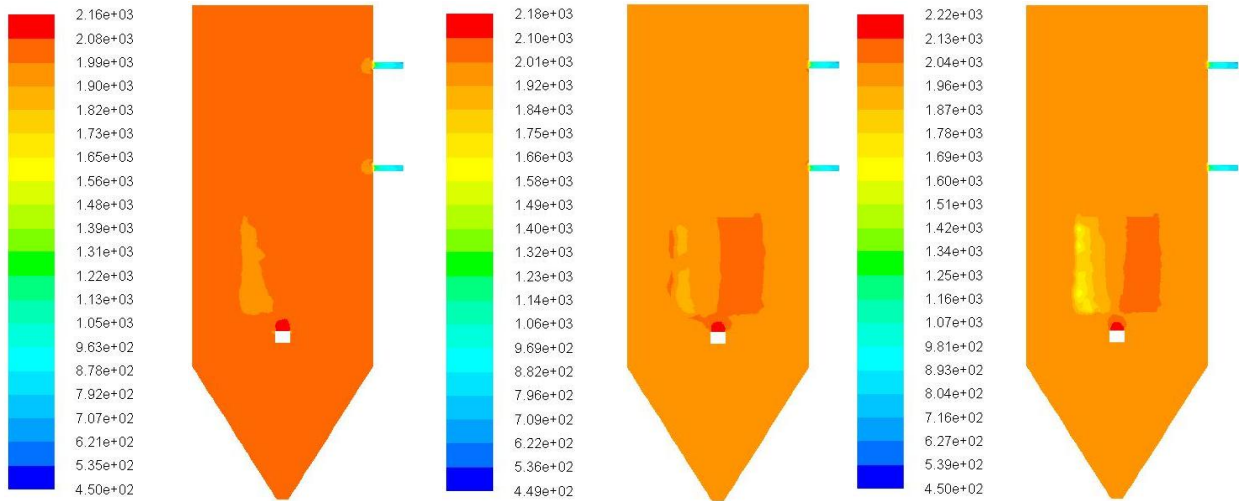




(d) 60 lph, 20 rpm

(e) 60 lph, 60 rpm

(f) 60 lph, 100 rpm



(g) 120 lph, 20 rpm

(h) 120 lph, 60 rpm

(i) 120 lph, 100 rpm

Figure 4-14: Total Pressure profile for the flow rates of 5 (a-c), 60 (d-f) and 120 (g-i) lph with anode rotation speed of 20 – 100 rpm respectively.

The pressure contours for all flow rates were determined. Here, the pressure contours for 5, 60 and 120 lph (minimum, mid-point and maxima) with rotation speed of 20, 60 and 100 (minimum, mid-point and maxima) are presented in Figure 4-14 (a-i).

Figure 4-14 (a-c) represents the pressure distribution for flow rate of 5 lph at the rotation speed of 20, 60 and 100 rpm. When the rotation speed was 20 rpm, there was no negative pressure zone in the reactor which was present in case of same flow rate without rotation. The pressure inside the reactor was also more than the case, when

impeller was stagnant. As the rotation of the impeller increases, the resultant pressure inside the reactor increases. The high pressure zones (20, 60 and 100 rpm) can be seen around the impeller with a constant pressure distribution in rest of the reactor. This implies that the turbulence inside the reactor at low flow rate was only caused by the rotation of the impeller. As the rotation speed of the impeller increases, the pressure along the impeller increases. The impeller in accordance with pressure index can be divided into right and left half as can be clearly seen in Figure 4-14 (a-c). The pressure index shows high pressure zones in the right part of the impeller and slightly low pressure zones on the left part of the impeller. This confirms the movement of fluid from right to left of the impeller as the rotation of the impeller was clockwise.

As the flow rate was increased to 60 lph as shown in Figure 4-14 (d-f) with rotation speed varying from 20 – 100 rpm. The pressure distribution for the rotation speed of 20 to 60 rpm, increases with increasing rotation speed and remain uniform in the entire volume of reactor except for the zone surrounding impeller. As the rotation speed was further increased above 60 rpm, the back mixing starts resulting in lower pressure. The high rotation speed of the impeller along with higher flow rate of 60 lph; the back mixing of the reactants takes place inside the reactor.

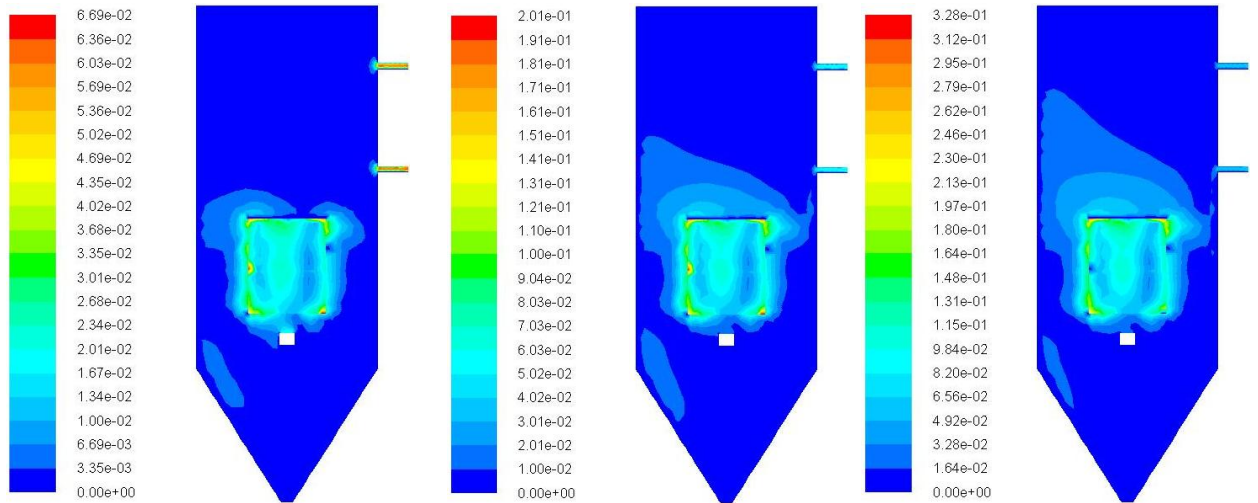
The pressure contours in the reactor for the flow rate of 120 lph with rotation speed varying from 20 to 100 rpm are shown in Figure 4-14 (g-i). These pressure contours for up to 60 rpm shows similar pattern as found for 60 lph but at higher pressure than the previous flow rate. The phenomenon of back mixing comes into play when rotation speed increases above 60 rpm. This shows that for the flow rate of 60 and 120 lph, lower rotation speed gives better pressure distribution profile.

It was evident that for all flow rates the presence of impeller has significantly changed the pressure distribution inside the reactor.

4.5.4 Velocity Magnitude Contour

The fluid velocity vector is one of the most important variables in fluid dynamics. The velocity magnitude and vector study give us the insight of movement of fluid in the reactor. The magnitude provides the rate at which dispersion of fluid occurs in the reactor.

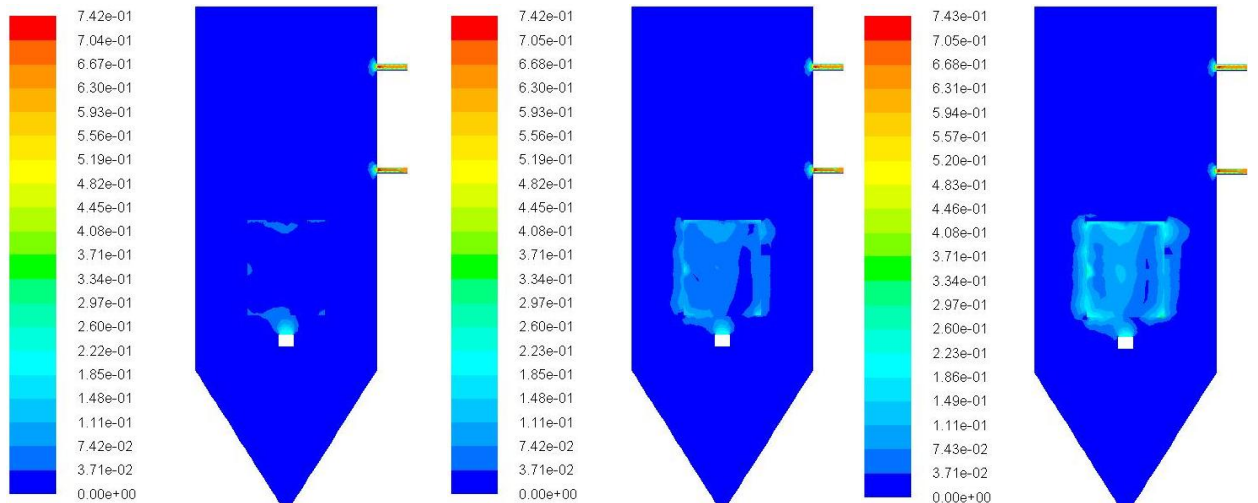
The velocity vector and magnitude contours for the flow rates of 5, 60 and 120 lph with rotation speed of 20, 60 and 100 rpm are shown in Figure 4-15 (a-c). For the flow rate of 5 lph, Figure 4-15 (a-c), the velocity magnitude increases around the impeller as the rotation speed increases from 20 to 100 rpm. There was a zone around the impeller which shows the velocity magnitude due to rotation of impeller. This zone increases with increase in rotation speed.



(a) 5 lph, 20 rpm

(b) 5 lph, 60 rpm

(c) 5 lph, 100 rpm



(d) 60 lph, 20 rpm

(e) 60 lph, 60 rpm

(f) 60 lph, 100 rpm

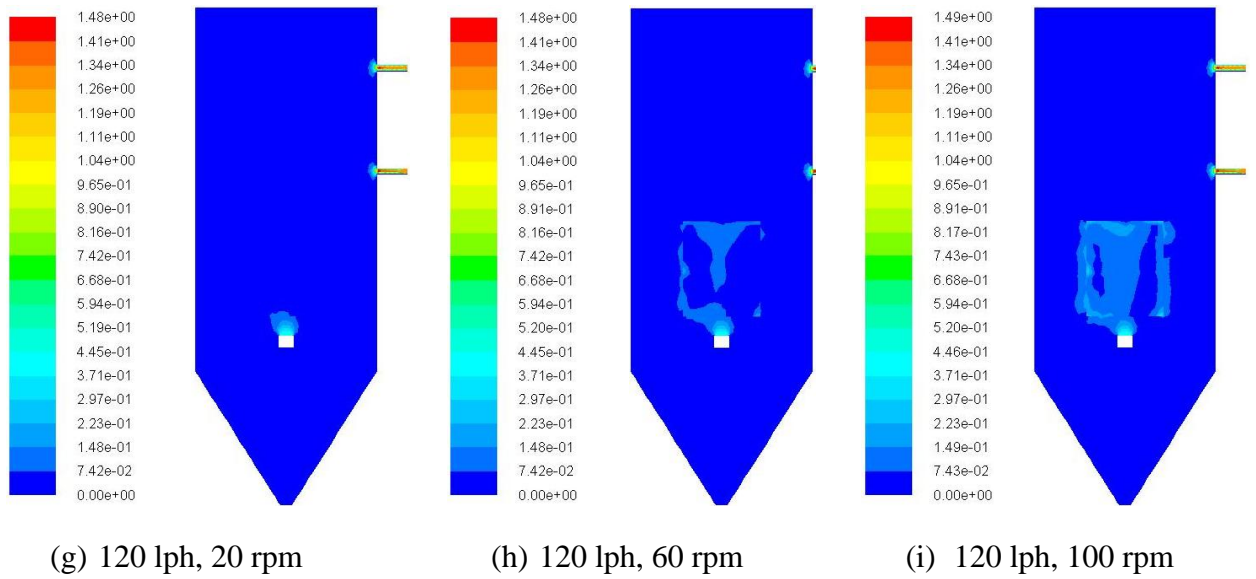


Figure 4-15: Velocity Magnitude Contour for the flow rates of 5 (a-c), 60 (d-f) and 120 (g-i) lph with anode rotation speed of 20 – 100 rpm respectively.

There was a swirl movement below the impeller from left to right side of the impeller which indicates the turbulence caused by the impeller in the reactor.

For the flow rate of 60 lph; when the rotation speed was lower (20 rpm), then there was a uniform magnitude distribution in the reactor. The impeller was visible only around its corners. When the rpm was increased to 60 rpm, the velocity magnitude increases and the distribution of magnitude was only around the impeller. This confirms that turbulence inside the reactor was mainly caused by the rotation of the impeller. For the same flow rate when the rpm was increased to 100 rpm, then there was much turbulence and velocity magnitude around the impeller. This indicates the chances of back mixing at this rotation speed.

For the flow rate of 120 rpm, the velocity magnitude for 20 rpm was uniform as presented in Figure 4-15 (g). The magnitude around the inlet and outlets are more than the other parts of the reactor. The magnitude around the impeller was uniform as in rest of the reactor. When the rotation speed was increased to 60 rpm, the velocity magnitude remains uniform in the reactor and shows similar pattern like 60 lph, but the intensity around the impeller was lower than that of 60 lph at 60 rpm. This was due to the fact that the short circuiting index increases at this level due to back mixing at higher flow rates. The same trend was followed by 120 lph at 100 rpm.

4.5.5 Velocity Vector

The velocity vector defines the directions of flow. This facilitates to understand the flow dynamics inside the reactor. The velocity vector for the flow rate of 5, 60 and 120 lph at rotation speed of impeller as 20, 60 and 100 rpm are presented in Figure 4-16 (a-i).

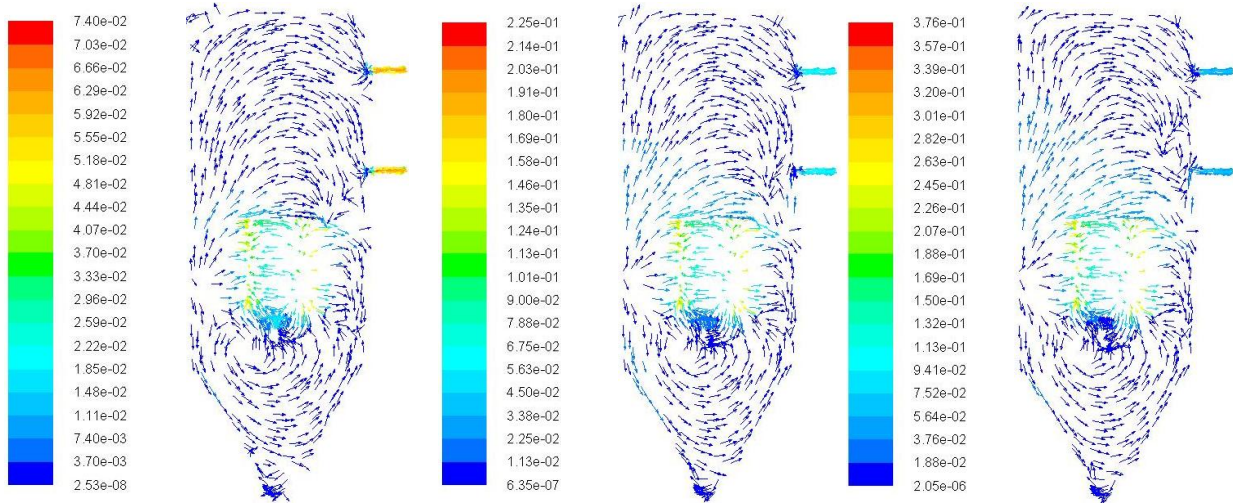
For the flow rate of 5 lph; when the rotation speed of impeller was 20 rpm, there can be seen an inside out movement of fluid along the impeller. The movement of fluid takes place from right to left as also depicted by velocity magnitude. At the bottom of hopper zone settling takes place which can be seen in Figure 4-16. There was deposition of flux at the bottom which indicates settling phenomenon. There was a single swirl movement from the bottom of the reactor defining the push from the inlet due to rotation of impeller. For the same flow rate when the rotation speed of the impeller was increased to 60 and 100 rpm, the inside out movement of the fluid through the impeller increases as presented in Figure 4-16 (b,c). A more stabilized zone was created at bottom for the rotation speed of 60 rpm.

For the flow rate of 60 lph; when the rotation speed was 20 rpm, the movement of fluid from 2 zones into the impeller can be seen as presented in Figure 4-16 (d). This was due to the fact that at this higher flow rate and rotation speed the turbulence was more than the previous studied flow rate. The bottom zone begins to divide into two different zones below the impeller defining the push of fluid into the impeller from both the zones. This provides better mixing opportunity for the fluid in the reactor. For the same flow rate, when rpm was increased to 60, the distinction of zones can clearly be seen as presented in Figure 4-16 (e). This confirms that the increase in rotation speed of the impeller imparts the turbulence inside the reactor.

For the same flow rate, when rpm was increased to 100, the pattern remains the same. This can be attributed that the maximum turbulence required inside the reactor was achieved at 60 rpm. Further, increase in rotation speed will only induce back mixing and wasteful use of energy.

For the flow rate of 120 lph, when the rotation speed of impeller was increased to 20, 60 and 100 rpm as presented in Figure 4-16 (g-i), there was high turbulence inside the

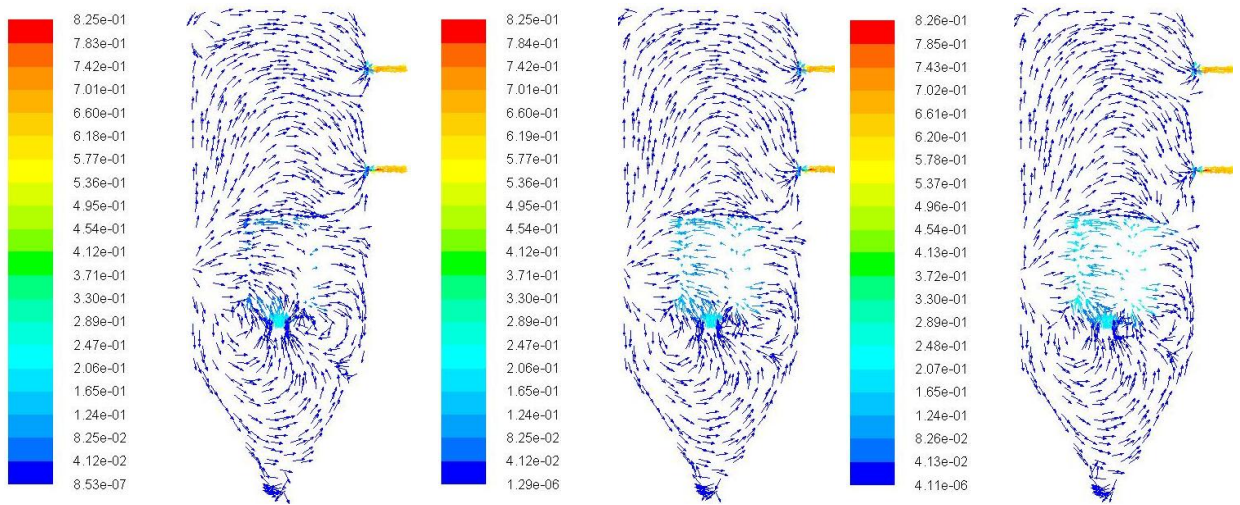
reactor for all three cases. The reactor divides into 4 zones imparting high turbulence in the fluid at the bottom of the reactor. This imparts the back mixing in the reactor. As the turbulence at the hopper bottom increases, the settle able solids are disturbed and induce back mixing.



(a) 5 lph, 20 rpm

(b) 5 lph, 60 rpm

(c) 5 lph, 100 rpm



(d) 60 lph, 20 rpm

(e) 60 lph, 60 rpm

(f) 60 lph, 60 rpm

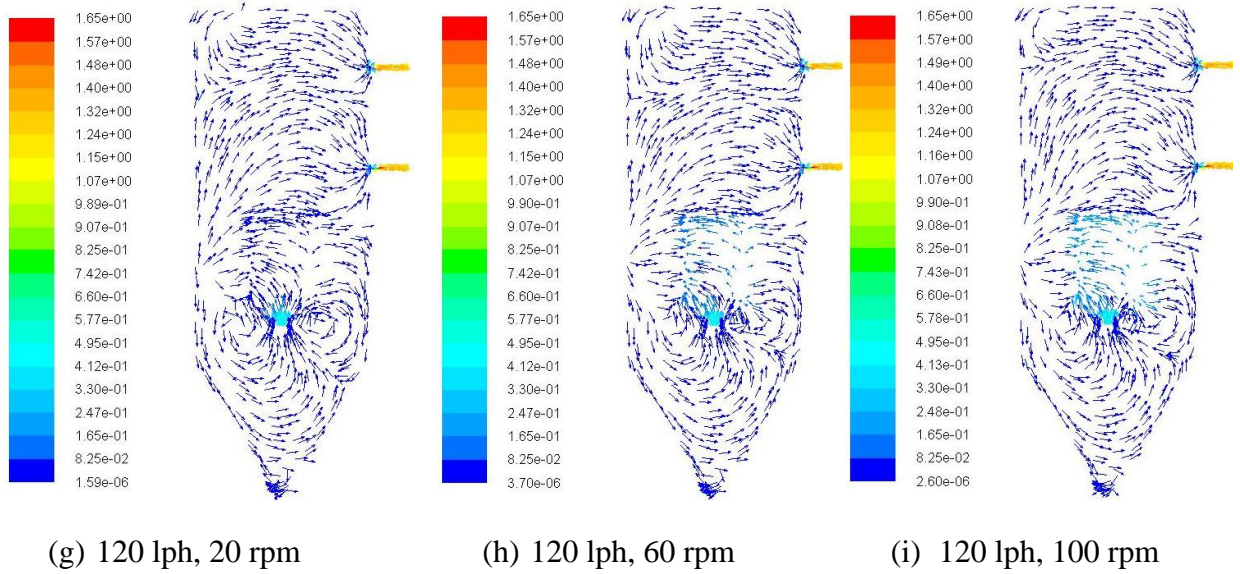


Figure 4-16: Velocity Vector profile for the flow rates of 5 (a-c), 60 (d-f) and 120 (g-i) lph with anode rotation speed of 20 – 100 rpm respectively.

4.5.6 Reynolds Number and Turbulent Kinetic Energy

The Reynolds number depicts the nature of flow. When the Reynolds number is greater than 4000, the flow is turbulent. For all the cases when impeller was rotated with varying rotation speed as depicted in Table 4-5, the flow was always turbulent. This confirms that the rotation of impeller in the reactor enhances the turbulence in the reactor. The change in velocities of various fluid elements cause turbulence in the reactor generating eddies in return (Ibrahim *et al.*, 2013a). The presence of turbulence enhancer and the fluid entrance effect causes the change in the velocity zones of the reactor. In this case, the 3D rotating type cylindrical anode; which was present at the distance of 3 cm from the inlet, acts as a turbulence enhancer. As shown in Table 4-5, the turbulence increases as the rotation speed of impeller increases.

Table 4-5: Reynolds number and type of flow

	Reynolds	
RPM	Number	Flow
20	67280	Turbulent

40	134560	Turbulent
60	201840	Turbulent
80	269120	Turbulent
100	336400	Turbulent

Table 4-6 compares the simulated values of the change in turbulent kinetic energy for different flow rates (5, 15, 30, 60, 90 and 120 lph). It can be observed that on increasing the flow rate, there is a notable increase in the turbulent kinetic energy. This confirms that as the flow rate increases the velocity of the fluid increases which in turn, increase the turbulence and turbulent kinetic energy of the system and thus provides better mixing and flow regime. The turbulent kinetic energy increases rapidly from 30 l/h to 60 l/h but as we further increase the flow rate, the increase in turbulent kinetic energy not appreciable as it was before.

Table 4-6: Comparison of turbulent kinetic energy for different flow rates with rotation speed

RPM ↓	Flow Rate					
	5	15	30	60	90	120
	Turbulent Kinetic Energy					
0	0.775	0.916	1.232	1.405	1.765	1.967
20	1.324	1.895	2.704	4.002	5.343	7.232
40	1.578	2.567	3.675	7.112	9.223	14.091
60	1.898	3.134	5.783	12.660	14.909	18.201
80	2.688	3.870	7.1422	17.989	19.001	25.43
100	3.450	4.344	8.556	20.344	22.587	28.560

4.5.7 Comparison between simulated and experimental mixing patterns

The mixing line represents ideal mixing condition with $I(\theta) = \exp(-\theta)$. The inlet flow transmits its energy to the liquid in the tank and causes generation of convective

streams and turbulent eddies, which give rise to the mixing of the contents of the tank. The comparative presentations of simulated and experimental with ideal mixing line are depicted in Figure 4-17 for the flow rate of 60 lph while anode rotation speed ranging from 0 to 100 rpm.

As shown in Figure 4-17 (a), the anode rotation was set to 0 rpm. The computed and experimental $I(\theta)$ shows a relatively similar behaviour and pattern but both were away from ideal mixing line. As we increase the anode rotation speed, the computed and experimental $I(\theta)$ begins to match perfectly with each other giving an insight that the modelled and experimental data are in correlation with each other. Thus, they both follow ideal mixing line as anode rotation increases upto 60 rpm. Above 60 rpm, the phenomenon of back mixing comes into play and the deviation of both the data sets from ideal mixing line can be observed from Figure 4-17 (e-f).

The observation finds that the computed values can predict in excellent the experimental data. The visible fluid mixing state was perfectly matching with the experimental mixing state. All the figures depict that the computed $I(\theta)$ approaches the ideal mixing line with increase in impeller rotation, N . It happens because of the increase of rate of mixing with increase in impeller rotation, which accounts for the amount of mechanical energy given to the liquid.

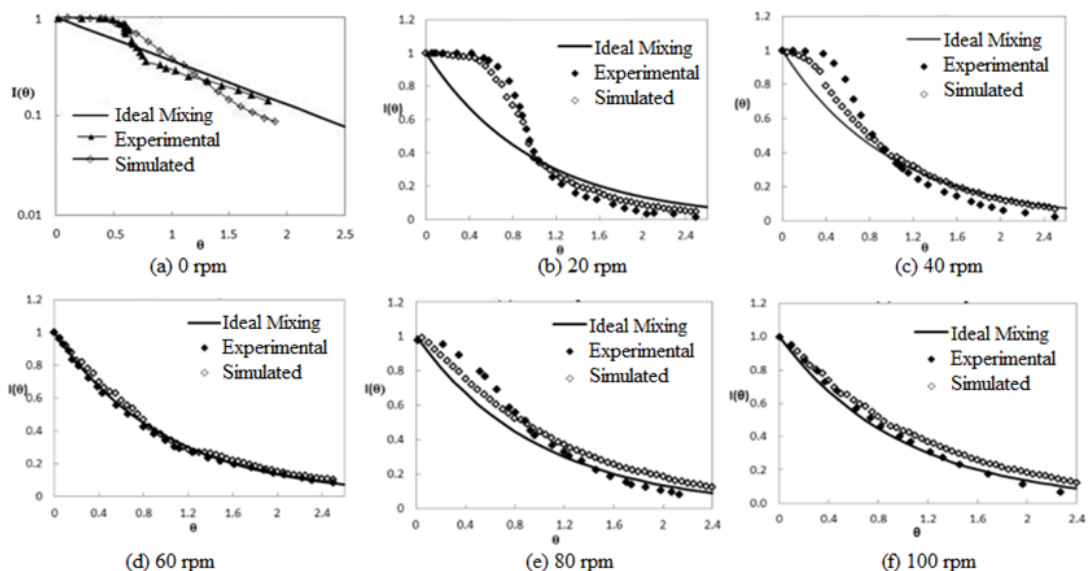


Figure 4-17: Comparison of simulated, experimental and ideal mixing line for anode rotation of (a) 0 rpm, (b) 20 rpm, (c) 40 rpm, (d) 60 rpm, (e) 80 rpm, and (f) 100 rpm respectively.

CHAPTER 5

TREATMENT OF STW USING 3D ROTATING ANODE

This chapter deals with the application of 3D rotating anode reactor in the electrochemical treatment of synthetic textile wastewater (STW). The synthetic textile wastewater was prepared using red azo dye as prescribed in the literature. The experimental investigations performed using 3D rotating electrochemical reactor was divided into three parts. Firstly, six operating parameters (anode rotation (n), current density (j), flow rate (q), EC time (t), initial pH (pH_0), supporting electrolyte concentration (m)) were investigated using PB design to identify the variables that significantly affect the COD and color removal efficiency. The batch studies were performed using three configurations viz. batch reactor, batch recirculation reactor and single pass system to use the results for the development of continuous flow regime reactor. Secondly, the significantly important operating parameters screened from PB design with more specific operating range were used as input variables for Box-Behnken (BB) design. The Box-Behnken (BB) design was used to develop and optimize a characteristic equation for color and COD removal efficiency along with electrode consumption and specific electrical energy consumption for unit COD removal for continuous flow regime. All the experiments were conducted in triplets and the average of the same is reported as required. Lastly, the analytical studies on the treated samples and on the solid residues were performed to decipher the probable removal mechanism.

The mechanistic study using zeta potential measurement was performed to understand the role of electrostatic interaction between aluminium species and the dye molecules. Then the characterization of generated solid residues was performed by X-ray diffraction (XRD), scanning electron microscope (SEM), energy dispersive spectroscopy of X-rays (EDX), etc to evaluate the possible end use of the solid residues.

5. EC Treatment of synthetic textile wastewater (STW) with 3D rotating anode electrochemical reactor

5.1 The Electrochemical treatment

A typical electrochemical treatment process consists of an electrolytic cell, which uses electrical energy to affect a chemical change. In simplest forms, an electrolytic cell consists of two electrodes i.e. anode and cathode, immersed in an electrical conducting solution (the electrolyte), and are connected together, external to the solution, via an electrical circuit which includes a current source and control device. The chemical processes occurring in such cells are oxidation and reduction, taking place at the electrode/electrolyte interface. The electrode at which reduction occurs is referred to as the cathode and conversely, the anode is the electrode at which oxidation processes occur.

The current flow in an electrochemical cell is maintained by the flow of electrons resulting from the driving force of the electrical source. In order to allow the current to flow, there must be an electrolyte, which facilitate the flow of current by the motion of its ionic charged species. Type of electrolyte have significant effect on the process in the formation of oxidizing species during the process (Chen, 2004).

5.2 Criteria for Reactor performance

The performance of the EC process depends on many operational parameters such as pH of the solution, applied current to the reactor, conductivity of the (wastewater) solution, electrolysis time as well as electrode specifications such as arrangement of electrode, electrode shape, distance between the electrodes, etc. Major operational parameters influencing the EC efficiency are presented schematically given in Figure 5-1. The effects of each parameter in details are described in the chapter - 2. However, in this study, effects of six of the operating parameters namely, *anode rotation (n)* (by rotating anode at specified speed); *current density (j)* (applied current to the unit area of active electrode surface); *flow rate (q)* (the input of wastewater in litre per hour);

EC time (t) (duration of applying current to the wastewater); *initial pH (pH₀)* (by adjusting the pH with acid or base) and *supporting electrolyte concentration (m)* were investigated. The upper and lower limits of the operating parameters were defined according to the literature available and the limits for *anode rotation (n)* were taken from the CFD simulation considering the turbulence caused by eddies.

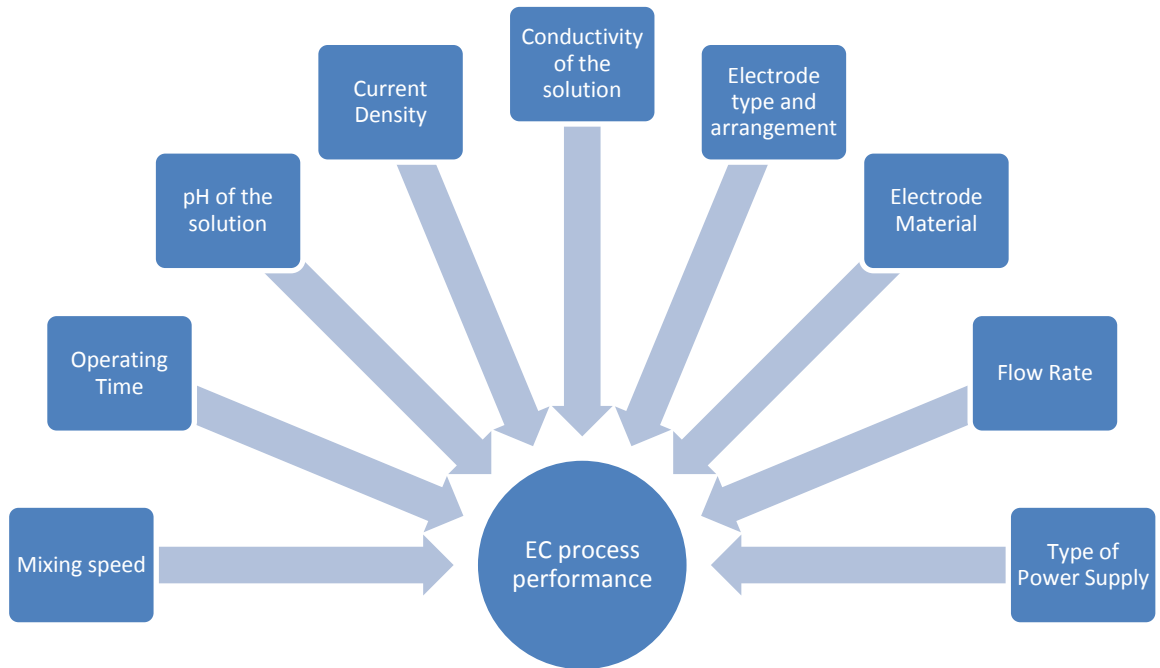


Figure 5-1: Schematic display of the various operating parameters influencing the EC process performance.

5.3 The 3D rotating anode reactor

A conical hopper bottom perplex vessel was used as a electrochemical reactor with 3D perforated rotating cylindrical impeller acting as an anode is shown schematically with all the connections in Figure 5-2 was used for the evaluation of EC process performance. The synthetic textile wastewater (STW) was used for all the experimental investigations. The characteristics of the STW were already described along with the detailed description of the system in chapter – 3.

The DC power unit supplies negative current to the long rod making it cathode and positive to perforated cylinder making it anode. This was a hydrodynamic electrode

system in which electrode (anode) rotates during the electrolysis inducing a flux of analyte to the electrode. The 3D rotating cylindrical impeller was designed to facilitate better mixing during the electrolysis process. The additional advantage it would offer was to prevent oxide layer formation, which in turn would slow down the fouling of electrode. The surface of the electrode was kept perforated to further improve the mixing phenomenon for better yield of the process.

The experimental investigations to evaluate the performance of EC process were conducted to validate the expected advantages due to 3D rotating anode system which were estimated during the RTD and CFD study of the system.

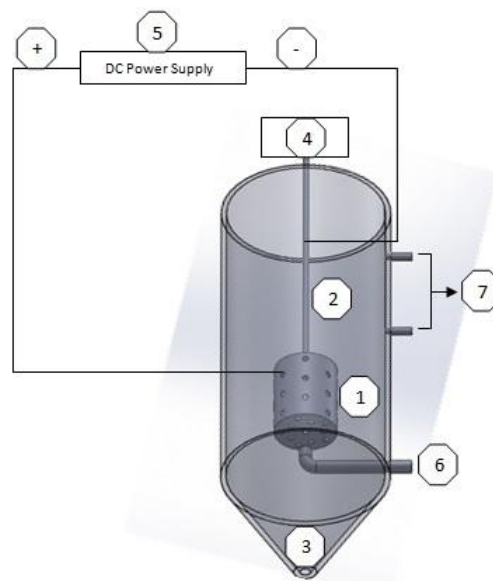


Figure 5-2: Geometry of Proposed Reactor. 1) 3D Aluminum perforated cylindrical anode. 2) Aluminum rod cathode. 3) Conical Hopper Bottom for Sludge collection. 4) Mechanical stirrer. 5) DC Power Supply Unit. 6) Inlet for Wastewater. 7) Outlet for Treated Water

5.4 Screening of the operating parameters using Plackett-Burman (PB) Design

PB design was used to screen the significant operating parameters. Six parameters (anode rotation (n), current density (j), flow rate (q), EC time (t), initial pH (pH_0), supporting electrolyte concentration (m)) were investigated using PB design to identify the variables that significantly affect the COD and color removal efficiency.

Response of each variable was evaluated at two levels, high and low, denoted by (+) and (-) signs respectively.

Responses (COD and Color) were measured in the terms of removal efficiency. The main effects plot was the most useful tool when there are several factors for consideration. The changes in the levels were used to deduce degree of influence of the responses. The factors exhibiting highest slope in the absolute terms can be considered as the most significant operating parameters for electrochemical treatment. First-order model linear equation was used to elucidate the significantly important factors by PB design:

$$y = \beta_0 + \sum_{i=1}^n(\beta_i X_i) \quad (5.1)$$

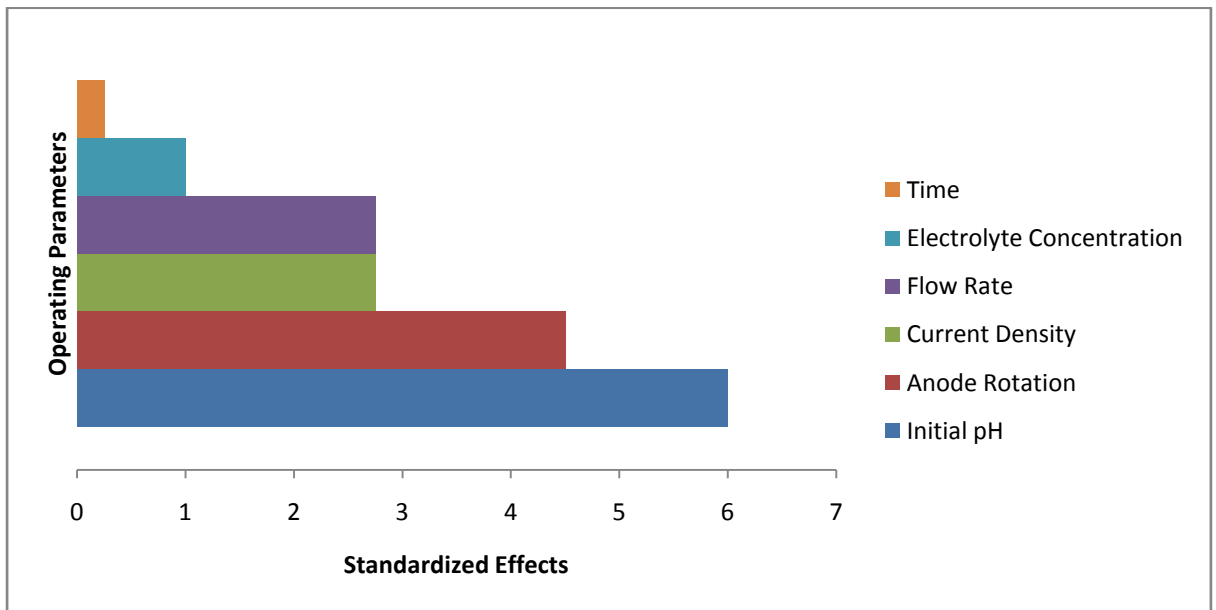
Where, y represents the response (i.e. COD or color removal efficiencies), β_0 is the model intercepts, β_i is the linear coefficient, X_i is the level of the independent variable, and n is the number of involved variables. Regression analysis was further done to find the operating parameters which were significant at 5% level ($P < 0.05$). Regression coefficients and their significance for the response of PB design are presented in Table 5-1. The PB design was used to represents the effect of the tested parameters (in terms of actual values) for the COD and color removal efficiencies (Şahan *et al.*, 2010).

Table 5-1: Regression coefficient and their significances for responses (COD and Color) in the Plackett-Burman design.

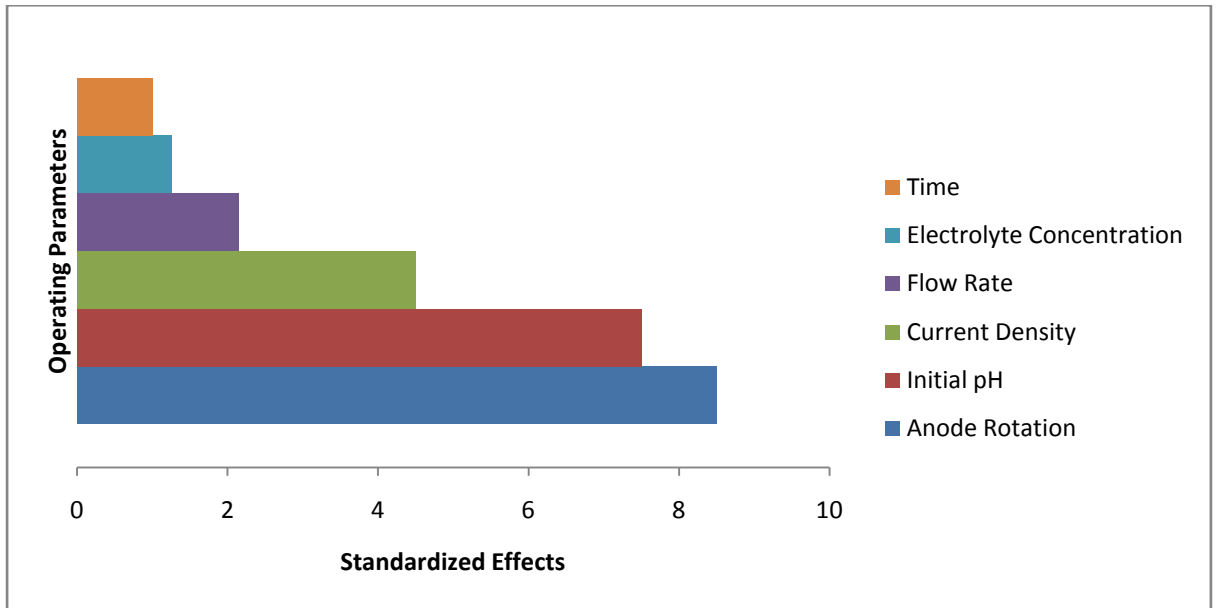
Factors	Level		COD				Color			
	(-1)	(+1)	Coefficient	T Value	P Value	Effect	Coefficient	T Value	P Value	Effect
Constant			50.10	53.23	0.0000		87.91	193.26	0.0000	
Anode Rotation	10	500	7.22	7.67	0.001	14..45	2.08	4.58	0.006	4.16
Current Density	1	20	4.05	4.31	0.008	8.11	1.25	2.75	0.040	1.25
Flow Rate	1	150	1.94	2.06	0.09	3.88	1.25	2.75	0.040	2.50
EC time	10	120	-0.77	-0.82	0.44	-1.55	-0.08	-0.18	0.86	-0.16
Initial pH	2	10	-6.55	-6.97	0.001	-13.11	-2.75	-6.05	0.002	-5.50

Supporting electrolyte concentration	0	5	1.10	1.18	0.29	2.21	-0.41	-0.92	0.40	-0.82
--------------------------------------	---	---	------	------	------	------	-------	-------	------	-------

The Pareto chart of standardized effects as depicted in Figure 5-3 shows the 95% confidence interval for responses, percent COD and color removal (Amini *et al.*, 2008; Luna *et al.*, 2010). The interaction plot depicts interaction of various parameters for COD and color removal. If the lines are parallel in the interaction graph, then it implies that there is no interaction between the factors. Non-parallel lines in the interaction plot indicate existence of an interaction between the factors. The greater the difference between the slopes of the lines of two factors in the range tested, the greater is the interaction (Kim *et al.*, 2003).



(a) Color Removal



(b) COD Removal

Figure 5-3: Pareto chart of standardized effects for the Plackett-Burman design for response (a) Color removal and (b) COD removal

It was evident that *anode rotation* (n), *current density* (j), *initial pH* (pH_0) and *flow rate* (q) have significant effects on COD and color removal efficiencies. Other factors also have effects but not sufficiently significant for removal of the COD and color. The treatment time and supporting electrolyte concentration have role in energy consumption and it was further studied through batch experiments after limiting the lower and upper level of the operating parameters using steepest ascent/descent.

5.4.1 Method of Steepest ascent/descent

PB design helped in finding out the most significant operating parameters affecting COD and color removal efficiency. However, the optimum levels of these selected operating parameters were yet to be found. The method of steepest ascent was applied for moving sequentially along the path of steepest ascent/descent, that was, in the direction of the maximum increase/decrease in the response (Montgomery, 2012; H.Myers, C.Montgomery and Anderson-Cook, M, 2016). The path of steepest ascent/descent was employed to find out the plateau by increasing the n and j and by

decreasing the pH_0 of STW (Koby, Demirbas, *et al.*, 2006; Şahan *et al.*, 2010). Based on plateau formed by steepest ascent/descent using 0, 0+1 Δt , 0+2 Δt , 0+3 Δt , 0+4 Δt , 0+5 Δt0+n Δt ; the lower (-1), middle (0) and upper (+1) range of significant operating parameters for batch experiments and Box-Behnken (BB) design were chosen as presented in Table 5-2.

Table 5-2: Range of operating parameters used in STW degradation for batch and Box-Behnken (BB) design.

Factor	Variable	Unit	Range and Levels		
			-1	0	+1
A	Current Density	mA/cm ²	2	6	10
B	Flow Rate	lph	5	60	120
C	Supporting Electrolyte Concentration	g/l	1	3	5
D	Anode Rotation Speed	rpm	0	60	100

5.5 Performance of the 3D rotating anode (Batch Studies)

The performance of the 3D rotating anode configurations was evaluated in three flow regimes namely, batch, batch recycle, and single pass system with STW. Out of these three flow regimes, the results of batch and batch recirculation reactor were found out to be better than one through the reactor system. The results of the same were then used to decide the range of operating parameters in order to optimize the EC process for continuous mode of operation using Box-Behnken design. The effect of the *anode rotation speed (n)*, *current density (j)*, *initial pH (pH₀)*, *electrolyte flow rate (q)*, *EC time (t)*, and *supporting electrolyte concentration (m)* on the COD removal efficiencies along with total specific electrical consumption have been evaluated with the experimental investigations.

5.5.1 Batch Reactor

Batch experiments were performed to optimize the six operating parameters as described above. The chemical oxygen demand (COD) of the treated samples was collected at an interval of 20 minutes to assess the treatment efficiency. The COD and

color of the effluent was measured using a Shimadzu UV-1800 spectrophotometer. The process performance of the 3D rotating anode was defined as two forms, one with respect to the percentage COD removal and second is specific electrical energy consumption for unit COD removal in J/mg COD.

The reaction rate (for COD removal) in the batch configuration for 3D rotating anode can be expressed as;

$$-\left(\frac{A_e}{V_e}\right) \frac{dC}{dt} = \frac{i}{zF} = k_L C \quad (5.2)$$

Integrating the above equation gives;

$$C = C_0 \exp(k_L a_S t) \quad (5.3)$$

Where;

V_e = effluent volume (cc),

A_e = effective anode area (cm²),

i = current density (A/dm²),

z = number of electrons involved in the electrochemical reaction,

F = Faraday constant,

C = COD (mg/l) at the time t ,

C_0 = initial COD (mg/l) and,

a_S = specific anode surface $\left(\frac{1}{cm}\right) = \left(\frac{A_e}{V_e}\right)$.

A plot of t vs $-\ln(C/C_0)$ provides the rate constant k_L .

The batch experiments showed that the *anode rotation (n)*; *current density (j)* and *initial pH (pH₀)* considerably influence the removal efficiency of the process while *EC time (t)* and *supporting electrolyte concentration (m)* were mainly affecting the specific electrical energy consumption as discussed later.

5.5.2 Effect of Anode Rotation Speed

In order to investigate the effect of anode rotation speed on the color and COD removal efficiencies, the experiments were carried out at six different anode rotation speeds: 0, 20, 40, 60, 80 and 100 rpm for the conditions: initial COD concentration = 861 ppm; Current Density = 6 mA/cm²; pH = 6. Figure 5-4 and Figure 5-5 represents that increasing the anode rotation speed in turn speed up COD removal and color removal. For instance, COD and color removal efficiency at 0 rpm was 73.53% and 97.65% and at 60 rpm they speed up to 92.85% and 98.86% respectively. This can be ascribed to the increment in the rate of diffusion of Al³⁺ from the surface of the anode and in turn enhancing the intensity of turbulence to induce good mixing conditions inside the reactor (Winnick, 1996). This results in reduction of diffusion layer thickness. The turbulence generated from anode rotation increases the collision frequency of the flocs generated resulting into coalescence into larger flocs which are easy to be buoyant by cathodic hydrogen bubbles formed (El-Ashtoukhy and Yasmine, 2014).

As the rotation speed was further increased to 80 and 100 rpm, the COD and color removal efficiency were decreased due to high turbulence; in turn resulting in breakdown of flocs generated back into the system. It results into an increase in the axial velocity in such a way that it hampers the flocs by inducing the cyclonic effect in the reactor at high rotation speed.

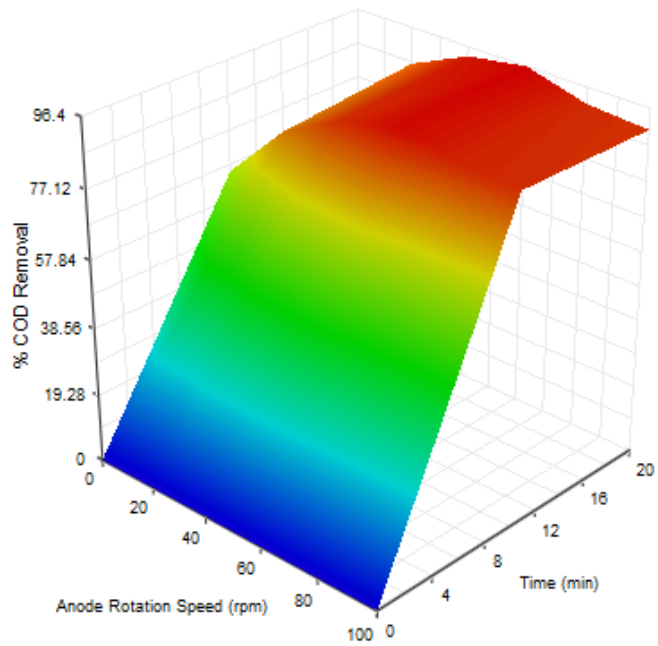


Figure 5-4: Effect of Anode rotation speed on percentage COD removal. (CD =6 mA/cm², pH = 6, initial COD = 861 ppm)

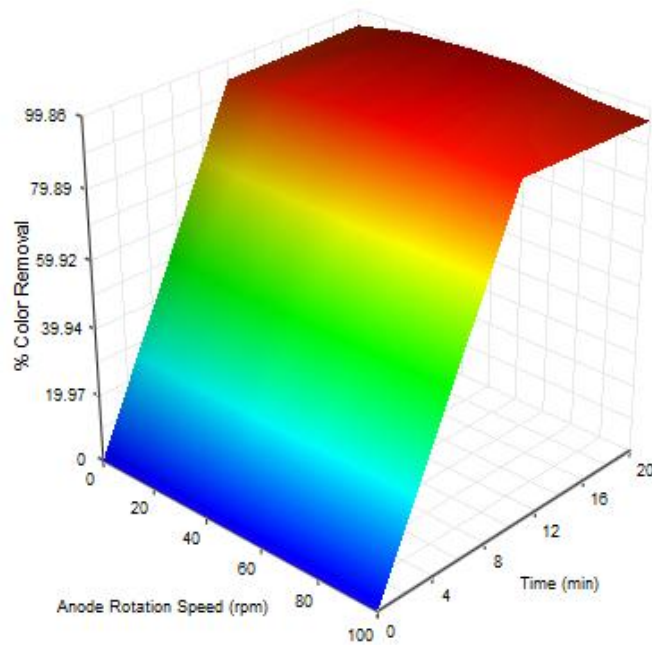


Figure 5-5: Effect of Anode rotation speed on percentage Color removal. (CD =6 mA/cm², pH = 6, initial COD = 861 ppm)

5.5.3 Effect of Current Density

It is one of the major operating parameters in the electrochemical treatment of wastewaters. This drives the process performance along with the specific electrical energy consumption to make the process effective. The experiments were varied with different current densities of 2, 4, 6, 8 and 10 mA/cm². The anode rotation speed was kept fixed at a constant value of 60 rpm and an initial pH of 6. The current density is determined by dividing the measured current to the total effective anode area (El-Ashtoukhy and Yasmine, 2014). It controls the reaction rate of the EC (S. Vasudevan and Lakshmi, 2012). As the current density increases upto 6 mA/cm², the efficiency of the system increases as depicted in Figure 5-6 and as the current density was further increased to 10 mA/cm², there was only marginal increase in the COD removal efficiency. This phenomenon can be explained by the following effects:

- (i) The increase in the quantity of coagulant i.e. Al³⁺ content as per Faraday law in the solution.
- (ii) As the current density increases, the discharge rate of H₂ increases; resulting in the floated electro coagulated dye molecules to the surface of the solution.
- (iii) The rotation of anode along with generation of H₂ bubbles enhances the mass transfer of Al³⁺. This in turn decreases anode passivation (El-Shazly and Daous, 2013).
- (iv) The dye removal efficiency increases when the current density increases because of the fact that negatively charged dye molecules were being neutralized by positively charged anode surface. The comparison of various current densities with respect to various EC time can mislead as the two variables can be compared at the same time. As the time changes, the concentration, total amount of dissolved Al³⁺ and the degree of mixing of hydrolyzed Al³⁺ species with the wastewater and concentration of dye in the wastewater as the dye concentration decreases with increase in current density and EC time. The steady diffusion of OH⁻ from cathode to the

wastewater with increasing EC time with respect to pH is also affected by time and current density (El-Ashtoukhy and Yasmine, 2014).

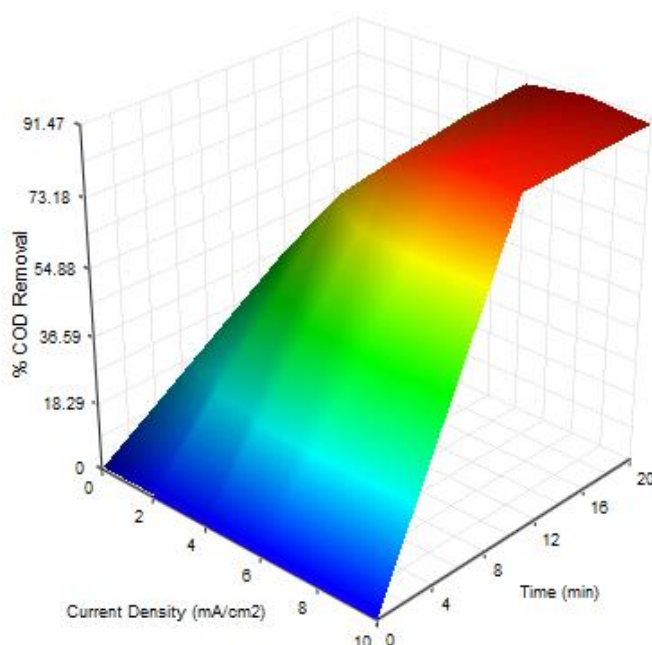


Figure 5-6: Effect of Current density on percentage COD removal. (Anode Rotation Speed = 60 rpm, pH = 6, initial COD = 861 ppm)

5.5.4 Effect of the initial pH (pH₀)

The effect of pH on the treatment was examined by adjusting the pH of the wastewater to the desired value by addition of 0.1M NaOH and 0.1M HCl solutions. All the experiments were carried out with varying the pH values as 4, 6, 8, and 10 keeping the current density constant at 6 mA/cm² and the initial COD concentration was 861 ppm. As shown in Figure 5-7; the highest removal efficiency was achieved in the pH range of 6-8. As the rate of chemical dissolution of aluminium anode increases in alkaline solutions (Cañizares *et al.*, 2005). The amphoteric nature of aluminium hydroxide affects the formation of Al(OH)₃ flocs at different pH values. At very low pH around 2 to 3, cationic monomeric species like Al³⁺ and Al(OH)²⁺ are prevalent. As the pH range increases from acidic to alkaline i.e. 4 to 9, the hydroxide species formed by the reaction of Al³⁺ and OH⁻ at anode and cathode are carrying positive charge. There are various of monomeric species formed such as Al(OH)²⁺, Al(OH)₂²⁺ and various polymeric species such as Al₆(OH)₁₅³⁺, Al₇(OH)₁₇⁴⁺, Al₁₃(OH)₃₄⁵⁺ and

$\text{Al}_{13}(\text{OH})_{32}^{7+}$. They have large capacity of adsorption as these species mutate into insoluble amorphous $\text{Al}(\text{OH})_3(\text{s})$ via intricate polymerization/precipitation kinetics in turn effectively remove pollutants via adsorption to produce charge neutralization. This in turn increases the net catching reaction. This confirms that the formation of insoluble amorphous $\text{Al}(\text{OH})_3(\text{s})$ is superlative in the pH range of 4 to 9 (Merzouk *et al.*, 2009). As the pH value increases to 11 and above, these aluminium species transform into $\text{Al}(\text{OH})_4^-$ which is a water soluble complex in turn making it of no use for treatment of wastewater (Holt *et al.*, 2002; Huang, Chen and Yang, 2009; Gupta *et al.*, 2013).

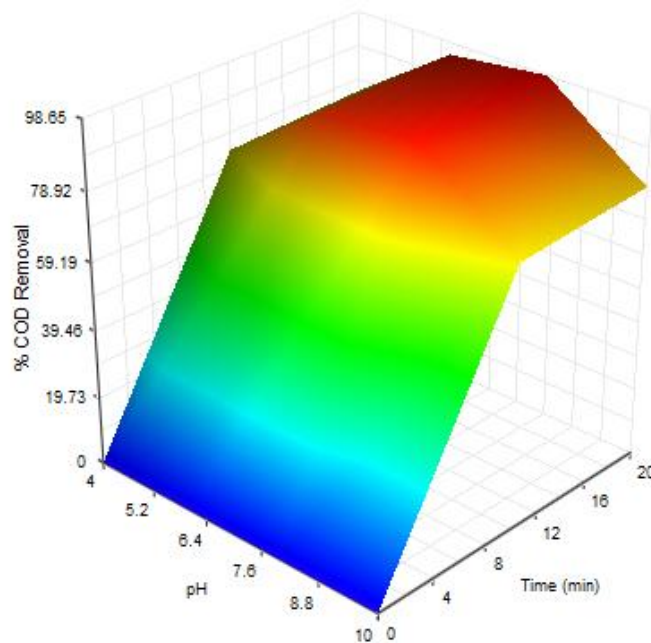


Figure 5-7: Effect of pH on percentage COD removal. (Anode Rotation Speed = 60 rpm, current density = 6 mA/cm², initial COD = 861 ppm)

As the pH for treatment ranges from 4 to 9; it favours the adsorption of dye molecules onto positively charged hydrolyzed insoluble gelatinous hydroxo cationic complexes. The H₂ bubbles at this pH range were also very tiny which render better floatation. As the pH lowers to 2 to 3, the tenuously hydrolyzed and soluble Al³⁺ products dissolves in this pH range with a decrement in adsorbed and separated amount of dye molecules. The H₂ bubbles formed in this range are of large size and have low floatation ability (El-Ashtoukhy and Yasmine, 2014).

5.5.5 Effect of NaCl/electrolyte concentration

The specific conductivity of the wastewater was varied using sodium chloride with values of 4, 24, 30, 54 $\text{ohm}^{-1} \text{cm}^{-1}$ as depicted in Figure 5-8. The COD removal efficiency increases as the conductivity of the solution increases as the current for a given cell voltage increases and in turn the energy consumption decreases.

Addition of NaCl not only enhance the conductivity of the wastewater but it enhances the EC process by eliminating passivation of anode formed at high current densities and for high EC reaction times. The Al_2O_3 oxide layer formed at anode which in turn restrain the dissolution of Al^{3+} from anode is eliminated by anti-passive Cl^- ions; thus controlling anode passivity. The presence of HCO_3^- and SO_4^{2-} ions leads to precipitation of calcium and magnesium ions that in turn forms a layer of insulation around the surface of electrodes thus facilitating passivation of electrode. This layer increases the layer potential and results in decrement of current efficiency, hampering the EC treatment process. The presence of chloride ions abates the inimical effects of the same. In order to ensure effective EC process there should be 10-15% Cl^- ions present in the solution among the total percentage of anions present (El-Ashtoukhy and Yasmine, 2014). The power consumption decreases with addition of NaCl because of increase in conductivity which leads to higher current efficiency as the internal cell resistance decreases and formation of high amount of hydroxide ions facilitating the treatment process.

The presence of Cl^- ions destructs the passive layer which is formed at a pH around 7 as per potential-pH diagram of the system Al- H_2O . The Al reacts to passive species at high current densities. The dissolution can occur via defects in passive layer formed at high electrode potential; thus eliminating passive layer formation and improving the COD removal efficiency of the system.

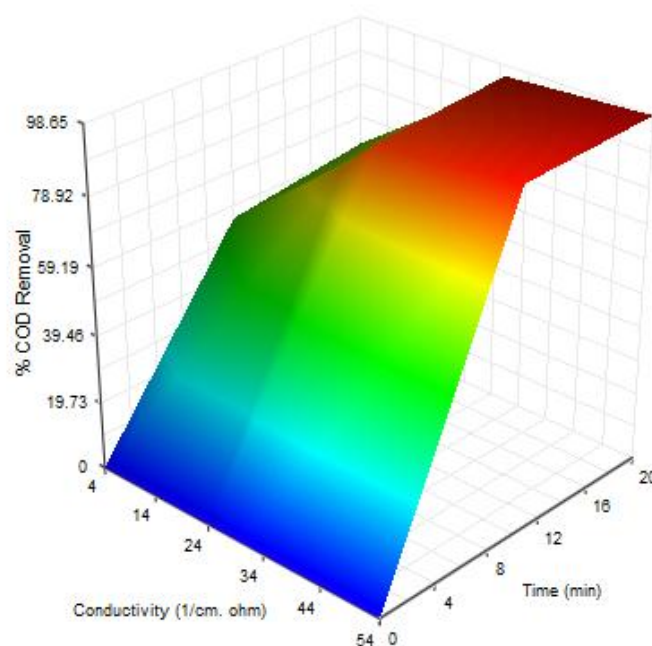


Figure 5-8: Effect of conductivity on percentage COD removal. (Current density = 6 mA/cm², Anode Rotation Speed = 60 rpm, pH = 8, initial COD = 861 ppm)

5.5.6 Effect of type of supporting electrolyte

The effect of supporting electrolyte was studied by using four different electrolytes: NaCl, NaOH, NH₄Cl and KCl. The properties of electrolyte devices their interaction with electro active species and hence dominate the electrode reactions (Huang, Chen and Yang, 2009). NaOH provides best removal efficiency as compared to other electrolytes. NaOH electrolyte favours the removal efficiency due to the fact that aluminium is an amphoteric metal that deliquesce electrochemically in NaOH and increases the dissolution rate of Al to Al³⁺. The anode passivity was prevented by the addition of NaOH as it dissolves Al₂O₃ to sodium aluminate. The size of the H₂ bubbles developed from NaOH solution are small and have effective surface area to float the pollutant to the surface easily as to those generated in the acidic range (Janssen and Hoogland, 1973). NH₄Cl has lowest efficiency due to fact that in acidic range the formation of Al(OH)₃ is hindered which is the main contributor in the dye removal process.

5.5.7 EC Treatment time (t)

The EC treatment time affects the treatment efficiency in conjunction to current density. The EC time 10, 20, 30, 40, 50 and 60 minutes were taken for experimental studies. The treatment efficiency was achieved in the span of 20 minutes. Further, increasing the treatment time (t) shows marginal increase with respect to increasing current density. And at higher current density ($> 8 \text{ mA/cm}^2$) and treatment time ($t > 20$ minutes), the temperature of the system was found to be few degrees higher, indicating that the additional charge has been turned into heat energy. As the treatment was 20 minutes. Over the first 5 min, the anodic dissolution produces the aluminum ions, which then reacts with hydroxide ions to produce Al(OH)_3 . The initiation of polymerization reaction takes place in 5–10 min after enough Al(OH)_3 was produced. The pollutant was mainly removed by monomeric species (Al(OH)_2^+ and Al(OH)_3) for first 10 minutes. It was well evident that, higher and longer the molecular weight and chain, the effectiveness of the inorganic polymer was increased for adsorbing, coagulating or flocculating pollutants (Lin and Lin, 1993; Ghaly *et al.*, 2014).

5.5.8 Rate Constant

The heterogeneous rate constant $k \text{ min}^{-1}$ with respect to the variation of anode rotation (n), current density (j), initial pH (pH_0) was also studied in the batch mode of operation. The results are presented in Table 5-3, which denotes that the rate constant gives a higher value of 0.024 min^{-1} at 60 rpm. Beyond this anode rotation speed, there was a decrease in the value of rate constant to 0.020 and 0.019 min^{-1} for 80 and 100 rpm, respectively. This was due to the diffusion controlled cathodic reduction and anodic oxidation of STW favoured at higher anode rotation speed.

Table 5-3: Effect of the anode rotation (n) on the performance of 3D rotating anode batch reactor.

Anode Rotation (n), rpm	Rate Constant, k (min⁻¹)
20	0.016
40	0.018
60	0.024
80	0.020
100	0.019

When the current density was increased upto 6 mA/cm², there was a noticeable improvement in the rate constant k as depicted in Table 5-4. The rate of transfer beyond 6 mA/cm² decreases due to the fact that an increase in the current density decreases the current efficiency and increases power consumption. In general, at higher current density gives higher capacity utilization, at the expense of more energy loss.

Table 5-4: Effect of the current density (j) on the performance of 3D rotating anode batch reactor.

Current Density (j), mA/cm²	Rate Constant, k (min⁻¹)
2	0.007
4	0.012
6	0.018
8	0.017
10	0.016

The rate transfer constant (Table 5-5) shows a good improvement of pH from basic to acidic and neutral condition. The optimum range of pH for the treatment of STW was found to be 6-8.

Table 5-5: Effect of the initial pH (pH_0) on the performance of 3D rotating anode batch reactor.

Initial pH (pH_0)	Rate Constant, k (min^{-1})
4	0.019
6	0.018
8	0.017
10	0.011

5.5.9 Batch Recirculation Reactor

The dynamic response of the 3D rotating anode reactor on the percentage COD removal at various input flow rates (q) was studied at constant condition of anode rotation (n) = 60 rpm, current density = 6 mA/cm², initial pH (pH_0) = 6 and initial COD concentration (C_0) = 861 mg/l.

5.5.9.1 Effect of the Electrolyte Flow Rate

The flow rate of the inlet STW during the treatment in batch recirculation mode was also found to affect the performance of the 3D rotating anode reactor in terms of COD removal efficiencies. The effect of flow rate on COD removal efficiency in the batch recirculation mode for the desired contact time has been studied. It was found that increasing the recirculation flow rate in turn increases the percentage COD removal. At 5 lph, a COD removal of 79.15% was observed and at 60 lph, it was increased to 94.40%. This can be the result of enhancement of the transfer coefficient at higher flow rates. At 90 and 120 lph of flow rate the back mixing phenomenon comes into play and the treatment efficiency was hindered due to the back mixing of the flocs generated at the time of treatment. So, the flow rate of 60 lph can be fixed as the optimum value.

The contact time can be calculated by using (R. Saravanathamizhan, Paranthaman, Balasubramanian and Ahmed Basha, 2008):

$$t_c = t \left(\frac{V_R}{V} \right) \quad (5.4)$$

Where, t_c and t are the contact and sampling time of the process.

V_R and V are the volume of the reactor and total volume used.

In the case of the 3D rotating anode batch recirculation reactor a higher circulation flow rate improved the process performance in all aspects. Keeping all the operating parameters as of the batch system, the performance in terms of percentage COD removal improved from 92.85% to 94.40% in 20 minutes of *treatment time* (t). Similarly, all the other operating parameters had incremental effect on the percentage COD removal.

Table 5-6: Effect of the electrolyte flow rate (q) on the performance of 3D rotating anode batch recirculation reactor.

Flow Rate (q), lph	Rate Constant, k (min^{-1})
5	0.009
15	0.010
30	0.011
60	0.012
90	0.012
120	0.012

The Table 5-6 depicts the increase in rate constant with the increase in the flow rate from 5 to 120 lph. The reason for increase in the rate constant till the flow rate of 60 lph can be due to the improved ionic conductivity by the bulk movement and the reduction of the resistance on the electrode surface. Comparing the batch recirculation system for the flow rate of 60 lph, with the batch system, it was observed that the batch recirculation system was superior than batch reactor in percentage COD removal and rate constant.

5.5.10 Single Pass System

The STW was not re-circulated nor did it remain like a batch system in the reactor. It was passed through the reactor in a single span of time only. The flow rates for single pass system were selected as 1 – 6 lph. This has given an insight in the process performance of the reactor in single pass system. The increase in the electrolyte flow rate (1 – 6 lph) lowers the rate constant (

Table 5-7).

Table 5-7: Effect of the flow rate (q) on the performance of 3D rotating anode single pass system.

Flow Rate (q), lph	Rate Constant, k (min ⁻¹)
1	0.0033
2	0.0034
3	0.0035
4	0.0020
5	0.0015
6	0.0010

Table 5-8 indicates that the increase in the current density improves the COD removal efficiency but at the expense of more energy consumption and unwanted side reactions.

Table 5-8: Effect of the current density (j) on the performance of 3D rotating anode single pass system.

Current Density (j), mA/cm ²	Rate Constant, k (min ⁻¹)
2	0.0025
4	0.0033

6	0.0040
8	0.0062
10	0.0088

5.6 Response Surface Methodology (RSM)

5.6.1 Interaction and optimization of parameters

In the present study, the response surface methodology (RSM) was used to determine the relation between percentage of chemical oxygen demand removal and operating parameters such as current density, electrolyte flow rate, supporting electrolyte concentration and anode rotation speed along with specific electrical energy consumption. Response surface methodology is a resourceful tool that is being used comprehensively in chemical process optimisation (Saravanathamizhan *et al.*, 2007; R Saravanathamizhan *et al.*, 2008; Montgomery, 2012; Palani and Balasubramanian, 2012). Table 5-9 provides the operating parameters along with their ranges. The current density, electrolyte flow rate, supporting electrolyte concentration and anode rotation speed are referred to by encoded variables as A, B, C and D respectively.

The Box–Behnken (BB) experimental design of response surface methodology was being chosen in order to find the relationship between the response functions and variables using the statistical software tool Design Expert 7 trial version. The three-level second-order design requires moderately lesser number of experimental data for specific prediction (Palani and Balasubramanian, 2012). A total number of 27 experiments with three centre points are carried out to investigate the percentage of COD removal with specific electrical energy consumption for the same. RSM is used to study the interaction between the variables and the analysis of variance (ANOVA). The value of R^2 determines the quality of the fit for this model.

Table 5-9: Range of variables used in textile wastewater degradation

Factor	Variable	Unit	Range and Levels		
			-1	0	+1
A	Current Density	mA/cm ²	2	6	10
B	Flow Rate	lph	5	60	120
C	Supporting Electrolyte Concentration	g/l	1	3	5
D	Anode Rotation Speed	Rpm	0	60	100

5.6.2 Development of regression equation

The operating parameters and dye removal were examined using CCD to establish a correlation between them. The analysis recommended a quadratic model for the response function. Table 5-10 gives the experimental runs for a three-level four factor Box–Behnken experimental design with three center points. The analysis focused on the impudence of independent variables, i.e. current density (A), electrolyte flow rate (B), supporting electrolyte concentration (C) and anode rotation speed (D) on maximum percentage COD removal with minimum specific electrical energy consumption (SEEC).

Table 5-10: Design of Experiments using RSM

Set No.	A: Current Density	B: Flow Rate	C: Supporting Electrolyte Concentration	D: Anode Rotation	Response 1: COD Removal Efficiency	Response 2: Specific Energy Consumption
	mA/cm ²	lph	g/l	Rpm	%age	J/mg COD
1	6	120	3	100	83.90	0.096
2	10	5	3	60	83.65	0.160

3	2	60	1	60	75.67	0.082
4	10	120	3	60	83.80	0.068
5	6	60	5	0	79.67	0.113
6	6	5	1	60	79.49	0.087
7	6	5	3	0	71.86	0.129
8	6	5	3	100	78.25	0.108
9	2	60	5	60	75.15	0.070
10	6	60	1	0	75.98	0.127
11	2	60	3	0	64.02	0.097
12	6	5	5	60	81.02	0.072
13	6	120	5	60	87.34	0.053
14	6	120	3	0	75.83	0.098
15	10	60	3	100	80.59	0.146
16	6	60	3	60	96.26	0.027
17	6	60	5	100	84.75	0.097
18	10	60	5	60	87.03	0.115
19	10	60	1	60	86.90	0.136
20	6	60	3	60	96.40	0.028
21	6	60	1	100	84.63	0.120
22	6	120	1	60	86.25	0.072
23	2	5	3	60	68.79	0.044
24	6	60	3	60	96.13	0.027
25	10	60	3	0	81.15	0.185
26	2	60	3	100	75.98	0.120
27	2	120	3	60	78.52	0.099

The quality of model was evaluated with the help of correlation coefficient value. The predicted R^2 is the quality measurement of the model to envisage the response value

and the adjusted R^2 is the extent of the amount of disparity about the mean as explained by the model (Montgomery, 2012). In this study, the value of the adjusted and predicted R^2 is 0.9882 and 0.9689 for COD removal; and 0.9982 and 0.9953 for SEEC, respectively. This depicts good concurrence between the experimental and predicted values. Table 5-11 shows that Quadratic model was best fitting the experimental data as supported by ANOVA which showed F-value of 157.76 and 1038.14 for responses of COD removal and specific electrical energy consumption (SEEC), indicating that the model was significant. There was only a 0.01% chance that a “Model F-Value” this large could occur due to noise (Montgomery, 2012).

Table 5-11: ANOVA for (a) COD removal and (b) specific electrical energy consumption (SEEC)

(a) COD Removal						
Source	Sum of Squares	df	Mean Square	F Value	p-value (Prob> F)	
Model	1553.27	14	110.94	157.76	< 0.0001	Significant
A-CD	376.54	1	376.54	535.44	< 0.0001	
B-FR	80.14	1	80.14	113.96	< 0.0001	
C-NaCl	4.48	1	4.48	6.38	0.0266	
D-Anode Rotation	131.42	1	131.42	186.88	< 0.0001	
AB	23.06	1	23.06	32.79	< 0.0001	
AC	0.10	1	0.10	0.15	0.7051	
AD	38.09	1	38.09	54.16	< 0.0001	
BC	0.04	1	0.04	0.05	0.8145	
BD	0.96	1	0.96	1.37	0.2637	
CD	3.75	1	3.757397	5.343023	0.0394	
A ²	540.68	1	540.6853	768.8552	< 0.0001	

B ²	341.43	1	341.4349	485.5208	< 0.0001	
C ²	119.82	1	119.8245	170.3906	< 0.0001	
D ²	522.74	1	522.7484	743.3488	< 0.0001	
Residual	8.43	12	0.703234			
Lack of Fit	8.40	10	0.840235	46.08233	0.0214	Not Significant
Pure Error	0.03	2	0.018233			
Cor. Total	1561.71	26				

(b) Specific Electrical Energy Consumption						
Source	Sum of Squares	df	Mean Square	F Value	p-value (Prob> F)	
Model	0.041672	14	0.002977	1038.14	< 0.0001	Significant
A-CD	0.00761	1	0.00761	2654.25	< 0.0001	
B-FR	0.001174	1	0.001174	409.4951	< 0.0001	
C-NaCl	0.000806	1	0.000806	281.2793	< 0.0001	
D- Anode Rotation	0.000302	1	0.000302	105.484	< 0.0001	
AB	0.005428	1	0.005428	1893.076	< 0.0001	
AC	2.03E-05	1	2.03E-05	7.062635	0.0209	
AD	0.001013	1	0.001013	353.3912	< 0.0001	
BC	3.89E-06	1	3.89E-06	1.356612	0.2668	
BD	9.62E-05	1	9.62E-05	33.54637	< 0.0001	
CD	1.77E-05	1	1.77E-05	6.167687	0.0288	

A ²	0.012114	1	0.012114	4225.14	< 0.0001	
B ²	0.00184	1	0.00184	641.5841	< 0.0001	
C ²	0.003443	1	0.003443	1200.983	< 0.0001	
D ²	0.019424	1	0.019424	6774.61	< 0.0001	
Residual	3.44E-05	12	2.87E-06			
Lack of Fit	3.37E-05	10	3.37E-06	10.12193	0.0932	Not Significant
Pure Error	6.67E-07	2	3.33E-07			
Cor. Total	0.041707	26				

The mathematical relationship between the independent variables and their responses can be related in terms of encoded variables as:

$$\begin{aligned}
 \text{COD} = & +96.15 + 5.75 * A + 2.650505 * B + 0.627958 * C + 3.31339 * \\
 & D - 2.39 * A * B + 0.16 * A * C - 3.04 * A * D - 0.10 * B * C + \\
 & 0.48 * B * D - 0.95 * C * D - 10.06 * A^2 - 8.01 * B^2 - 4.73 * C^2 - \\
 & 10.40 * D^2
 \end{aligned} \tag{5.5}$$

$$\begin{aligned}
 \text{SEEC} = & +0.02 + 0.02 * A - 0.01 * B - 0.0084 * C - 0.0050 * D - \\
 & 0.03 * A * B - 0.0022 * A * C - 0.0157 * A * D - 0.00099 * B * C + \\
 & 0.0048 * B * D - 0.0020 * C * D + 0.04 * A^2 + 0.018 * B^2 + 0.025 * \\
 & C^2 + 0.063 * D^2
 \end{aligned} \tag{5.6}$$

5.6.3 Adequacy

The model predictions using the relation equations were compared with the experimental observations in Figure 5-9 and Figure 5-10. The comparison shows that the model predictions harmonized agreeably with the experimental values.

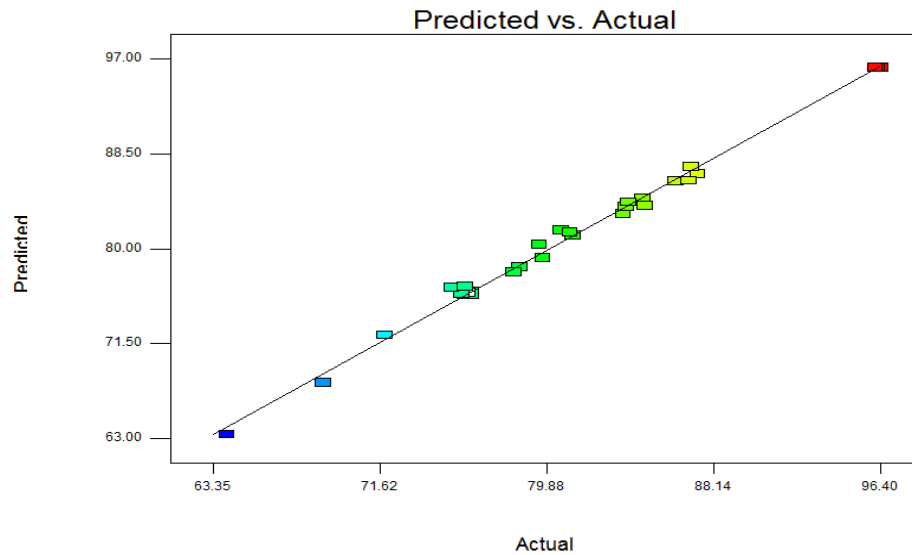


Figure 5-9: Actual vs Predicted COD Removal Efficiencies

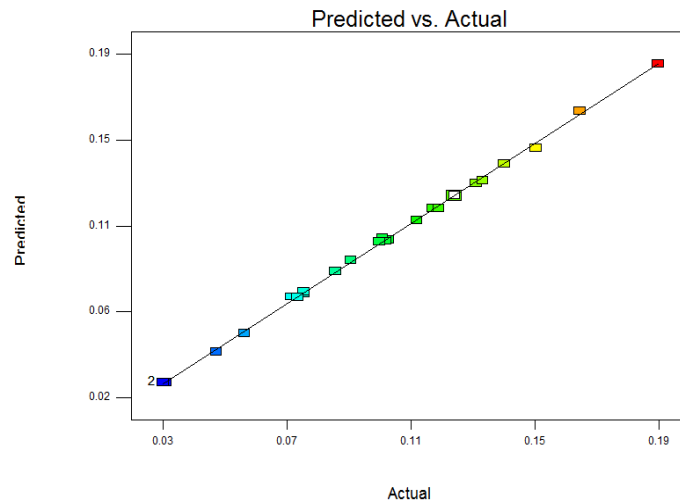


Figure 5-10: Actual vs Predicted Specific Electrical Energy Consumption

The residual data also helps in analysis of suitability of model. Normal probability and residual plots helps in its diagnosis. The residuals should follow a normal distribution indicating that the points in the normal probability plot are adhering to a straight line (Hassani *et al.*, 2015). As depicted in

Figure 5-11 and Figure 5-12; the normal probability against the internally studentized residual plot was in normal distribution. The comparison of the deviation of actual points from the fitted surface relative to pure error was tested by “Lack of fit” (Anderson and Whitcomb, no date). The Prob. > F of “lack-of-fit” for the model was

0.0214 and 0.0932 for COD and SEEC respectively. This depicts that the lack of fit was insignificant relative to the pure error. The applicability of the model for predicting the response variables within the range of operating parameters were being studied to exhibit a non-significant lack of fit in the model.

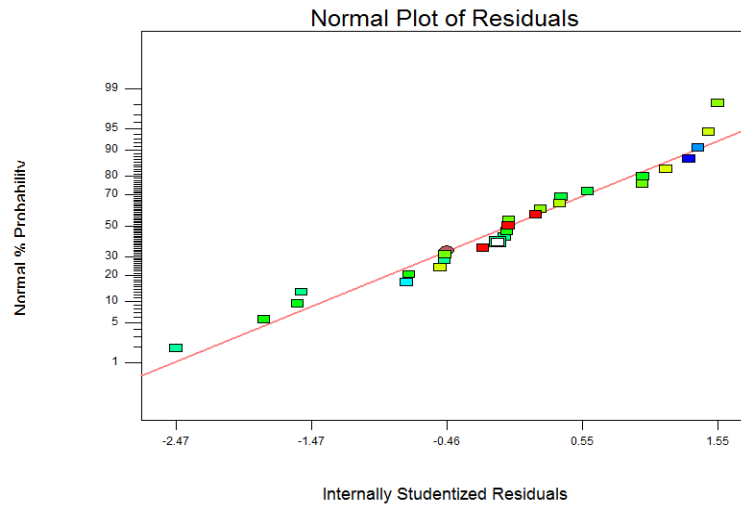


Figure 5-11: Normal probability curve for COD Removal

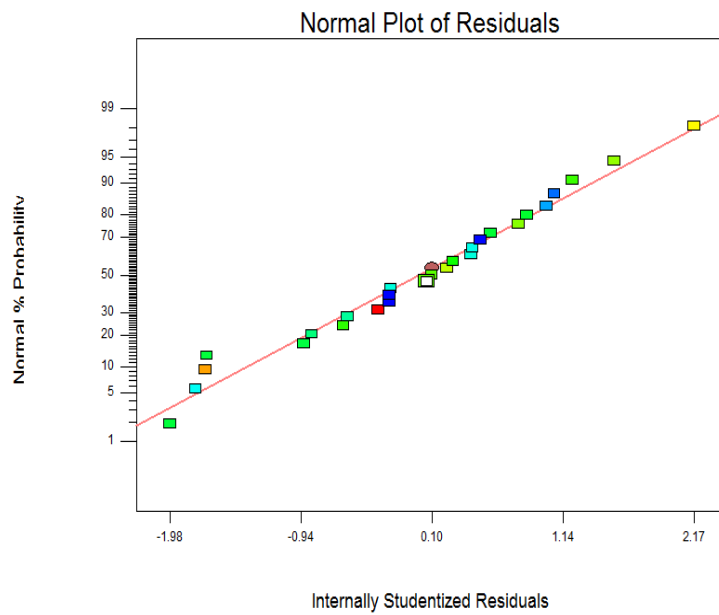
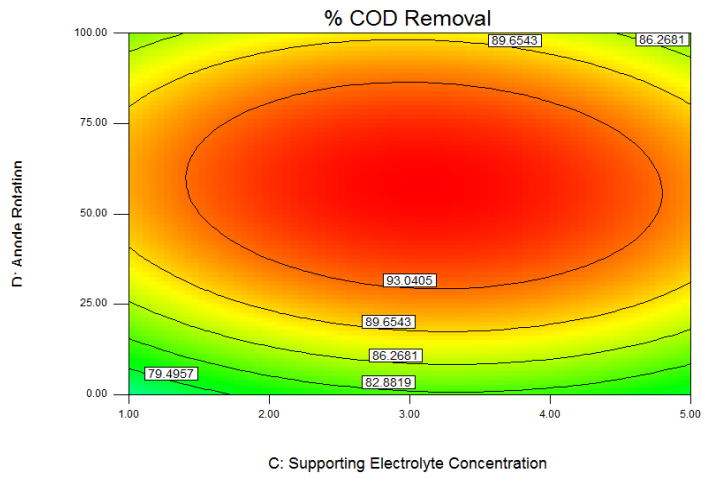


Figure 5-12: Normal probability curve for Specific Electrical Energy Consumption (SEEC)

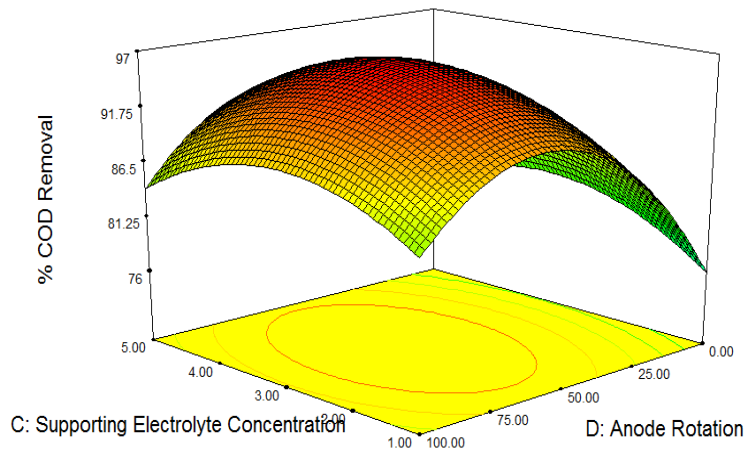
5.6.4 Combined Effects of operating parameters on COD and SEEC

In order to verify the impudence of operating parameters on STW degradation, the optimization was done and the results of analysis carried out are being presented in Figure 5-13 - Figure 5-18 depicting the effects on percentage COD removal and SEEC respectively. It can be ascertained from Figure 5-13 - Figure 5-15; that the percentage of chemical oxygen demand removal increases with anode rotation speed with variation of supporting electrolyte concentration, current density and flow rate; and reaches a maximum at 60 rpm. No significant development in percentage chemical oxygen demand removal was obtained when the anode rotation speed was increased beyond 60 rpm. This was due to the fact that increasing the anode rotation speed beyond the optimum rotation speed favours the anodic reduction, and in addition induces back mixing phenomenon in the system (Palani and Balasubramanian, 2012). As the anode rotation speed increases, the turbulence inside the system increases. This in turn, improves the mixing inside the reactor and reduces the diffusion layer thickness at the surface of the electrode which increases the percentage COD removal (Palani and Balasubramanian, 2012). This inspection matches qualitatively with the experimental findings of El-Ashtoukhy et al. 2014 (El-Ashtoukhy and Yasmine, 2014).

As shown in Figure 5-16 - Figure 5-18; the specific electrical energy consumption decreases with increase in supporting electrolyte concentration. The increase in supporting electrolyte concentration increases the conductivity of the wastewater, in turn increasing the current potential of the system and thus reducing the specific electrical energy consumption. In case of current density and flow rate; as they increases the SEEC increases. As the anode rotation increases beyond an optimum level, the SEEC increases due to the fact that increased turbulence beyond optimum level favours anodic reduction and back mixing.

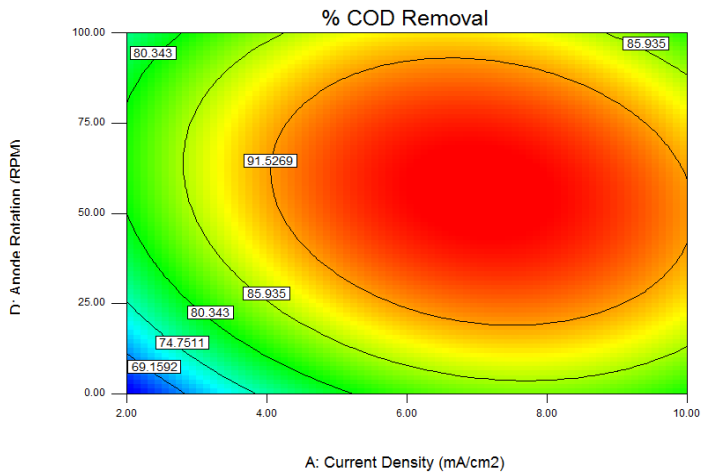


(a)

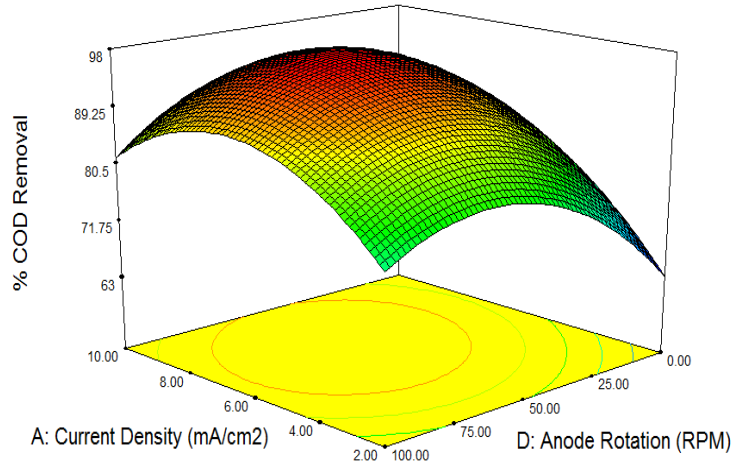


(b)

Figure 5-13: Combined Effects of supporting electrolyte concentration and anode rotation speed on percentage COD removal: (a) Contour plot and (b) Response Surface

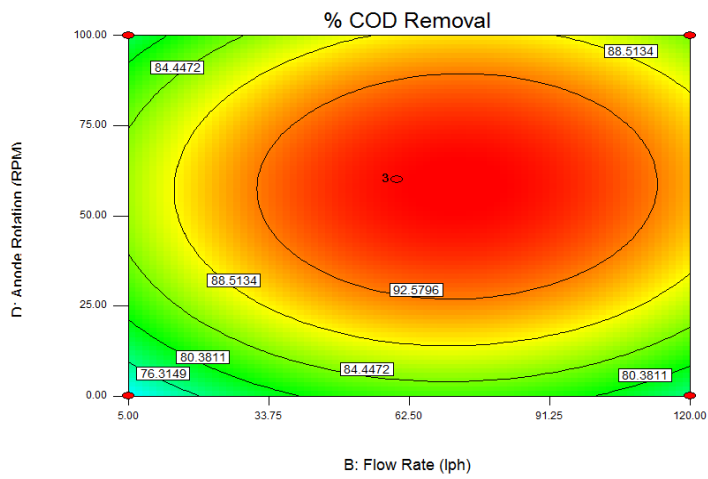


(a)

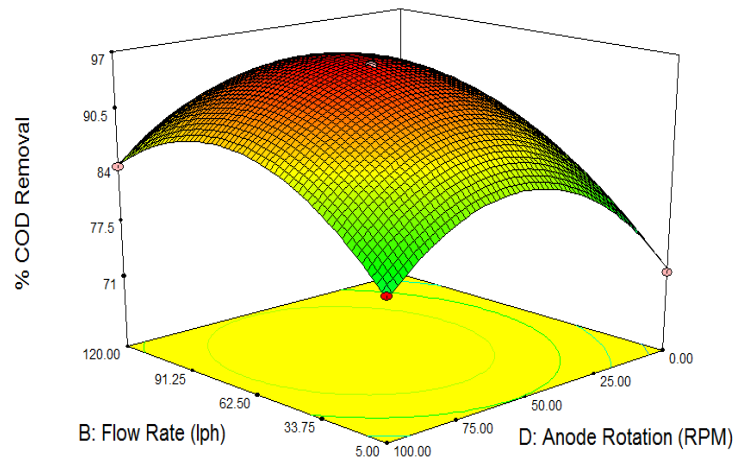


(b)

Figure 5-14: Combined Effects of current density and anode rotation speed on percentage COD removal: (a) Contour plot and (b) Response Surface

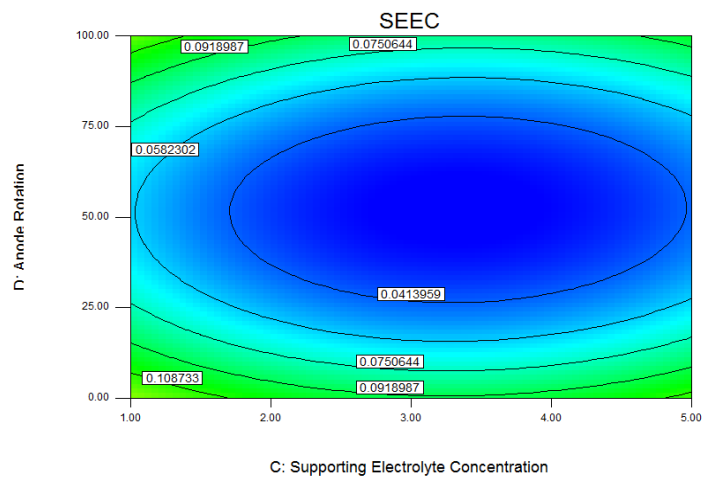


(a)

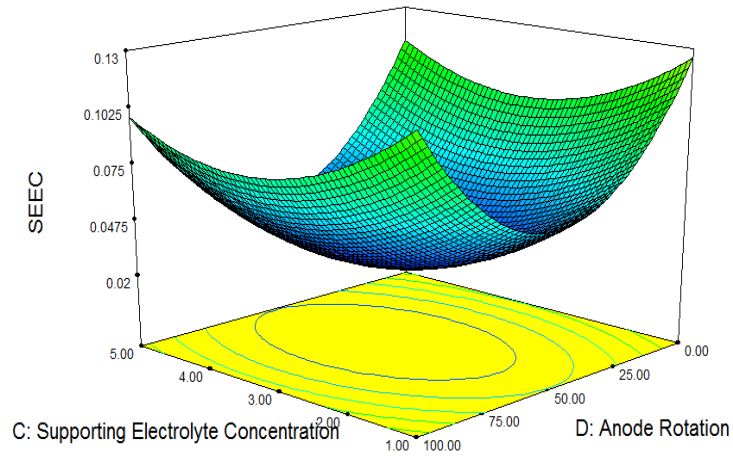


(b)

Figure 5-15: Combined Effects of flow rate and anode rotation speed on percentage COD removal: (a) Contour plot and (b) Response Surface

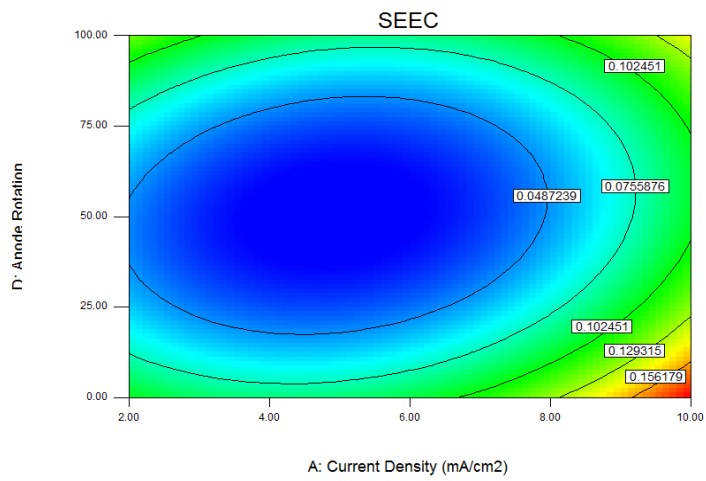


(a)

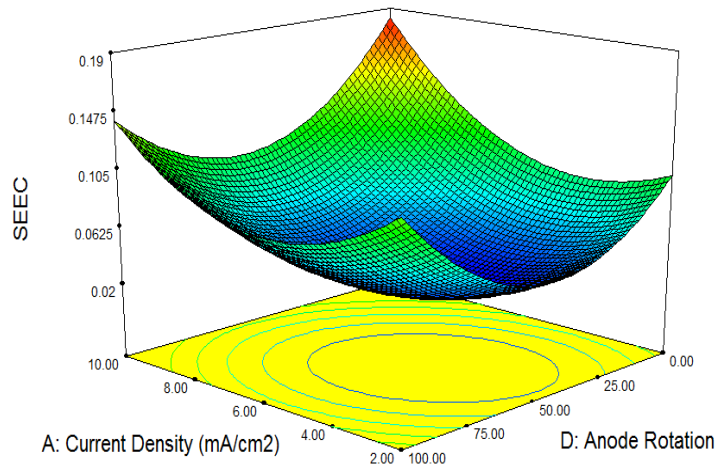


(b)

Figure 5-16: Combined Effects of supporting electrolyte concentration and anode rotation speed on specific electrical energy consumption: (a) Contour plot and (b) Response Surface

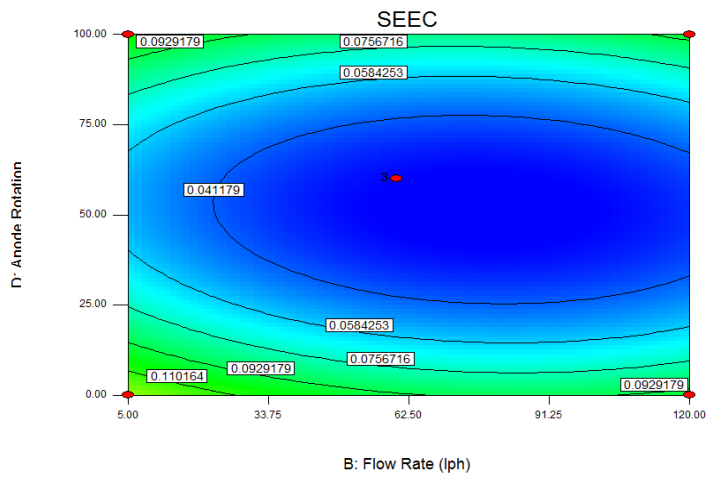


(a)

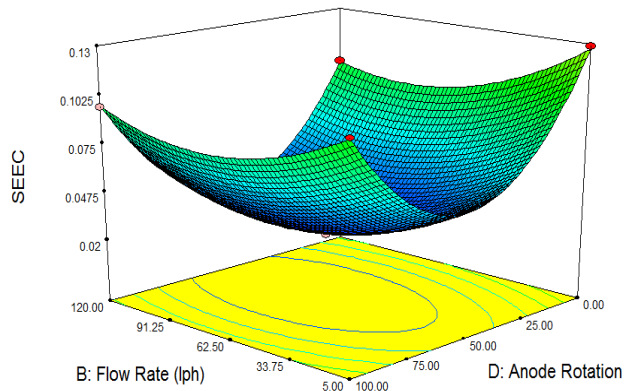


(b)

Figure 5-17: Combined Effects of current density and anode rotation speed on specific electrical energy consumption: (a) Contour plot and (b) Response Surface



(a)



(b)

Figure 5-18: Combined Effects of flow rate and anode rotation on specific electrical energy consumption: (a) Contour plot and (b) Response Surface

5.6.5 Optimization of Model and its verification

The main objective of the optimization was to determine the optimum values of operating variables for maximum percentage of COD removal with minimum specific electrical energy consumption (SEEC). In optimization process, the target COD removal percentage = max and specific electrical energy consumption (SEEC) = min. The comparisons of optimized and experimental results are shown in Table 5-12. As shown in Table 5-12; the experimental verification of optimized/predicted results shows good agreement with the experimental results (Sinha, Singh and Mathur, 2014).

Table 5-12: Comparison of optimized and experimental results for COD removal and specific electrical energy consumption (SEEC)

Current Density (mA/cm ²)	Flow Rate (lph)	Supporting Electrolyte Concentration (g)	Anode Rotation (rpm)	Percentage COD Removal		Specific Electrical Energy Consumption	
				Optimized/Predicted	Experimental	Optimized/Predicted	Experimental
6.26	74.21	3.04	54	96.86	95.98	0.025	0.026
6.25	70.90	3.55	53	96.59	96.02	0.025	0.026
6.25	84.28	3.23	56	96.50	95.67	0.025	0.027
5.89	71.88	3.20	60	96.50	95.38	0.025	0.026
6.24	66.71	3.03	49	96.53	95.57	0.026	0.027
6.05	75.35	3.54	55	96.43	94.98	0.024	0.025
6.01	76.27	3.50	56	96.41	95.08	0.024	0.026
5.90	72.20	3.03	56	96.50	95.72	0.024	0.025

5.96	73.24	3.11	53	96.52	95.23	0.024	0.026
6.36	81.11	3.11	52	96.66	96.1	0.025	0.027

5.7 Comparison of Plate Electrode and 3D stationary anode reactor

The use of plate electrode reactor for the electrochemical treatment of textile wastewater is commonly used as per available literature (Irdemez, Yildiz and Tosunolu, 2006; Yahiaoui *et al.*, 2011; Bayar *et al.*, 2014; Rodríguez *et al.*, 2015). The performance of 3D stationary anode reactor was compared with plate electrode reactor for treatment of synthetic textile wastewater. The aluminium was used as anode and cathode material for present experimental investigations. For each set of operating parameters; experiments were carried out in triplets and average values of response are reported. The performance of both the reactors was evaluated in terms of color removal efficiency, COD removal efficiency and energy consumption.

5.7.1 Color Removal

The color removal efficiency of 3D stationary and plate electrode reactor was studied for current density of 2 – 10 mA/cm². There was an improvement in color removal efficiency for the similar applied current density for 3D stationary anode reactor as compared to plate electrode reactor. As the current density increases the color removal efficiency increases for both the reactor configurations. When current density was increased from 8 – 10 mA/cm², the improvement in color removal efficiency was limited due to the fact that the fouling of electrode begins at these values of current density as presented in

Table 5-13.

Table 5-13: Color Removal efficiency comparison between conventional plate electrode reactor and 3D stationary anode reactor

Current Density (mA/cm ²)	Color Removal Efficiency (%)	
	Plate Electrode Reactor	Stationary 3D Electrode Reactor
2	88.50	92.50
4	90.58	93.58
6	92.88	95.88
8	93.66	97.66
10	93.89	97.97

As shown in Table 5-13, the conventional plate electrode reactor has inferior color removal efficiency as compared to 3D stationary anode reactor. This was due to the fact that the 3D anode acts as a turbulence enhancer and increases the mass transfer near the electrode which in turn increases the efficiency of the system. There was a constant improvement in stationary 3D anode reactor efficiency in comparison to conventional plate electrode reactor.

5.7.2 COD Removal

There was a significant effect of current density on treatment efficiency in an electrochemical technique (Ni'am *et al.*, 2007). It was observed that increase in the current density resulted in an increase in COD removal efficiency, when other affecting parameters were kept constant. This effect can be explained by the Faraday's law, according to which an increase in current density will lead more generation of

metal ions and hence more metal hydroxides generation ultimately resulting in increased removal efficiencies (El-Shazly and Daous, 2013).

The mechanism of COD removal involves two stages namely destabilization and aggregation. The optimum COD removal depends on these stages which in turn (as a function of) depend on current density. As shown in Figure 5-19; the COD removal efficiency of plate electrode reactor was deficient than 3D stationary anode reactor. It was due to the fact that 3D stationary anode enhances the turbulence in the reactor which in turn provides better mixing conditions and hence reducing short circuiting and fouling of electrode.

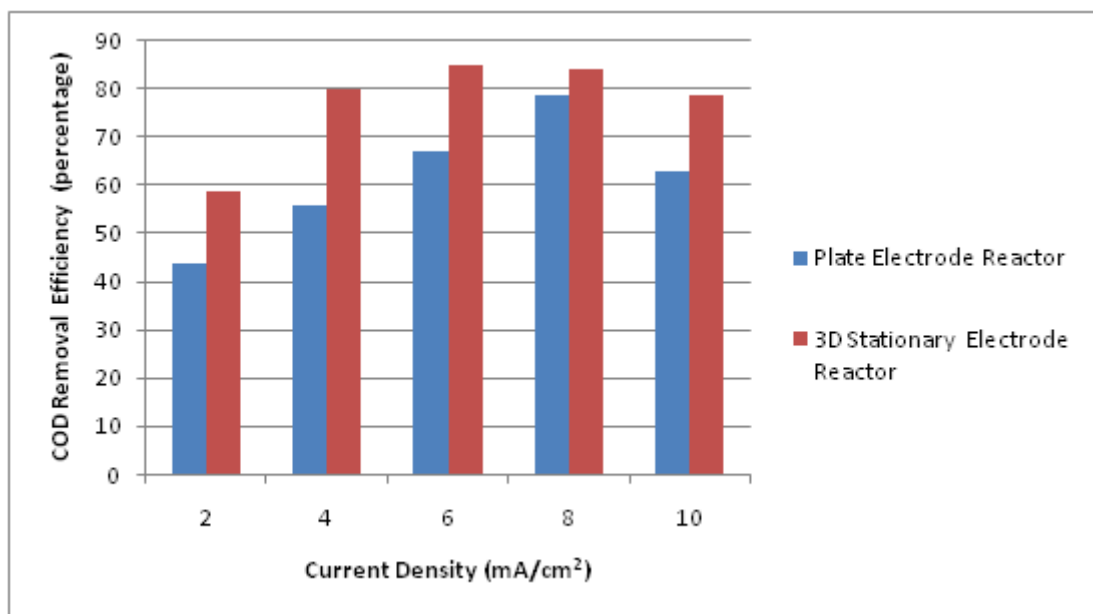


Figure 5-19: Effect of current density on COD removal efficiency of plate electrode reactor and 3D stationary anode reactor

5.7.3 Energy Consumption

In electro coagulation technique of treatment, total electrical energy consumed depends on applied voltage, current and detention. Many researchers have shown that optimized combination of applied voltage, time and current assure high treatment efficiency. The applied current directly affects metal ion generation and consequently treatment; but if too high current is supplied it will be wasted in heating up of the system i.e. efficiency of the system will decrease (Lai and Lin, 2004). Thus, energy

consumed for unit COD removal was calculated for 3D stationary anode reactor and plate electrode reactor.

For all experiments in continuous flow reactor, energy consumed for 60 minutes of running time, after pseudo steady state was calculated. Energy consumed for unit removal of COD (1 mg of COD) in each experiment was calculated and reported here as specific energy consumed. Specific energy consumed for unit COD removal was analyzed with corresponding Y_{COD} to find out the energy efficiency of the system.

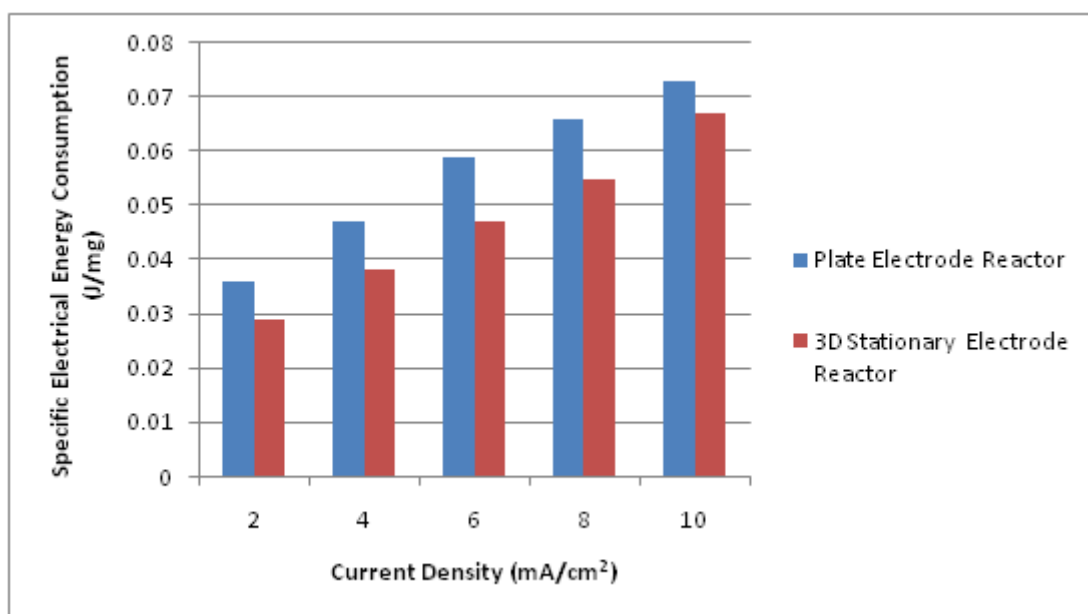


Figure 5-20: Effect of current density on SEEC of plate electrode reactor and 3D stationary anode reactor

As shown in Figure 5-20; the energy consumed for unit removal of COD for current density ranging from 2 – 10 mA/cm² shows an increasing behaviour as the removal efficiencies depicts similar behaviour. The energy consumed for unit COD removal in plate electrode reactor was always higher than the 3D stationary anode reactor. This can be attributed from the COD and color removal efficiencies of both the systems. So, the energy consumption in plate electrode reactor was more than 3D stationary anode reactor for same current density.

5.8 Comparison of 3D stationary and rotating anode reactor

The comparison of color, COD removal efficiency, anode consumption and specific electrical energy consumption (SEEC) between 3D stationary and rotating anode reactor gives the insight of better performance of the 3D rotating anode reactor for the treatment of textile wastewater. The better efficiency highlights the impact of better mixing imparted by 3D rotating anode which increases the mass transfer inside the reactor and in turn enhances the efficiency of the system.

5.8.1 Color Removal

The color removal efficiency of stationary and 3D rotating cylindrical anode reactor was studied for anode rotation speed ranging between 0 - 100 rpm. The flow rate was adjusted for desired detention time. Various runs were carried out to study the effect of EC on absorbance of the effluent coming out after EC.

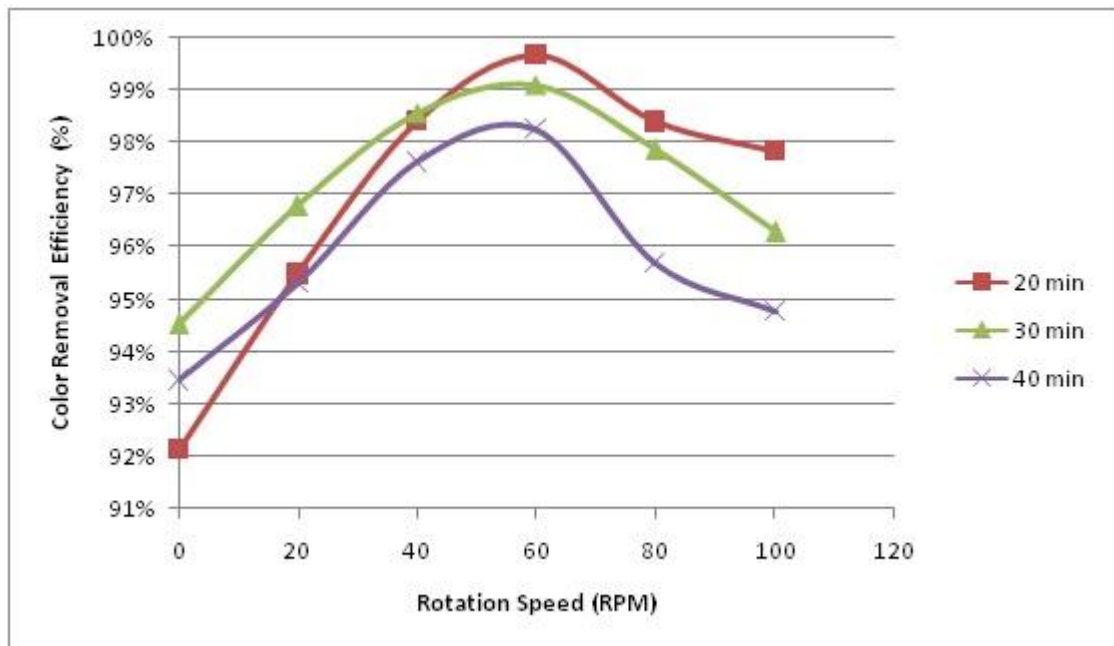


Figure 5-21: Color Removal comparison between continuous 3D stationary and rotating Reactor

As depicted in Figure 5-21; as the detention time increases the color removal efficiency increases when the anode was stationary (at 0 rpm) till 30 min of detention

time. Above 30 min of detention time, the efficiency decreases as the phenomenon of back mixing comes into play. For the rotating configuration; as the anode rotation speed increases from 20 rpm to 100 rpm, the efficiency increases along with detention time due to the fact that the 3D rotating anode acts as a turbulence enhancer. As it attains the rotation of 60 rpm for detention time of 20 min, the maximum removal efficiency was achieved. As it can be seen if the detention time or rotation speed increases further; the efficiency decreases, probably due to enhanced turbulence resulting in breaking down of flocs and back mixing in the system.

5.8.2 COD Removal

As shown in Figure 5-22; in case of non rotating reactor configuration (at 0 rpm), when the detention time is changed from 20 to 30 min with a constant current density 8 mA/cm^2 , the COD removal was increased from 71.77% to 78.18%. This coincides with the fact that for shorter detention time of 20 min, the time was not sufficient to complete the process. Therefore, the COD removal is better at 30 min of detention time. Whereas; in case of rotating reactor configuration, the optimum detention time was found to be 20 min as the rotation of the anode increases the turbulence inside the reactor. This shortens the detention time for the pollutant to get treated as the mixing inside the reactor increases. The maximum COD removal achieved was 96.40% for 6 mA/cm^2 as shown in Figure 5-22.

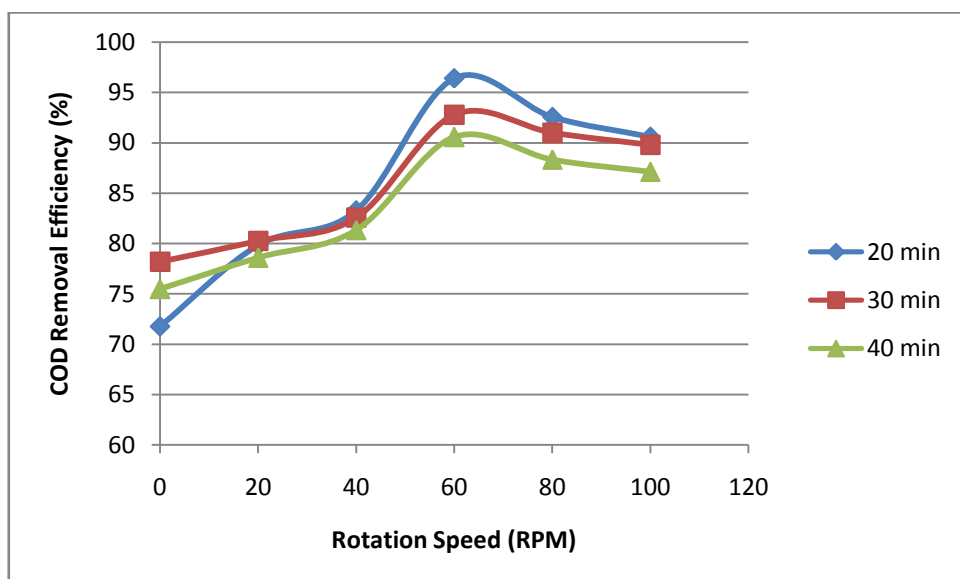


Figure 5-22: Effect of detention time on COD removal efficiency of Non Rotating and rotating 3D cylindrical anode reactor

The detention time was further increased to 40 and 50 min, the COD removal efficiency decreased to 64.98% and 75.91% for non-rotating and rotating reactor configurations respectively. It was due to the fact that for increased detention time, the pollutant in wastewater goes on decreasing and simultaneously aluminium hydroxides generation increases. This increased aluminium hydroxides does not found pollutants for removal, so beyond optimal point, COD removal efficiency remains nearly constant (Kumar *et al.*, 2004).

While for quicker detention time i.e. 10 min, the COD removal efficiency was not good. It was observed to be 46.48% and 69.40% for non-rotating and rotating configurations respectively. It was due to the fact that the metal ion (Al^{3+}) dosage was not sufficient to destabilize all colloidal and finely suspended particles (Ni'am *et al.*, 2007).

5.8.3 Anode Consumption

In electro coagulation technique of treatment, total electrode consumption depends on applied current density and detention time. Many researchers have shown that optimized combination of applied current density and detention time assure high treatment efficiency with optimized electrode consumption. The applied current directly affects metal ion generation and consequently treatment; but if too high current is supplied it will be wasted in heating up of the system i.e. efficiency of the system will decrease (Lai and Lin, 2004). Thus, electrode consumption for unit COD removal was calculated for stationary and Rotating anode.

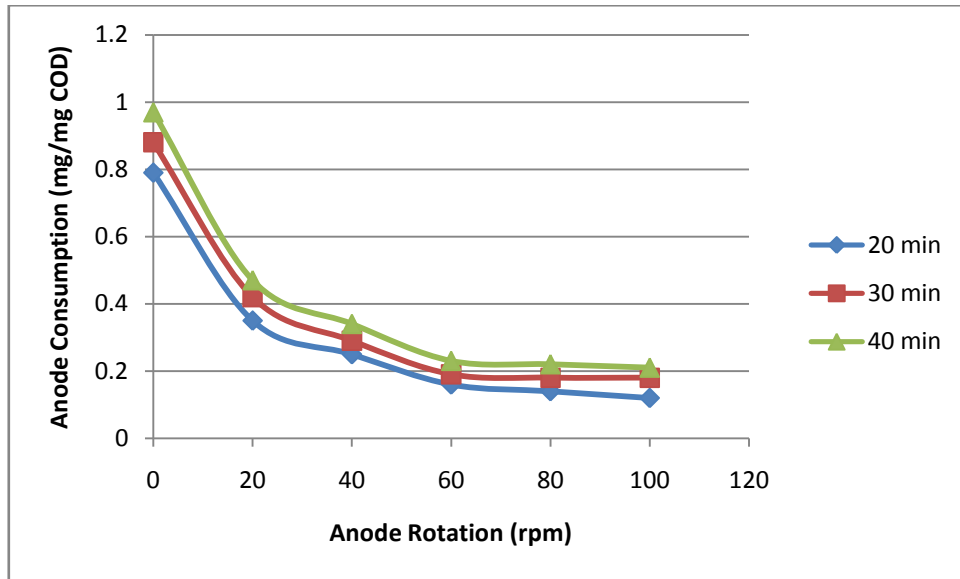


Figure 5-23: Effect of anode rotation speed on electrode consumption

As shown in Figure 5-23; the electrode consumed for unit removal of COD for 20 min of detention time for non rotating reactor configuration (at 0 rpm) is 0.79 mg but for rotating reactor configuration it varies from 0.35 to 0.12 mg as current density was increased which was approximately 50-80% less than non rotating reactor configuration.

As the detention time was increased to 30 and 40 min, the electrode consumption for non rotating reactor configuration is 0.97 mg but for rotating reactor configuration it was found out to be 0.47 to 0.21 mg.

5.8.4 Energy Consumption

In electro coagulation technique of treatment, total electrical energy consumed depends on applied voltage, current and detention. Many researchers have shown that optimized combination of applied voltage, time and current assure high treatment efficiency. The applied current directly affects metal ion generation and consequently treatment; but if too high current is supplied it will be wasted in heating up of the system i.e. efficiency of the system will decrease (Lai and Lin, 2004). Thus, energy consumed for unit COD removal was calculated for stationary and Rotating anode.

As shown in Figure 5-24; the energy consumed for unit removal of COD for 20 min of detention time for non rotating reactor configuration (at 0 rpm) is 0.047 J/mg but for rotating reactor configuration it varies from 0.016 to 0.046 J/mg as current density was increased which was approximately 50% less than non rotating reactor configuration.

As the detention time was increased to 30 min, the energy consumption for non rotating reactor configuration is 0.055 J/mg but for rotating reactor configuration it was calculated to be 0.017 to 0.049 J/mg COD.

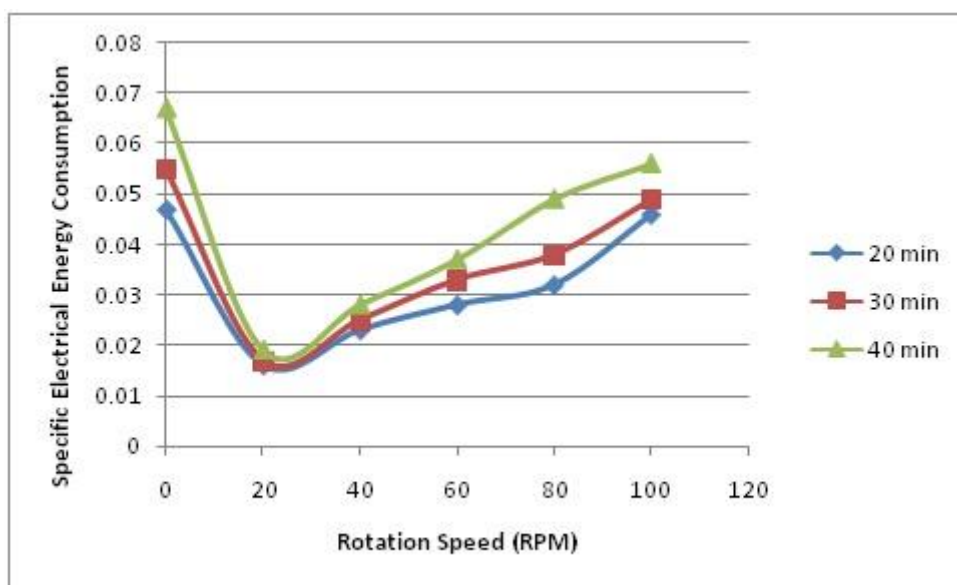


Figure 5-24: Specific Electrical Energy consumption

Further on increasing the detention time to 40 min; the energy consumption for both non-rotating and rotating reactor configuration increases; whereas COD removal decreases due to the fact that now the energy is wasted up in heating.

So, the energy consumed for maximum COD removal was found to be 0.028 J/mg, which was 40.42% less for the similar results in non rotating reactor configuration.

5.9 Zeta Potential

The electrostatic interaction between pollutant and electrochemically generated aluminium species helps in understanding the removal mechanism. When the net

charge on the particle is zero, it is referred as iso-electric point at a particular pH value. So, without variation of pH, it is inevitable to measure zeta potential of the solution (Cañizares *et al.*, 2006; Srivastava *et al.*, 2006).

The increase in pH from 4 to 6, the zeta potential shifts towards the neutral side. This confirms that the release of cations from electrodes decreases with increase in pH. Further increase in pH value to 8, shifts the zeta potential more towards the neutral or positive side. This can be due to the fact that heavy particles of aluminium hydroxide are formed and precipitates out and settle to the bottom of the reactor. The settling process also favours the sweeping of pollutant in the system. The mechanisms observed in this study for removal of pollutant were charge neutralisation mainly of negatively charged colloids by cationic hydrolysis products formed at less initial pH. The other mechanism followed was sweep coagulation of the colloidal impurities by the amorphous hydroxide precipitate at higher initial pH (Singh, Srivastava and Mall, 2013b).

5.10 Adsorption study

5.10.1 Adsorption isotherms

The adsorption data obtained at different initial pollutant concentration is fitted into four different isotherm models viz. Langmuir, Freundlich, Temkin and Dubinin-Radushkevich to investigate the reaction kinetics and removal mechanism.

The isotherms values shown in Table 5-14; implies that the adsorption data fitted well with all the isotherms. As the value of R^2 is highest in Tempkin isotherm but the Q_m value of 735.92 mg/g observed for the Langmuir isotherm model makes it more acceptable. As depicted by the $1/n$ value of >1 observed for Freudlinch isotherm shows and confirms that adsorption is favourable (Adeogun and Balakrishnan, 2016).

Table 5-14: Isotherm parameters for EC removal of STW

Isotherm	Parameters	Values
Langmuir	$Q_{\max}/\text{mg g}^{-1}$	735.92
	$b/L \text{ mg}^{-1}$	0.26
	R_L	0.054
	R^2	0.996
Freundlich	$K_F/\text{mg g}^{-1} (\text{mg L}^{-1})^{-1/n}$	176.85
	N	0.52
	R^2	0.991
Tempkin	$A_T/L \text{ g}^{-1}$	12.43
	$B_T/J \text{ mol}^{-1} \text{ g mg}^{-1}$	2.03
	R^2	0.997
Dubinin-Radushkevich	$Q_s/\text{mg g}^{-1}$	624.26
	$E/\text{kJ mol}^{-1}$	5.56×10^{-7}
	R^2	0.951

5.10.2 Reaction kinetics

The plots of four different kinetic models viz. Pseudo First Order, Second Order, Elovich and Avramin used to explain the adsorption data are studied. The pseudo-first-order kinetic model fitted well with experimental data in comparison to other models studied. The R^2 value is also highest for pseudo-first-order kinetic model. As the input pollutant concentration increases up to 75 mg/L, the rate constant for all studied models increases while it decreases at 100 mg/L. This can be the effect of lesser electrostatic interaction between the particles, thus reducing the adsorption rate. The Elovich constant also shows that this process of adsorption is behaving in multiple steps indicating more than one mechanism of adsorption (Adeogun and Balakrishnan, 2016).

5.10.3 Adsorption mechanism

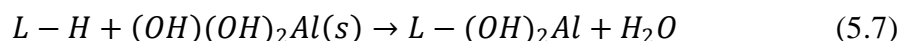
The intra-particulate diffusion model is studied for investigation of removal mechanism by adsorption. The adsorption data is fitted into this model. The study of this model shows the multi-linearity function of the data imparting the subsistence of two successive adsorption steps. The study of these two stages shows that the first stage is faster and short than the second stage. In first stage, boundary layer diffusion is occurring. The second stage is intra-particle diffusion stage which also acts as a rate controlling step (Adeogun and Balakrishnan, 2016).

5.11 *Solid Residue Generation and Analysis*

The analysis of the sludge is being done in order to understand the removal mechanism taking place in this new 3D RCE electrochemical reactor. The XRD, TGA, DTA and DTG analysis is done on sludge to understand the nature of residues formed during the treatment process.

5.11.1 XRD Analysis

The X-ray analysis reveals the major species formed during electrochemical treatment and helps to understand the insight of the mechanism taking place for removal of pollutant. It was analysed for current density of 6 mA/cm², having pH varied from 4-8 with anode rotation of 60 rpm, NaCl concentration of 3 g/l and electrolysis time of 20 min. According to the following reaction, the pollutant can act as a ligand (L) to bind aluminium hydroxides or hydrates, during the treatment process (Zidane *et al.*, 2008):



The species generated at pH ~ 4 were largely monomeric in nature and only traces of polymeric species are recorded. It can be in relation to electrostatic phenomena that are taking place and further ascribed to the appearance of hydrate particles or aluminium hydroxides having positive or negative charge. These species are generally

($[\text{Al}(\text{OH}_2)_6]^{3+}$, $[\text{Al}(\text{OH})_4]^-$ or $[\text{Al}(\text{OH})_4(\text{OH})_2]^-$) which are capable of attracting the opposite charge on pollutant and remove it from solution (Ibanez *et al.*, 1998).

The presence of both monomeric and polymeric hydroxides as major species produced during electrochemical treatment of simulated textile wastewater with pH ~ 6 as shown in Figure 5-25. As indicated, the interaction between pollutant and monomeric species ($\text{Al}(\text{OH})_3$) for removal of pollutant takes place. Apart from this, the pollutant was efficiently coagulated with polymeric species. The mechanism mainly followed with polymeric species is adsorption and charge neutralization (Zidane *et al.*, 2008). The capability of polymeric aluminum species to have both positive and negative charge makes them feasible for attraction of oppositely charged polluting species. The importance of attraction phenomenon between polluting species and polymeric aluminum species are more significant than in between polluting species and monomeric aluminum species ($\text{Al}(\text{OH})_2^+$, $\text{Al}(\text{OH})_2^+$, and $\text{Al}(\text{OH})_4^-$).

The electrochemical treatment was done over a time of 20 minutes. Over the first 5 min, the anodic dissolution produces the aluminum ions, which then reacts with hydroxide ions to produce $\text{Al}(\text{OH})_3$. The initiation of polymerization reaction takes place in 5–10 min after enough $\text{Al}(\text{OH})_3$ was being produced. The pollutant was mainly removed by monomeric species ($\text{Al}(\text{OH})_2^+$ and $\text{Al}(\text{OH})_3$) for first 10 minutes. It is well evident that, higher and longer the molecular weight and chain, the effectiveness of the inorganic polymer is increased for adsorbing, coagulating, or flocculating pollutants (Lin and Lin, 1993; Ghaly *et al.*, 2014).

The metallic hydroxide ($\text{Al}(\text{OH})_3$) particles were produced upto an ample concentration when the electrochemical treatment is pursued for 20 min which in turn initiate polymerization reactions. This induces the formation of white gelatinous precipitate (polymeric species) (Zidane *et al.*, 2008). These polymeric species contribute in removal of reasonably high amount of pollutant.

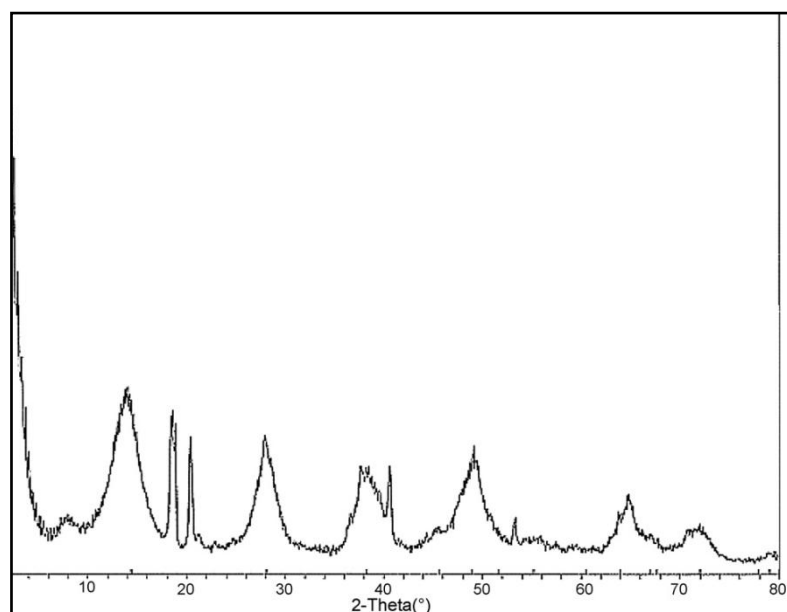


Figure 5-25: XRD Analysis of Sludge generated during electrolysis at pH ~ 6 (Major Species are $\text{Al}(\text{OH})_3$, Aluminium chloride Hydroxide Hydrate and Aluminium Oxide Chloride Hydroxide).

The XRD analysis of sludge generated during pH ~ 8 shows that it behaves similar to that generated at pH ~ 6. The removal mechanism is based on co-precipitation with metallic hydroxides ($\text{Al}(\text{OH})_3$, $\text{AlCl}(\text{OH})_2 \cdot 2\text{H}_2\text{O}$, $\text{Al}_{45}\text{O}_{45}(\text{OH})_{45}\text{Cl}$). At this pH, the formation of metallic hydroxide was limited and a small fraction of Al^{3+} which was generated by anodic dissolution remains in the system in the form of aluminate ion ($\text{Al}(\text{OH})_4^-$). This is the dominating species above pH ~ 8 (Holt *et al.*, 2002).

5.11.2 SEM-EDAX and Pore size distribution of solid residue

The evaluation of the surface of sludge and scum produced at the time of treatment shows that the texture of sludge was amorphous and that of scum was hard. These residues contain pores of various sizes. All the residues were mesoporous in nature. BET and BJH surface area and pore volume were highest for sludge residue as shown in Table 5-15.

EDX analysis was used to evaluate the elemental composition in solid EC residue. The sludge contained 19.06% of carbon, 35.87% of oxygen, 36.45% of aluminium,

1.69% of chlorine, 1.42% of sodium by mass whereas, the scum contains 33.25% of carbon, 30.15% of oxygen, 20.75% of aluminum, 6.12% chlorine and 5.25% sodium. This confirms that the scum contains higher amount of carbon whereas, the sludge contains higher amount of aluminum. This confirms that the treatment occurred by the combination of aggregation, sweep coagulation and floatation.

Table 5-15: Textural characteristics of solid residues

Textual Characteristics			
Parameters	Scum with Wastewater	Sludge with Wastewater	Sludge without Wastewater
BET Surface Area (m²/g)	21.22	388.95	370.44
BJH Surface Area (m²/g)	22.47	383.12	360.82
BJH Pore Volume (cm³/g)	0.0409	0.318	0.2615
BJH Pore Diameter (Å⁰)	71.07	32.63	29.86

5.11.3 Thermal Degradation Analysis

The thermal degradation kinetics of sludge residue is studied with the help of thermo gravimetric analysis (TGA) in the air atmosphere (Kushwaha, Srivastava and Mall, 2010; Mondal *et al.*, 2013a). TGA (thermo gravimetric analysis), DTA (differential thermal analysis) and DTG (differential thermal gravimetry) graphs provides quantitative and qualitative information regarding energy content, nature of degradation etc. which helps to identify the prior disposal mechanism of residue (sludge) (Singh, Srivastava and Mall, 2014).

The weight loss of 10.08% is recorded by TGA (thermo gravimetric analysis) in the temperature range of 25⁰C to 100⁰C. This weight loss can be due to which may be due to the moisture loss and evolution of some volatile molecules including water (Mondal *et al.*, 2013a). The analysis shows that the ignition temperature of sludge is near 200⁰C; as the utmost loss in weight which is around 42.24% is pragmatic in range of 200⁰C - 450⁰C (Kushwaha, Srivastava and Mall, 2010; Mondal *et al.*, 2013a). The oxidative degradation of sludge produces an exothermic peak in range of 200⁰C - 450⁰C. At the end of oxidation of sludge, a 28.50% of ash weight percentage is recorded.

The heat release of high calorific value is recorded by TGA analysis of sludge in air medium which is 4.80 MJ/Kg. This is approximately 23-26% of average gross calorific value of Indian coal which is around 18.19 MJ/Kg (Mishra, 2009). This shows that the sludge contains a noteworthy quantity of carbon. Therefore, the best suitable option for disposal of this sludge is using it as a fuel to extract energy in boilers/incinerators. This can also be used as an ingredient for making blended fuel briquettes along with other high calorific value fuels such as industrial and agricultural wastes (Mondal *et al.*, 2013b). The residue at last obtained as ash can be used for amalgamation with the cementitious compounds or fire brick production with fire clay (Kushwaha, Srivastava and Mall, 2010).

CHAPTER 6

CONCLUSIONS AND RECOMMENDATIONS

This chapter deals with the summary of the present research work and its major findings on the basis of results and discussions presented heretofore for the development of 3D rotating anode electrochemical reactor and its application in treatment of synthetic textile wastewater (STW).

In the first section, the major findings on the hydrodynamics of the 3D rotating anode with hopper bottom electrochemical reactor in the absence and presence of the stationary 3D anode are presented. The normalized mixing time and plug flow behaviour of the reactor in presence and absence of impeller is also presented. This section also includes the effect on the hydrodynamics of the reactor when rotation was introduced through the 3D rotating anode. This includes the reduction in short circuiting index and effect of mixing on flow behaviour of the 3D rotating anode electrochemical reactor.

The next section summarizes the performance evaluation of the 3D rotating anode electrochemical reactor for the treatment of synthetic textile wastewater (STW). The screening of significant operating parameters with PB design and the outcome of the batch studies including the effect of the separating parameters on the treatment of STW. Further the multi-objective optimization findings of Box-Behnken (BB) design and development of regression equation for color and COD removal along with electrode and specific electrical energy consumption.

Recommendations and the future scope for the further studies on the developed electrochemical reactor are also presented in the end.

6.1 Hydrodynamics of the 3D rotating anode electrochemical reactor with RTD and CFD

Based on the analysis of the residence time distribution (RTD) and computational fluid dynamics (CFD) of the 3D rotating anode (impeller) electrochemical reactor using tracer injection method, the following conclusions can be drawn:

- The CFD and RTD help to evaluate and simulate the performance and hydrodynamics of the reactor. The flow dynamics of the reactor changes significantly when the impeller is introduced into the reactor. The simulated age distribution was found in good agreement with the experimental data.
- For all studied flow rates, the pressure profile shows 140 - 160% improvement in uniform pressure distribution inside the reactor due to the impeller. The velocity magnitude shows higher velocity zones created around the impeller which indicates the turbulence caused by the introduction of the impeller. The velocity vectors show the generation of two vector zones imparting the fluid inside and out of the impeller causing more turbulence as compared to the case where the impeller is absent. The presence of impeller causes a reduction in mixing time, in the range of 18 to 44%.
- The tracer mass fraction curve indicates symmetrical shape in a case where the impeller is present as compared to when the impeller is absent. The short circuiting index also decreases with increase in flow rate when the impeller is present, and it is always less than the case where the impeller is absent. The flow regime tends to become plug flow when the impeller is present with an increase in flow rate.
- In absence of the impeller, the maximum velocity was found nearer to the wall of the electrochemical reactor. This shows that the introduction of impeller imparts more turbulence in the reactor which in turn provides better mixing and makes the flow regime plug flow. The laminar flow MRF model could capture the initial transient variation of Q , which latter becomes constant.
- The 3D rotating anode clearly affects the performance of the reactor and increases the mean residence time of the fluid inside the proposed reactor configuration. The mixing was found to be dependent of the RPM of the rotating anode (impeller). The mixing behaviour was changed from dispersion to ideal mixing state as rpm of the rotating anode (impeller) increases. The rotation of impeller was responsible for the formation of low pressure and

high-pressure zones. The velocity vectors had confirmed the formation of four loops at higher rotation speed.

- The variance and the mean time were found to be equal at high rotation speed and shows ideal condition at 60 rpm. Above that the back mixing hampers the system. The back mixing and bypass volume affects the performance of the 3D rotating anode electrochemical reactor at high anode rotation speed and at high input flow rates respectively. The values of turbulent intensity exhibit a constant behaviour beyond a certain rotational speed and at low flow rates. The reactor can be operated efficiently at 60 lph and 60 rpm. At higher flow rates, the value of turbulent intensity increases linearly, whereas vorticity magnitude does not increase considerably. Since the vorticity magnitude represents micro-mixing inside the reactor, it can be summarized that at higher flow rates the mixing inside the reactor is suppressed.
- The effective volume ratio increases with increasing rotation speed and found out to be best suited at flow rate of 60 lph with anode rotation speed set at 60 rpm. The short-circuiting index is also found out to be minimum at these values. The 3D rotating anode acts as a turbulence enhancer for the configuration and in turn increases the mass transfer inside the reactor.
- The passivation of the anode, dead volume, short circuiting is not present in the proposed configuration.

6.2 Treatment of synthetic textile wastewater using 3D rotating anode

The newly designed 3D rotating anode electrochemical reactor was then evaluated for the treatment of synthetic textile wastewater (STW). The following conclusions can be drawn:

- In this section, the multi-objective optimization of EC treatment of synthetic textile wastewater was performed by 3D rotating anode. The use of 3D rotating anode facilitates better mixing and yielded better performance.
- Plackett-Burman (PB) model has been used as a first step to determine the most important operating parameters. The batch studies were performed to analyse the effect of the various operating parameters on the performance of the batch reactors. The optimum conditions for batch mode were found to be at a current density of 6 mA/cm^2 , anode rotation speed of 60 rpm, pH of 6, and a COD removal efficiency of 91.50%. The optimum conditions for batch recirculation mode were found to be at a current density of 6 mA/cm^2 , flow rate of 60 lph, anode rotation speed of 60 rpm, pH of 6, and a COD removal efficiency of 94.40%. The optimum conditions for once through mode were found to be at a current density of 8 mA/cm^2 , flow rate of 4 lph, anode rotation speed of 60 rpm, pH of 6, and a COD removal efficiency of 85.28%. The Box-Behnken design was further used to optimize the selected factors so as to achieve maximum COD and color removal efficiencies.
- Analysis of variance was used for developing a polynomial model and graphical response surfaces and contour plots. These were used to locate the optimum point. Maximum COD and color removal efficiency of 96.40% and 99.88% respectively was observed for optimum conditions of current density of 6 mA/cm^2 , flow rate of 60 lph, anode rotation speed of 60 rpm, pH of 6, supporting electrolyte concentration of 3 g/l.
- The higher COD removal efficiency (90-97%) is observed for lower specific energy consumption (0.028-0.056) viz a viz the prevalent plate electrode.
- A mathematical correlation is developed to design operating parameters for given quality of waste and desired efficiency. The values of the adjusted and predicted R^2 were 0.9882 and 0.9689 for COD removal and 0.9982 and 0.9953 for specific electrical energy consumption, respectively.

- This shows good agreement between the experimental and predicted values of COD removal efficiencies and specific electrical energy consumption (SEEC).
- The model F-value recorded is 157.76 and 1038.14 for COD removal and SEEC respectively, signifying that the model is significant. The XRD analysis shows that both monomeric and polymeric species are present and aiding in the treatment of wastewater through pH 6-8. TGA analysis showed that the heat release by sludge in air atmosphere is 4.80 MJ/kg respectively. This residue can be used in blended fuel briquettes. Zeta potential analysis shows the removal by both the charge neutralization and sweep coagulation.
- The removal follows pseudo-first order reaction following Langmuir isotherm and intra-particle diffusion model explaining two step adsorption mechanism. The study shows that the removal mechanism is physisorption and broadly chemisorption.

6.3 Recommendations

This study has brought forth a number of considerations which may be of interest to pursue further research in the area of EC treatment of various industrial effluents using 3D rotating anode electrochemical reactor. Based on the experiences gained during the present work, following recommendations are being made for future research:

- The RTD and CFD with rotation of cathode can be studied to investigate the effects of cathode rotation.
- The baffling of the reactor can be done to lower the rotations requirements for better mixing.
- The vortex formation using Fluent's volume of fluid (VOF) can be studied with baffle and unbaffled 3D rotating anode electrochemical reactor.

- Other electrode materials like SS/Fe/RuO₂/Ti etc. may be studied in combinations (anode and cathode) for batch and continuous EC process.
- Conversion of EC sludge generated after the treatment into a material that can be used as a potential catalyst can be done in future to effectively handle the solid residue.
- For successful industrial application of EC process using 3D rotating anode, quantitative scale-up from batch and continuous laboratory scale is required. The key independent scale-up parameters must be identified to ensure dimensional consistency between small and large scale processes.

BIBLIOGRAPHY

Adeogun, A. I. and Balakrishnan, R. B. (2016) 'Electrocoagulation removal of anthraquinone dye Alizarin Red S from aqueous solution using aluminum electrodes: kinetics, isothermal and thermodynamics studies', *Journal of Electrochemical Science and Engineering*, (April). doi: 10.5599/jese.290.

Agustin, M. B., Sengpracha, W. P. and Phutdhawong, W. (2008) 'Electrocoagulation of palm oil mill effluent', *Int J Environ Res Public Health*, 5, pp. 177–180. Available at:http://www.ncbi.nlm.nih.gov/entrez/query.fcgi?cmd=Retrieve&db=PubMed&dopt=Citation&list_uids=19139537.

Al Aji, B., Yavuz, Y. and Koparal, A. S. (2012) 'Electrocoagulation of heavy metals containing model wastewater using monopolar iron electrodes', *Separation and Purification Technology*, 86, pp. 248–254. doi: 10.1016/j.seppur.2011.11.011.

Akyol, A. (2012) 'Treatment of paint manufacturing wastewater by electrocoagulation', *Desalination*, 285, pp. 91–99. doi: 10.1016/j.desal.2011.09.039.

Alinsafi, A., Khemis, M., Pons, M. N., Leclerc, J. P., Yaacoubi, A., Benhammou, A. and Nejmeddine, A. (2005) 'Electro-coagulation of reactive textile dyes and textile wastewater', *Chemical Engineering and Processing: Process Intensification*, 44(4), pp. 461–470. doi: 10.1016/j.cep.2004.06.010.

Alvarez, M. M., Zalc, J. M., Shinbrot, T., Arratia, P. E. and Muzzio, F. J. (2002) 'Mechanisms of mixing and creation of structure in laminar stirred tanks', *AIChE Journal*, 48(10), pp. 2135–2148. doi: 10.1002/aic.690481005.

Amani-Ghadim, A. R., Aber, S., Olad, A. and Ashassi-Sorkhabi, H. (2013) 'Optimization of electrocoagulation process for removal of an azo dye using response surface methodology and investigation on the occurrence of destructive side reactions', *Chemical Engineering and Processing: Process Intensification*, 64, pp. 68–78. doi: 10.1016/j.cep.2012.10.012.

American Public Health Association, American Water Works Association and Water Environment Federation (1999) 'Standard Methods for the Examination of Water and

Wastewater', *Standard Methods*, p. 541.

Amini, M., Younesi, H., Bahramifar, N., Lorestani, A. A. Z., Ghorbani, F., Daneshi, A. and Sharifzadeh, M. (2008) 'Application of response surface methodology for optimization of lead biosorption in an aqueous solution by *Aspergillus niger*', *Journal of Hazardous Materials*, 154(1–3), pp. 694–702. doi: Doi 10.1016/J.Jhazmat.2007.10.114.

Anderson, M. J. and Whitcomb, P. J. (no date) *RSM Simplified : Optimizing Processes Using Response Surface Methods for Design of Experiments, Second Edition*. Available at: https://books.google.co.in/books?id=WI2KDQAAQBAJ&printsec=frontcover&source=gbs_ge_summary_r&cad=0#v=onepage&q&f=false (Accessed: 13 July 2017).

Anglada, Á., Urtiaga, A. and Ortiz, I. (2009) 'Contributions of electrochemical oxidation to waste-water treatment: Fundamentals and review of applications', *Journal of Chemical Technology and Biotechnology*, pp. 1747–1755. doi: 10.1002/jctb.2214.

Aoudj, S., Khelifa, A., Drouiche, N., Belkada, R. and Miroud, D. (2015) 'Simultaneous removal of chromium(VI) and fluoride by electrocoagulation-electroflotation: Application of a hybrid Fe-Al anode', *Chemical Engineering Journal*, 267, pp. 153–162. doi: 10.1016/j.cej.2014.12.081.

Aoudj, S., Khelifa, A., Drouiche, N., Hecini, M. and Hamitouche, H. (2010) 'Electrocoagulation process applied to wastewater containing dyes from textile industry', *Chemical Engineering and Processing: Process Intensification*, 49(11), pp. 1176–1182. doi: 10.1016/j.cep.2010.08.019.

Arratia, P. E., Lacombe, J. P., Shinbrot, T. and Muzzio, F. J. (2004) 'Segregated regions in continuous laminar stirred tank reactors', *Chemical Engineering Science*, 59(7), pp. 1481–1490. doi: 10.1016/j.ces.2003.06.003.

Arslan-Alaton, I., Kabdaşlı, I., Vardar, B. and Tünay, O. (2009) 'Electrocoagulation of simulated reactive dyebath effluent with aluminum and stainless steel electrodes', *Journal of Hazardous Materials*, 164(2–3), pp. 1586–1594. doi: 10.1016/j.jhazmat.2008.09.004.

Asselin, M., Drogui, P., Benmoussa, H. and Blais, J. F. (2008) 'Effectiveness of electrocoagulation process in removing organic compounds from slaughterhouse wastewater using monopolar and bipolar electrolytic cells', *Chemosphere*, 72(11), pp. 1727–1733. doi: 10.1016/j.chemosphere.2008.04.067.

Asselin, M., Drogui, P., Brar, S. K., Benmoussa, H. and Blais, J. F. (2008) 'Organics removal in oily bilgewater by electrocoagulation process', *Journal of Hazardous Materials*, 151(2–3), pp. 446–455. doi: 10.1016/j.jhazmat.2007.06.008.

Balla, W., Essadki, A. H., Gourich, B., Dassaa, A., Chenik, H. and Azzi, M. (2010) 'Electrocoagulation/electroflotation of reactive, disperse and mixture dyes in an external-loop airlift reactor', *Journal of Hazardous Materials*, 184(1–3), pp. 710–716. doi: 10.1016/j.jhazmat.2010.08.097.

Barrera-Díaz, C., Roa-Morales, G., Ávila-Córdoba, L., Pavón-Silva, T. and Bilyeu, B. (2006) 'Electrochemical Treatment Applied to Food-Processing Industrial Wastewater', *Industrial and Engineering Chemistry Research*, 45(1), pp. 34–38. doi: 10.1021/ie050594k.

Barrett, E. P., Joyner, L. G. and Halenda, P. P. (1951) 'The Determination of Pore Volume and Area Distributions in Porous Substances. I. Computations from Nitrogen Isotherms', *Journal of the American Chemical Society*, 73(1), pp. 373–380. doi: 10.1021/ja01145a126.

Bayar, S., Boncukcuoglu, R., Yilmaz, a E. and Fil, B. a (2014) 'Pre-Treatment of Pistachio Processing Industry Wastewaters (PPIW) by Electrocoagulation using Al Plate Electrode', *Separation Science and Technology*, 49(7), pp. 1008–1018. doi: Doi 10.1080/01496395.2013.878847.

Bayar, S., Yildiz, Y. S., Yilmaz, A. E. and Irdemez, S. (2011) 'The effect of stirring speed and current density on removal efficiency of poultry slaughterhouse wastewater by electrocoagulation method', *Desalination*, 280(1–3), pp. 103–107. doi: 10.1016/j.desal.2011.06.061.

Bayar, S., Yıldız, Y. Ş., Yılmaz, A. E. and İrdemez, Ş. (2011) 'The effect of stirring speed and current density on removal efficiency of poultry slaughterhouse wastewater by electrocoagulation method', *Desalination*, 280(1), pp. 103–107. doi:

10.1016/j.desal.2011.06.061.

Bayramoglu, M., Eyvaz, M. and Kobya, M. (2007) 'Treatment of the textile wastewater by electrocoagulation. Economical evaluation', *Chemical Engineering Journal*, 128(2–3), pp. 155–161. doi: 10.1016/j.cej.2006.10.008.

Bayramoglu, M., Kobya, M., Can, O. T. and Sozbir, M. (2004) 'Operating cost analysis of electrocoagulation of textile dye wastewater', *Separation and Purification Technology*, 37(2), pp. 117–125. doi: 10.1016/j.seppur.2003.09.002.

Bayramoglu, M., Kobya, M., Eyvaz, M. and Senturk, E. (2006) 'Technical and economic analysis of electrocoagulation for the treatment of poultry slaughterhouse wastewater', *Separation and Purification Technology*, 51(3), pp. 404–408. doi: 10.1016/j.seppur.2006.03.003.

Bejankiwar, R. S. (2002) 'Electrochemical treatment of cigarette industry wastewater: Feasibility study', *Water Research*, 36(17), pp. 4386–4390. doi: 10.1016/S0043-1354(02)00155-0.

Bektaş, N., Öncel, S., Akbulut, H. Y. and Dimoglo, A. (2004) 'Removal of boron by electrocoagulation', *Environmental Chemistry Letters*, 2(2), pp. 51–54. doi: 10.1007/s10311-004-0075-6.

Bianco, B., De Michelis, I. and Vegliò, F. (2011) 'Fenton treatment of complex industrial wastewater: Optimization of process conditions by surface response method', *Journal of Hazardous Materials*, 186(2–3), pp. 1733–1738. doi: 10.1016/j.jhazmat.2010.12.054.

Bouhezila, F., Hariti, M., Lounici, H. and Mameri, N. (2011) 'Treatment of the OUED SMAR town landfill leachate by an electrochemical reactor', *Desalination*, 280(1–3), pp. 347–353. doi: 10.1016/j.desal.2011.07.032.

Boye, B., Brillas, E. and Dieng, M. M. (2003) 'Electrochemical degradation of the herbicide 4-chloro-2-methylphenoxyacetic acid in aqueous medium by peroxi-coagulation and photoperoxi-coagulation', *Journal of Electroanalytical Chemistry*, 540, pp. 25–34. doi: 10.1016/S0022-0728(02)01271-8.

Boye, B., Dieng, M. M. and Brillas, E. (2003) 'Electrochemical degradation of 2,4,5-

trichlorophenoxyacetic acid in aqueous medium by peroxi-coagulation. Effect of pH and UV light', *Electrochimica Acta*, 48(7), pp. 781–790. doi: 10.1016/S0013-4686(02)00747-8.

Brannock, M. W. D., De Wever, H., Wang, Y. and Leslie, G. (2009) 'Computational fluid dynamics simulations of MBRs: Inside submerged versus outside submerged membranes', *Desalination*, 236(1), pp. 244–251. doi: 10.1016/j.desal.2007.10.073.

Bratby, J. (2006) *Coagulation and Flocculation in Water and Wastewater Treatment*, IWA. doi: 10.2166/9781780402321.

Brillas, E., Boye, B., Ángel Baños, M., Calpe, J. C. and Garrido, J. A. (2003) 'Electrochemical degradation of chlorophenoxy and chlorobenzoic herbicides in acidic aqueous medium by the peroxi-coagulation method', *Chemosphere*, 51(4), pp. 227–235. doi: 10.1016/S0045-6535(02)00836-6.

Brillas, E. and Martínez-Huitle, C. A. (2015) 'Decontamination of wastewaters containing synthetic organic dyes by electrochemical methods. An updated review', *Applied Catalysis B: Environmental*, pp. 603–643. doi: 10.1016/j.apcatb.2014.11.016.

Burghardt, A. and Lipowska, L. (1972) 'Mixing phenomena in a continuous flow stirred tank reactor', *Chemical Engineering Science*. Available at: <http://www.sciencedirect.com/science/article/pii/0009250972850401> (Accessed: 3 May 2017).

Butler, E., Hung, Y.-T., Yeh, R. Y.-L. and Suleiman Al Ahmad, M. (2011a) 'Electrocoagulation in Wastewater Treatment', *Water*, 3(4), pp. 495–525. doi: 10.3390/w3020495.

Butler, E., Hung, Y.-T., Yeh, R. Y.-L. and Suleiman Al Ahmad, M. (2011b) 'Electrocoagulation in Wastewater Treatment', *Water*, pp. 495–525. doi: 10.3390/w3020495.

Can, O. T., Bayramoglu, M. and Kobya, M. (2003) 'Decolorization of reactive dye solutions by electrocoagulation using aluminum electrodes', *Industrial Engineering Chemistry Research*, 42(14), pp. 3391–3396. doi: 10.1021/ie020951g.

Can, O. T., Kobya, M., Demirbas, E. and Bayramoglu, M. (2006) 'Treatment of the

textile wastewater by combined electrocoagulation', *Chemosphere*, 62(2), pp. 181–187. doi: 10.1016/j.chemosphere.2005.05.022.

Cañizares, P., Carmona, M., Lobato, J., Martínez, F. and Rodrigo, M. A. (2005) 'Electrodissolution of Aluminum Electrodes in Electrocoagulation Processes', *Industrial & Engineering Chemistry Research*. American Chemical Society, 44(12), pp. 4178–4185. doi: 10.1021/ie048858a.

Cañizares, P., Jiménez, C., Martínez, F., Sáez, C. and Rodrigo, M. A. (2007) 'Study of the electrocoagulation process using aluminum and iron electrodes', *Industrial and Engineering Chemistry Research*, 46(19), pp. 6189–6195. doi: 10.1021/ie070059f.

Cañizares, P., Martínez, F., Jiménez, C., Lobato, J. and Rodrigo, M. A. (2006) 'Comparison of the aluminum speciation in chemical and electrochemical dosing processes', *Industrial and Engineering Chemistry Research*, 45(26), pp. 8749–8756. doi: 10.1021/ie060824a.

Capela, I., Bilé, M. J., Silva, F., Nadais, H., Prates, A. and Arroja, L. (2009) 'Hydrodynamic behaviour of a full-scale anaerobic contact reactor using residence time distribution technique', *Journal of Chemical Technology and Biotechnology*, 84(5), pp. 716–724. doi: 10.1002/jctb.2104.

Chaturvedi, S. I. (2013) 'Electrocoagulation: A Novel Waste Water Treatment Method', *International Journal of Modern Engineering Research (IJMER)*, 3(1), pp. 93–100.

Chavalparit, O. and Ongwandee, M. (2009) 'Optimizing electrocoagulation process for the treatment of biodiesel wastewater using response surface methodology.', *Journal of environmental sciences (China)*, 21(11), pp. 1491–6.

Chen, G. (2004) 'Electrochemical technologies in wastewater treatment', *Separation and Purification Technology*, 38(1), pp. 11–41. doi: 10.1016/j.seppur.2003.10.006.

Chen, X., Chen, G. and Yue, P. L. (2000) 'Separation of pollutants from restaurant wastewater by electrocoagulation', *Separation and Purification Technology*, 19(1–2), pp. 65–76. doi: 10.1016/S1383-5866(99)00072-6.

Chopra, A. K., Kumar Sharma, A. and Kumar, V. (2011) 'Overview of Electrolytic

treatment: An alternative technology for purification of wastewater', *Archives of Applied Science Research Arch. Appl. Sci. Res.*, 3(35), pp. 191–206.

Chou, W.-L., Wang, C.-T. and Huang, K.-Y. (2010) 'Investigation of process parameters for the removal of polyvinyl alcohol from aqueous solution by iron electrocoagulation', *Desalination*, 251(1), pp. 12–19. doi: 10.1016/j.desal.2009.10.008.

Chou, W. L., Wang, C. T. and Huang, K. Y. (2010) 'Investigation of process parameters for the removal of polyvinyl alcohol from aqueous solution by iron electrocoagulation', *Desalination*, 251(1–3), pp. 12–19. doi: 10.1016/j.desal.2009.10.008.

Coskun, T., Ilhan, F., Demir, N. M., Debik, E. and Kurt, U. (2012) 'Optimization of energy costs in the pretreatment of olive mill wastewaters by electrocoagulation', *Environmental Technology*, 33(7), pp. 801–807. doi: Doi 10.1080/09593330.2011.595829.

Cotillas, S., Llanos, J., Cañizares, P., Mateo, S. and Rodrigo, M. A. (2013) 'Optimization of an integrated electrodisinfection/electrocoagulation process with Al bipolar electrodes for urban wastewater reclamation', *Water Research*, 47(5), pp. 1741–1750. doi: 10.1016/j.watres.2012.12.029.

Daneshvar, N., Ashassi-Sorkhabi, H. and Tizpar, A. (2003) 'Decolorization of orange II by electrocoagulation method', *Separation and Purification Technology*, 31(2), pp. 153–162. doi: 10.1016/S1383-5866(02)00178-8.

Daneshvar, N., Khataee, A. R., Amani Ghadim, A. R. and Rasoulifard, M. H. (2007) 'Decolorization of C.I. Acid Yellow 23 solution by electrocoagulation process: Investigation of operational parameters and evaluation of specific electrical energy consumption (SEEC)', *Journal of Hazardous Materials*, 148(3), pp. 566–572. doi: 10.1016/j.jhazmat.2007.03.028.

Davila, J. A., MacHuca, F. and Marrianga, N. (2011) 'Treatment of vinasses by electrocoagulation-electroflotation using the Taguchi method', *Electrochimica Acta*, 56(22), pp. 7433–7436. doi: 10.1016/j.electacta.2011.07.015.

Den, W. and Huang, C. (2005) 'Electrocoagulation for removal of silica nanoparticles from chemical-mechanical-planarization wastewater', *Colloids and Surfaces A: Physicochemical and Engineering Aspects*, 254(1–3), pp. 81–89. doi: 10.1016/j.colsurfa.2004.11.026.

Dierberg, F. E., DeBusk, T. A., Jackson, S. D., Chimney, M. J. and Pietro, K. (2002) 'Submerged aquatic vegetation-based treatment wetlands for removing phosphorus from agricultural runoff: response to hydraulic and nutrient loading', *Water Research*, 36(6), pp. 1409–1422. doi: 10.1016/S0043-1354(01)00354-2.

Dierberg, F. E., Juston, J. J., DeBusk, T. A., Pietro, K. and Gu, B. (2005) 'Relationship between hydraulic efficiency and phosphorus removal in a submerged aquatic vegetation-dominated treatment wetland', *Ecological Engineering*, 25(1), pp. 9–23. doi: 10.1016/j.ecoleng.2004.12.018.

Dimoglo, A., Akbulut, H. Y., Cihan, F. and Karpuzcu, M. (2004) 'Petrochemical wastewater treatment by means of clean electrochemical technologies', *Clean Technologies and Environmental Policy*, 6(4), pp. 288–295. doi: 10.1007/s10098-004-0248-9.

Djoudi, W., Aissani-Benissad, F. and Ozil, P. (2012) 'Flow modeling in electrochemical tubular reactor containing volumetric electrode: Application to copper cementation reaction', *Chemical Engineering Research and Design*, 90(10), pp. 1582–1589. doi: 10.1016/j.cherd.2012.02.003.

Do, D. D., Herrera, L. F. and Nicholson, D. (2011) 'A method for the determination of accessible surface area, pore volume, pore size and its volume distribution for homogeneous pores of different shapes', *Adsorption*, 17(2), pp. 325–335. doi: 10.1007/s10450-010-9314-2.

Drouiche, N., Ghaffour, N., Lounici, H. and Mameri, M. (2007) 'Electrocoagulation of chemical mechanical polishing wastewater', *Desalination*, 214(1–3), pp. 31–37. doi: 10.1016/j.desal.2006.11.009.

Duan, J. and Gregory, J. (2003) 'Coagulation by hydrolysing metal salts', *Advances in Colloid and Interface Science*, 100–102(SUPPL.), pp. 475–502. doi: 10.1016/S0001-8686(02)00067-2.

Durango-Usuga, P., Guzmán-Duque, F., Mosteo, R., Vazquez, M. V., Peuela, G. and Torres-Palma, R. A. (2010) 'Experimental design approach applied to the elimination of crystal violet in water by electrocoagulation with Fe or Al electrodes', *Journal of Hazardous Materials*, 179(1–3), pp. 120–126. doi: 10.1016/j.jhazmat.2010.02.067.

Egedy, A., Varga, T. and Chován, T. (2013) 'Compartment model structure identification with qualitative methods for a stirred vessel', *Mathematical and Computer Modelling of Dynamical Systems*, 19(2), pp. 115–132. doi: 10.1080/13873954.2012.700939.

Eiband, M. M. S. G., Kamli, K. C., Gama, K., Melo, J. V. De, Martínez-Huitle, C. A. and Ferro, S. (2014) 'Elimination of Pb²⁺ through electrocoagulation: Applicability of adsorptive stripping voltammetry for monitoring the lead concentration during its elimination', *Journal of Electroanalytical Chemistry*, 717–718, pp. 213–218. doi: 10.1016/j.jelechem.2014.01.032.

El-Ashtoukhy, E. and Yasmine, F. (2014) 'Oil Removal from Oil-Water Emulsion by Electrocoagulation in a Cell with Rotating Cylinder Anode', *The Electrochemical Society of Japan*, 82(11), pp. 974–978. doi: <http://dx.doi.org/10.5796/electrochemistry.82.974>.

El-Naas, M. H., Al-Zuhair, S., Al-Lobaney, A. and Makhlof, S. (2009) 'Assessment of electrocoagulation for the treatment of petroleum refinery wastewater', *Journal of Environmental Management*, 91(1), pp. 180–185. doi: 10.1016/j.jenvman.2009.08.003.

El-Shazly, A. and Daous, M. (2013) 'Investigations and Kinetics Study for the Effect of Solution Flow Rate on the Performance of Electrocoagulation Unit Used for Nutrients Removal', *Int. J. Electrochem. Sci.* Available at: <http://electrochemsci.org/papers/vol8/81212509.pdf> (Accessed: 25 April 2016).

Enciso, R., Delgadillo, J. A., Domínguez, O. and Rodríguez-Torres, I. (2017) 'Analysis and validation of the hydrodynamics of an electrodialysis cell using computational fluid dynamics', *Desalination*, 408, pp. 127–132. doi: 10.1016/j.desal.2017.01.015.

Essadki, A. H., Bennajah, M., Gourich, B., Vial, C., Azzi, M. and Delmas, H. (2008)

‘Electrocoagulation/electroflotation in an external-loop airlift reactor-Application to the decolorization of textile dye wastewater: A case study’, *Chemical Engineering and Processing: Process Intensification*, 47(8), pp. 1211–1223. doi: 10.1016/j.cep.2007.03.013.

Essadki, A. H., Gourich, B., Azzi, M., Vial, C. and Delmas, H. (2010) ‘Kinetic study of defluoridation of drinking water by electrocoagulation/electroflotation in a stirred tank reactor and in an external-loop airlift reactor’, *Chemical Engineering Journal*, 164(1), pp. 106–114. doi: 10.1016/j.cej.2010.08.037.

Eyvaz, M., Kirlaroglu, M., Aktas, T. S. and Yuksel, E. (2009) ‘The effects of alternating current electrocoagulation on dye removal from aqueous solutions’, *Chemical Engineering Journal*, 153(1–3), pp. 16–22. doi: DOI 10.1016/j.cej.2009.05.028.

Fajardo, A. S., Rodrigues, R. F., Martins, R. C., Castro, L. M. and Quinta-Ferreira, R. M. (2015) ‘Phenolic wastewaters treatment by electrocoagulation process using Zn anode’, *Chemical Engineering Journal*, 275, pp. 331–341. doi: 10.1016/j.cej.2015.03.116.

Fimbres-Weihs, G. A. and Wiley, D. E. (2010) ‘Review of 3D CFD modeling of flow and mass transfer in narrow spacer-filled channels in membrane modules’, *Chemical Engineering and Processing: Process Intensification*, 49(7), pp. 759–781. doi: 10.1016/j.cep.2010.01.007.

Fogler, H. S. (1999a) ‘Elements of chemical reaction engineering’, *Chemical Engineering Science*, 42, p. 1000. doi: 10.1016/0009-2509(87)80130-6.

Fogler, H. S. (1999b) ‘Elements of chemical reaction engineering.’, *Elements of Chemical Reaction Engineering*, p. 646. doi: 10.1016/0009-2509(87)80130-6.

Fogler, H. S. (2006a) ‘Distributions of residence times for chemical reactors’, *Elements of Chemical Reaction Engineering*, pp. 867–944.

Fogler, H. S. (2006b) *Elements of Chemical Reaction Engineering*, *Chemical Engineering Science*. doi: 10.1016/0009-2509(87)80130-6.

Fogler, H. S. (2016) *Elements of chemical reaction engineering*, *Prentice Hall*. doi:

10.1016/0009-2509(87)80130-6.

Fu, F. and Wang, Q. (2011) 'Removal of heavy metal ions from wastewaters: A review', *Journal of Environmental Management*, pp. 407–418. doi: 10.1016/j.jenvman.2010.11.011.

Ganesan, P., Lakshmi, J., Sozhan, G. and Vasudevan, S. (2013) 'Removal of manganese from water by electrocoagulation: Adsorption, kinetics and thermodynamic studies', *Canadian Journal of Chemical Engineering*, 91(3), pp. 448–458. doi: 10.1002/cjce.21709.

García-García, P., López-López, A., Moreno-Baquero, J. M. and Garrido-Fernández, A. (2011) 'Treatment of wastewaters from the green table olive packaging industry using electro-coagulation', *Chemical Engineering Journal*, 170(1), pp. 59–66. doi: 10.1016/j.cej.2011.03.028.

Garcia-Segura, S., Eiband, M. M. S. G., de Melo, J. V. and Martínez-Huitle, C. A. (2017) 'Electrocoagulation and advanced electrocoagulation processes: A general review about the fundamentals, emerging applications and its association with other technologies', *Journal of Electroanalytical Chemistry*, pp. 267–299. doi: 10.1016/j.jelechem.2017.07.047.

Ge, J., Qu, J., Lei, P. and Liu, H. (2004) 'New bipolar electrocoagulation-electroflotation process for the treatment of laundry wastewater', *Separation and Purification Technology*, 36(1), pp. 33–39. doi: 10.1016/S1383-5866(03)00150-3.

Gengec, E., Kobya, M., Demirbas, E., Akyol, A. and Oktor, K. (2012) 'Optimization of baker's yeast wastewater using response surface methodology by electrocoagulation', *Desalination*, 286, pp. 200–209. doi: 10.1016/j.desal.2011.11.023.

Ghaly, a. E., Ananthashankar, R., Alhattab, M. and Ramakrishnan, V. V. (2014) 'Production, characterization and treatment of textile effluents: a critical review', *Journal of Chemical Engineering & Process Technology*, 5(1), pp. 1–18. doi: 10.4172/2157-7048.1000182.

Ghosh, D., Medhi, C. R. and Purkait, M. K. (2008) 'Treatment of fluoride containing

drinking water by electrocoagulation using monopolar and bipolar electrode connections', *Chemosphere*, 73(9), pp. 1393–1400. doi: 10.1016/j.chemosphere.2008.08.041.

Ghosh, D., Solanki, H. and Purkait, M. K. (2008) 'Removal of Fe(II) from tap water by electrocoagulation technique', *Journal of Hazardous Materials*, 155(1–2), pp. 135–143. doi: 10.1016/j.jhazmat.2007.11.042.

Golder, A. K., Samanta, A. N. and Ray, S. (2007a) 'Removal of Cr³⁺ by electrocoagulation with multiple electrodes: Bipolar and monopolar configurations', *Journal of Hazardous Materials*, 141(3), pp. 653–661. doi: 10.1016/j.jhazmat.2006.07.025.

Golder, A. K., Samanta, A. N. and Ray, S. (2007b) 'Removal of Cr³⁺ by electrocoagulation with multiple electrodes: Bipolar and monopolar configurations', *Journal of Hazardous Materials*, 141(3), pp. 653–661. doi: 10.1016/j.jhazmat.2006.07.025.

Gomes, J. A. G., Daida, P., Kesmez, M., Weir, M., Moreno, H., Parga, J. R., Irwin, G., McWhinney, H., Grady, T., Peterson, E. and Cocke, D. L. (2007) 'Arsenic removal by electrocoagulation using combined Al-Fe electrode system and characterization of products', *Journal of Hazardous Materials*, 139(2), pp. 220–231. doi: 10.1016/j.jhazmat.2005.11.108.

Gomes, J. A. G., Daida, P., Kesmez, M., Weir, M., Moreno, H., Parga, J. R., Irwin, G., McWhinney, H., Grady, T., Peterson, E. and Cocke, D. L. (2007) 'Arsenic removal by electrocoagulation using combined Al-Fe electrode system and characterization of products', *Journal of Hazardous Materials*, 139(2), pp. 220–231. doi: 10.1016/j.jhazmat.2005.11.108.

Gong, C., Zhang, Z., Li, H., Li, D., Wu, B., Sun, Y. and Cheng, Y. (2014) 'Electrocoagulation pretreatment of wet-spun acrylic fibers manufacturing wastewater to improve its biodegradability', *Journal of Hazardous Materials*, 274, pp. 465–472. doi: 10.1016/j.jhazmat.2014.04.033.

Gregory, J. and Duan, J. (2001) 'Hydrolyzing metal salts as coagulants *', *Pure and Applied Chemistry*, 73(12), pp. 2017–2026. doi: 10.1351/pac200173122017.

Gupta, V. K., Ali, I., Gupta, V. K. and Ali, I. (2013) 'Chapter 6 – Water Treatment by Electrical Technologies', in *Environmental Water*, pp. 155–178. doi: 10.1016/B978-0-444-59399-3.00006-4.

H.Myers, R., C.Montgomery, D. and Anderson-Cook, M, C. (2016) *Response Surface Methodology: Process and Product Optimization Using Designed Experiments*, WILEY SERIES IN PROBABILITY AND STATISTICS Established. doi: 10.1017/CBO9781107415324.004.

Hakizimana, J. N., Gourich, B., Chafi, M., Stiriba, Y., Vial, C., Drogui, P. and Naja, J. (2017) 'Electrocoagulation process in water treatment: A review of electrocoagulation modeling approaches', *Desalination*, 404. doi: 10.1016/j.desal.2016.10.011.

Hakizimana, J. N., Gourich, B., Chafi, M., Stiriba, Y., Vial, C., Drogui, P. and Naja, J. (2017) 'Electrocoagulation process in water treatment: A review of electrocoagulation modeling approaches', *Desalination*, 404, pp. 1–21. doi: 10.1016/j.desal.2016.10.011.

Hamdan, S. S. and El-Naas, M. H. (2014) 'Characterization of the removal of Chromium(VI) from groundwater by electrocoagulation', *Journal of Industrial and Engineering Chemistry*, 20(5), pp. 2775–2781. doi: 10.1016/j.jiec.2013.11.006.

Hanafi, F., Assobhei, O. and Mountadar, M. (2010) 'Detoxification and discoloration of Moroccan olive mill wastewater by electrocoagulation', *Journal of Hazardous Materials*, 174(1–3), pp. 807–812. doi: 10.1016/j.jhazmat.2009.09.124.

Hanay, A., Boncukcuoğlu, R., Kocakerim, M. M. and Yilmaz, A. E. (2003) 'Boron removal from geothermal waters by ion exchange in a batch reactor', *Fresenius Environmental Bulletin*, 12(10), pp. 1190–1194.

Hanay, Ö. and Hasar, H. (2011) 'Effect of anions on removing Cu²⁺, Mn²⁺ and Zn²⁺ in electrocoagulation process using aluminum electrodes.', *Journal of hazardous materials*, 189, pp. 572–576. doi: 10.1016/j.jhazmat.2011.02.073.

Ben Hariz, I., Halleb, A., Adhoum, N. and Monser, L. (2013) 'Treatment of petroleum refinery sulfidic spent caustic wastes by electrocoagulation', *Separation and Purification Technology*, 107, pp. 150–157. doi: 10.1016/j.seppur.2013.01.051.

Hassani, A., Kiranşan, M., Darvishi Cheshmeh Soltani, R., Khataee, A. and Karaca, S.

(2015) 'Optimization of the adsorption of a textile dye onto nanoclay using a central composite design', *Turkish Journal of Chemistry*, 39(4), pp. 734–749. doi: 10.3906/kim-1412-64.

Heidmann, I. and Calmano, W. (2008a) 'Removal of Zn(II), Cu(II), Ni(II), Ag(I) and Cr(VI) present in aqueous solutions by aluminium electrocoagulation', *Journal of Hazardous Materials*, 152(3), pp. 934–941. doi: 10.1016/j.jhazmat.2007.07.068.

Heidmann, I. and Calmano, W. (2008b) 'Removal of Zn(II), Cu(II), Ni(II), Ag(I) and Cr(VI) present in aqueous solutions by aluminium electrocoagulation', *Journal of Hazardous Materials*, 152(3), pp. 934–941. doi: 10.1016/j.jhazmat.2007.07.068.

Henry Ezechi, E., Hasnain Isa, M., Kutty, S. R. bin M. and Ahmed, Z. (2015) 'Electrochemical removal of boron from produced water and recovery', *Journal of Environmental Chemical Engineering*, 3(3), pp. 1962–1973. doi: 10.1016/j.jece.2015.05.015.

Holt, P. K., Barton, G. W., Wark, M. and Mitchell, C. A. (2002) 'A quantitative comparison between chemical dosing and electrocoagulation', *Colloids and Surfaces A: Physicochemical and Engineering Aspects*, 211(2–3), pp. 233–248. doi: 10.1016/S0927-7757(02)00285-6.

Hu, C. Y., Lo, S. L. and Kuan, W. H. (2014) 'High concentration of arsenate removal by electrocoagulation with calcium', *Separation and Purification Technology*, 126, pp. 7–14. doi: 10.1016/j.seppur.2014.02.015.

Hu, C. Y., Lo, S. L., Li, C. M. and Kuan, W. H. (2005) 'Treating chemical mechanical polishing (CMP) wastewater by electro-coagulation-flotation process with surfactant', *Journal of Hazardous Materials*, 120(1–3), pp. 15–20. doi: 10.1016/j.jhazmat.2004.12.038.

Huang, C.-H., Chen, L. and Yang, C.-L. (2009) 'Effect of anions on electrochemical coagulation for cadmium removal', *Separation and Purification Technology*, 65(2), pp. 137–146. doi: 10.1016/j.seppur.2008.10.029.

Ibanez, J. G., Singh, M. M., Szafran, Z. and Pike, R. M. (1998) 'Laboratory Experiments On Electrochemical Remediation Of The Environment. Part 4. Color

Removal of Simulated Wastewater by Electrocoagulation-Electroflotation', *J. Chem. Educ.*, 75(8), pp. 1040–1041.

Ibrahim, D. S., Veerabahu, C., Palani, R., Devi, S. and Balasubramanian, N. (2013a) 'Flow dynamics and mass transfer studies in a tubular electrochemical reactor with a mesh electrode', *Computers & Fluids*, 73, pp. 97–103. doi: 10.1016/j.compfluid.2012.12.001.

Ibrahim, D. S., Veerabahu, C., Palani, R., Devi, S. and Balasubramanian, N. (2013b) 'Flow dynamics and mass transfer studies in a tubular electrochemical reactor with a mesh electrode', *Computers and Fluids*, 73, pp. 97–103. doi: 10.1016/j.compfluid.2012.12.001.

Inan, H., Dimoglo, A., Şimşek, H. and Karpuzcu, M. (2004) 'Olive oil mill wastewater treatment by means of electro-coagulation', *Separation and Purification Technology*, 36(1), pp. 23–31. doi: 10.1016/S1383-5866(03)00148-5.

Irdemez, ahset, Yildiz, Y. S. and Tosunolu, V. (2006) 'Optimization of phosphate removal from wastewater by electrocoagulation with aluminum plate electrodes', *Separation and Purification Technology*, 52(2), pp. 394–401. doi: 10.1016/j.seppur.2006.05.020.

Isa, M. H., Ezechi, E. H., Ahmed, Z., Magram, S. F. and Kutty, S. R. M. (2014) 'Boron removal by electrocoagulation and recovery', *Water Research*, 51, pp. 113–123. doi: 10.1016/j.watres.2013.12.024.

Izquierdo, C. J., Canizares, P., Rodrigo, M. A., Leclerc, J. P., Valentin, G. and Lapique, F. (2010) 'Effect of the nature of the supporting electrolyte on the treatment of soluble oils by electrocoagulation', *Desalination*, 255(1–3), pp. 15–20. doi: 10.1016/j.desal.2010.01.022.

Janpoor, F., Torabian, A. and Khatibikamal, V. (2011) 'Treatment of laundry wastewater by electrocoagulation', *Journal of Chemical Technology and Biotechnology*, 86(8), pp. 1113–1120. doi: 10.1002/jctb.2625.

Janssen, L. J. J. and Hoogland, J. G. (1973) 'The effect of electrolytically evolved gas bubbles on the thickness of the diffusion layer—II', *Electrochimica Acta*. Pergamon,

18(8), pp. 543–550. doi: 10.1016/0013-4686(73)85016-9.

Jarvis, P., Jefferson, B. and Parsons, S. A. (2004) ‘Characterising natural organic matter flocs’, in *Water Science and Technology: Water Supply*, pp. 79–87.

Jiang, J. Q. (2015) ‘The role of coagulation in water treatment’, *Current Opinion in Chemical Engineering*, pp. 36–44. doi: 10.1016/j.coche.2015.01.008.

Jones, P. N., Özcan-Taşkin, N. G. and Yianneskis, M. (2009) ‘The use of momentum ratio to evaluate the performance of CSTRs’, *Chemical Engineering Research and Design*, 87(4), pp. 485–491. doi: 10.1016/j.cherd.2008.12.005.

Jüttner, K., Galla, U. and Schmieder, H. (2000) ‘Electrochemical approaches to environmental problems in the process industry’, *Electrochimica Acta*, 45(15–16), pp. 2575–2594. doi: 10.1016/S0013-4686(00)00339-X.

Kamaraj, R. and Vasudevan, S. (2015) ‘Evaluation of electrocoagulation process for the removal of strontium and cesium from aqueous solution’, *Chemical Engineering Research and Design*, 93, pp. 522–530. doi: 10.1016/j.cherd.2014.03.021.

Kannan, N., Karthikeyan, G. and Tamilselvan, N. (2006) ‘Comparison of treatment potential of electrocoagulation of distillery effluent with and without activated Areca catechu nut carbon’, *Journal of Hazardous Materials*, 137(3), pp. 1803–1809. doi: 10.1016/j.jhazmat.2006.05.048.

Kara, S. (2013) ‘Treatment of transport container washing wastewater by electrocoagulation’, *Environmental Progress and Sustainable Energy*, 32(2), pp. 249–256. doi: 10.1002/ep.11616.

Katal, R. and Pahlavanzadeh, H. (2011) ‘Influence of different combinations of aluminum and iron electrode on electrocoagulation efficiency: Application to the treatment of paper mill wastewater’, *Desalination*, 265(1–3), pp. 199–205. doi: 10.1016/j.desal.2010.07.052.

Khaled, B., Wided, B., Bchir, H., Elimame, E., Mouna, L. and Zied, T. (2014) ‘Investigation of electrocoagulation reactor design parameters effect on the removal of cadmium from synthetic and phosphate industrial wastewater’, *Arabian Journal of Chemistry*. doi: 10.1016/j.arabjc.2014.12.012.

Khandegar, V. and Saroha, A. K. (2012) 'Electrochemical treatment of distillery spent wash using aluminum and iron electrodes', *Chinese Journal of Chemical Engineering*, 20(3), pp. 439–443. doi: 10.1016/S1004-9541(11)60204-8.

Khandegar, V. and Saroha, A. K. (2013) 'Electrocoagulation for the treatment of textile industry effluent--a review.', *Journal of environmental management*, 128(July 2013), pp. 949–63. doi: 10.1016/j.jenvman.2013.06.043.

Kim, H. K., Kim, J. G., Cho, J. D. and Hong, J. W. (2003) 'Optimization and characterization of UV-curable adhesives for optical communications by response surface methodology', *Polymer Testing*, 22(8), pp. 899–906. doi: 10.1016/S0142-9418(03)00038-2.

Kim, T.-H., Park, C., Shin, E.-B. and Kim, S. (2002) 'Decolorization of disperse and reactive dyes by continuous electrocoagulation process', *Desalination*, 150(2), pp. 165–175. doi: 10.1016/S0011-9164(02)00941-4.

Kirzhner, F., Zimmels, Y. and Shraiber, Y. (2008) 'Combined treatment of highly contaminated winery wastewater', *Separation and Purification Technology*, 63(1), pp. 38–44. doi: 10.1016/j.seppur.2008.03.034.

Kobyas, M., Bayramoglu, M. and Eyvaz, M. (2007) 'Techno-economical evaluation of electrocoagulation for the textile wastewater using different electrode connections', *Journal of Hazardous Materials*, 148(1–2), pp. 311–318. doi: 10.1016/j.jhazmat.2007.02.036.

Kobyas, M. and Delipinar, S. (2008) 'Treatment of the baker's yeast wastewater by electrocoagulation', *Journal of Hazardous Materials*, 154(1–3), pp. 1133–1140. doi: 10.1016/j.jhazmat.2007.11.019.

Kobyas, M., Demirbas, E., Can, O. T. and Bayramoglu, M. (2006) 'Treatment of levafix orange textile dye solution by electrocoagulation', *Journal of Hazardous Materials*, 132(2–3), pp. 183–188. doi: 10.1016/j.jhazmat.2005.07.084.

Kobyas, M., Hiz, H., Senturk, E., Aydiner, C. and Demirbas, E. (2006) 'Treatment of potato chips manufacturing wastewater by electrocoagulation', *Desalination*, 190(1–3), pp. 201–211. doi: 10.1016/j.desal.2005.10.006.

- Kobyas, M., Senturk, E. and Bayramoglu, M. (2006) 'Treatment of poultry slaughterhouse wastewaters by electrocoagulation', *Journal of Hazardous Materials*, 133(1–3), pp. 172–176. doi: 10.1016/j.jhazmat.2005.10.007.
- Kobyas, M., Ulu, F., Gebologlu, U., Demirbas, E. and Oncel, M. S. (2011) 'Treatment of potable water containing low concentration of arsenic with electrocoagulation: Different connection modes and Fe-Al electrodes', *Separation and Purification Technology*, 77(3), pp. 283–293. doi: 10.1016/j.seppur.2010.12.018.
- Körbahti, B. K. (2007) 'Response surface optimization of electrochemical treatment of textile dye wastewater', *Journal of Hazardous Materials*, 145(1–2), pp. 277–286. doi: 10.1016/j.jhazmat.2006.11.031.
- Körbahti, B. K. and Tanyolaç, A. (2008) 'Electrochemical treatment of simulated textile wastewater with industrial components and Levafix Blue CA reactive dye: Optimization through response surface methodology', *Journal of Hazardous Materials*, 151(2–3), pp. 422–431. doi: 10.1016/j.jhazmat.2007.06.010.
- Körbahti, B. K. and Tanyolaç, A. (2009) 'Continuous electrochemical treatment of simulated industrial textile wastewater from industrial components in a tubular reactor', *Journal of Hazardous Materials*, 170(2–3), pp. 771–778. doi: 10.1016/j.jhazmat.2009.05.032.
- Krishna, B. M., Murthy, U. N., Manoj Kumar, B. and Lokesh, K. S. (2010) 'Electrochemical pretreatment of distillery wastewater using aluminum electrode', *Journal of Applied Electrochemistry*, 40(3), pp. 663–673. doi: 10.1007/s10800-009-0041-x.
- Kumar, N. S. and Goel, S. (2010) 'Factors influencing arsenic and nitrate removal from drinking water in a continuous flow electrocoagulation (EC) process', *Journal of Hazardous Materials*, 173(1–3), pp. 528–533. doi: 10.1016/j.jhazmat.2009.08.117.
- Kumar, P. R., Chaudhari, S., Khilar, K. C. and Mahajan, S. P. (2004) 'Removal of arsenic from water by electrocoagulation', *Chemosphere*, 55(9), pp. 1245–1252. doi: 10.1016/j.chemosphere.2003.12.025.
- Kuokkanen, V., Kuokkanen, T., Rämö, J. and Lassi, U. (2013) 'Recent Applications

of Electrocoagulation in Treatment of Water and Wastewater—A Review’, *Green and Sustainable Chemistry*, 3(2), pp. 89–121. doi: 10.4236/gsc.2013.32013.

Kuokkanen, V., Kuokkanen, T., Rämö, J., Lassi, U. and Roininen, J. (2015) ‘Removal of phosphate from wastewaters for further utilization using electrocoagulation with hybrid electrodes - Techno-economic studies’, *Journal of Water Process Engineering*, 8, pp. e50–e57. doi: 10.1016/j.jwpe.2014.11.008.

Kuramitz, H., Saitoh, J., Hattori, T. and Tanaka, S. (2002) ‘Electrochemical removal of p-nonylphenol from dilute solutions using a carbon fiber anode’, *Water Research*, 36(13), pp. 3323–3329. doi: 10.1016/S0043-1354(02)00040-4.

Kurt, U., Gonullu, M. T., Ilhan, F. and Varinca, K. (2008) ‘Treatment of Domestic Wastewater by Electrocoagulation in a Cell with Fe–Fe Electrodes’, *Environmental Engineering Science*, 25(2), pp. 153–162. doi: 10.1089/ees.2006.0132.

Kushwaha, J. P., Srivastava, V. C. and Mall, I. D. (2010) ‘Organics removal from dairy wastewater by electrochemical treatment and residue disposal’, *Separation and Purification Technology*. Elsevier B.V., 76(2), pp. 198–205. doi: 10.1016/j.seppur.2010.10.008.

Lacasa, E., Cañizares, P., Sáez, C., Fernández, F. J. and Rodrigo, M. A. (2011a) ‘Electrochemical phosphates removal using iron and aluminium electrodes’, *Chemical Engineering Journal*, 172(1), pp. 137–143. doi: 10.1016/j.cej.2011.05.080.

Lacasa, E., Cañizares, P., Sáez, C., Fernández, F. J. and Rodrigo, M. A. (2011b) ‘Removal of arsenic by iron and aluminium electrochemically assisted coagulation’, *Separation and Purification Technology*, 79(1), pp. 15–19. doi: 10.1016/j.seppur.2011.03.005.

Lai, C. L. and Lin, S. H. (2003) ‘Electrocoagulation of chemical mechanical polishing (CMP) wastewater from semiconductor fabrication’, *Chemical Engineering Journal*, 95(1), pp. 205–211. doi: 10.1016/S1385-8947(03)00106-2.

Lai, C. L. and Lin, S. H. (2004) ‘Treatment of chemical mechanical polishing wastewater by electrocoagulation: System performances and sludge settling characteristics’, *Chemosphere*, 54(3), pp. 235–242. doi:

10.1016/j.chemosphere.2003.08.014.

Lakshmanan, D., Clifford, D. A. and Samanta, G. (2010) 'Comparative study of arsenic removal by iron using electrocoagulation and chemical coagulation', *Water Research*, 44(19), pp. 5641–5652. doi: 10.1016/j.watres.2010.06.018.

Lakshmi Kruthika, N., Karthika, S., Bhaskar Raju, G. and Prabhakar, S. (2013) 'Efficacy of electrocoagulation and electrooxidation for the purification of wastewater generated from gelatin production plant', *Journal of Environmental Chemical Engineering*, 1(3), pp. 183–188. doi: 10.1016/j.jece.2013.04.017.

Lee, C. S., Robinson, J. and Chong, M. F. (2014) 'A review on application of flocculants in wastewater treatment', *Process Safety and Environmental Protection*, pp. 489–508. doi: 10.1016/j.psep.2014.04.010.

Lekhlif, B., Oudrhiri, L., Zidane, F., Drogui, P. and Blais, J. F. (2014) 'Study of the electrocoagulation of electroplating industry wastewaters charged by nickel (II) and chromium (VI)', *Journal of Materials and Environmental Science*, 5(1), pp. 111–120.

Li, X., Song, J., Guo, J., Wang, Z. and Feng, Q. (2011) 'Landfill leachate treatment using electrocoagulation', in *Procedia Environmental Sciences*, pp. 1159–1164. doi: 10.1016/j.proenv.2011.09.185.

Lin, S. H. and Lin, C. M. (1993) 'Treatment of textile waste effluents by ozonation and chemical coagulation', *Water Research*, 27(12), pp. 1743–1748. doi: 10.1016/0043-1354(93)90112-U.

Lin, S. H. and Peng, C. F. (1994) 'Treatment of textile wastewater by electrochemical method', *Water Research*, 28(2), pp. 277–282. doi: 10.1016/0043-1354(94)90264-X.

Lin, S. H. and Wu, C. L. (1996) 'Electrochemical removal of nitrite and ammonia for aquaculture', *Water Research*, 30(3), pp. 715–721. doi: 10.1016/0043-1354(95)00208-1.

Lin, S. and Peng, C. (1994) 'Treatment of textile wastewater by electrochemical method', *Water Research*, 28(2), pp. 277–282. doi: 10.1016/0043-1354(94)90264-X.

Luna, A. S., Costa, A. L. H., da Costa, A. C. A. and Henriques, C. A. (2010)

‘Competitive biosorption of cadmium(II) and zinc(II) ions from binary systems by *Sargassum filipendula*’, *Bioresource Technology*, 101(14), pp. 5104–5111. doi: 10.1016/j.biortech.2010.01.138.

Mahvi, A. H., Ebrahimi, S. J. A. din, Mesdaghinia, A., Gharibi, H. and Sowlat, M. H. (2011) ‘Performance evaluation of a continuous bipolar electrocoagulation/electrooxidation-electroflotation (ECEO-EF) reactor designed for simultaneous removal of ammonia and phosphate from wastewater effluent’, *Journal of Hazardous Materials*, 192(3), pp. 1267–1274. doi: 10.1016/j.jhazmat.2011.06.041.

Martínez-Delgadillo, S. A., Mollinedo-Ponce, H., Mendoza-Escamilla, V. and Barrera-Díaz, C. (2010) ‘Residence time distribution and back-mixing in a tubular electrochemical reactor operated with different inlet flow velocities, to remove Cr(VI) from wastewater’, *Chemical Engineering Journal*, 165(3), pp. 776–783. doi: 10.1016/j.cej.2010.09.066.

Matilainen, A., Vepsäläinen, M. and Sillanpää, M. (2010) ‘Natural organic matter removal by coagulation during drinking water treatment: A review’, *Advances in Colloid and Interface Science*, 159(2), pp. 189–197. doi: 10.1016/j.cis.2010.06.007.

Meas, Y., Ramirez, J. A., Villalon, M. A. and Chapman, T. W. (2010) ‘Industrial wastewaters treated by electrocoagulation’, in *Electrochimica Acta*, pp. 8165–8171. doi: 10.1016/j.electacta.2010.05.018.

Merzouk, B., Gourich, B., Sekki, A., Madani, K., Vial, C. and Barkaoui, M. (2009) ‘Studies on the decolorization of textile dye wastewater by continuous electrocoagulation process’, *Chemical Engineering Journal*, 149(1–3), pp. 207–214. doi: 10.1016/j.cej.2008.10.018.

Meunier, N., Drogui, P., Montané, C., Hausler, R., Mercier, G. and Blais, J. F. (2006) ‘Comparison between electrocoagulation and chemical precipitation for metals removal from acidic soil leachate’, *Journal of Hazardous Materials*, 137(1), pp. 581–590. doi: 10.1016/j.jhazmat.2006.02.050.

Millar, G. J., Lin, J., Arshad, A. and Couperthwaite, S. J. (2014) ‘Evaluation of electrocoagulation for the pre-treatment of coal seam water’, *Journal of Water Process Engineering*, 4(C), pp. 166–178. doi: 10.1016/j.jwpe.2014.10.002.

Mishra, A. (2009) 'Assessment of Coal Quality of Some Indian Coals', *Mining Engineering*.

Modirshahla, N., Behnajady, M. A. and Kooshaiian, S. (2007) 'Investigation of the effect of different electrode connections on the removal efficiency of Tartrazine from aqueous solutions by electrocoagulation', *Dyes and Pigments*, 74(2), pp. 249–257. doi: 10.1016/j.dyepig.2006.02.006.

Modirshahla, N., Behnajady, M. A. and Mohammadi-Aghdam, S. (2008) 'Investigation of the effect of different electrodes and their connections on the removal efficiency of 4-nitrophenol from aqueous solution by electrocoagulation', *Journal of Hazardous Materials*, 154(1–3), pp. 778–786. doi: 10.1016/j.jhazmat.2007.10.120.

MOLLAH, M., MORKOVSKY, P., GOMES, J., KESMEZ, M., PARGA, J. and COCKE, D. (2004) 'Fundamentals, present and future perspectives of electrocoagulation', *Journal of Hazardous Materials*, 114(1–3), pp. 199–210. doi: 10.1016/j.jhazmat.2004.08.009.

Mollah, M. Y. A., Morkovsky, P., Gomes, J. A. G., Kesmez, M., Parga, J. and Cocke, D. L. (2004) 'Fundamentals, present and future perspectives of electrocoagulation', *Journal of Hazardous Materials*, pp. 199–210. doi: 10.1016/j.jhazmat.2004.08.009.

Mondal, B., Srivastava, V. C., Kushwaha, J. P., Bhatnagar, R., Singh, S. and Mall, I. D. (2013a) 'Parametric and multiple response optimization for the electrochemical treatment of textile printing dye-bath effluent', *Separation and Purification Technology*. Elsevier B.V., 109, pp. 135–143. doi: 10.1016/j.seppur.2013.02.026.

Mondal, B., Srivastava, V. C., Kushwaha, J. P., Bhatnagar, R., Singh, S. and Mall, I. D. (2013b) 'Parametric and multiple response optimization for the electrochemical treatment of textile printing dye-bath effluent', *Separation and Purification Technology*, 109, pp. 135–143. doi: 10.1016/j.seppur.2013.02.026.

Montgomery, D. C. (2000) *Design and Analysis of Experiments, 5th Edition, America*. doi: 978-0-470-56319-9.

Montgomery, D. C. (2012) *Design and Analysis of Experiments, Design*. doi:

10.1198/tech.2006.s372.

Moreira, F. C., Boaventura, R. A. R., Brillas, E. and Vilar, V. J. P. (2017) 'Electrochemical advanced oxidation processes: A review on their application to synthetic and real wastewaters', *Applied Catalysis B: Environmental*, 202, pp. 217–261. doi: 10.1016/j.apcatb.2016.08.037.

Moreno-Casillas, H. A., Cocke, D. L., Gomes, J. A. G., Morkovsky, P., Parga, J. R. and Peterson, E. (2007) 'Electrocoagulation mechanism for COD removal', *Separation and Purification Technology*, 56(2), pp. 204–211. doi: 10.1016/j.seppur.2007.01.031.

Moussavi, G., Majidi, F. and Farzadkia, M. (2011) 'The influence of operational parameters on elimination of cyanide from wastewater using the electrocoagulation process', *Desalination*, 280(1–3), pp. 127–133. doi: 10.1016/j.desal.2011.06.052.

Murugananthan, M., Bhaskar Raju, G. and Prabhakar, S. (2004) 'Removal of sulfide, sulfate and sulfite ions by electro coagulation', *Journal of Hazardous Materials*, 109(1–3), pp. 37–44. doi: 10.1016/j.jhazmat.2003.12.009.

Murugananthan, M., Raju, G. B. and Prabhakar, S. (2004) 'Separation of pollutants from tannery effluents by electro flotation', *Separation and Purification Technology*, 40(1), pp. 69–75. doi: 10.1016/j.seppur.2004.01.005.

Naje, A. S., Chelliapan, S., Zakaria, Z. and Abbas, S. A. (2015) 'Enhancement of an electrocoagulation process for the treatment of textile wastewater under combined electrical connections using titanium plates', *International Journal of Electrochemical Science*, 10(6), pp. 4495–4512.

Naje, A. S., Chelliapan, S., Zakaria, Z., Ajeel, M. A. and Alaba, P. A. (2017) 'A review of electrocoagulation technology for the treatment of textile wastewater', *Reviews in Chemical Engineering*, 33(3), pp. 263–292. doi: 10.1515/revce-2016-0019.

Nanseu-Njiki, C. P., Tchamango, S. R., Ngom, P. C., Darchen, A. and Ngameni, E. (2009) 'Mercury(II) removal from water by electrocoagulation using aluminium and iron electrodes', *Journal of Hazardous Materials*, 168(2–3), pp. 1430–1436. doi: 10.1016/j.jhazmat.2009.03.042.

Ni'am, M. F., Othman, F., Sohaili, J. and Fauzia, Z. (2007) 'Removal of COD and Turbidity to Improve Wastewater Quality Using Electrocoagulation Technique', *The Malaysian Journal of Analytical Sciences*, 11(1), pp. 198–205.

Nuñez, P., Hansen, H. K., Aguirre, S. and Maureira, C. (2011) 'Electrocoagulation of arsenic using iron nanoparticles to treat copper mineral processing wastewater', in *Separation and Purification Technology*, pp. 285–290. doi: 10.1016/j.seppur.2011.02.028.

Orkun, M. O. and Kuleyin, A. (2012) 'Treatment performance evaluation of chemical oxygen demand from landfill leachate by electro-coagulation and electro-fenton technique', *Environmental Progress & Sustainable Energy*, 31(1), pp. 59–67. doi: 10.1002/Ep.10522.

Palani, R., AbdulGani, A. and Balasubramanian, N. (2017) 'Treatment of Tannery Effluent Using a Rotating Disc Electrochemical Reactor', *Water Environment Research*, 89(1), pp. 77–85. doi: 10.2175/106143016X14609975746046.

Palani, R. and Balasubramanian, N. (2012) 'Electrochemical treatment of Methyl Orange dye wastewater by rotating disc electrode: Optimisation using response surface methodology', *Coloration Technology*, 128(6), pp. 434–439. doi: 10.1111/j.1478-4408.2012.00387.x.

Panizza, M. and Cerisola, G. (2010) 'Applicability of electrochemical methods to carwash wastewaters for reuse. Part 1: Anodic oxidation with diamond and lead dioxide anodes', *Journal of Electroanalytical Chemistry*, 638(1), pp. 28–32. doi: 10.1016/j.jelechem.2009.10.025.

Parga, J. R., Cocke, D. L., Valverde, V., Gomes, J. A. G., Kesmez, M., Moreno, H., Weir, M. and Mencer, D. (2005) 'Characterization of electrocoagulation for removal of chromium and arsenic', *Chemical Engineering and Technology*, 28(5), pp. 605–612. doi: 10.1002/ceat.200407035.

Patel, U. D., Ruparelia, J. P. and Patel, M. U. (2011) 'Electrocoagulation treatment of simulated floor-wash containing Reactive Black 5 using iron sacrificial anode', *Journal of Hazardous Materials*, 197, pp. 128–136. doi: 10.1016/j.jhazmat.2011.09.064.

- Pearse, M. J. (2003) 'Historical use and future development of chemicals for solid-liquid separation in the mineral processing industry', in *Minerals Engineering*, pp. 103–108. doi: 10.1016/S0892-6875(02)00288-1.
- Pérez, M., Torrades, F., Domènech, X. and Peral, J. (2002) 'Fenton and photo-Fenton oxidation of textile effluents', *Water Research*, 36(11), pp. 2703–2710. doi: 10.1016/S0043-1354(01)00506-1.
- Pernitsky, D. J. and Edzwald, J. K. (2006) 'Selection of alum and polyaluminum coagulants: Principles and applications', *Journal of Water Supply: Research and Technology - AQUA*, 55(2), pp. 121–141. doi: 10.2166/aqua.2006.062.
- Persson, J. (2000) 'The hydraulic performance of ponds of various layouts', *Urban Water*, 2(3), pp. 243–250. doi: 10.1016/S1462-0758(00)00059-5.
- Pi, K. W., Xiao, Q., Zhang, H. Q., Xia, M. and Gerson, A. R. (2014) 'Decolorization of synthetic Methyl Orange wastewater by electrocoagulation with periodic reversal of electrodes and optimization by RSM', *Process Safety and Environmental Protection*, 92(6), pp. 796–806. doi: 10.1016/j.psep.2014.02.008.
- Pociecha, M. and Lestan, D. (2010) 'Using electrocoagulation for metal and chelant separation from washing solution after EDTA leaching of Pb, Zn and Cd contaminated soil', *Journal of Hazardous Materials*, 174(1–3), pp. 670–678. doi: 10.1016/j.jhazmat.2009.09.103.
- Ricordel, C. and Djelal, H. (2014) 'Treatment of landfill leachate with high proportion of refractory materials by electrocoagulation: System performances and sludge settling characteristics', *Journal of Environmental Chemical Engineering*, 2(3), pp. 1551–1557. doi: 10.1016/j.jece.2014.06.014.
- Rincón, G. J. and La Motta, E. J. (2014) 'Simultaneous removal of oil and grease, and heavy metals from artificial bilge water using electro-coagulation/flotation', *Journal of Environmental Management*, 144, pp. 42–50. doi: 10.1016/j.jenvman.2014.05.004.
- Roa-Morales, G., Campos-Medina, E., Aguilera-Cotero, J., Bilyeu, B. and Barrera-Díaz, C. (2007) 'Aluminum electrocoagulation with peroxide applied to wastewater from pasta and cookie processing', *Separation and Purification Technology*, 54(1),

pp. 124–129. doi: 10.1016/j.seppur.2006.08.025.

Rodríguez, G., Sierra-Espinosa, F. Z., Teloxa, J., Álvarez, A. and Hernández, J. A. (2015) ‘Hydrodynamic design of electrochemical reactors based on computational fluid dynamics’, *Desalination and Water Treatment*, 3994(March), pp. 1–12. doi: 10.1080/19443994.2015.1114169.

Rodríguez, J., Friedrich, B. and Stopić, S. (2007) ‘Continuous Electrocoagulation Treatment of Wastewater from Copper Production’, *World of Metallurgy – ERZMETALL*, 2(Figure 1), pp. 81–87.

Şahan, T., Ceylan, H., Şahiner, N. and Aktaş, N. (2010) ‘Optimization of removal conditions of copper ions from aqueous solutions by *Trametes versicolor*’, *Bioresource Technology*, 101(12), pp. 4520–4526. doi: 10.1016/j.biortech.2010.01.105.

Sahu, O., Mazumdar, B. and Chaudhari, P. K. (2014) ‘Treatment of wastewater by electrocoagulation: A review’, *Environmental Science and Pollution Research*, pp. 2397–2413. doi: 10.1007/s11356-013-2208-6.

Sahu, O. P. and Chaudhari, P. K. (2013) ‘Review on Chemical treatment of Industrial Waste Water Review on Chemical treatment’, *Journal of Applied Science Environmental Management*, 17(2), pp. 241–257. doi: <http://dx.doi.org/10.4314/jasem.v17i2.8>.

Sánchez-Bayo, F. (2006) ‘Comparative acute toxicity of organic pollutants and reference values for crustaceans. I. Branchiopoda, Copepoda and Ostracoda’, *Environmental Pollution*, 139(3), pp. 385–420. doi: 10.1016/j.envpol.2005.06.016.

Santo, C. E., Vilar, V. J. P., Botelho, C. M. S., Bhatnagar, A., Kumar, E. and Boaventura, R. A. R. (2012) ‘Optimization of coagulation-flocculation and flotation parameters for the treatment of a petroleum refinery effluent from a Portuguese plant’, *Chemical Engineering Journal*, 183, pp. 117–123. doi: 10.1016/j.cej.2011.12.041.

Saravanathamizhan, R., Mohan, N., Balasubramanian, N., Ramamurthi, V. and Ahmed Basha, C. (2007) ‘Evaluation of electro-oxidation of textile effluent using response surface methods’, *Clean - Soil, Air, Water*, 35(4), pp. 355–361. doi:

10.1002/clen.200700005.

Saravanathamizhan, R., Paranthaman, R., Balasubramanian, N. and Ahmed Basha, C. (2008) 'Tanks in Series Model for Continuous Stirred Tank Electrochemical Reactor', *Industrial & Engineering Chemistry Research*, 47(9), pp. 2976–2984. doi: 10.1021/ie071426q.

Saravanathamizhan, R., Paranthaman, R., Balasubramanian, N. and Basha, C. A. (2008a) 'Residence time distribution in continuous stirred tank electrochemical reactor', *Chemical Engineering Journal*, 142(2), pp. 209–216. doi: 10.1016/j.cej.2008.02.017.

Saravanathamizhan, R., Paranthaman, R., Balasubramanian, N. and Basha, C. A. (2008b) 'Residence time distribution in continuous stirred tank electrochemical reactor', *Chemical Engineering Journal*, 142(2), pp. 209–216. doi: 10.1016/j.cej.2008.02.017.

Saravanathamizhan, R., Soloman, P. a, Balasubramanian, N., Basha, C. A. and Do, W. (2008) 'Optimization of In-situ Electro-oxidation of Formaldehyde by the Response Surface Method', *Chem. Biochem. Eng.*, 22(2), pp. 213–220.

Şengil, I. A., Kulaç, S. and Özacar, M. (2009) 'Treatment of tannery liming drum wastewater by electrocoagulation', *Journal of Hazardous Materials*, 167(1–3), pp. 940–946. doi: 10.1016/j.jhazmat.2009.01.099.

Şengil, I. A. and özacar, M. (2006) 'Treatment of dairy wastewaters by electrocoagulation using mild steel electrodes', *Journal of Hazardous Materials*, 137(2), pp. 1197–1205. doi: 10.1016/j.jhazmat.2006.04.009.

Shafaei, A., Rezayee, M., Arami, M. and Nikazar, M. (2010) 'Removal of Mn²⁺ ions from synthetic wastewater by electrocoagulation process', *Desalination*, 260(1), pp. 23–28. doi: 10.1016/j.desal.2010.05.006.

Siles, J. A., Gutiérrez, M. C., Martín, M. A. and Martín, A. (2011) 'Physical-chemical and biomethanization treatments of wastewater from biodiesel manufacturing', *Bioresource Technology*, 102(10), pp. 6348–6351. doi: 10.1016/j.biortech.2011.02.106.

Singh, H., Fletcher, D. F. and Nijdam, J. J. (2011) 'An assessment of different turbulence models for predicting flow in a baffled tank stirred with a Rushton turbine', *Chemical Engineering Science*, 66(23), pp. 5976–5988. doi: 10.1016/j.ces.2011.08.018.

Singh, S., Haberl, R., Moog, O., Shrestha, R. R., Shrestha, P. and Shrestha, R. (2009) 'Performance of an anaerobic baffled reactor and hybrid constructed wetland treating high-strength wastewater in Nepal—A model for DEWATS', *Ecological Engineering*, 35(5), pp. 654–660. doi: 10.1016/j.ecoleng.2008.10.019.

Singh, S., Srivastava, V. C. and Mall, I. D. (2013a) 'Mechanism of dye degradation during electrochemical treatment', *Journal of Physical Chemistry C*, 117(29), pp. 15229–15240. doi: 10.1021/jp405289f.

Singh, S., Srivastava, V. C. and Mall, I. D. (2013b) 'Mechanistic study of electrochemical treatment of basic green 4 dye with aluminum electrodes through zeta potential, TOC, COD and color measurements, and characterization of residues', *RSC Advances*, 3(37), p. 16426. doi: 10.1039/c3ra41605d.

Singh, S., Srivastava, V. C. and Mall, I. D. (2013c) 'Multistep optimization and residue disposal study for electrochemical treatment of textile wastewater using aluminum electrode', *International Journal of Chemical Reactor Engineering*, 11(1). doi: 10.1515/ijcre-2012-0019.

Singh, S., Srivastava, V. C. and Mall, I. D. (2014) 'Electrochemical treatment of dye bearing effluent with different anode-cathode combinations: Mechanistic study and sludge analysis', *Industrial and Engineering Chemistry Research*, 53(26), pp. 10743–10752. doi: 10.1021/ie4042005.

Sinha, R., Singh, A. and Mathur, S. (2014) 'Multiobjective optimization for minimum residual fluoride and specific energy in electrocoagulation process', *Desalination and Water Treatment*, 57(9), pp. 4194–4204. doi: 10.1080/19443994.2014.990929.

Sridhar, R., Sivakumar, V., Prince Immanuel, V. and Prakash Maran, J. (2011) 'Treatment of pulp and paper industry bleaching effluent by electrocoagulant process', *Journal of Hazardous Materials*, 186(2–3), pp. 1495–1502. doi: 10.1016/j.jhazmat.2010.12.028.

- Srivastava, V. C., Swamy, M. M., Mall, I. D., Prasad, B. and Mishra, I. M. (2006) 'Adsorptive removal of phenol by bagasse fly ash and activated carbon: Equilibrium, kinetics and thermodynamics', *Colloids and Surfaces A: Physicochemical and Engineering Aspects*, 272(1–2), pp. 89–104. doi: 10.1016/j.colsurfa.2005.07.016.
- TA, C. and BRIGNAL, W. (1998) 'Application of computational fluid dynamics technique to storage reservoir studies', *Water Science and Technology*, 37(2), pp. 219–226. doi: 10.1016/S0273-1223(98)00027-4.
- Tanyildizi, M. T. (2011) 'Modeling of adsorption isotherms and kinetics of reactive dye from aqueous solution by peanut hull', *Chemical Engineering Journal*, 168(3), pp. 1234–1240. doi: 10.1016/j.cej.2011.02.021.
- Tchamango, S., Nanseu-Njiki, C. P., Ngameni, E., Hadjiev, D. and Darchen, A. (2010) 'Treatment of dairy effluents by electrocoagulation using aluminium electrodes', *Science of the Total Environment*, 408(4), pp. 947–952. doi: 10.1016/j.scitotenv.2009.10.026.
- Tchobanoglous, G., Burton, F. L. (Franklin L., Stensel, H. D. and Metcalf & Eddy. (2003) *Wastewater engineering: treatment and reuse*. McGraw-Hill. Available at: https://books.google.co.in/books/about/Wastewater_Engineering.html?id=U9OmPwAACA AJ&redir_esc=y&hl=en (Accessed: 3 May 2017).
- Tezcan Un, U., Kandemir, A., Erginel, N. and Ocal, S. E. (2014) 'Continuous electrocoagulation of cheese whey wastewater: An application of response surface methodology', *Journal of Environmental Management*, 146, pp. 245–250. doi: 10.1016/j.jenvman.2014.08.006.
- Tezcan Un, U., Koparal, A. S. and Bakir Ogutveren, U. (2009) 'Electrocoagulation of vegetable oil refinery wastewater using aluminum electrodes', *Journal of Environmental Management*, 90(1), pp. 428–433. doi: 10.1016/j.jenvman.2007.11.007.
- Tezcan Un, U., Koparal, A. S. and Bakir Ogutveren, U. (2013) 'Fluoride removal from water and wastewater with a batch cylindrical electrode using electrocoagulation', *Chemical Engineering Journal*, 223, pp. 110–115. doi: 10.1016/j.cej.2013.02.126.

Tezcan Un, U. and Ozel, E. (2013) 'Electrocoagulation of yogurt industry wastewater and the production of ceramic pigments from the sludge', *Separation and Purification Technology*, 120, pp. 386–391. doi: 10.1016/j.seppur.2013.09.031.

Thakur, C., Srivastava, V. C. and Mall, I. D. (2009) 'Electrochemical treatment of a distillery wastewater: Parametric and residue disposal study', *Chemical Engineering Journal*, 148(2–3), pp. 496–505. doi: 10.1016/j.cej.2008.09.043.

Thiam, A., Zhou, M., Brillas, E. and Sirés, I. (2014) 'Two-step mineralization of Tartrazine solutions: Study of parameters and by-products during the coupling of electrocoagulation with electrochemical advanced oxidation processes', *Applied Catalysis B: Environmental*, 150–151, pp. 116–125. doi: 10.1016/j.apcatb.2013.12.011.

Thilakavathi, R., Rajasekhar, D., Balasubramanian, N., Srinivasakannan, C. and Shoaibi, A. Al (2012) 'CFD Modeling of Continuous Stirred Tank Electrochemical Reactor', 7, pp. 1386–1401.

Top, S., Sekman, E., Hoşver, S. and Bilgili, M. S. (2011) 'Characterization and electrocoagulative treatment of nanofiltration concentrate of a full-scale landfill leachate treatment plant', *Desalination*, 268(1), pp. 158–162. doi: 10.1016/j.desal.2010.10.012.

Trompette, J. L. and Vergnes, H. (2009) 'On the crucial influence of some supporting electrolytes during electrocoagulation in the presence of aluminum electrodes', *Journal of Hazardous Materials*, 163(2–3), pp. 1282–1288. doi: 10.1016/j.jhazmat.2008.07.148.

Tsai, D. D. W., Ramaraj, R. and Chen, P. H. (2012) 'A Method of Short-Circuiting Comparison', *Water Resources Management*, 26(9), pp. 2689–2702. doi: 10.1007/s11269-012-0040-2.

Uğurlu, M., Gürses, A., Doğar, Ç. and Yalçın, M. (2008) 'The removal of lignin and phenol from paper mill effluents by electrocoagulation', *Journal of Environmental Management*, 87(3), pp. 420–428. doi: 10.1016/j.jenvman.2007.01.007.

UNESCO (2012) *World Water Development Report Volume 4: Managing Water*

under Uncertainty and Risk, Water demand: What drives consumption? doi: 10.1608/FRJ-3.1.2.

Valero, D., Ortiz, J. M., García, V., Expósito, E., Montiel, V. and Aldaz, A. (2011) 'Electrocoagulation of wastewater from almond industry', *Chemosphere*, 84(9), pp. 1290–1295. doi: 10.1016/j.chemosphere.2011.05.032.

Vasudevan, S., Kannan, B. S., Lakshmi, J., Mohanraj, S. and Sozhan, G. (2011) 'Effects of alternating and direct current in electrocoagulation process on the removal of fluoride from water', *Journal of Chemical Technology and Biotechnology*, 86(3), pp. 428–436. doi: 10.1002/jctb.2534.

Vasudevan, S. and Lakshmi, J. (2011) 'Effects of alternating and direct current in electrocoagulation process on the removal of cadmium from water - A novel approach', *Separation and Purification Technology*, 80(3), pp. 643–651. doi: 10.1016/j.seppur.2011.06.027.

Vasudevan, S. and Lakshmi, J. (2012) 'Effect of alternating and direct current in an electrocoagulation process on the removal of cadmium from water', *Water Science and Technology*, 65(2), pp. 353–360. doi: 10.2166/wst.2012.859.

Vasudevan, S. and Lakshmi, J. (2012) 'Electrochemical removal of boron from water: Adsorption and thermodynamic studies', *Canadian Journal of Chemical Engineering*, 90(4), pp. 1017–1026. doi: 10.1002/cjce.20585.

Vasudevan, S., Lakshmi, J. and Sozhan, G. (2011) 'Effects of alternating and direct current in electrocoagulation process on the removal of cadmium from water', *Journal of Hazardous Materials*, 192(1), pp. 26–34. doi: 10.1016/j.jhazmat.2011.04.081.

Vasudevan, S., Lakshmi, J. and Sozhan, G. (2013) 'Electrochemically assisted coagulation for the removal of boron from water using zinc anode', *Desalination*, 310, pp. 122–129. doi: 10.1016/j.desal.2012.01.016.

Vasudevan, S., Sheela, S. M., Lakshmi, J. and Sozhan, G. (2010) 'Optimization of the process parameters for the removal of boron from drinking water by electrocoagulation - A clean technology', *Journal of Chemical Technology and Biotechnology*, 85(7), pp. 926–933. doi: 10.1002/jctb.2382.

Vázquez, A., Rodríguez, I. and Lázaro, I. (2012) 'Primary potential and current density distribution analysis: A first approach for designing electrocoagulation reactors', *Chemical Engineering Journal*, 179, pp. 253–261. doi: 10.1016/j.cej.2011.10.078.

Vegini, A. A., Meier, H. F., Less, J. J. and Mori, M. (2008) 'Computational fluid dynamics (CFD) Analysis of cyclone separators connected in series', *Industrial and Engineering Chemistry Research*, 47(1), pp. 192–200. doi: 10.1021/ie061501h.

Vepsäläinen, M. (2012) *Electrocoagulation in the treatment of industrial waters and wastewaters*, VTT science.

Vepsäläinen, M., Kivisaari, H., Pulliainen, M., Oikari, A. and Sillanpää, M. (2011) 'Removal of toxic pollutants from pulp mill effluents by electrocoagulation', *Separation and Purification Technology*, 81(2), pp. 141–150. doi: 10.1016/j.seppur.2011.07.017.

Verma, A. K., Dash, R. R. and Bhunia, P. (2012) 'A review on chemical coagulation/flocculation technologies for removal of colour from textile wastewaters', *Journal of Environmental Management*, pp. 154–168. doi: 10.1016/j.jenvman.2011.09.012.

Vu, T. P., Vogel, A., Kern, F., Platz, S., Menzel, U. and Gadow, R. (2014) 'Characteristics of an electrocoagulation-electroflotation process in separating powdered activated carbon from urban wastewater effluent', *Separation and Purification Technology*, 134, pp. 196–203. doi: 10.1016/j.seppur.2014.07.038.

Walsh, F. C. (2001) 'Electrochemical technology for environmental treatment and clean energy conversion', *Pure and Applied Chemistry*, 73(12), pp. 1819–1837. doi: 10.1351/pac200173121819.

Walsh, F. C. and Pletcher, D. (2014) 'Electrochemical Engineering and Cell Design', in *Developments in Electrochemistry: Science Inspired by Martin Fleischmann*, pp. 95–111. doi: 10.1002/9781118694404.ch6.

Wan, W., Pepping, T. J., Banerji, T., Chaudhari, S. and Giammar, D. E. (2011) 'Effects of water chemistry on arsenic removal from drinking water by

electrocoagulation', *Water Research*, 45(1), pp. 384–392. doi: 10.1016/j.watres.2010.08.016.

Wang, C. T., Chou, W. L. and Kuo, Y. M. (2009) 'Removal of COD from laundry wastewater by electrocoagulation/electroflotation', *Journal of Hazardous Materials*, 164(1), pp. 81–86. doi: 10.1016/j.jhazmat.2008.07.122.

Wang, Y., Sanly, Brannock, M. and Leslie, G. (2009) 'Diagnosis of membrane bioreactor performance through residence time distribution measurements — a preliminary study', *Desalination*, 236(1–3), pp. 120–126. doi: 10.1016/j.desal.2007.10.058.

Winnick, J. (1996) 'A first course in electrochemical engineering. By Frank Walsh, Electrochemical Consultancy, Hants, England, 1993, 381 pp., \$45.00', *AIChE Journal*, 42(4), pp. 1195–1197. doi: 10.1002/aic.690420437.

World Water Assessment Programme (2012) *World Water Development Report Volume 4: Managing Water under Uncertainty and Risk, Water demand: What drives consumption?* doi: 10.1608/FRJ-3.1.2.

Xanthos, S., Gong, M., Ramalingam, K., Fillos, J., Deur, A., Beckmann, K. and McCorquodale, J. A. (2011) 'Performance Assessment of Secondary Settling Tanks Using CFD Modeling', *Water Resources Management*. Springer Netherlands, 25(4), pp. 1169–1182. doi: 10.1007/s11269-010-9620-1.

Yahiaoui, O., Lounici, H., Abdi, N., Drouiche, N., Ghaffour, N., Pauss, A. and Mameri, N. (2011) 'Treatment of olive mill wastewater by the combination of ultrafiltration and bipolar electrochemical reactor processes', *Chemical Engineering and Processing: Process Intensification*, 50(1), pp. 37–41. doi: 10.1016/j.cep.2010.11.003.

Yang, Q., Drak, A., Hasson, D. and Semiat, R. (2007) 'RO module RTD analyses based on directly processing conductivity signals', *Journal of Membrane Science*, 306(1–2), pp. 355–364. doi: 10.1016/j.memsci.2007.09.018.

Yavuz, Y., Öcal, E., Koparal, A. S. and Ögütveren, Ü. B. (2011) 'Treatment of dairy industry wastewater by EC and EF processes using hybrid Fe-Al plate electrodes',

Journal of Chemical Technology and Biotechnology, 86(7), pp. 964–969. doi: 10.1002/jctb.2607.

Yilmaz, A. E., Boncukcuoğlu, R. and Kocakerim, M. M. (2007a) ‘A quantitative comparison between electrocoagulation and chemical coagulation for boron removal from boron-containing solution’, *Journal of Hazardous Materials*, 149(2), pp. 475–481. doi: 10.1016/j.jhazmat.2007.04.018.

Yilmaz, A. E., Boncukcuoğlu, R. and Kocakerim, M. M. (2007b) ‘An empirical model for parameters affecting energy consumption in boron removal from boron-containing wastewaters by electrocoagulation’, *Journal of Hazardous Materials*, 144(1–2), pp. 101–107. doi: 10.1016/j.jhazmat.2006.09.085.

Yilmaz, A. E., Boncukcuoğlu, R., Kocakerim, M. M. and Keskinler, B. (2005) ‘The investigation of parameters affecting boron removal by electrocoagulation method’, *Journal of Hazardous Materials*, 125(1–3), pp. 160–165. doi: 10.1016/j.jhazmat.2005.05.020.

Yilmaz, A. E., Boncukcuoğlu, R., Kocakerim, M. M., Yilmaz, M. T. and Paluluoğlu, C. (2008) ‘Boron removal from geothermal waters by electrocoagulation’, *Journal of Hazardous Materials*, 153(1–2), pp. 146–151. doi: 10.1016/j.jhazmat.2007.08.030.

Yu, Y. X., Wang, X. X., Yang, D., Lei, B. L., Zhang, X. Y. L. and Zhang, X. Y. L. (2014) ‘Evaluation of human health risks posed by carcinogenic and non-carcinogenic multiple contaminants associated with consumption of fish from Taihu Lake, China’, *Food and Chemical Toxicology*, 69, pp. 86–93. doi: 10.1016/j.fct.2014.04.001.

Zaied, M. and Bellakhal, N. (2009) ‘Electrocoagulation treatment of black liquor from paper industry’, *Journal of Hazardous Materials*, 163(2–3), pp. 995–1000. doi: 10.1016/j.jhazmat.2008.07.115.

Zaroual, Z., Azzi, M., Saib, N. and Chainet, E. (2006) ‘Contribution to the study of electrocoagulation mechanism in basic textile effluent’, *Journal of Hazardous Materials*, 131(1–3), pp. 73–78. doi: 10.1016/j.jhazmat.2005.09.021.

Zhang, L., Pan, Q. and Rempel, G. L. (2007) ‘Residence time distribution in a multistage agitated contactor with newtonian fluids: CFD prediction and experimental

validation', *Industrial and Engineering Chemistry Research*, 46(11), pp. 3538–3546. doi: 10.1021/ie060567+.

Zhao, X., Zhang, B., Liu, H., Chen, F., Li, A. and Qu, J. (2012) 'Transformation characteristics of refractory pollutants in plugboard wastewater by an optimal electrocoagulation and electro-Fenton process', *Chemosphere*, 87(6), pp. 631–636. doi: 10.1016/j.chemosphere.2012.01.054.

Zhu, J., Wu, F., Pan, X., Guo, J. and Wen, D. (2011) 'Removal of antimony from antimony mine flotation wastewater by electrocoagulation with aluminum electrodes', *Journal of Environmental Sciences*, 23(7), pp. 1066–1071. doi: 10.1016/S1001-0742(10)60550-5.

Zidane, F., Drogui, P., Lekhlif, B., Bensaid, J., Blais, J. F., Belcadi, S. and kacemi, K. El (2008) 'Decolourization of dye-containing effluent using mineral coagulants produced by electrocoagulation', *Journal of Hazardous Materials*, 155(1–2), pp. 153–163. doi: 10.1016/j.jhazmat.2007.11.041.

Zodi, S., Louvet, J. N., Michon, C., Potier, O., Pons, M. N., Lopicque, F. and Leclerc, J. P. (2011) 'Electrocoagulation as a tertiary treatment for paper mill wastewater: Removal of non-biodegradable organic pollution and arsenic', *Separation and Purification Technology*, 81(1), pp. 62–68. doi: 10.1016/j.seppur.2011.07.002.

Zodi, S., Potier, O., Lopicque, F. and Leclerc, J. P. (2009a) 'Treatment of the textile wastewaters by electrocoagulation: Effect of operating parameters on the sludge settling characteristics', *Separation and Purification Technology*, 69(1), pp. 29–36. doi: 10.1016/j.seppur.2009.06.028.

Zodi, S., Potier, O., Lopicque, F. and Leclerc, J. P. (2009b) 'Treatment of the textile wastewaters by electrocoagulation: Effect of operating parameters on the sludge settling characteristics', *Separation and Purification Technology*, 69(1), pp. 29–36. doi: 10.1016/j.seppur.2009.06.028.

Zodi, S., Potier, O., Lopicque, F. and Leclerc, J. P. (2010) 'Treatment of the industrial wastewaters by electrocoagulation: Optimization of coupled electrochemical and sedimentation processes', *Desalination*, 261(1–2), pp. 186–190. doi: 10.1016/j.desal.2010.04.024.



Performance evaluation of 3D rotating anode in electro coagulation reactor: Part I: Effect of impeller



Aditya Choudhary, Sanjay Mathur*

Department of Civil Engineering, Malaviya National Institute of Technology, JLN Marg, Malaviya Nagar, Jaipur, Rajasthan 302017, India

ARTICLE INFO

Keywords:

3D rotating anode
Computational fluid dynamics (CFD)
Velocity profile
Velocity vector
Simulated textile wastewater
Residence time distribution (RTD)
Chemical oxygen demand (COD)
Color removal efficiency
Specific energy consumption

ABSTRACT

A hopper bottom electro chemical reactor with perforated 3D anode is attempted to avoid commonly encountered problems in conventional electrochemical reactor like short circuiting, development of dead zones, formation of oxide layer on anode surface etc. The RTD experiments and CFD simulations established that the present configuration performs better than commonly used plate electrode electrochemical reactors. The synthetic textile wastewater is treated in the proposed configuration. A higher COD removal efficiency (85.12%), color removal efficiency (97.97%) and low specific energy consumption (0.047 J/mg) are observed vis-à-vis plate electrode electrochemical reactors.

1. Introduction

In current scenario, water consumption and wastewater generation is becoming a cosmic issue in this era of industrial revolution. The conventional technologies presently available are costly and have become inefficient due to their own limitations to treat the wastewater to a desired level. The introduction of electrochemical technologies for the treatment of industrial wastewater is of great influence and readily replacing the conventional treatment technologies. In recent years, various treatment technologies have been used such as advanced electro oxidation, photo oxidation, electro coagulation, electro floatation, etc. [1–6].

The design of electrochemical reactor plays an important role in the process of treatment. It drives the dynamics of the fluid to be treated inside the electrochemical reactor. The effective geometry and design eradicate the issues that come into play with regular electrochemical reactors. The proper design and geometry of the electrochemical reactor helps the fluid to be treated in a uniform fashion leaving no dead zones, short circuiting, channeling and fouling of electrode [7–10]. All the issues can be addressed with efficient mixing inside the electrochemical reactor [11–14].

The residence time distribution (RTD) is an attribute of mixing in the electrochemical reactor. It provides information about the residence of elements inside the reactor. It helps to develop an accurate kinetic model for electrochemical reactor. The RTD also helps to design the reactor with desired fluid dynamics, which helps in scaling up of the

reactor [15–20].

In the present work, a reactor configuration with a 3D rotating anode acting as turbulence enhancer is presented to overcome the disadvantages experienced with the usual reactors like fluid channeling/short circuiting, back mixing, formation of dead zones and oxide layer formation on electrode etc., which may lead to loss of process efficiency and higher energy consumption. The 3D anode also acts as an impeller; hence in the following text anode is referred as impeller.

The study is being presented in two parts. The effect of the 3D impeller on the flow dynamics and improvement of yield is presented in this paper. The effect of rotation of 3D anode yielding performance improvement is being presented in second part of this series.

2. Literature review

The considerable amount of experimental and theoretical work has been done on RTD of the electrochemical reactor. Recently, the presence of inlet and outlet condition, presence of impeller and its mixing speed on the efficiency of mixing process have been investigated using RTD [17,21,22]. The mass tracer fraction helps in the study of flow behaviour and exit age distribution curves of parallel plate electrochemical reactor using single and two/three tank in series RTD model [23–25]. A significant improvement in mixing performance of an electrochemical reactor can be achieved by adding a draft tube at low impeller clearance [26].

The velocity, pressure and vector distribution in a chemical reactor

* Corresponding author.

E-mail address: smathur.ce@mmit.ac.in (S. Mathur).

<http://dx.doi.org/10.1016/j.jwpe.2017.08.020>

Received 17 May 2017; Received in revised form 23 August 2017; Accepted 25 August 2017
2214-7144/ © 2017 Elsevier Ltd. All rights reserved.



Contents lists available at ScienceDirect

Journal of Water Process Engineering

journal homepage: www.elsevier.com/locate/jwpe

Performance evaluation of 3D rotating anode in electro coagulation reactor: Part II: Effect of rotation

Aditya Choudhary, Sanjay Mathur^{*}

Department of Civil Engineering, Malaviya National Institute of Technology, JLN Marg, Malaviya Nagar, Jaipur, Rajasthan 302017, India

ARTICLE INFO

Keywords:

3D rotating anode
Hopper bottom electrochemical reactor
Computational fluid dynamics (CFD)
Velocity and vector profile
Simulated synthetic textile wastewater
Residence time distribution (RTD)
Chemical oxygen demand (COD)
Color removal efficiency
Specific electrical energy consumption (SEEC)

ABSTRACT

A hopper bottom electro chemical reactor with rotating 3D anode is attempted to avoid commonly encountered problems in electrochemical reactor like short circuiting, development of dead zones, formation of oxide layer on anode surface etc. The RTD experiments and CFD simulations established that the present configuration is free from these operational difficulties. The simulated synthetic textile wastewater is treated in the proposed configuration. A higher COD removal efficiency (96.40%), color removal efficiency (99.88%) and low specific energy consumption (0.028 J/mg) are observed vis-à-vis stationary 3D anode reactor.

1. Introduction

Electro coagulation, a process when coagulant is generated electrochemically and used to remove wide range of pollutants from water and wastewater [1]. The design of electrochemical reactor systems is of great interest for electrochemical engineers in various wastewater producing industries. The electrochemical wastewater treatment through redox reactions is readily replacing the conventional treatment technologies for wastewater treatment. Many toxic wastewater producing industries require costly physicochemical pre treatment as they are mostly non biodegradable waste [2]. There are various types of electrochemical reactors that are employed in various electrochemical applications for the treatment of toxic and non biodegradable wastewater. There are numerous designs of electrochemical reactors employed viz. conventional stack cell, flow cell mesh electrode, rotating disc, 3D electrode, parallel plate electrode etc. The process yield, efficiency and mass transfer of the reactor readily depends upon the geometry of the electrochemical reactor [3,4]. Electrochemical reactors offer a continuous production of treated water along with no requirement of expensive pre treatment. When they are operated in constant current mode, it is easy and flexible to scale-up the system. These systems are rapid in homogenous or heterogeneous reactions at higher temperatures [5–7]. These electrochemical reactors can also be used in applications for removal of metals, toxic waste, disinfection, organic and inorganic degradation [7–11].

The continuous flow stirred-tank reactor (CSTR) has been explored

by many researchers and investigators for treatment of various types of industrial wastewater through electrochemical treatment technology viz. phenol from wastewater, pharmaceutical wastewater, textile wastewater, petroleum refinery effluent, paint wastewater, precious metals from wastewater, heavy metals from wastewater, oil emulsions from wastewater, defluoridation [12–29]. The removal of contaminant and efficiency of the system primarily depends upon the residence time of the contaminant in the treatment system. During this residence time the contaminant gets the juncture to undergo treatment. The design of suitable electrochemical reactor in accordance to efficient treatment is important. Mixing inside the reactor depends upon the type and design of electrochemical reactor. Induced or natural mixing inside the system can affect the treatment time, hydrodynamics, and efficiency of the system [30–32]. Maximum production rate along with conversion can be obtained when mixing inside the reactor improves and thus promotes efficient mass transfer [7,33]. The hydraulic and mean residence time along with liquid distribution in the entire reactor is determined by the hydrodynamics of the reactor which plays important role in treatment of the system [34,35]. Hydrodynamics provides an insight of an operating electrochemical reactor and in turn helps to understand numerous inter related facets for treatment viz. flow patterns inside the reactor, mixing patterns, kinetics, heat and mass transfer inside the electrochemical reactor. This provides better understanding and insight to design a specific system which can target specifically on the conditions that aggravate in lower efficiency of the reactor. In order to design an efficient electrochemical reactor various factors needs to be taken

^{*} Corresponding author.

E-mail address: smathur.ce@mmit.ac.in (S. Mathur).

<http://dx.doi.org/10.1016/j.jwpe.2017.08.019>

Received 17 May 2017; Received in revised form 14 August 2017; Accepted 24 August 2017

Available online 12 September 2017

2214-7144/ © 2017 Elsevier Ltd. All rights reserved.

Nature Environment and Pollution Technology

(AN INTERNATIONAL OPEN ACCESS JOURNAL ON DIVERSE ASPECTS OF ENVIRONMENT)
ISSN 0972-6268(PRINT); ISSN 2395-3454(ONLINE)

[A UGC (India) Approved Journal]

Published by

Technoscience Publications

2, Shila Apartment, Shila Nagar, KARAD-415 110, Maharashtra, India

Tel: 02164-223070, Mob: 9890248152, e-mail: contact@neptjournal.com, journalnept@gmail.com

Date: 18/2/2017

1. NAAS Rating of the Journal (2016) = 4.94
2. Scopus H-Index = 5
3. Scopus SJR (2015) = 0.14
4. Cites per Doc. (2Yr) 2015 equivalent to Impact Factor™ = 0.124
5. Index Copernicus = 100.23 (2015)
6. ISI Journal Impact Factor (2016) = 1.953
7. Journal is approved by UGC (India)

Final Acceptance Letter

Paper No. B-3452

To,

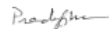
A Choudhary and S Mathur
Department of Civil Engineering,
Malaviya National Institute of Technology,
Jaipur, Rajasthan, India

Dear Sir/Madam

We are happy to inform you that your paper entitled "**Removal Kinetics and performance evaluation of 3D Rotating Cylindrical Anode Reactor for textile wastewater treatment**" has been accepted for publication in the scientific journal Nature Environment and Pollution Technology (p-ISSN 0972-6268; e-ISSN 2395-3454). The paper is likely to come in Vol. 16, No. 4 (December), Year 2017. .

Thanking you,

Yours sincerely,



P. K. Goel
Editor

For full papers of current and old issues, Online submission
of the research papers, Sample copy of the journal and
literature survey visit our website:

www.neptjournal.com

Tel: 02164-223070, Mob: 9890248152, e-mails: contact@neptjournal.com, journalnept@gmail.com

PAPER • OPEN ACCESS

Performance Evaluation of Non Rotating and Rotating Anode Reactor in Electro Coagulation Process

To cite this article: Aditya Choudhary and Sanjay Mathur Dr. 2017 *IOP Conf. Ser.: Mater. Sci. Eng.* **225** 012131

View the [article online](#) for updates and enhancements.

Related content

- [Experimental performance evaluation of heat pump-based steam supply system](#)
T Kaida, I Sakuraba, K Hashimoto et al.
- [Characterization and performance evaluation of a vertical seismic isolator using link and crank mechanism](#)
N Tsujiuchi, A Ito, Y Sekiya et al.
- [Fluid-Structure interaction analysis and performance evaluation of a membrane blade](#)
M. Saeedi, R. Wüchner and K.-U. Bletzinger

Performance Evaluation of Non Rotating and Rotating Anode Reactor in Electro Coagulation Process

Aditya Choudhary^a and Dr. Sanjay Mathur^b

^a Research Scholar, Department of Civil Engineering, Malaviya National Institute of Technology, Jaipur – 302017

^b Associate Professor, Department of Civil Engineering, Malaviya National Institute of Technology, Jaipur - 302017

Abstract: Electro coagulation process using various designs and configurations have been tested from time to time and found to impart major role in the process. Mostly non rotating configurations were used in the available literature. The usage of rotating electrode reactors has come to light and found out to be effective configuration. The effect of rotating and non rotating reactor configurations along with other affecting parameters likes current density, detention time and energy consumption were investigated. Set of experiments were conducted using simulated sample prepared by dissolving basic red dye in tap water to carry out the performance evaluation of the two type of reactors configuration. A comparative study between the two configurations was made to investigate their effectiveness in term of COD removal efficiency and economics of treatment. The results show that rotating reactor configuration have consumed 15-17% less energy for maximum COD removal of 96.40% and thus have better removal efficiency and lower specific energy consumption than non rotating reactor configuration.

Keywords: COD removal, Electro coagulation, Energy Consumption, Rotating and Non Rotating reactor configuration, Textile wastewater

1. INTRODUCTION

The major challenge standing in front of the modern world is demand, supply and availability of clean water for domestic and industrial use [1]. Due to large quantity and diverse nature of industrial wastewater, the issue of its treatment remains a major environmental concern. So, the gap in demand and supply has made it compulsory to reuse the treated wastewater.

The textile wastewater from dyeing and finishing process has been a serious environmental concern for decades. The textile wastewater contains high color, varying pH, high COD concentration, high turbidity, suspended particles and low biodegradability [2]–[5] which makes it difficult to use conventional technologies available. A host of modern era imparted the use of very promising technique based on electrochemical technology like electro coagulation, electro flotation [6] etc. EC has been a very complex process involving various multitude mechanisms operating simultaneously to treat wastewater.

A wide variety of opinions exist in literature for key mechanism and reactor configurations. A systematic and holistic approach is required to understand EC and its controlling parameters [1]. Over the broad range of time period over which this technology is used it is surprising the



Content from this work may be used under the terms of the [Creative Commons Attribution 3.0 licence](https://creativecommons.org/licenses/by/3.0/). Any further distribution of this work must maintain attribution to the author(s) and the title of the work, journal citation and DOI.

Published under licence by IOP Publishing Ltd

1



**AMITY SCHOOL OF
ENGINEERING & TECHNOLOGY**

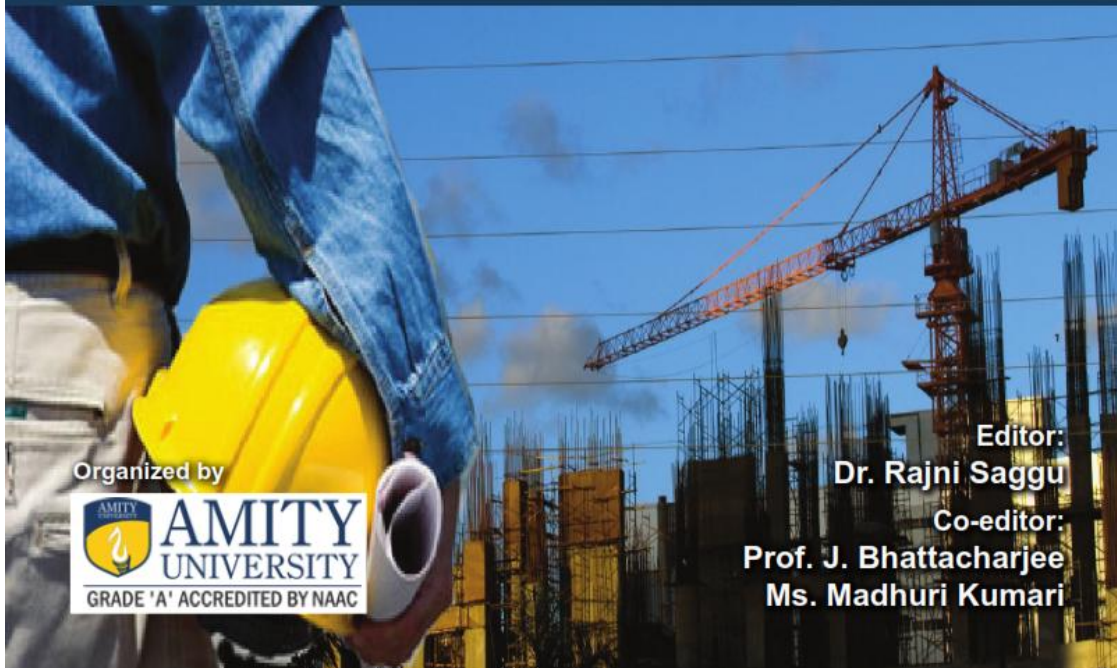
presents

**PROCEEDINGS OF THE
INTERNATIONAL CONFERENCE ON**

**Trends and Recent Advances
in Civil Engineering**

TRACE 2016

11th & 12th August 2016 | Amity University Uttar Pradesh



Organized by



Editor:
Dr. Rajni Saggu

Co-editor:
**Prof. J. Bhattacharjee
Ms. Madhuri Kumari**

*Proceedings of
International Conference
on
Trends and Recent Advances in
Civil Engineering*

TRACE 2016

**11-12 August 2016
Amity University Uttar Pradesh, Sector 125, Noida**

**Editor:
Dr. Rajni Saggu**

**Co-editor
Prof J Bhattacharjee
Ms Madhuri Kumari**

Organized by



**Department of Civil Engineering
Amity School of Engineering and Technology
Amity University Uttar Pradesh, Noida, India**

Textile Wastewater Removal by Electrocoagulation in a 3D Rotating Cylindrical Anode Reactor: An Innovative Approach

Aditya Choudhary¹ and Dr. Sanjay Mathur²

¹Department of Civil Engineering, Malaviya National Institute of Technology, Jaipur, Rajasthan, India;
Email: adityacmnit@gmail.com

²Department of Civil Engineering, Malaviya National Institute of Technology, Jaipur, Rajasthan, India;
Email: smathur.ce@mnit.ac.in

ABSTRACT: The removal and performance of a batch electrocoagulation 3D rotating cylindrical anode reactor for reactive dye effluent was investigated. The cell used a rotating 3D Al cylinder as anode and long rod of aluminium as cathode. The performance of this unique reactor was investigated for various operating parameters, such as anode rotation speed (0-100 rpm), current density (2-10 mA/cm²), duration of electrolysis, NaCl concentration, initial pH. Increasing the anode rotation speed and current density led to increase the rate of COD removal; current density of 6 mA/cm² and rotation speed of 60 rpm allowed achieving maximum efficiency of the system with 96.40% of COD removal. The optimum pH range for the electrocoagulation is 6-8; the acidic range (pH 4-5) hinders the process. The increase in NaCl concentration increases the rate of dye removal.

INTRODUCTION

The rapid speed of industrialization and discharge of untreated wastewater in the receiving streams severely affects the aquatic life and in turn the ground water resources. In this contamination process, the textile wastewater shares a hefty amount of water pollution mainly transpiring from various textile units after respective dyeing process. The removal of various dyes from textile wastewater is of great need and concern as they not only impart colouring impacts but also high BOD and COD of the wastewater severely affects the receiving stream or body. Dissociation of many dyes produce carcinogen compounds which in turn possess serious health risk to living beings via food chain especially in developing countries (Deb and Majumdar, 2013). The annual production capacity for dyes and pigments are about 700,000 and 10,000 tonnes respectively across the globe (Gong et al. 2007, Maneet al. 2007). There are conventional processes available for the treatment of textile wastewater including biological process, biodegradation, coagulation and flocculation, adsorption, advanced oxidation, adsorption (Annadurai et al. 2008, Kim et al. 2004, Lin and Peng 1996, Nakagawa et al., 2004, Papić, et al. 2004). These biological processes in turn are less efficient in treatment of dye wastewater (Elisangela et al., 2009, Lin and Peng 1996). The drawbacks of these processes led to search of alternative technology for wastewater treatment known as Electrocoagulation. It has an advantage of “in situ” delivery of reactive agents with less space required for its functioning. The potential of EC as a treatment technology for different type of wastewater has been reported by various researchers. It has been reported for treatment of dyes; heavy metals; oil emulsions; complex organics; suspended solids; bacteria, viruses and cysts (Aleboyeh et al. 2008, Can, Kobya, Demirbas, & Bayramoglu, 2006; Vlyssides, Papaioannou, Loizidouy, Karlis, & Zorpas, 2000; Xiong, Strunk, Xia, Zhu, & Karlsson, 2001).

In this investigation, an electrochemical reactor with an innovative design was used for EC/treatment of textile wastewater. A rotating 3D perforated cylindrical aluminium anode and cathode were designed to induce high turbulence even at low rotational speeds in the textile wastewater/solution (Winnick, 1996).

BRIEF BIO-DATA

Mr. Aditya Choudhary is a Research scholar in Department of Civil Engineering, Malaviya National Institute of Technology (MNIT), Jaipur. He has received his B.Tech degree in Biotechnology from Amity University, Noida. He has received his Master's degree from MNIT, Jaipur in Environmental Engineering. He has joined PhD in 2012 under supervision of Dr. Sanjay Mathur, Department of Civil Engineering, MNIT, Jaipur. His research interests are mainly in the areas of wastewater treatment. During his research work he has published three research papers in international journals. He has attended various National and International Conferences & workshops.